DESIGN OF PERFORATED THIN-WALLED STEEL COLUMNS

ZHENYU YAO
KIM JR RASMUSSEN

SCHOOL OF CIVIL
ENGINEERING

THE UNIVERSITY OF
SYDNEY

THE UNIVERSITY OF
SYDNEY

DESIGN OF PERFORATED THIN-WALLED STEEL COLUMNS

RESEARCH REPORT R949

ZHENYU YAO
KIM JR RASMUSSEN

June 2014

Copyright Notice

ABSTRACT

The strength database from the parametric study presented in (Yao and Rasmussen 2014) was used to evaluate an overall number of 19 design methods based on the DSM for non-perforated and perforated thin-walled steel columns with the Ramberg-Osgood material model defined by *n*=20. These methods included the current codified DSM, the design options proposed by Moen and Schafer (2011), the methods based on simple modifications to these aforementioned methods, the methods considering buckling interactions (in addition to LG interaction), and the methods based on regression analyses.

A concerted effort was made to compare the 19 DSM methods by presenting the detailed statistics of the predictions for each section type and failure mode, as well as figures illustrating the corresponding simulation-to-predicted ratios. This led to the best-performing method proposed for the design of perforated cold-formed carbon steel columns. This method was based on modifying the Option 4 method proposed by Moen and Schafer (2011) such that (i) DG interaction was included, (ii) $P_{cr\text{-}l\text{-}nh}$ and $P_{cr\text{-}d\text{-}nh}$ based on gross section were used, and (iii) a factor based on a regression analysis was added to improve the final design strength.

The proposed method was based on a reliability analysis with a target reliability index of 2.5, carried out on 60132 data points. A linear regression equation was taken to calculate the additional factor in the method. Two sets of best-fit constants were proposed for the regression equation, one for general section types including C, Z, Hat, Rack, and Stiffened C sections, the other for Stiffened C section only. When calculating the design strength of a perforated column as per the proposed method, the major effort will be calculating the elastic local and distortional buckling loads $P_{cr\text{-}l\text{-}nh}$ and $P_{cr\text{-}d\text{-}nh}$ based on the gross section (which can be readily calculated by a SAFSM software such as THIN-WALL or CUFSM), and the elastic global buckling load $P_{cr\text{-}e\text{-}h}$ including the influence of hole(s).

KEYWORDS

Cold-formed, Thin-walled, Columns, Perforations, Design, Interactive buckling, Direct Strength Method, Reliability analysis, Resistance factor

TABLE OF CONTENTS

1. Introduction

This report aims to evaluate the existing design methods and develop a new design approach for predicting the strength of perforated thin-walled columns. The study was based on:

(i)   The numerous column data for five types of cross-section shapes (C, Z, Hat, Rack and Stiffened C) obtained from the FE simulations in (Yao and Rasmussen 2014).

(ii)   The Direct Strength Method (DSM) included in the North American and Australian/New Zealand standards for cold-formed steel design (AS/NZS:4600 2005; NAS 2007).

Although the parametric studies described in (Yao and Rasmussen 2014) were performed with Ramberg-Osgood material models defined by n=5 and 20 (the C-section columns also considered n=10), only the data related to n=20 were chosen for the evaluation and formulation of the design equations in this report. This is because this study mainly concerns cold-formed carbon steel members, while the material models defined by n=5 or n=10 are more related to stainless steel. Future research is planned to include these data in design formulations.

An overall total of 19 different design methods based on the DSM were explored. Their descriptions are tabulated in Table 1 which also includes the method identification number and the database used to evaluate the method.

The main body of this report provides the tabulated statistics of the predictions using each design method, along with figures plotting the simulation-to-predicted ratios for all the members considered, which are classified according to either the failure mode or section type. The detailed simulation-to-predicted ratios for each section type with classified failure modes are provided in the appendices to this report. It should be noted that the classification of failure modes was performed visually, hence it was approximate and subject to the judgement of the author.

2. Review of existing DSM design practices

2.1. Design strength by AS/NZS 4600 DSM

As an alternative to the traditional Effective Width Method, the DSM was first adopted in Appendix I of the North American Specifications (NAS) (2004), and later in Section 7 of AS/NZS 4600 (2005) for the design of non-perforated cold-formed steel columns and beams. The existing DSM is composed of equations for three

strength limit states, i.e. global buckling or yielding, local-global buckling interaction, and distortional buckling. For completeness, the respective equations for the three limit states are stated as follows:

(i) The nominal axial strength, P_{ne}, for flexural, torsional, or torsional-flexural buckling is

$$\text{For } \lambda_c \leq 1.5: \quad P_{ne} = \left(0.658^{\lambda_c^2} \right) P_y \tag{1}$$

$$\text{For } \lambda_c > 1.5: \quad P_{ne} = \left(\frac{0.877}{\lambda_c^2} \right) P_y \tag{2}$$

where $\lambda_c = \sqrt{P_y / P_{cr-e-nh}}$, $P_y = A_g F_y$, $P_{cr-e-nh}$ = critical elastic global column buckling load based on A_g , and A_g = gross area of the cross-section.

(ii) The nominal axial strength, P_{nle}, for local buckling (including local-global buckling interaction) is

$$\text{For } \lambda_{le} \leq 0.776, \quad P_{nle} = P_{ne} \tag{3}$$

$$\text{For } \lambda_{le} > 0.776, \quad P_{nle} = \left[1 - 0.15 \left(\frac{P_{cr-l-nh}}{P_{ne}} \right)^{0.4} \right] \left(\frac{P_{cr-l-nh}}{P_{ne}} \right)^{0.4} P_{ne} \tag{4}$$

where $\lambda_{le} = \sqrt{P_{ne} / P_{cr-l-nh}}$, and $P_{cr-l-nh}$ = critical elastic local column buckling load based on A_g , and P_{ne} = nominal axial strength for global buckling as defined in (1) and (2).

(iii) The nominal axial strength, P_{nd}, for distortional buckling is

$$\text{For } \lambda_d \leq 0.561, \quad P_{nd} = P_y \tag{5}$$

$$\text{For } \lambda_d > 0.561, \quad P_{nd} = \left[1 - 0.25 \left(\frac{P_{cr-d-nh}}{P_y} \right)^{0.6} \right] \left(\frac{P_{cr-d-nh}}{P_y} \right)^{0.6} P_y \tag{6}$$

where $\lambda_d = \sqrt{P_y / P_{cr-d-nh}}$, $P_{cr-d-nh}$ = critical elastic distortional column buckling load based on A_g .

Table 1: Description of design methods explored in this report

DSM Method	Simulation Database	Description
1	non-perforated, perforated, all	AS/NZS 4600 DSM
2	non-perforated, all	minimum of LG and DG interaction equations based on AS/NZS 4600 DSM
3	non-perforated	minimum of LG, DG, and LD interaction equations based on AS/NZS 4600 DSM
4	non-perforated	LDG interaction equation based on AS/NZS 4600 DSM
5	all	Option 2 in (Moen and Schafer 2011), i.e. P_{yn} everywhere, P_{cr} (i.e. P_{cr-1-h}, P_{cr-d-h}, P_{cr-e-h}) includes the influence of holes by the simplified methods in (Moen and Schafer 2009)
6	all	Option 4 in (Moen and Schafer 2011), i.e. limit P_{n1} to P_{yn}, transition P_{nd} to P_{yn}, P_{cr} includes the influence of holes by the simplified methods in (Moen and Schafer 2009)
7	all	AS/NZS 4600 DSM with P_{yn} everywhere and P_{cr} based on gross area (i.e. $P_{cr-1-nh}$, $P_{cr-d-nh}$, $P_{cr-e-nh}$)
8	all	AS/NZS 4600 DSM with P_y in the slenderness, P_{yn} elsewhere and P_{cr} based on gross area
9	all	Modification 1 to Option 4 in (Moen and Schafer 2011) – replace P_{cr-e-h} by $P_{cr-e-nh}$
10	all	Modification 2 to Option 4 in (Moen and Schafer 2011) – replace P_{cr-1-h} by $P_{cr-1-nh}$
11	all	Modification 3 to Option 4 in (Moen and Schafer 2011) – replace P_{cr-d-h} by $P_{cr-d-nh}$
12	all	Modification 4 to Option 4 in (Moen and Schafer 2011) – replace the D equation by the AS/NZS 4600 DSM D equation, limit P_{nd} to P_{yn}; use P_{cr-d-h}
13	all	Modification 5 to Option 4 in (Moen and Schafer 2011) – minimum of (i) regression analyses of LG equation using $P_{cr-1-nh}$, (ii) D equation, and (iii) G equation
14	all	Modification 6 to Option 4 in (Moen and Schafer 2011) – minimum of (i) regression analyses of LG equation using $P_{cr-1-nh}$ and (ii) D equation

Table 5.1: Description of design methods explored in this report (continued)

15	all	Modification 7 to Option 4 in (Moen and Schafer 2011) – minimum of (i) regression analyses of LG equation using $P_{cr-l-nh}$ and (ii) G equation
16	all	Modification 8 to Option 4 in (Moen and Schafer 2011) – use $P_{cr-l-nh}$ and $P_{cr-d-nh}$, factor final strengths
17	all	Modification 9 to Option 4 in (Moen and Schafer 2011) – use $P_{cr-l-nh}$ and $P_{cr-d-nh}$, regression analyses of final strengths; separate regression parameters for stiffened C section columns
18	all	Modification 10 to Option 4 in (Moen and Schafer 2011) – replace D equation by DG interaction equation, use $P_{cr-l-nh}$ and $P_{cr-d-nh}$, factor final strengths
19	all, non-perforated	Modification 11 to Option 4 in (Moen and Schafer 2011) – replace D equation by DG interaction equation, use $P_{cr-l-nh}$ and $P_{cr-d-nh}$, regression analyses of final strengths; separate regression parameters for stiffened C section columns

Firstly, the AS/NZS 4600 DSM design expressions (i.e. DSM Method 1) as shown in Equations (1)-(6) were applied to 1506 non-perforated steel columns included in the parametric studies. These data included non-perforated columns with five cross-section shapes (i.e. C, Z, Hat, Rack and Stiffened C) which covered both the practical slenderness ranges and the geometric limits of the major cross-sections pre-qualified by the AS/NZS 4600 DSM.

A first order second moment (FOSM) reliability analysis was performed to evaluate the AS/NZS 4600 DSM rules, as well as all subsequent design expressions. The primary aim was to obtain the resistance factor ϕ conforming to the load and resistance factor design (LRFD) for cold-formed carbon steel. The analysis was based on the equations provided in Chapter F of the AISI Specification (NAS 2007). The following statistical data was used:

> ➤ The LRFD reliability target index β_0=2.5 for cold-formed carbon steel structural members.

> ➤ The mean value of the fabrication factor F_m=1.0 and its coefficient of variation V_F=0.05.

> ➤ The mean value of the material factor M_m=1.10 and its coefficient of variation V_M=0.10.

> ➤ A representative ratio of dead load to live load for cold-formed members G_n/Q_n=0.2.

> ➤ A representative ratio of mean dead load to nominal dead load G_m/G_n=1.05.

> ➤ A representative ratio of mean live load to nominal live load Q_m/Q_n=1.0.

> ➤ The coefficient of variation of the dead load V_D=0.1.

> ➤ The coefficient of variation of the live load V_L=0.25.

> ➤ Dead load factor γ_G=1.2.

> ➤ Live load factor γ_Q=1.5.

To determine the resistance factor ϕ, the reliability analysis used the mean professional factor P_m, defined as the mean of the test-to-predicted (or simulation-to-predicted) ratio, and the coefficient of variation, V_p, of the same ratio defined as the standard deviation of the test-to-predicted ratio divided by the P_m value.

2.1.1. Method 1 – non-perforated

The resulting resistance factors by DSM Method 1, i.e. the AS/NZS 4600 DSM, for non-perforated columns are listed in Table 2 for failure modes L, LG, G, D, and L+LG+G+D, and in Table 3 for LD, DG, LDG, LD+DG+LDG, and all failure modes. Essentially Table 2 includes the failure modes that are considered by the current DSM, and Table 3 includes the interactive modes involving distortional deformations that are not covered in the standard.

Table 2 and Table 3 show that the overall resistance factor ϕ is 0.824 which is slightly below the prescribed value 0.85 in the AS/NZS 4600 DSM. In terms of failure mode the resistance factors ϕ in a descending order are 0.914 (G), 0.893 (LG), 0.882 (L), 0.838 (LDG), 0.824 (D), 0.794 (LD), and 0.698 (DG), which suggests that the AS/NZS 4600 DSM produced inferior predictions for failure modes involving distortional buckling. A quite reliable prediction (ϕ =0.874) was achieved if only the modes (i.e. L, LG, G and D) covered by the current DSM were considered, while a resistance factor ϕ of only 0.757 was obtained for other interactive modes (i.e. LD, DG, LDG). This observation is also valid for each individual section. It is found that the overall resistance factor ϕ also varies between different section types such that the ϕ values in a descending order are 0.896(Z), 0.834 (Rack), 0.830 (C), 0.737 (Hat), and 0.609 (Stiffened C). Therefore, depending on the specific section type and failure mode, the reliability of the prediction can vary considerably. For example, the safest predictions are for Rack section columns failing in G mode with ϕ =0.971 and the least safe ones are for Stiffened C section columns failing in DG interaction with ϕ of only 0.508. From a design point of view, an engineer not knowing the actual failure mode should use the prescribed ϕ value of 0.85 in the AS/NZS 4600 DSM only for C, Z and Rack sections (as their overall ϕ values are 0.830, 0.896 and 0.834 respectively), while the "actual" ϕ values of 0.737 and 0.609 should be used for Hat and Stiffened C sections respectively. Nevertheless, this approach of using the overall ϕ value including different failure modes can still over-predict the member strength if the column is in reality predisposed to a failure mode which has a lower ϕ value than the overall ϕ value. Therefore, a more conservative design approach could be to use the minimum ϕ value of all failure modes, for instance, to use ϕ =0.683 (for the LDG mode) for designing non-perforated Rack section columns.

Table 2: Resistance factors for non-perforated columns failing in modes L, LG, G, D, and L+LG+G+D by **DSM Method 1** – AS/NZS 4600 DSM

prediction method	Section shape	Failure mode																			
		L				LG				G				D				All L, LG, G, D			
		P_m	V_p	ϕ	n	P_m	V_p	ϕ	n	P_m	V_p	ϕ	n	P_m	V_p	ϕ	n	P_m	V_p	ϕ	n
DSM Method 1	C	1.108	0.135	0.889	292	1.075	0.082	0.911	94	1.025	0.083	0.869	34	1.159	0.217	0.822	80	1.104	0.146	0.873	500
	Z	1.107	0.097	0.927	147	1.053	0.145	0.834	28	1.070	0.030	0.935	52	1.032	0.058	0.890	50	1.079	0.097	0.902	277
	Hat	0.930	0.056	0.803	42	1.046	0.145	0.829	13	1.093	0.013	0.959	3	1.021	0.092	0.859	9	0.972	0.104	0.808	67
	Rack	1.042	0.084	0.882	11	1.088	0.081	0.923	22	1.110	0.027	0.971	8	1.025	0.045	0.890	8	1.071	0.074	0.914	49
	Stiffened C	1.026	0.072	0.877	10	1.078	0.034	0.940	3	1.097	0.006	0.963	4	1.215	0.272	0.782	5	1.089	0.156	0.849	22
	All sections	1.090	0.128	0.882	502	1.070	0.100	0.893	160	1.060	0.058	0.914	101	1.104	0.186	0.824	152	1.085	0.132	0.874	915

Table 3: Resistance factors for non-perforated failing in modes LD, DG, LDG, LD+DG+LDG, and all failure modes by **DSM Method 1** – AS/NZS 4600 DSM

prediction method	Section shape	Failure mode																			
		LD				DG				LDG				All LD, DG, LDG				ALL Failure modes			
		P_m	V_p	ϕ	n	P_m	V_p	ϕ	n	P_m	V_p	ϕ	n	P_m	V_p	ϕ	n	P_m	V_p	ϕ	n
DSM Method 1	C	0.929	0.130	0.750	65	0.920	0.173	0.701	54	1.130	0.165	0.870	22	0.957	0.172	0.730	141	1.072	0.162	0.830	641
	Z	1.000	0.060	0.862	84	1.065	0.086	0.900	62	1.155	0.131	0.931	134	1.089	0.125	0.884	280	1.085	0.110	0.896	557
	Hat	0.886	0.073	0.757	12	0.894	0.208	0.645	41	0.944	0.170	0.722	21	0.907	0.182	0.682	74	0.938	0.151	0.737	141
	Rack	0.900	0.070	0.771	3	0.996	0.093	0.836	17	0.957	0.214	0.683	18	0.970	0.160	0.753	38	1.027	0.125	0.834	87
	Stiffened C	0.851	0.219	0.602	5	0.809	0.285	0.508	36	0.915	0.184	0.685	17	0.844	0.253	0.563	58	0.911	0.252	0.609	80
	All sections	0.958	0.107	0.794	169	0.945	0.193	0.698	210	1.096	0.171	0.838	212	1.003	0.179	0.757	591	1.053	0.155	0.824	1506
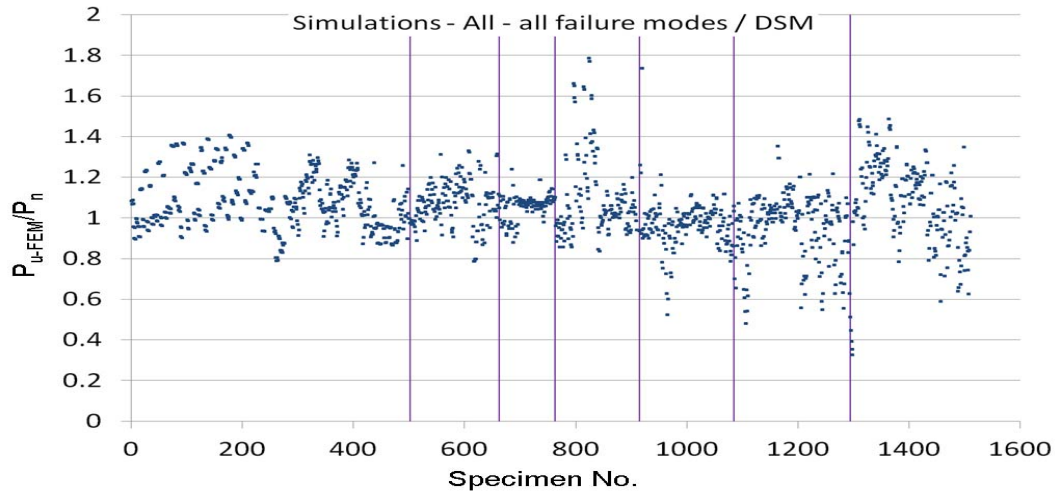
Fig. 1: Simulation-to-predicted ratios for all non-perforated columns by DSM Method 1 with classified failure modes (from left to right: L, LG, G, D, LD, DG, and LDG)
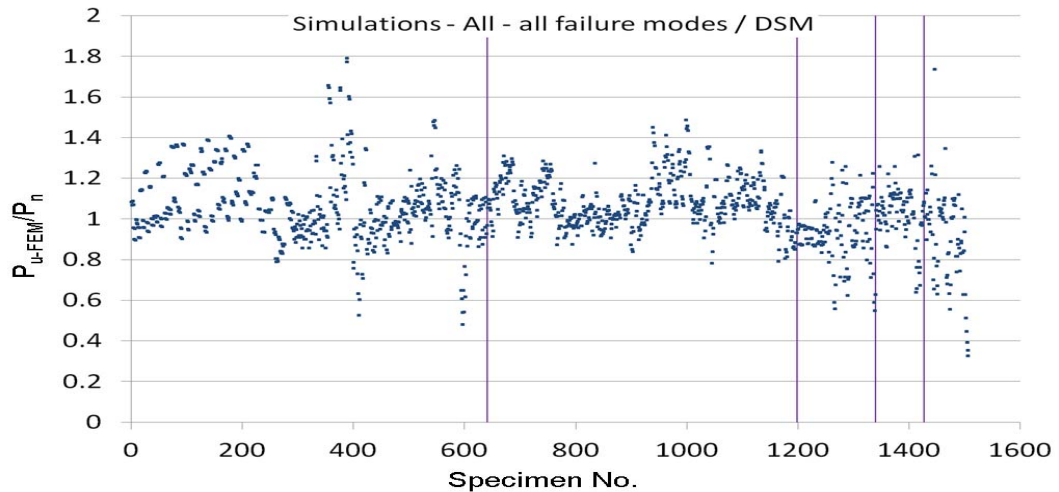
Fig. 2: Simulation-to-predicted ratios for all non-perforated columns by DSM Method 1 with classified section types (from left to right: C, Z, Hat, Rack and Stiffened C)

Along with the statistical tables, two figures are also provided to plot the simulation-to-predicted ratios ($P_{u\text{-}FEM}/P_n$) for all non-perforated members, with Fig. 1 classified by failure mode (from left to right: L, LG, G, D, LD, DG, and LDG) and Fig. 2 classified according to section type (from left to right: C, Z, Hat, Rack and Stiffened C). In addition, Section A.1 of Appendix A provides more detailed figures that plot the simulation-to-predicted ratios for each section type with classified failure modes. In general, these figures show less reliable predictions (with smaller mean and/or larger variation) for failure modes D, LD, DG, and LDG, and also for Hat and Stiffened C sections, which agrees with the results presented in Table 2 and Table 3. In addition, the following describes the observations for any substantial deviations from unity in the value of $P_{u\text{-}FEM}/P_n$:

(i) For C section columns failing in an L mode, significant over-predictions ($P_{u\text{-}FEM}/P_n$ <0.9) occurred for sections C66, C68 and C69. This is because on one hand C66 had very small lips

(hence its λ_d was much higher than its λ_l, where $\lambda_d = \sqrt{P_y/P_{cr\text{-}d\text{-}nh}}$ and $\lambda_l = \sqrt{P_y/P_{cr\text{-}l\text{-}nh}}$) so that considerable distortional deformations were involved in its L mode. On the other hand, C68 and C69 were the sections that had the widest flanges (b_1) relative to their web widths (d) so that local buckling failure was triggered mainly in the two flanges. This mode seemed to have a more pronounced weakening effect on the load-carrying capacity compared to sections with narrow flanges which contributed to a stiffening effect.

In addition, under-predictions occurred for a large number of sections with moderate to high cross-sectional slenderness and whose λ_l was significantly higher than λ_d (such as C35 and C45). These members exhibited considerable post-buckling reserve of strength associated with plate local buckling. In general it was found that the higher (lower) the λ_l than the corresponding λ_d, the safer (less safe) the predictions for local buckling failures.

(ii)　　　For C section columns failing in a D mode, considerable under-predictions were observed for slender sections such as C21, C32, C43, C49, and C51, indicating that those columns exhibited considerable post-buckling reserve of strength that was not reflected in the current DSM.

(iii)　　　For C section columns failing in an LD mode, severe over-predictions occurred for sections C55, C59, C60 and C63 featuring large cross-sectional slenderness with λ_l much higher than λ_d. This indicates that severe interaction with local buckling could cause significant strength erosion in an LD mode.

(iv)　　　For C section columns failing in a DG mode, the most severe over-predictions ($P_{u\text{-}FEM}/P_n$ as low as 0.48) occurred for columns made from section C65. This is because C65 featured very small lips and therefore its λ_d was much higher than its λ_l, and thus its global failure mode showed a strong interaction with the D mode. This demonstrates the profoundly adverse effect of DG interaction on the strength of the column.

(v)　　　For C section columns failing in an LDG mode, significant under-predictions occurred for short columns made from section C43 which had the highest ratio of web width to flange width. No special characteristic was detected in their failure modes, but it was found that it was the D equation in the AS/NZS 4600 DSM that under-predicted the strength of this section.

(vi)　　　For Z section columns failing in an L mode, as with C sections, over-predictions occurred for sections with $\lambda_d > \lambda_l$, while under-predictions occurred for sections with moderate to high cross-sectional slenderness with $\lambda_d < \lambda_l$.

(vii)　　　For Z section columns failing in an LG mode, over-predictions were produced solely by section Z71 which featured no lips. It therefore did not have a distortional mode and Equations (5) and (6) were not used in prediction.

(viii)　　　For Z section columns failing in an LDG mode, large variations in the predictions were observed. The strength of most columns was safely or overly safely predicted by the AS/NZS 4600

DSM, despite the fact that they failed in an obvious LDG interaction. On the other hand, unsafe predictions were produced by short to moderate-length columns made from sections Z35, Z69 and Z70 which featured high cross-sectional slenderness ($\lambda_1 > 4.0$) with $\lambda_1 > \lambda_d$ but $\lambda_1 < \lambda_d + 1.0$. It is also interesting to note that while the strengths of Z35 and Z69 were over-predicted for short to moderate-length columns, they were under-predicted for longer columns. This difference was reflected in their failure modes such that the former involved more noticeable distortional deformations.

(ix)　　For Hat section columns failing in an L mode, a great majority of their strengths were over-predicted by the AS/NZS 4600 DSM. This is because most Hat sections featured wide flanges (b_1) relative to the web width (d), and thus local buckling failure mainly occurred in the flanges, as with sections C68 and C69 as discussed in (i).

(x)　　For Hat section columns failing in a DG mode, substantial over-predictions ($P_{\text{u-FEM}}/P_n$ as low as 0.55) occurred for moderate to long columns made from sections H1, H4, H8, H19, H20, and H21, of which H1, H4, H8 and H21 featured wide flanges and moderate to high cross-sectional slenderness with $\lambda_1 > \lambda_d$.

(xi)　　For Hat section columns failing in an LDG mode, over-predictions　　($P_{\text{u-FEM}}/P_n$ <0.8) occurred for columns of a moderate length ($0.8 < \lambda_c < 1.1$) and made from sections H1, H3 and H8 which featured wide flanges. It is also worth noting that among those sections, H1 and H8 with a shorter length ($\lambda_c = 0.55$) were however notably under-predicted ($P_{\text{u-FEM}}/P_n = 1.17$), which is because those short columns failed by predominant local buckling.

(xii)　　For Rack sections, as opposed to L, LG, G and D modes which showed quite uniform and conservative predictions, the predictions associated with LD, DG and LDG modes were poor. In particular, the LD mode resulted in an unconservative mean prediction while the LDG mode showed large variations.

(xiii)　　For Rack sections failing in a DG mode, the only significant over-prediction was from the column made from section R9 and with a moderate length, where R9 featured the widest flanges relative to the web width.

(xiv)　　For Rack sections failing in an LDG mode, the strengths of columns made from R9 and R10 were all significantly over-predicted, and these sections also featured wide flanges.

(xv)　　For Stiffened C sections, considerable variations in strength prediction were found with failure modes involving the D mode, and thus a resistance factor ϕ of only 0.563 was obtained for those modes (i.e. LD, DG and LDG) excluded in the AS/NZS 4600 DSM, while the ϕ value of 0.849, consistent with the prescribed value of 0.85 in the current DSM, was achieved for the other modes.

(xvi)　　For Stiffened C sections failing in a D mode, the strengths of sections SC4, SC5 and SC10 were significantly under-predicted. These sections featured moderate to high cross-sectional slenderness with λ_d much higher than λ_1, hence indicating a considerable post-buckling reserve of

strength. However, the strength of the columns made from stocky sections (SC3 and SC6) was slightly over-predicted.

(xvii)   For Stiffened C sections failing in an LD mode, notable over-predictions were found with sections SC7 and SC9 which had high cross-sectional slenderness with $\lambda_1 > \lambda_d$. This indicates that a severe interaction with local buckling contributed to a noticeable erosion of strength in the LD mode.

(xviii)   A majority of pinned-end Stiffened C section columns that failed in a DG mode showed the lowest mean and the most severe variations in $P_{u\text{-FEM}}/P_n$ values among all the sections and failure modes. In particular, over-predictions occurred for sections SC1, SC4, SC5, SC8 and SC10 which featured moderate to high cross-sectional slenderness with $\lambda_d > \lambda_1$. Of them, the strength of SC10 was over-predicted the most with a $P_{u\text{-FEM}}/P_n$ value of as low as 0.33, which was due to the fact that SC10 had very small lips (so its λ_d was much higher than its λ_1), and hence a strong DG interaction. It is also worth noting that this degree of over-prediction increased with an increase in the member length, in contrast to the other sections where the most severe over-predictions usually occurred at a moderate member length.

(xix)   For Stiffened C sections failing in an LDG mode, the strength of most of the columns was over-predicted. These columns had a moderate member length and were made from sections SC7, SC8 and SC9 featuring moderate to high cross-sectional slenderness. Severe interaction with distortional buckling, as shown in their failure modes, had a profoundly adverse influence on the strength of the column failing in an LDG mode.

Summarising the above observations prompts the following preliminary conclusions:

(i) The local buckling strength tended to be over-predicted by the AS/NZS 4600 DSM if λ_d was much higher than λ_1 (since considerable distortional deformations could participate in the local failure mode), or if the flange width was large relative to the web width. Regarding the latter, Yap and Hancock (2008; 2011) also made similar observations, i.e. the strength of sections failing in all flange elements tended to be overestimated by the DSM L curve expressed by Equations (3) and (4) , and proposed that the exponent of 0.4 be raised to 0.5 as in the Winter strength formula for a single element in order to provide safe predictions. Among those sections with wide flanges and inferior strength, C68 is pre-qualified by the AS/NZS 4600 DSM, while C69 is nearly pre-qualified. Besides, most Hat sections are not pre-qualified because the limits set out in Table 7.1.1 of AS/NZS 4600 are very impractical and most of the sections used in this study are actually practical sections produced by major manufacturers.

(ii)   On the other hand the local buckling strength could be under-predicted for sections whose λ_1 was significantly higher than λ_d so that a substantial reserve of post-buckling strength could occur.

(iii)   A considerable post-buckling reserve of strength could also occur in pure distortional buckling if the section was slender and its λ_d was much higher than its λ_1, and thus leading to an under-prediction of strength.

(iv)   Severe interaction with local buckling could cause a significant strength erosion in a D mode, which usually occurred for slender sections whose λ_1 was much higher than λ_d. This was in line with the finding by Silvestre et al. (2012) that LD interaction only caused a significant strength erosion for the most slender columns. Among those sections, C55, C59, C60, C63, SC9 were nearly pre-qualified, while SC7 was not pre-qualified.

(v)   DG interaction could significantly reduce the strength of a column, which usually occurred for sections with small lips, wide flanges, or sections of moderate to high slenderness with $\lambda_d > \lambda_1$ (or with $\lambda_1 > \lambda_d$ but $\lambda_1 < \lambda_d +1.0$). The most severe DG and LDG interaction usually occurred in columns of a moderate length.

(vi)   Sections with wide flanges proved to have inferior structural performance such that they not only had slightly poor local buckling strength, but were also susceptible to DG interaction which could lead to significant strength erosion.

(vii)   The AS/NZS 4600 DSM tended to over-predict the strength of sections with no lips. Because such sections do not have a distortional mode, the D equation is not used in the prediction. Further research is needed to study the strength of this class of section.

(viii)   Z sections in general did not seem to be very sensitive to interactive buckling because the current DSM could provide safe predictions even when there was obvious LDG interaction. Only when considerable D mode was engaged did the strength of those sections severely erode. Moreover, it is unusual that interaction with local buckling seemed to benefit the ultimate strength of the Z section columns (except for sections without lips), which resulted in under-predictions of strength for a large proportion of columns.

2.1.2. Method 1 – perforated and all

Although in principle the AS/NZS 4600 DSM should not be applied to perforated columns, its performance was nevertheless evaluated in this study. The resulting statistics are tabulated in Table 4 and Table 5, along with two figures (Fig. 3 and Fig. 4) showing the simulation-to-predicted ratios ($P_{\text{u-FEM}}/P_n$) for all perforated columns classified by failure mode and section type respectively. More detailed figures regarding the simulation-to-predicted ratios for each section are provided in Section A.2 for perforated members only and in Section A.3 for non-perforated plus perforated members.

In comparison with Fig. 1 and Fig. 2, Fig. 3 and Fig. 4 illustrate the additional considerable variations in $P_{\text{u-FEM}}/P_n$ due to the influence of perforations. Overall, the tabulated results show that the resistance factor ϕ was reduced from 0.824 for non-perforated members to only 0.663 for perforated members, demonstrating the

significant erosion of the reliability of the prediction if the presence of holes is not considered in the design method. To further show the influence of holes on each individual failure mode and section type, the percentage differences in the values of ϕ, as well as P_m and V_p, between the non-perforated and perforated members are presented in Table 6 and Table 7. It is seen from the ϕ values that the D mode was most adversely affected by holes with a reduction in ϕ of 22.9%, while the least adversely affected one was the L mode where a 9.6% reduction in ϕ was obtained. On the other hand the most adversely affected section was Hat section with a 28% reduction in ϕ (closely followed by Rack section with a reduction in ϕ of 26.5%), whereas Stiffened C section was least adversely affected by holes with a reduction in ϕ of 14.9%. In addition, if one looks at a particular section with a particular mode, Rack section failing in an LG mode was most adversely affected with a large 41.6% reduction in ϕ, contrary to the least reduction of only 3.8% for Hat section failing in a G mode. These results proved that the presence of holes had a varying influence on different section types and failure modes.

In addition, statistics are also provided for all (non-perforated plus perforated) columns, as shown in Table 8 and Table 9. As the overwhelming majority of the columns were perforated, the difference in the numbers is subtle comparing with Table 4 and Table 5 for perforated columns only. For instance, the overall resistance factor ϕ increased from 0.663 to 0.666 when non-perforated columns were added in the predictions.

Table 4: Resistance factors for perforated columns failing in modes L, LG, G, D, and L+LG+G+D by **DSM Method 1** – AS/NZS 4600 DSM

prediction method	Section shape	Failure mode																			
		L				LG				G				D				All L, LG, G, D			
		P_m	V_p	ϕ	n	P_m	V_p	ϕ	n	P_m	V_p	ϕ	n	P_m	V_p	ϕ	n	P_m	V_p	ϕ	n
DSM Method 1	C	1.059	0.149	0.834	6631	0.983	0.119	0.804	4151	0.868	0.143	0.690	1617	1.037	0.271	0.669	3598	1.015	0.188	0.756	15997
	Z	1.049	0.122	0.855	3565	0.966	0.182	0.726	1330	1.016	0.068	0.871	2496	0.874	0.147	0.690	2394	0.986	0.144	0.782	9785
	Hat	0.820	0.115	0.673	1372	0.898	0.203	0.653	481	1.070	0.058	0.923	134	0.786	0.201	0.574	432	0.843	0.170	0.645	2419
	Rack	0.950	0.107	0.787	450	0.798	0.246	0.539	1043	0.905	0.177	0.685	375	0.831	0.109	0.687	383	0.852	0.201	0.621	2251
	Stiffened C	0.928	0.114	0.763	307	0.915	0.138	0.732	140	0.964	0.102	0.803	192	0.993	0.252	0.662	240	0.951	0.171	0.727	879
	All sections	1.022	0.157	0.797	12325	0.946	0.171	0.723	7145	0.957	0.128	0.774	4814	0.953	0.253	0.635	7047	0.979	0.185	0.733	31331

Table 5: Resistance factors for perforated failing in modes LD, DG, LDG, LD+DG+LDG, and all failure modes by **DSM Method 1** – AS/NZS 4600 DSM

prediction method	Section shape	Failure mode																			
		LD				DG				LDG				All LD, DG, LDG				ALL Failure modes			
		P_m	V_p	ϕ	n	P_m	V_p	ϕ	n	P_m	V_p	ϕ	n	P_m	V_p	ϕ	n	P_m	V_p	ϕ	n
DSM Method 1	C	0.798	0.176	0.605	3092	0.764	0.209	0.550	2535	0.984	0.191	0.729	840	0.809	0.210	0.581	6467	0.956	0.217	0.679	22464
	Z	0.876	0.132	0.705	4031	0.956	0.134	0.768	2927	1.020	0.170	0.780	5923	0.960	0.167	0.738	12881	0.972	0.158	0.756	22666
	Hat	0.711	0.181	0.534	573	0.710	0.297	0.436	1886	0.791	0.257	0.523	943	0.733	0.274	0.470	3402	0.779	0.240	0.531	5821
	Rack	0.731	0.101	0.609	134	0.820	0.196	0.603	815	0.824	0.187	0.614	882	0.815	0.190	0.605	1831	0.836	0.198	0.613	4082
	Stiffened C	0.712	0.201	0.519	240	0.724	0.296	0.445	1691	0.802	0.217	0.570	783	0.745	0.270	0.482	2714	0.796	0.266	0.518	3593
	All sections	0.827	0.167	0.635	8070	0.808	0.247	0.544	9854	0.957	0.210	0.688	9371	0.865	0.227	0.604	27295	0.926	0.212	0.663	58626

Table 6: Difference in resistance factors between perforated and non-perforated columns failing in modes L, LG, G, D, and L+LG+G+D by **DSM Method 1** – AS/NZS 4600 DSM

prediction method	Section shape	Failure mode														
		L			LG			G			D			All L, LG, G, D		
		P_m	V_p	ϕ	P_m	V_p	ϕ	P_m	V_p	ϕ	P_m	V_p	ϕ	P_m	V_p	ϕ
DSM Method 1	C	-4.4%	10.4%	-6.2%	-8.6%	45.1%	-11.7%	-15.3%	72.3%	-20.6%	-10.5%	24.9%	-18.6%	-8.1%	28.8%	-13.4%
	Z	-5.2%	25.8%	-7.8%	-8.3%	25.5%	-12.9%	-5.0%	126.7%	-6.8%	-15.3%	153.4%	-22.5%	-8.6%	48.5%	-13.3%
	Hat	-11.8%	105.4%	-16.2%	-14.1%	40.0%	-21.2%	-2.1%	346.2%	-3.8%	-23.0%	118.5%	-33.2%	-13.3%	63.5%	-20.2%
	Rack	-8.8%	27.4%	-10.8%	-26.7%	203.7%	-41.6%	-18.5%	555.6%	-29.5%	-18.9%	142.2%	-22.8%	-20.4%	171.6%	-32.1%
	Stiffened C	-9.6%	58.3%	-13.0%	-15.1%	305.9%	-22.1%	-12.1%	1600.0%	-16.6%	-18.3%	-7.4%	-15.3%	-12.7%	9.6%	-14.4%
	All sections	-6.2%	22.7%	-9.6%	-11.6%	71.0%	-19.0%	-9.7%	120.7%	-15.3%	-13.7%	36.0%	-22.9%	-9.8%	40.2%	-16.1%

Table 7: Difference in resistance factors between perforated and non-perforated columns failing in modes LD, DG, LDG, LD+DG+LDG, and all failure modes by **DSM Method 1** – AS/NZS 4600 DSM

prediction method	Section shape	Failure mode														
		LD			DG			LDG			All LD, DG, LDG			ALL Failure modes		
		P_m	V_p	ϕ	P_m	V_p	ϕ	P_m	V_p	ϕ	P_m	V_p	ϕ	P_m	V_p	ϕ
DSM Method 1	C	-14.1%	35.4%	-19.3%	-17.0%	20.8%	-21.5%	-12.9%	15.8%	-16.2%	-15.5%	22.1%	-20.4%	-10.8%	34.0%	-18.2%
	Z	-12.4%	120.0%	-18.2%	-10.2%	55.8%	-14.7%	-11.7%	29.8%	-16.2%	-11.8%	33.6%	-16.5%	-10.4%	43.6%	-15.6%
	Hat	-19.8%	147.9%	-29.5%	-20.6%	42.8%	-32.4%	-16.2%	51.2%	-27.6%	-19.2%	50.5%	-31.1%	-17.0%	58.9%	-28.0%
	Rack	-18.8%	44.3%	-21.0%	-17.7%	110.8%	-27.9%	-13.9%	-12.6%	-10.1%	-16.0%	18.8%	-19.7%	-18.6%	58.4%	-26.5%
	Stiffened C	-16.3%	-8.2%	-13.8%	-10.5%	3.9%	-12.4%	-12.3%	17.9%	-16.8%	-11.7%	6.7%	-14.4%	-12.6%	5.6%	-14.9%
	All sections	-13.7%	56.1%	-20.0%	-14.5%	28.0%	-22.1%	-12.7%	22.8%	-17.9%	-13.8%	26.8%	-20.2%	-12.1%	36.8%	-19.5%

Table 8: Resistance factors for all columns failing in modes L, LG, G, D, and L+LG+G+D by **DSM Method 1** – AS/NZS 4600 DSM

prediction method	Section shape	Failure mode																			
		L				LG				G				D				All L, LG, G, D			
		P_m	V_p	ϕ	n	P_m	V_p	ϕ	n	P_m	V_p	ϕ	n	P_m	V_p	ϕ	n	P_m	V_p	ϕ	n
DSM Method 1	C	1.061	0.149	0.836	6923	0.985	0.119	0.806	4245	0.872	0.144	0.691	1651	1.039	0.270	0.671	3678	1.018	0.187	0.758	16497
	Z	1.051	0.122	0.857	3712	0.968	0.182	0.727	1358	1.017	0.068	0.872	2548	0.877	0.148	0.692	2444	0.989	0.144	0.785	10062
	Hat	0.823	0.115	0.676	1414	0.902	0.203	0.656	494	1.071	0.057	0.924	137	0.791	0.202	0.575	441	0.847	0.170	0.648	2486
	Rack	0.952	0.107	0.789	461	0.804	0.247	0.542	1065	0.909	0.177	0.688	383	0.835	0.113	0.687	391	0.857	0.202	0.624	2300
	Stiffened C	0.931	0.114	0.765	317	0.919	0.138	0.734	143	0.967	0.102	0.805	196	0.997	0.254	0.663	245	0.955	0.172	0.728	901
	All sections	1.025	0.156	0.800	12827	0.949	0.170	0.726	7305	0.959	0.128	0.776	4915	0.956	0.252	0.638	7199	0.982	0.184	0.736	32246

Table 9: Resistance factors for all failing in modes LD, DG, LDG, LD+DG+LDG, and all failure modes by **DSM Method 1** – AS/NZS 4600 DSM

prediction method	Section shape	Failure mode																			
		LD				DG				LDG				All LD, DG, LDG				ALL Failure modes			
		P_m	V_p	ϕ	n	P_m	V_p	ϕ	n	P_m	V_p	ϕ	n	P_m	V_p	ϕ	n	P_m	V_p	ϕ	n
DSM Method 1	C	0.801	0.176	0.607	3157	0.767	0.210	0.551	2589	0.988	0.191	0.731	862	0.812	0.210	0.583	6608	0.959	0.216	0.682	23105
	Z	0.878	0.132	0.707	4115	0.958	0.134	0.769	2989	1.023	0.171	0.782	6057	0.963	0.167	0.740	13161	0.974	0.158	0.759	23223
	Hat	0.714	0.182	0.536	585	0.714	0.297	0.438	1927	0.794	0.256	0.526	964	0.737	0.273	0.473	3476	0.782	0.240	0.534	5962
	Rack	0.734	0.106	0.609	137	0.824	0.196	0.606	832	0.826	0.189	0.614	900	0.819	0.191	0.607	1869	0.840	0.199	0.615	4169
	Stiffened C	0.715	0.203	0.520	245	0.726	0.296	0.446	1727	0.804	0.217	0.571	800	0.748	0.270	0.483	2772	0.798	0.267	0.519	3673
	All sections	0.830	0.167	0.637	8239	0.811	0.247	0.547	10064	0.960	0.210	0.690	9583	0.868	0.227	0.606	27886	0.929	0.212	0.666	60132
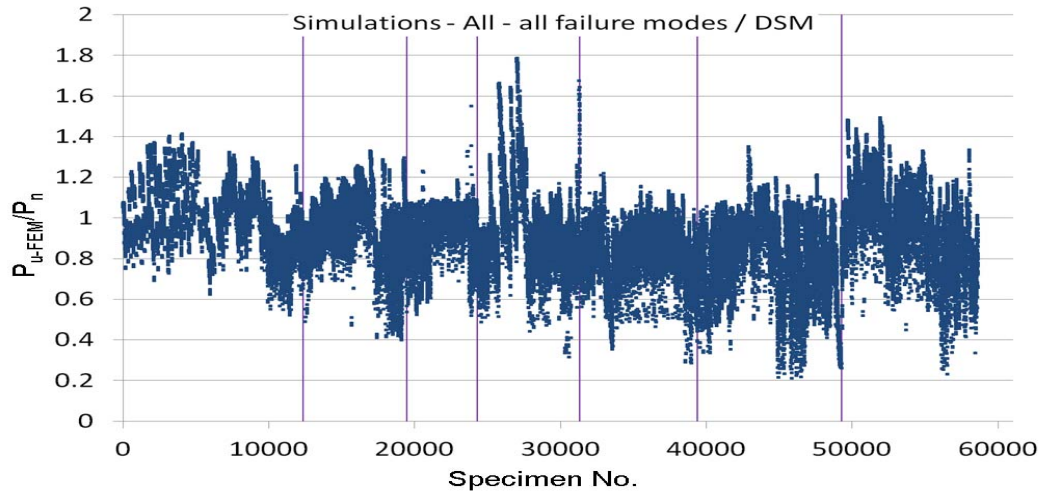
Fig. 3: Simulation-to-predicted ratios for all perforated columns by DSM Method 1 with classified failure modes (from left to right: L, LG, G, D, LD, DG, and LDG)
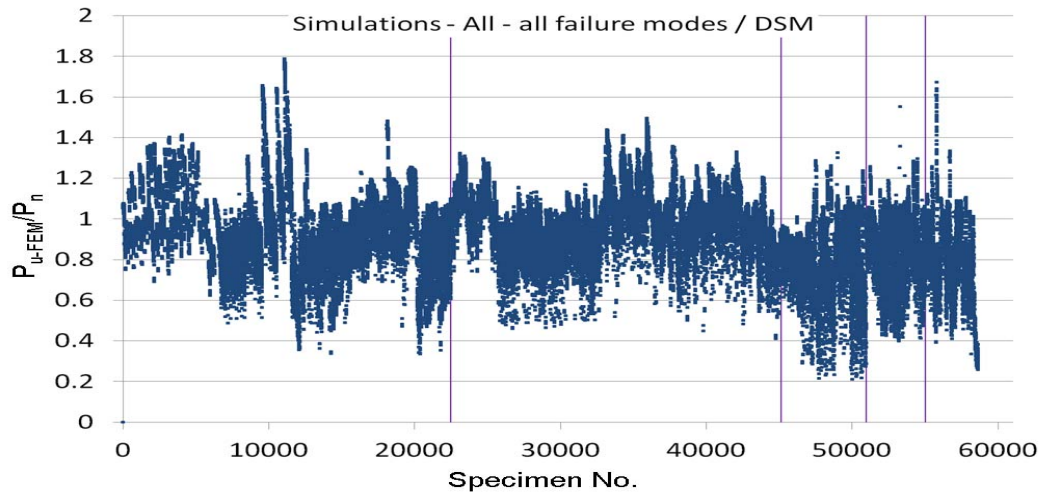
Fig. 4: Simulation-to-predicted ratios for all perforated columns by DSM Method 1 with classified section types (from left to right: C, Z, Hat, Rack and Stiffened C)

2.2. Design strength based on AS/NZS 4600 DSM and interaction with D mode

The discussions presented in Section 2.1 demonstrate that when the current DSM was used for strength prediction, the discrepancy mainly stemmed from two sources, one was the existence of perforations, while more fundamentally, the other was the interaction of buckling modes. It has been shown that the current DSM generally performed poorly against the failure modes (i.e. LD, DG, LDG) that are not covered by it, or more typically, the failure modes involving distortional buckling.

Previous research on the design against interactive buckling has been presented in detail in Section 1.4.3 of (Yao 2013). In short, LG interaction has been extensively studied and its influence is widely recognised, and as a consequence, it has been considered in the current DSM equations. In contrast, other interactive buckling phenomena (i.e. LD, DG, LDG) are less understood. Of them, LD interaction has received a considerable amount of attention, but the literature regarding DG and LDG interaction is not adequate. The design approaches based on the DSM which considered LD and DG interaction were first explored by Schafer (2002) when the current codified DSM was under development. However, LD and DG interaction were not included in the current DSM equations mainly due to the lack of experimental and numerical evidence to prove their adverse effects and also the poor performance found with the formulation considering LD interaction. This DSM-based design approach to account for LD interaction has since been evaluated by several researchers (Yang and Hancock 2004; Kwon, Kim et al. 2009; Yap and Hancock 2011; Silvestre, Camotim et al. 2012), and proved necessary for safely predicting the strength of columns subject to LD interaction. The approach was either to replace P_{ne} by P_{nd} in Equations (3)-(4) or to replace P_y by P_{nl} (which was based on P_y in lieu of P_{ne}) in Equations (5) and (6). The former was adopted most often, and given by the expressions:

$$\text{For } \lambda_{ld} \leq 0.776, \quad P_{nld} = P_{nd} \tag{7}$$

$$\text{For } \lambda_{ld} > 0.776, \quad P_{nld} = \left[1 - 0.15\left(\frac{P_{cr\text{-}l\text{-}nh}}{P_{nd}}\right)^{0.4}\right]\left(\frac{P_{cr\text{-}l\text{-}nh}}{P_{nd}}\right)^{0.4} P_{nd} \tag{8}$$

where $\lambda_{ld} = \sqrt{P_{nd} / P_{cr\text{-}l\text{-}nh}}$. In addition, the DG interaction equation proposed by Schafer (2002) was also assessed in the works by Yang and Hancock (2004), Rossi et al. (2010), Yap and Hancock (2011), Casafont (2011) and Silvestre et al. (2012) and shown to substantially improve the strength prediction for columns affected by strong DG interaction. This DSM-based DG approach was given by

$$\text{For } \lambda_{dc} \leq 0.561, \quad P_{nde} = P_{ne} \tag{9}$$

$$\text{For } \lambda_{dc} > 0.561, \quad P_{nde} = \left[1 - 0.25\left(\frac{P_{cr\text{-}d\text{-}nh}}{P_{ne}}\right)^{0.6}\right]\left(\frac{P_{cr\text{-}d\text{-}nh}}{P_{ne}}\right)^{0.6} P_{ne} \tag{10}$$

where $\lambda_{dc} = \sqrt{P_{ne}/P_{cr\text{-}d\text{-}nh}}$. Furthermore, a DSM-based approach to account for LDG interaction was first explored by Yap and Hancock (2011) and then by Silvestre et al. (2012), whose expressions were as follows:

$$\text{For } \lambda_{ldc} \leq 0.776, \quad P_{nlde} = P_{nde} \tag{11}$$

$$\text{For } \lambda_{ldc} > 0.776, \quad P_{nlde} = \left[1 - 0.15\left(\frac{P_{cr\text{-}l\text{-}nh}}{P_{nde}}\right)^{0.4}\right]\left(\frac{P_{cr\text{-}l\text{-}nh}}{P_{nde}}\right)^{0.4} P_{nde} \tag{12}$$

where $\lambda_{\mathrm{ldc}} = \sqrt{P_{\mathrm{nde}} / P_{\mathrm{cr-l-nh}}}$. Compared to the predictions obtained by the LD or DG approaches, the results produced by this LDG approach typically featured an increased mean and a significantly larger scatter.

The following sections describe the performance of three DSM-based methods considering different combinations of interactions. Non-perforated columns were first used in the assessment of these methods, followed by applying the best-performing option to all (non-perforated plus perforated) columns.

2.2.1. Method 2 – LG and DG interactions – non-perforated

Table 10 and Table 11 list the statistics of the predictions for non-perforated columns using DSM Method 2, i.e. minimum of the LG interaction Equations (3)-(4) and the DG interaction Equations (9)-(10). Meanwhile, Table 12 and Table 13 present the percentage differences of the statistics between DSM Method 2 and DSM Method 1 (the current DSM that considers only LG interaction).

Overall, DSM Method 2 improved the overall resistance factor ϕ of the predictions from 0.824 to 0.851 which satisfied the prescribed value of 0.85 as in the code. This improvement mainly came from the DG and LDG modes and the results regarding the other modes were barely influenced. In particular, the value of ϕ was improved from 0.698 to 0.795 (i.e. 13.9% increase although it was still lower than 0.85) for DG mode, and from 0.838 to 0.921 for LDG mode (i.e. 9.9% increase). The section that benefited most from the inclusion of DG interaction was Stiffened C section (which showed in the combined LD, DG and LDG statistics a 13.9% increase in P_{m} and 20.2% decrease in V_{p}, resulting in a 24.3% increase in ϕ), followed by Hat and Rack sections (13.0% increases in ϕ) with only slightly beneficial influence on C and Z sections (1.6% and 3.4% increase in ϕ respectively). These results agreed with the fact that Stiffened C, Hat and Rack sections were susceptible to DG interaction and a large number of columns failed in this mode. Therefore, including DG interaction in the current DSM is warranted because it can decrease the variations and increase the resistance factors for almost all sections (expect for a slightly adverse effect on the LG and LDG modes for C section columns).

The simulation-to-predicted ratios ($P_{\mathrm{u\text{-}FEM}}/P_{\mathrm{n}}$) are also provided in Fig. 5 and Fig. 6 for all non-perforated columns classified by failure mode and section type respectively. More detailed figures regarding each section type can be found in Section B.1. It is seen that including DG interaction in the prediction did not eliminate all the over-predictions. A close examination showed that substantial over-predictions mainly came from three sources, one from severe LD interaction represented by sections such as C60, SC7, SC8 and SC9, another one from severe DG interaction involving moderate to long-length columns made from sections such as C65, H1, H8, H21, SC5, and SC10 and the third one from severe LDG interaction occurring in moderate-length members made from H1 and R9. Those sections mentioned in the last two items featured either wide flanges (H1, H8, H21, and R9) or very small lips hence very high distortional slenderness (C65, SC5 and SC10). The over-predictions for these sections demonstrate that the inclusion of DG interaction in the strength prediction was not adequate to reliably predict the strength erosion for such sections subject to severe interaction with distortional buckling.

Table 10: Resistance factors for non-perforated columns failing in modes L, LG, G, D, and L+LG+G+D by **DSM Method 2** – minimum of LG and DG interaction equations based on AS/NZS 4600 DSM

prediction method	Section shape	Failure mode																			
		L				LG				G				D				All L, LG, G, D			
		P_m	V_p	ϕ	n	P_m	V_p	ϕ	n	P_m	V_p	ϕ	n	P_m	V_p	ϕ	n	P_m	V_p	ϕ	n
DSM Method 2	C	1.108	0.135	0.889	292	1.106	0.115	0.908	94	1.025	0.083	0.869	34	1.159	0.217	0.822	80	1.110	0.149	0.874	500
	Z	1.107	0.097	0.927	147	1.053	0.145	0.834	28	1.071	0.030	0.935	52	1.032	0.058	0.890	50	1.081	0.093	0.908	277
	Hat	0.930	0.056	0.803	42	1.059	0.148	0.835	13	1.093	0.013	0.959	3	1.021	0.092	0.859	9	0.975	0.107	0.807	67
	Rack	1.042	0.084	0.882	11	1.142	0.073	0.975	22	1.110	0.027	0.971	8	1.025	0.045	0.890	8	1.095	0.080	0.931	49
	Stiffened C	1.026	0.072	0.877	10	1.127	0.036	0.983	3	1.097	0.006	0.963	4	1.215	0.272	0.782	5	1.096	0.156	0.855	22
	All sections	1.090	0.128	0.882	502	1.098	0.119	0.898	160	1.060	0.058	0.915	101	1.104	0.186	0.824	152	1.090	0.133	0.877	915

Table 11: Resistance factors for non-perforated columns failing in modes LD, DG, LDG, LD+DG+LDG, and all failure modes by **DSM Method 2** – minimum of LG and DG interaction equations based on AS/NZS 4600 DSM

prediction method	Section shape	Failure mode																			
		LD				DG				LDG				All LD, DG, LDG				ALL Failure modes			
		P_m	V_p	ϕ	n	P_m	V_p	ϕ	n	P_m	V_p	ϕ	n	P_m	V_p	ϕ	n	P_m	V_p	ϕ	n
DSM Method 2	C	0.929	0.130	0.750	65	0.953	0.126	0.773	54	1.198	0.207	0.865	22	0.980	0.178	0.742	141	1.081	0.163	0.836	641
	Z	1.000	0.060	0.862	84	1.095	0.078	0.931	62	1.195	0.101	0.997	134	1.115	0.116	0.914	280	1.098	0.107	0.910	557
	Hat	0.886	0.073	0.757	12	0.981	0.144	0.778	41	1.000	0.150	0.787	21	0.971	0.143	0.771	74	0.973	0.126	0.789	141
	Rack	0.900	0.070	0.771	3	1.054	0.061	0.908	17	1.071	0.161	0.830	18	1.050	0.127	0.851	38	1.076	0.103	0.894	87
	Stiffened C	0.851	0.219	0.602	5	0.931	0.221	0.657	36	1.056	0.125	0.858	17	0.961	0.202	0.700	58	0.998	0.197	0.733	80
	All sections	0.958	0.107	0.794	169	1.005	0.145	0.795	210	1.155	0.140	0.921	212	1.045	0.157	0.815	591	1.073	0.144	0.851	1506

Table 12: Difference in resistance factors between **DSM Method 2** and **DSM Method 1** for non-perforated columns failing in modes L, LG, G, D, and L+LG+G+D

prediction method	Section shape	Failure mode												All L, LG, G, D		
		L			LG			G			D					
		P_m	V_p	ϕ	P_m	V_p	ϕ	P_m	V_p	ϕ	P_m	V_p	ϕ	P_m	V_p	ϕ
DSM Method 2	C	0.0%	0.0%	0.0%	2.9%	40.2%	-0.3%	0.0%	0.0%	0.0%	0.0%	0.0%	0.0%	0.5%	2.1%	0.1%
	Z	0.0%	0.0%	0.0%	0.0%	0.0%	0.0%	0.1%	0.0%	0.0%	0.0%	0.0%	0.0%	0.2%	-4.1%	0.7%
	Hat	0.0%	0.0%	0.0%	1.2%	2.1%	0.7%	0.0%	0.0%	0.0%	0.0%	0.0%	0.0%	0.3%	2.9%	-0.1%
	Rack	0.0%	0.0%	0.0%	5.0%	-9.9%	5.6%	0.0%	0.0%	0.0%	0.0%	0.0%	0.0%	2.2%	8.1%	1.9%
	Stiffened C	0.0%	0.0%	0.0%	4.5%	5.9%	4.6%	0.0%	0.0%	0.0%	0.0%	0.0%	0.0%	0.6%	0.0%	0.7%
	All sections	0.0%	0.0%	0.0%	2.6%	19.0%	0.6%	0.0%	0.0%	0.1%	0.0%	0.0%	0.0%	0.5%	0.8%	0.3%

Table 13: Difference in resistance factors between **DSM Method 2** and **DSM Method 1** for non-perforated columns failing in modes LD, DG, LDG, LD+DG+LDG, and all failure modes

prediction method	Section shape	Failure mode									All LD, DG, LDG			ALL Failure modes		
		LD			DG			LDG								
		P_m	V_p	ϕ	P_m	V_p	ϕ	P_m	V_p	ϕ	P_m	V_p	ϕ	P_m	V_p	ϕ
DSM Method 2	C	0.0%	0.0%	0.0%	3.6%	-27.2%	10.3%	6.0%	25.5%	-0.6%	2.4%	3.5%	1.6%	0.8%	0.6%	0.7%
	Z	0.0%	0.0%	0.0%	2.8%	-9.3%	3.4%	3.5%	-22.9%	7.1%	2.4%	-7.2%	3.4%	1.2%	-2.7%	1.6%
	Hat	0.0%	0.0%	0.0%	9.7%	-30.8%	20.6%	5.9%	-11.8%	9.0%	7.1%	-21.4%	13.0%	3.7%	-16.6%	7.1%
	Rack	0.0%	0.0%	0.0%	5.8%	-34.4%	8.6%	11.9%	-24.8%	21.5%	8.2%	-20.6%	13.0%	4.8%	-17.6%	7.2%
	Stiffened C	0.0%	0.0%	0.0%	15.1%	-22.5%	29.3%	15.4%	-32.1%	25.3%	13.9%	-20.2%	24.3%	9.5%	-21.8%	20.4%
	All sections	0.0%	0.0%	0.0%	6.3%	-24.9%	13.9%	5.4%	-18.1%	9.9%	4.2%	-12.3%	7.7%	1.9%	-7.1%	3.3%
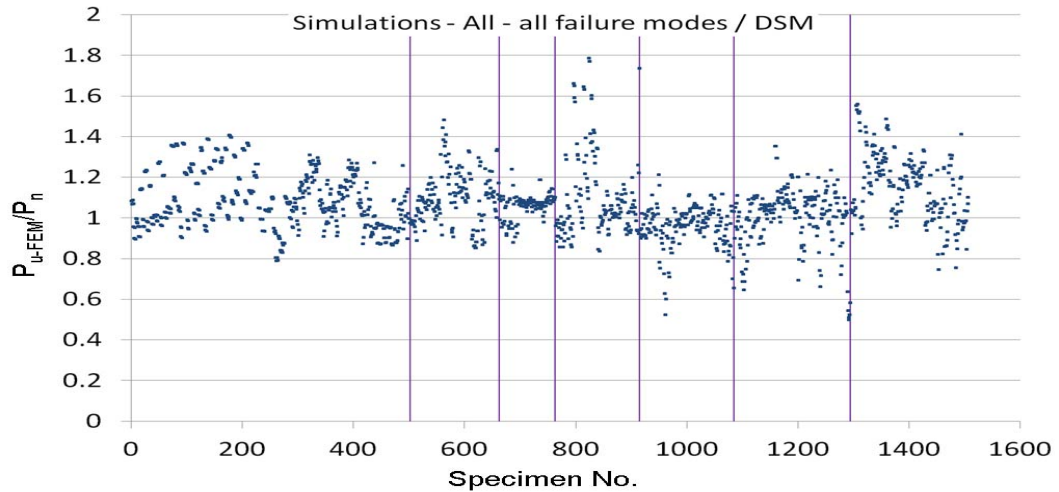
Fig. 5: Simulation-to-predicted ratios for all non-perforated columns by DSM Method 2 with classified failure modes (from left to right: L, LG, G, D, LD, DG, and LDG)
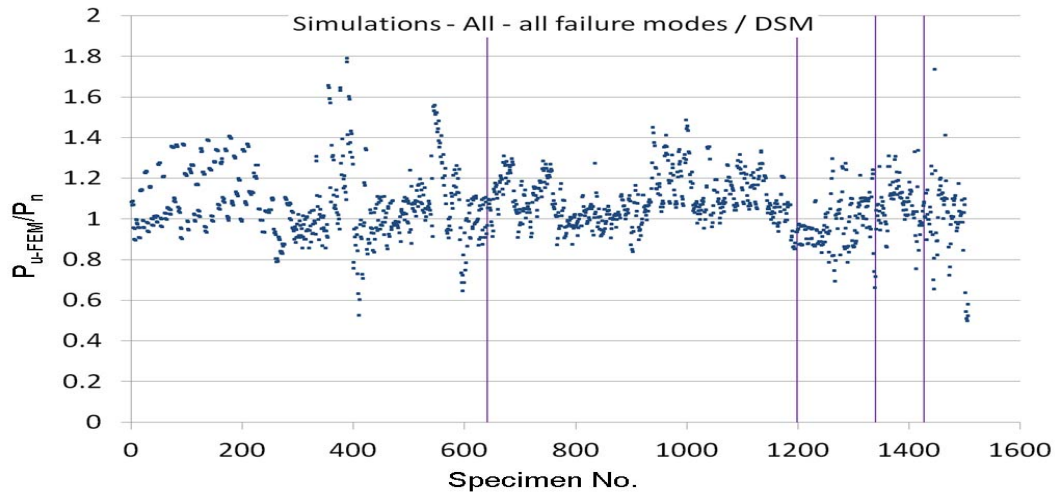
Fig. 6: Simulation-to-predicted ratios for all non-perforated columns by DSM Method 2 with classified section types (from left to right: C, Z, Hat, Rack and Stiffened C)

2.2.2. Method 3 – LG, DG and LD interactions – non-perforated

Table 14 and Table 15 present the statistics of the predictions for non-perforated columns using DSM Method 3, i.e. minimum of the LG interaction Equations (3)-(4), the DG interaction Equations (9)-(10), and the LD interaction Equations (7)-(8). The percentage differences of the statistics between DSM Method 3 and DSM Method 1 (i.e. the current DSM) are also given in Table 16 and Table 17.

The results show that DSM Method 3 in general performed poorly. Compared with the current DSM, although it raised the overall P_m value from 1.053 to 1.235, it resulted in a much larger scatter as shown by the overall V_p value increasing from 0.155 to 0.284, hence producing a lower overall resistance factor ϕ of 0.776 compared to 0.824. Also, in contrast to DSM Method 2 which did not change the statistics for the modes (i.e.

L, LG, G and D) that were covered by the current DSM, DSM Method 3 significantly worsened the prediction as indicated by the values of ϕ decreasing from 0.877 to 0.751. However, the inclusion of LD interaction in the strength prediction was indeed most beneficial to the LD mode, as shown by the considerable 61.3% and 40.3% increases in the values of P_m and ϕ respectively, although accompanied by a massive 94.4% increase in the value of V_p. It is also interesting to note that Stiffened C section columns failing in the LD mode benefited most as the V_p value for this section was reduced by 72.1%, contrary to the other sections which all showed an increase in their V_p values.

The simulation-to-predicted ratios ($P_{u\text{-FEM}}/P_n$) are provided in Fig. 7 and Fig. 8 for all non-perforated columns classified by failure mode and section type respectively. More detailed figures for each section type can be found in Section C.1. The results show that compared to DSM Method 1 and DSM Method 2, DSM Method 3 safely predicts the strength for the vast majority of members, despite the large scatter in the values of $P_{u\text{-FEM}}/P_n$ and that the predicted strengths of some columns could be as low as one third of the "actual" strengths. Besides, those column strengths that were significantly over-predicted came from sections C65, H1, H21, SC5, and SC10 which failed in DG interaction, and section R9 failing in LDG interaction.

Table 14: Resistance factors for non-perforated columns failing in modes L, LG, G, D, and L+LG+G+D by **DSM Method 3** – minimum of LG, DG, and LD interaction equations based on AS/NZS 4600 DSM

prediction method	Section shape	Failure mode																		
		L				LG				G				D				All L, LG, G, D			
		P_m	V_p	ϕ	n	P_m	V_p	ϕ	n	P_m	V_p	ϕ	n	P_m	V_p	ϕ	n	P_m	V_p	ϕ	n
DSM Method 3	C	1.108	0.135	0.889	292	1.297	0.272	0.834	94	1.025	0.083	0.869	34	1.658	0.424	0.780	80	1.226	0.323	0.714	500
	Z	1.126	0.122	0.917	147	1.053	0.145	0.834	28	1.071	0.030	0.935	52	1.252	0.204	0.908	50	1.131	0.148	0.892	277
	Hat	0.930	0.056	0.803	42	1.422	0.306	0.857	13	1.093	0.013	0.959	3	1.029	0.096	0.862	9	1.046	0.260	0.689	67
	Rack	1.042	0.084	0.882	11	1.190	0.182	0.894	22	1.110	0.027	0.971	8	1.066	0.079	0.906	8	1.124	0.148	0.887	49
	Stiffened C	1.026	0.072	0.877	10	1.766	0.102	1.470	3	1.097	0.006	0.963	4	1.292	0.307	0.776	5	1.200	0.263	0.785	22
	All sections	1.095	0.135	0.879	502	1.258	0.268	0.816	160	1.060	0.058	0.915	101	1.444	0.403	0.710	152	1.178	0.277	0.751	915

Table 15: Resistance factors for non-perforated columns failing in modes LD, DG, LDG, LD+DG+LDG, and all failure modes by **DSM Method 3** – minimum of LG, DG, and LD interaction equations based on AS/NZS 4600 DSM

prediction method	Section shape	Failure mode																		
		LD				DG				LDG				All LD, DG, LDG				ALL Failure modes			
		P_m	V_p	ϕ	n	P_m	V_p	ϕ	n	P_m	V_p	ϕ	n	P_m	V_p	ϕ	n	P_m	V_p	ϕ	n
DSM Method 3	C	1.580	0.260	1.040	65	0.964	0.124	0.783	54	1.939	0.257	1.284	22	1.400	0.360	0.756	141	1.264	0.338	0.714	641
	Z	1.584	0.149	1.249	84	1.095	0.079	0.931	62	1.462	0.186	1.091	134	1.417	0.207	1.024	280	1.275	0.218	0.903	557
	Hat	1.270	0.092	1.067	12	1.019	0.121	0.832	41	1.260	0.263	0.824	21	1.128	0.209	0.813	74	1.089	0.235	0.750	141
	Rack	1.357	0.113	1.117	3	1.103	0.208	0.796	17	1.175	0.177	0.889	18	1.157	0.191	0.858	38	1.138	0.168	0.874	87
	Stiffened C	1.220	0.061	1.050	5	0.946	0.236	0.651	36	1.174	0.176	0.891	17	1.037	0.229	0.721	58	1.082	0.249	0.726	80
	All sections	1.545	0.208	1.114	169	1.022	0.155	0.799	210	1.444	0.249	0.969	212	1.323	0.279	0.840	591	1.235	0.284	0.776	1506

Table 16: Difference in resistance factors between **DSM Method 3** and **DSM Method 1** for non-perforated columns failing in modes L, LG, G, D, and L+LG+G+D

prediction method	Section shape	Failure mode													
		L			LG			G			D			All L, LG, G, D		
		P_m	V_p	ϕ	P_m	V_p	ϕ	P_m	V_p	ϕ	P_m	V_p	ϕ	P_m	V_p	ϕ
DSM Method 3	C	0.0%	0.0%	0.0%	20.7%	231.7%	-8.5%	0.0%	0.0%	0.0%	43.1%	95.4%	-5.1%	11.1%	121.2%	-18.2%
	Z	1.7%	25.8%	-1.1%	0.0%	0.0%	0.0%	0.1%	0.0%	0.0%	21.3%	251.7%	2.0%	4.8%	52.6%	-1.1%
	Hat	0.0%	0.0%	0.0%	35.9%	111.0%	3.4%	0.0%	0.0%	0.0%	0.8%	4.3%	0.3%	7.6%	150.0%	-14.7%
	Rack	0.0%	0.0%	0.0%	9.4%	124.7%	-3.1%	0.0%	0.0%	0.0%	4.0%	75.6%	1.8%	4.9%	100.0%	-3.0%
	Stiffened C	0.0%	0.0%	0.0%	63.8%	200.0%	56.4%	0.0%	0.0%	0.0%	6.3%	12.9%	-0.8%	10.2%	68.6%	-7.5%
	All sections	0.5%	5.5%	-0.3%	17.6%	168.0%	-8.6%	0.0%	0.0%	0.1%	30.8%	116.7%	-13.8%	8.6%	109.8%	-14.1%

Table 17: Difference in resistance factors between **DSM Method 3** and **DSM Method 1** for non-perforated columns failing in modes LD, DG, LDG, LD+DG+LDG,

and all failure modes

	prediction method	Section shape	Failure mode													
		LD			DG			LDG			All LD, DG, LDG			ALL Failure modes		
		P_m	V_p	ϕ	P_m	V_p	ϕ	P_m	V_p	ϕ	P_m	V_p	ϕ	P_m	V_p	ϕ
DSM Method 3	C	70.1%	100.0%	38.7%	4.8%	-28.3%	11.7%	71.6%	55.8%	47.6%	46.3%	109.3%	3.6%	17.9%	108.6%	-14.0%
	Z	58.4%	148.3%	44.9%	2.8%	-8.1%	3.4%	26.6%	42.0%	17.2%	30.1%	65.6%	15.8%	17.5%	98.2%	0.8%
	Hat	43.3%	26.0%	41.0%	14.0%	-41.8%	29.0%	33.5%	54.7%	14.1%	24.4%	14.8%	19.2%	16.1%	55.6%	1.8%
	Rack	50.8%	61.4%	44.9%	10.7%	123.7%	-4.8%	22.8%	-17.3%	30.2%	19.3%	19.4%	13.9%	10.8%	34.4%	4.8%
	Stiffened C	43.4%	-72.1%	74.4%	16.9%	-17.2%	28.1%	28.3%	-4.3%	30.1%	22.9%	-9.5%	28.1%	18.8%	-1.2%	19.2%
	All sections	61.3%	94.4%	40.3%	8.1%	-19.7%	14.5%	31.8%	45.6%	15.6%	31.9%	55.9%	11.0%	17.3%	83.2%	-5.8%
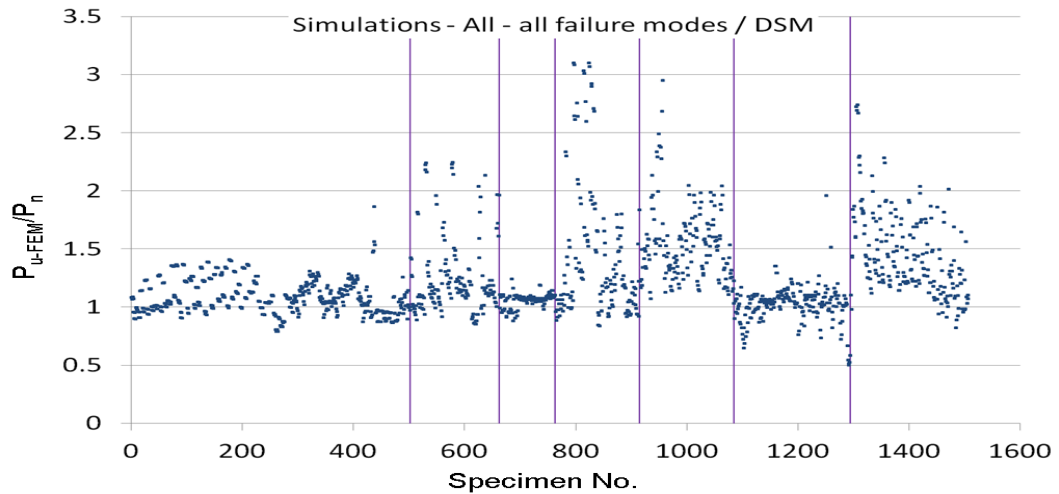
Fig. 7: Simulation-to-predicted ratios for all non-perforated columns by DSM Method 3 with classified failure modes (from left to right: L, LG, G, D, LD, DG, and LDG)
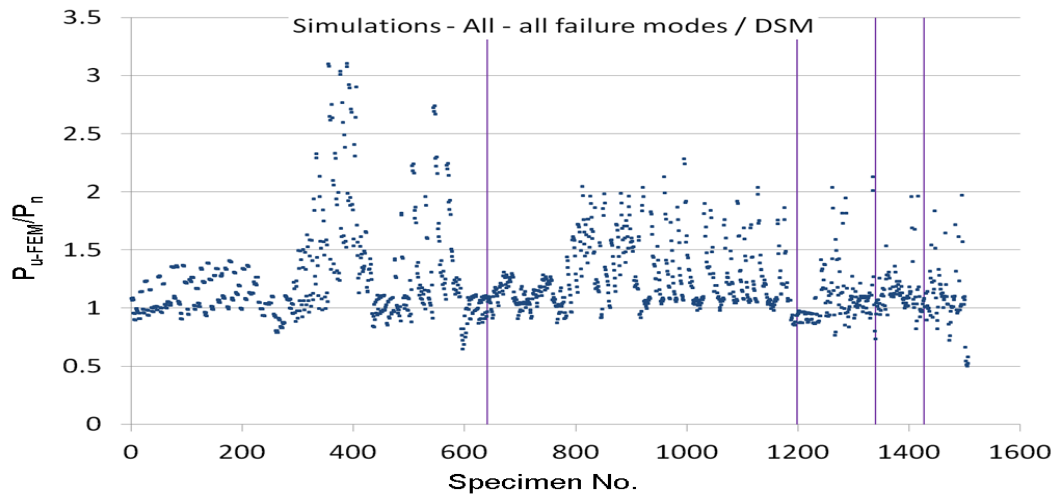

Fig. 8: Simulation-to-predicted ratios for all non-perforated columns by DSM Method 3 with classified section types (from left to right: C, Z, Hat, Rack and Stiffened C)

2.2.3. Method 4 – LDG interaction – non-perforated

Table 18 and Table 19 present the statistics of the predictions for non-perforated columns using DSM Method 4, i.e. LDG interaction Equations (11)-(12). The percentage differences of the statistics between DSM Method 4 and DSM Method 1 (the AS/NZS 4600 DSM) are also given in Table 20 and Table 21. As section Z71 did not have lips, its distortional buckling mode was non-existent, and thus it was not included in the prediction.

DSM Method 4 in general performed similarly to DSM Method 3, which was unsatisfactory. Compared with DSM Method1, although it increased the overall P_m value from 1.053 to 1.289, it almost doubled the variation of the predictions and resulted in a decreased ϕ value of 0.793 compared with 0.824. In particular,

although DSM Method 4 decreased the overall ϕ value for the L and D modes, it increased the overall ϕ value for the LG, LD, DG and LDG modes. Of all the modes, those that benefited most from the LDG interaction method were the LD and LDG modes which showed increases of about 40% in the values of ϕ, while the worst performing mode was the D mode with a 13.8 % decrease in the value of ϕ. On the other hand, the best and worst performing sections were Stiffened C and C sections respectively.

Fig. 9-Fig. 10 illustrate the simulation-to-predicted ratios ($P_{\text{u-FEM}}/P_{\text{n}}$) for all non-perforated columns classified by failure mode and section type respectively. More detailed figures for each section type can be found in Section D.1 . Compared with Fig. 7 and Fig. 8 for DSM Method 3, the distribution of the predictions shown in Fig. 9-Fig. 10 was very similar, though with safer predictions for some members failing in the DG mode and overly safe predictions for the LG and LDG modes. Significant over-predictions still existed and were mostly associated with sections S65, SC5 and SC10 failing in DG interaction. These sections featured very small lips hence much higher distortional slenderness than local slenderness.

Table 18: Resistance factors for non-perforated columns failing in modes L, LG, G, D, and L+LG+G+D by **DSM Method 4** – LDG interaction equation based on AS/NZS 4600 DSM

prediction method	Section shape	Failure mode																		
		L				LG				G				D				All L, LG, G, D			
		P_m	V_p	ϕ	n	P_m	V_p	ϕ	n	P_m	V_p	ϕ	n	P_m	V_p	ϕ	n	P_m	V_p	ϕ	n
DSM Method 4	C	1.108	0.135	0.889	292	1.562	0.248	1.050	94	1.026	0.083	0.869	34	1.658	0.424	0.780	80	1.276	0.332	0.730	500
	Z	1.126	0.122	0.917	147	1.239	0.110	1.023	16	1.074	0.043	0.934	52	1.252	0.204	0.908	50	1.146	0.146	0.907	265
	Hat	0.930	0.056	0.803	42	1.455	0.289	0.906	13	1.093	0.013	0.959	3	1.029	0.096	0.862	9	1.052	0.263	0.689	67
	Rack	1.042	0.084	0.882	11	1.215	0.178	0.919	22	1.110	0.027	0.971	8	1.066	0.079	0.906	8	1.135	0.150	0.893	49
	Stiffened C	1.026	0.072	0.877	10	1.818	0.100	1.517	3	1.097	0.006	0.963	4	1.292	0.307	0.776	5	1.207	0.273	0.776	22
	All sections	1.095	0.135	0.879	502	1.471	0.256	0.975	148	1.062	0.062	0.914	101	1.444	0.403	0.710	152	1.212	0.289	0.755	903

Table 19: Resistance factors for non-perforated columns failing in modes LD, DG, LDG, LD+DG+LDG, and all failure modes by **DSM Method 4** – LDG interaction equation based on AS/NZS 4600 DSM

prediction method	Section shape	Failure mode																		
		LD				DG				LDG				All LD, DG, LDG				ALL Failure modes			
		P_m	V_p	ϕ	n	P_m	V_p	ϕ	n	P_m	V_p	ϕ	n	P_m	V_p	ϕ	n	P_m	V_p	ϕ	n
DSM Method 4	C	1.580	0.260	1.040	65	0.974	0.112	0.802	54	2.147	0.235	1.477	22	1.436	0.376	0.750	141	1.311	0.348	0.726	641
	Z	1.584	0.149	1.249	84	1.134	0.132	0.913	62	1.690	0.143	1.343	134	1.535	0.203	1.116	280	1.346	0.236	0.925	545
	Hat	1.270	0.092	1.067	12	1.092	0.088	0.922	41	1.384	0.223	0.973	21	1.204	0.186	0.899	74	1.132	0.230	0.786	141
	Rack	1.357	0.113	1.117	3	1.112	0.213	0.795	17	1.283	0.164	0.990	18	1.213	0.193	0.896	38	1.169	0.174	0.890	87
	Stiffened C	1.220	0.061	1.050	5	0.969	0.241	0.660	36	1.380	0.130	1.115	17	1.111	0.252	0.742	58	1.137	0.260	0.749	80
	All sections	1.545	0.208	1.114	169	1.054	0.164	0.813	210	1.648	0.217	1.170	212	1.408	0.281	0.890	591	1.289	0.295	0.793	1494

Table 20: Difference in resistance factors between **DSM Method 4** and **DSM Method 1** for non-perforated columns failing in modes L, LG, G, D, and L+LG+G+D

prediction method	Section shape	Failure mode														
		L			LG			G			D			All L, LG, G, D		
		P_m	V_p	ϕ	P_m	V_p	ϕ	P_m	V_p	ϕ	P_m	V_p	ϕ	P_m	V_p	ϕ
DSM Method 4	C	0.0%	0.0%	0.0%	45.3%	202.4%	15.3%	0.1%	0.0%	0.0%	43.1%	95.4%	-5.1%	15.6%	127.4%	-16.4%
	Z	1.7%	25.8%	-1.1%	17.7%	-24.1%	22.7%	0.4%	43.3%	-0.1%	21.3%	251.7%	2.0%	6.2%	50.5%	0.6%
	Hat	0.0%	0.0%	0.0%	39.1%	99.3%	9.3%	0.0%	0.0%	0.0%	0.8%	4.3%	0.3%	8.2%	152.9%	-14.7%
	Rack	0.0%	0.0%	0.0%	11.7%	119.8%	-0.4%	0.0%	0.0%	0.0%	4.0%	75.6%	1.8%	6.0%	102.7%	-2.3%
	Stiffened C	0.0%	0.0%	0.0%	68.6%	194.1%	61.4%	0.0%	0.0%	0.0%	6.3%	12.9%	-0.8%	10.8%	75.0%	-8.6%
	All sections	0.5%	5.5%	-0.3%	37.5%	156.0%	9.2%	0.2%	6.9%	0.0%	30.8%	116.7%	-13.8%	11.7%	118.9%	-13.6%

Table 21: Difference in resistance factors between **DSM Method 4** and **DSM Method 1** for non-perforated columns failing in modes LD, DG, LDG, LD+DG+LDG, and all failure modes

| prediction method | Section shape | Failure mode | | | | | | | | | | | | | | |
|---|---|---|---|---|---|---|---|---|---|---|---|---|---|---|---|
| | | LD | | | DG | | | LDG | | | All LD, DG, LDG | | | ALL Failure modes | | |
| | | P_m | V_p | ϕ | P_m | V_p | ϕ | P_m | V_p | ϕ | P_m | V_p | ϕ | P_m | V_p | ϕ |
| DSM Method 4 | C | 70.1% | 100.0% | 38.7% | 5.9% | -35.3% | 14.4% | 90.0% | 42.4% | 69.8% | 50.1% | 118.6% | 2.7% | 22.3% | 114.8% | -12.5% |
| | Z | 58.4% | 148.3% | 44.9% | 6.5% | 53.5% | 1.4% | 46.3% | 9.2% | 44.3% | 41.0% | 62.4% | 26.2% | 24.1% | 114.5% | 3.2% |
| | Hat | 43.3% | 26.0% | 41.0% | 22.1% | -57.7% | 42.9% | 46.6% | 31.2% | 34.8% | 32.7% | 2.2% | 31.8% | 20.7% | 52.3% | 6.6% |
| | Rack | 50.8% | 61.4% | 44.9% | 11.6% | 129.0% | -4.9% | 34.1% | -23.4% | 44.9% | 25.1% | 20.6% | 19.0% | 13.8% | 39.2% | 6.7% |
| | Stiffened C | 43.4% | -72.1% | 74.4% | 19.8% | -15.4% | 29.9% | 50.8% | -29.3% | 62.8% | 31.6% | -0.4% | 31.8% | 24.8% | 3.2% | 23.0% |
| | All sections | 61.3% | 94.4% | 40.3% | 11.5% | -15.0% | 16.5% | 50.4% | 26.9% | 39.6% | 40.4% | 57.0% | 17.6% | 22.4% | 90.3% | -3.8% |
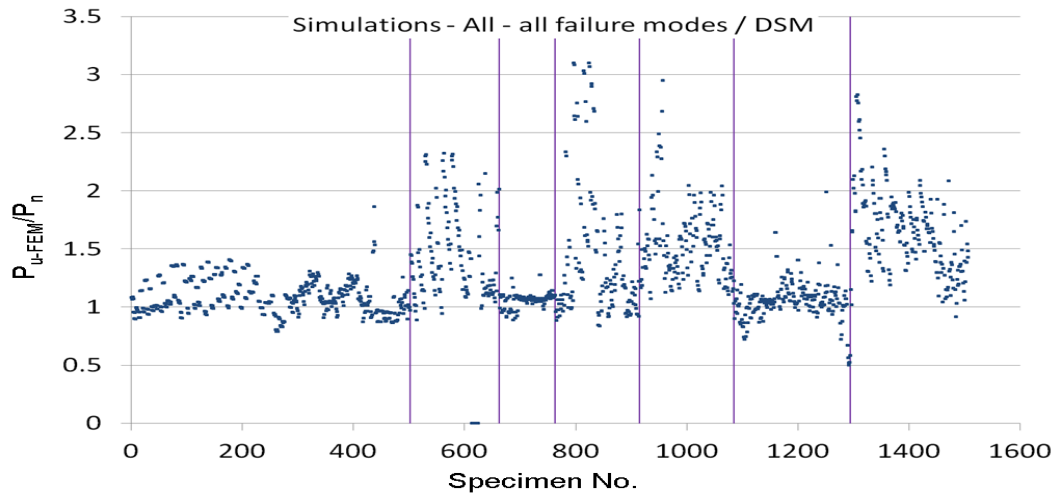
Fig. 9: Simulation-to-predicted ratios for all non-perforated columns by DSM Method 4 with classified failure modes (from left to right: L, LG, G, D, LD, DG, and LDG)
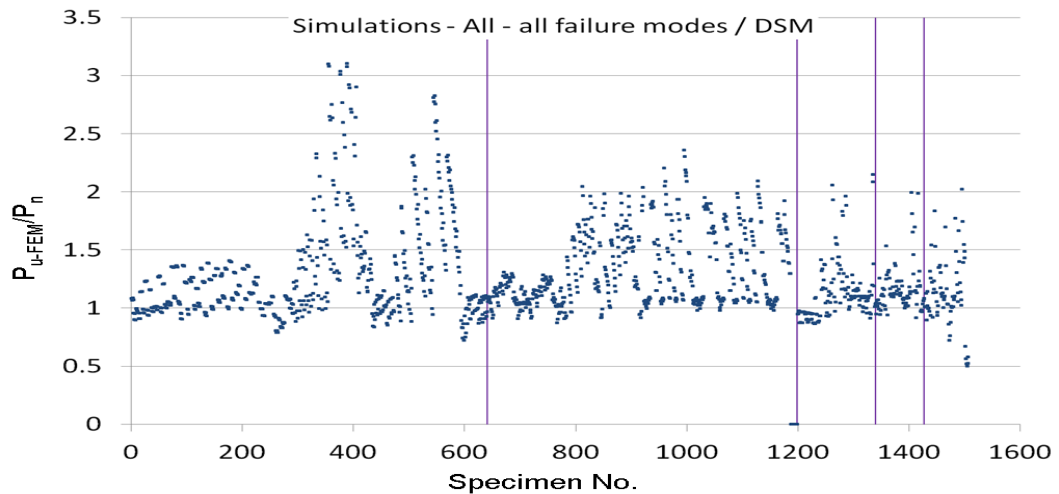

Fig. 10: Simulation-to-predicted ratios for all non-perforated columns by DSM Method 4 with classified section types (from left to right: C, Z, Hat, Rack and Stiffened C)

2.2.4. Method 2 – LG and DG interaction – all

The above discussions relating to DSM Method 2, 3, and 4 have clearly demonstrated the superior performance of DSM Method 2, in terms of reduced scatter and increased reliability, which calculates the column strength as the minimum of the LG and DG interaction equations. These results also showed that the inclusion of LD or LDG interaction in the strength prediction could increase the scatter significantly and also produce overly conservative strength predictions for a large number of members, which agreed with the finding by Schafer (2002) regarding LD interaction.

In this section, DSM Method 2 is also applied to all (non-perforated plus perforated) columns, and the results are shown in Table 22-Table 23 for the statistics of the predictions and in Fig. 11-Fig. 12 for the

simulation-to-predicted ratios. More detailed figures for each section type can be found in Section B.2. The percentage differences of the statistics between DSM Method 2 and DSM Method 1 (the AS/NZS 4600 DSM) for all columns are also given in Table 24 and Table 25.

Comparing Table 22 and Table 23 with Table 10 and Table 11 for non-perforated columns, the influence of including DG interaction in the strength prediction was very similar between the non-perforated and all (non-perforated plus perforated) columns. The comparison also indicates that the failure modes of perforated columns were generally consistent with those of non-perforated columns. While the scatter (V_p) was generally less than 0.2 for the various buckling and interactive buckling modes, as per Table 22 and Table 23, the overall resistance factor considering all modes was 0.692.

Table 22: Resistance factors for all columns failing in modes L, LG, G, D, and L+LG+G+D by **DSM Method 2** – minimum of LG and DG interaction equations based on AS/NZS 4600 DSM

prediction method	Section shape	Failure mode																			
		L				LG				G				D				All L, LG, G, D			
		P_m	V_p	ϕ	n	P_m	V_p	ϕ	n	P_m	V_p	ϕ	n	P_m	V_p	ϕ	n	P_m	V_p	ϕ	n
DSM Method 2	C	1.061	0.149	0.836	6923	1.013	0.139	0.809	4245	0.872	0.144	0.691	1651	1.039	0.270	0.671	3678	1.025	0.189	0.761	16497
	Z	1.051	0.122	0.857	3712	0.968	0.182	0.727	1358	1.017	0.067	0.872	2548	0.877	0.148	0.692	2444	0.989	0.144	0.785	10062
	Hat	0.823	0.115	0.676	1414	0.913	0.204	0.663	494	1.071	0.057	0.924	137	0.791	0.202	0.575	441	0.849	0.172	0.648	2486
	Rack	0.952	0.107	0.789	461	0.842	0.234	0.581	1065	0.909	0.177	0.688	383	0.835	0.113	0.687	391	0.874	0.192	0.647	2300
	Stiffened C	0.931	0.114	0.765	317	0.961	0.139	0.767	143	0.967	0.102	0.805	196	0.997	0.254	0.663	245	0.961	0.171	0.735	901
	All sections	1.025	0.156	0.800	12827	0.972	0.176	0.737	7305	0.959	0.128	0.776	4915	0.956	0.252	0.638	7199	0.988	0.184	0.740	32246

Table 23: Resistance factors for all columns failing in modes LD, DG, LDG, LD+DG+LDG, and all failure modes by **DSM Method 2** – minimum of LG and DG interaction equations based on AS/NZS 4600 DSM

prediction method	Section shape	Failure mode																			
		LD				DG				LDG				All LD, DG, LDG				ALL Failure modes			
		P_m	V_p	ϕ	n	P_m	V_p	ϕ	n	P_m	V_p	ϕ	n	P_m	V_p	ϕ	n	P_m	V_p	ϕ	n
DSM Method 2	C	0.801	0.176	0.607	3157	0.799	0.195	0.589	2589	1.038	0.231	0.720	862	0.831	0.218	0.589	6608	0.969	0.216	0.689	23105
	Z	0.878	0.132	0.707	4115	0.984	0.124	0.800	2989	1.059	0.149	0.834	6057	0.986	0.161	0.764	13161	0.987	0.154	0.773	23223
	Hat	0.714	0.182	0.536	585	0.783	0.250	0.525	1927	0.842	0.241	0.573	964	0.788	0.245	0.533	3476	0.813	0.218	0.576	5962
	Rack	0.734	0.106	0.609	137	0.876	0.208	0.632	832	0.930	0.164	0.718	900	0.892	0.191	0.661	1869	0.882	0.192	0.653	4169
	Stiffened C	0.715	0.203	0.520	245	0.836	0.241	0.570	1727	0.930	0.170	0.711	800	0.853	0.228	0.594	2772	0.879	0.220	0.621	3673
	All sections	0.830	0.167	0.637	8239	0.864	0.215	0.616	10064	1.012	0.185	0.758	9583	0.905	0.211	0.649	27886	0.949	0.201	0.692	60132

Table 24: Difference in resistance factors between **DSM Method 2** and **DSM Method 1** for all columns failing in modes L, LG, G, D, and L+LG+G+D

prediction method	Section shape	Failure mode														
		L			LG			G			D			All L, LG, G, D		
		P_m	V_p	ϕ	P_m	V_p	ϕ	P_m	V_p	ϕ	P_m	V_p	ϕ	P_m	V_p	ϕ
DSM Method 2	C	0.0%	0.0%	0.0%	2.8%	16.8%	0.4%	0.0%	0.0%	0.0%	0.0%	0.0%	0.0%	0.7%	1.1%	0.4%
	Z	0.0%	0.0%	0.0%	0.0%	0.0%	0.0%	0.0%	-1.5%	0.0%	0.0%	0.0%	0.0%	0.0%	0.0%	0.0%
	Hat	0.0%	0.0%	0.0%	1.2%	0.5%	1.1%	0.0%	0.0%	0.0%	0.0%	0.0%	0.0%	0.2%	1.2%	0.0%
	Rack	0.0%	0.0%	0.0%	4.7%	-5.3%	7.2%	0.0%	0.0%	0.0%	0.0%	0.0%	0.0%	2.0%	-5.0%	3.7%
	Stiffened C	0.0%	0.0%	0.0%	4.6%	0.7%	4.5%	0.0%	0.0%	0.0%	0.0%	0.0%	0.0%	0.6%	-0.6%	1.0%
	All sections	0.0%	0.0%	0.0%	2.4%	3.5%	1.5%	0.0%	0.0%	0.0%	0.0%	0.0%	0.0%	0.6%	0.0%	0.5%

Table 25: Difference in resistance factors between **DSM Method 2** and **DSM Method 1** for all columns failing in modes LD, DG, LDG, LD+DG+LDG, and all

failure modes

| prediction method	Section shape	Failure mode														
		LD			DG			LDG			All LD, DG, LDG			ALL Failure modes		
		P_m	V_p	ϕ	P_m	V_p	ϕ	P_m	V_p	ϕ	P_m	V_p	ϕ	P_m	V_p	ϕ
DSM Method 2	C	0.0%	0.0%	0.0%	4.2%	-7.1%	6.9%	5.1%	20.9%	-1.5%	2.3%	3.8%	1.0%	1.0%	0.0%	1.0%
	Z	0.0%	0.0%	0.0%	2.7%	-7.5%	4.0%	3.5%	-12.9%	6.6%	2.4%	-3.6%	3.2%	1.3%	-2.5%	1.8%
	Hat	0.0%	0.0%	0.0%	9.7%	-15.8%	19.9%	6.0%	-5.9%	8.9%	6.9%	-10.3%	12.7%	4.0%	-9.2%	7.9%
	Rack	0.0%	0.0%	0.0%	6.3%	6.1%	4.3%	12.6%	-13.2%	16.9%	8.9%	0.0%	8.9%	5.0%	-3.5%	6.2%
	Stiffened C	0.0%	0.0%	0.0%	15.2%	-18.6%	27.8%	15.7%	-21.7%	24.5%	14.0%	-15.6%	23.0%	10.2%	-17.6%	19.7%
	All sections	0.0%	0.0%	0.0%	6.5%	-13.0%	12.6%	5.4%	-11.9%	9.9%	4.3%	-7.0%	7.1%	2.2%	-5.2%	3.9%
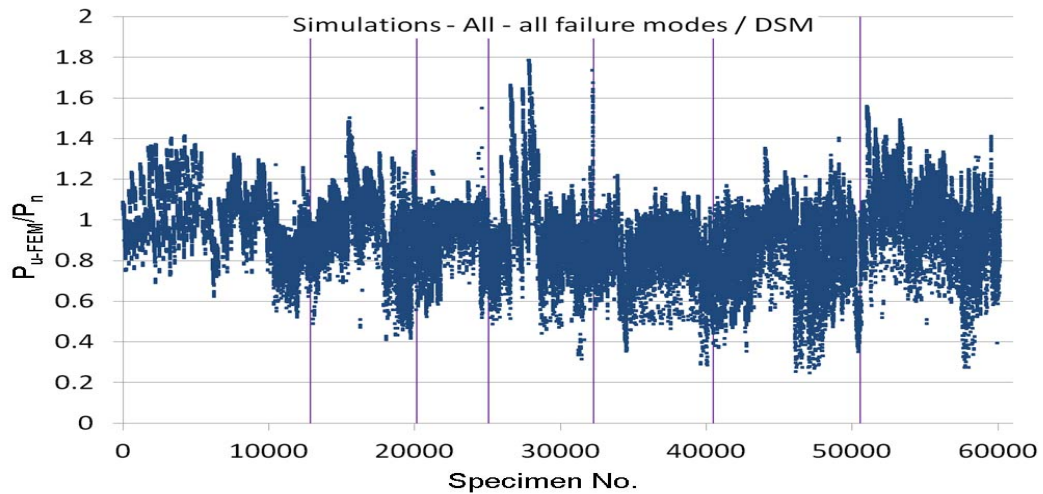
Fig. 11: Simulation-to-predicted ratios for all columns by DSM Method 2 with classified failure modes
(from left to right: L, LG, G, D, LD, DG, and LDG)
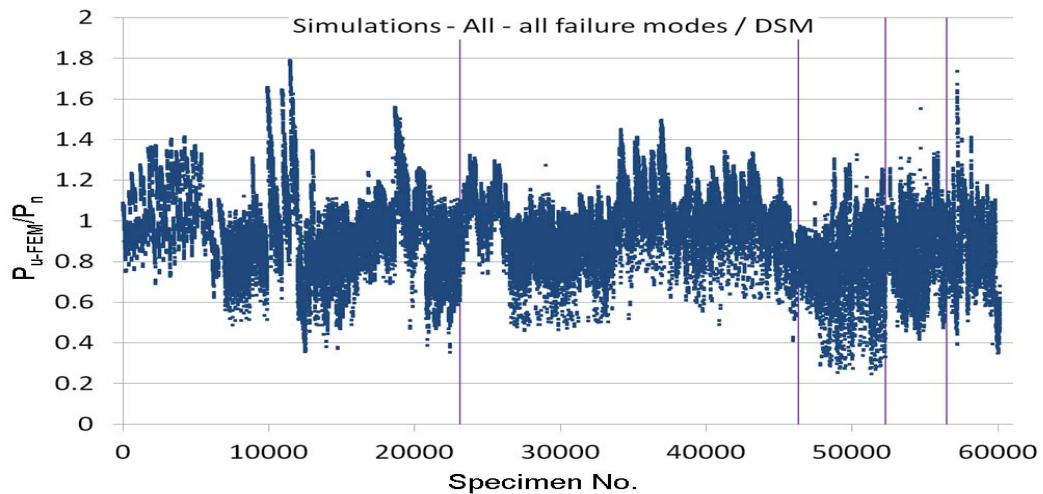
Fig. 12: Simulation-to-predicted ratios for all columns by DSM Method 2 with classified section types
(from left to right: C, Z, Hat, Rack and Stiffened C)

2.3. Design strength proposed by Moen and Schafer (2011)

Recent research by Moen and Schafer (2011) led to a set of modified DSM equations which considers the presence of holes. In brief, elastic buckling properties including the influence of holes (calculated by the simplified methods (Moen and Schafer 2009)) were used to replace the elastic buckling loads in the existing DSM provisions, while the DSM equations were modified to consider the inelastic failure caused by the presence of holes. Of the six proposed DSM options, two of them were evaluated in this study.

2.3.1. Method 5 – Option 2 in (Moen and Schafer 2011) – all

Design Option 2 in (Moen and Schafer 2011) (i.e. DSM Method 5 in this study) constituted using P_{yn} everywhere in Equations (1)-(6) and including hole(s) in P_{cr} determinations by means of the simplified methods proposed by Moen and Schafer (2009).

Table 26 and Table 27 present the statistics of the predictions for all columns using DSM Method 5, i.e. Option 2 in (Moen and Schafer 2011), while their simulation-to-predicted ratios ($P_{u\text{-FEM}}/P_n$) are illustrated in Fig. 13 and Fig. 14. More detailed figures for each section type can be found in Section E.1. Section Z71 was not included in these predictions because the approach in the simplified methods to calculate the local buckling load required the corners of the section to be restrained, which would erroneously prevent the local buckling mode of Z71 since this section does not have lips so its local buckling deformations involve flanges rotating about the web-flange corners.

The results show that compared with the results obtained by DSM Method 1 presented in Table 8 and Table 9, DSM Method 5 significantly improved the overall resistance factor ϕ from 0.666 to 0.746, although it was still unable to reach the prescribed value of 0.85 as in the current DSM provisions. An increase in P_m and a decrease in V_p were shown for all sections except that the value of V_p for C section increased significantly from 0.216 to 0.255. However, only Z section was satisfactorily predicted with an overall ϕ value of 0.900, followed by that for C section of 0.750, with Stiffened C section worst predicted with a ϕ value of 0.578. Moreover, in terms of failure mode, the mode that benefited most from considering holes in P_{cr} and P_y was the LD mode with an overall increase of 25.8 % in ϕ, while the least influenced one was the G mode with an overall increase of 9.3% in ϕ. Meanwhile, it is interesting that the L mode only saw an overall increase of 10% in the ϕ value.

Table 26: Resistance factors for all columns failing in modes L, LG, G, D, and L+LG+G+D by **DSM Method 5** – Option 2 in (Moen and Schafer 2011), i.e. P_{yn} everywhere, P_{cr} (i.e. $P_{cr\text{-}l\text{-}h}$, $P_{cr\text{-}d\text{-}h}$, $P_{cr\text{-}e\text{-}h}$) includes the influence of holes by the simplified methods in (Moen and Schafer 2009)

prediction method	Section shape	Failure mode																		
		L				LG				G				D				All L, LG, G, D			
		P_m	V_p	ϕ	n	P_m	V_p	ϕ	n	P_m	V_p	ϕ	n	P_m	V_p	ϕ	n	P_m	V_p	ϕ	n
DSM Method 5	C	1.230	0.176	0.932	6923	1.059	0.097	0.886	4245	0.940	0.098	0.786	1651	1.396	0.305	0.842	3678	1.194	0.243	0.810	16497
	Z	1.199	0.129	0.969	3712	1.109	0.087	0.937	784	1.041	0.043	0.905	2548	1.112	0.122	0.907	2444	1.127	0.124	0.916	9488
	Hat	0.901	0.083	0.764	1414	0.999	0.202	0.727	494	1.087	0.044	0.945	137	0.898	0.175	0.682	441	0.930	0.147	0.735	2486
	Rack	1.007	0.095	0.844	461	0.883	0.219	0.626	1065	0.990	0.114	0.814	383	0.949	0.081	0.805	391	0.937	0.169	0.718	2300
	Stiffened C	0.985	0.100	0.822	317	1.074	0.115	0.882	143	1.024	0.067	0.878	196	1.141	0.247	0.769	245	1.050	0.171	0.802	901
	All sections	1.170	0.182	0.880	12827	1.033	0.143	0.821	6731	1.004	0.086	0.848	4915	1.236	0.296	0.760	7199	1.130	0.221	0.798	31672

Table 27: Resistance factors for all columns failing in modes LD, DG, LDG, LD+DG+LDG, and all failure modes by **DSM Method 5** – Option 2 in (Moen and Schafer 2011), i.e. P_{yn} everywhere, P_{cr} (i.e. $P_{cr\text{-}l\text{-}h}$, $P_{cr\text{-}d\text{-}h}$, $P_{cr\text{-}e\text{-}h}$) includes the influence of holes by the simplified methods in (Moen and Schafer 2009)

| prediction method	Section shape	Failure mode																		
		LD				DG				LDG				All LD, DG, LDG				ALL Failure modes			
		P_m	V_p	ϕ	n	P_m	V_p	ϕ	n	P_m	V_p	ϕ	n	P_m	V_p	ϕ	n	P_m	V_p	ϕ	n
DSM Method 5	C	1.000	0.185	0.748	3157	0.863	0.159	0.671	2589	1.202	0.228	0.839	862	0.972	0.219	0.688	6608	1.130	0.255	0.750	23105
	Z	1.128	0.104	0.937	4115	1.028	0.095	0.862	2989	1.136	0.154	0.889	6057	1.109	0.135	0.890	13161	1.117	0.131	0.900	22649
	Hat	0.838	0.156	0.654	585	0.786	0.263	0.514	1927	0.888	0.227	0.620	964	0.823	0.243	0.559	3476	0.868	0.212	0.622	5962
	Rack	0.851	0.096	0.712	137	0.900	0.169	0.690	832	0.921	0.181	0.693	900	0.907	0.173	0.691	1869	0.923	0.171	0.705	4169
	Stiffened C	0.829	0.169	0.635	245	0.792	0.280	0.502	1727	0.872	0.219	0.618	800	0.818	0.256	0.542	2772	0.875	0.258	0.578	3673
	All sections	1.045	0.169	0.801	8239	0.888	0.213	0.635	10064	1.075	0.206	0.778	9583	0.999	0.215	0.712	27886	1.069	0.227	0.746	59558
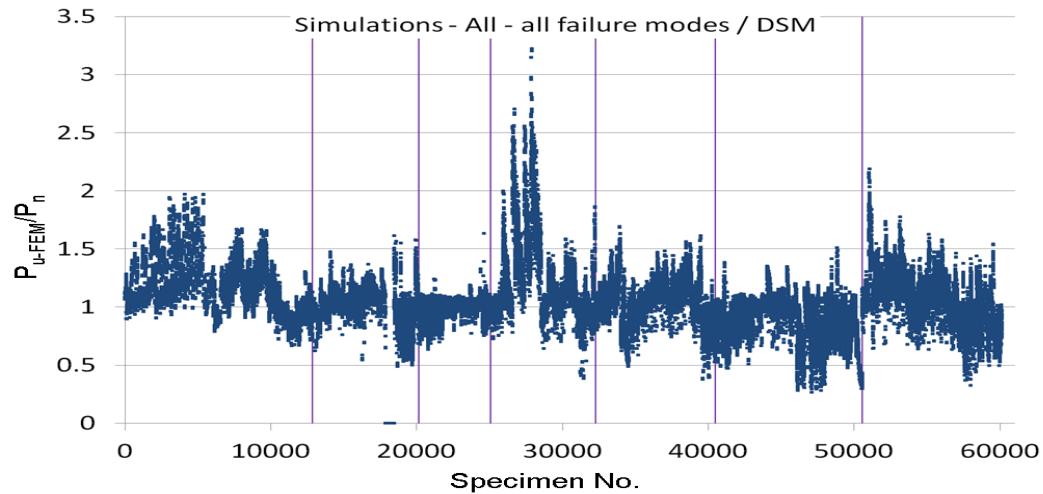
Fig. 13: Simulation-to-predicted ratios for all columns by DSM Method 5 with classified failure modes
(from left to right: L, LG, G, D, LD, DG, and LDG)
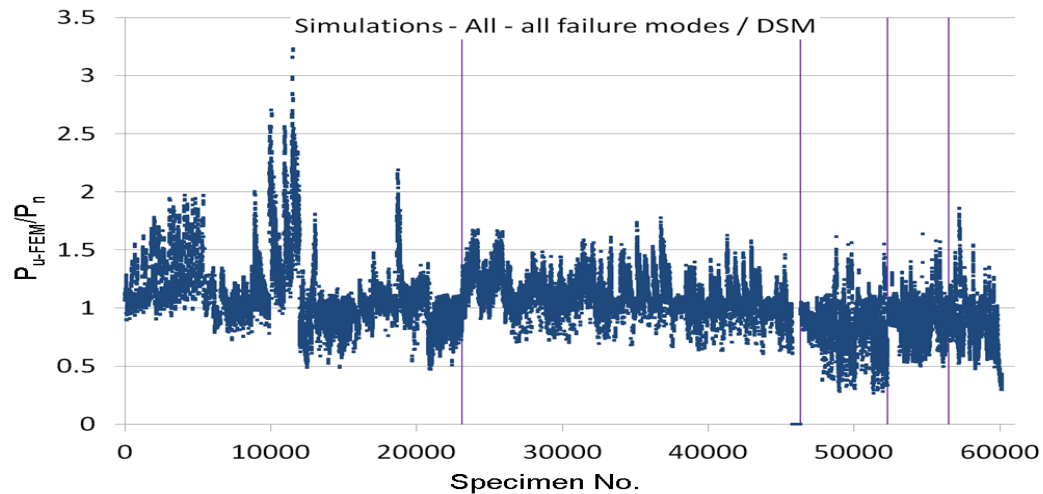
Fig. 14: Simulation-to-predicted ratios for all columns by DSM Method 5 with classified section types
(from left to right: C, Z, Hat, Rack and Stiffened C)

2.3.2. Method 6 – Option 4 in (Moen and Schafer 2011) – all

Moen (2008) found that the last method (i.e. DSM Method 5) presented in Section 2.3.1 was not optimal because capping the strength by P_{yn} missed a number of columns failing in the inelastic transition range. Therefore, DSM Method 6, i.e. the best-performing DSM option (Design Option 4) in (Moen and Schafer 2011) was proposed for designing perforated thin-walled steel columns and it was expressed as follows:

(i) The nominal axial strength, P_{ne}, for flexural, torsional, or torsional-flexural buckling is

$$\text{For } \lambda_c \leq 1.5: \quad P_{ne} = \left(0.658^{\lambda_c^2}\right)P_y \qquad (13)$$

$$\text{For } \lambda_c > 1.5: \quad P_{ne} = \left(\frac{0.877}{\lambda_c^2} \right) P_y \tag{14}$$

where $\lambda_c = \sqrt{P_y / P_{cr-e-h}}$, and P_{cr-e-h} includes the influence of holes.

(ii) The nominal axial strength, P_{nle}, for local buckling (local-global interactive buckling) is

$$\text{For } \lambda_{le} \leq 0.776, \quad P_{nle} = P_{ne} \leq P_{yn} \tag{15}$$

$$\text{For } \lambda_{le} > 0.776, \quad P_{nle} = \left[1 - 0.15 \left(\frac{P_{cr-l-h}}{P_{ne}} \right)^{0.4} \right] \left(\frac{P_{cr-l-h}}{P_{ne}} \right)^{0.4} P_{ne} \leq P_{yn} \tag{16}$$

where $\lambda_{le} = \sqrt{P_{ne} / P_{cr-l-h}}$, and P_{cr-l-h} includes the influence of holes.

(iii) The nominal axial strength, P_{nd}, for distortional buckling is

$$\text{For } \lambda_d \leq \lambda_{d1}, \quad P_{nd} = P_{yn} \tag{17}$$

$$\text{For } \lambda_{d1} < \lambda_d \leq \lambda_{d2}, \quad P_{nd} = P_{yn} - \left(\frac{P_{yn} - P_{d2}}{\lambda_{d2} - \lambda_{d1}} \right) \left(\lambda_{d2} - \lambda_{d1} \right) \tag{18}$$

$$\text{For } \lambda_d > \lambda_{d2}, \quad P_{nd} = \left[1 - 0.25 \left(\frac{P_{cr-d-h}}{P_y} \right)^{0.6} \right] \left(\frac{P_{cr-d-h}}{P_y} \right)^{0.6} P_y \tag{19}$$

where $\lambda_d = \sqrt{P_y / P_{cr-d-h}}$, $\lambda_{d1} = 0.561 \left(P_{yn} / P_y \right)$, $\lambda_{d2} = 0.561 \left(14 \left(P_y / P_{yn} \right)^{0.4} - 13 \right)$,

P_{cr-d-h} includes the influence of holes, and

$$P_{d2} = \left(1 - 0.25 \left(1/\lambda_{d2} \right)^{1.2} \right) \left(1/\lambda_{d2} \right)^{1.2} P_y \ . \tag{20}$$

All the elastic buckling loads ($P_{cre}, P_{crl}, P_{crd}$) in their proposals included the influence of holes which needed to be obtained with either general hand methods or the simplified methods developed by Moen and Schafer (2009) based on the linear elastic Semi-Analytical Finite Strip Method (SAFSM). In (Moen and Schafer 2009), the local buckling load was calculated by the SAFSM as the minimum of the elastic buckling load of the unstiffened strip at the edge of holes within the hole length and the elastic local buckling load of the gross cross-section. The distortional buckling load was calculated by the SAFSM while using proper modifications to the element thickness to represent the effect of perforations, while the global buckling load was predicted using approximate "weighted average" cross-sectional properties derived from classical stability solutions. Table 28 and Table 29 present the statistics of the predictions using the above described DSM Method 6 against all simulated columns, along with Fig. 15 and Fig. 16 illustrating the simulation-to-predicted

ratios ($P_{\text{u-FEM}}/P_n$) classified by failure mode and section type respectively. More detailed figures regarding each section type can be found in Section F.1. As with DSM Method 5, section Z71 was not included in the predictions.

In general, DSM Method 6 performed better than DSM Method 5 in terms of producing a significantly smaller scatter, as shown by its overall V_p value of 0.199 as compared to 0.227 for DSM Method 5. In comparison to DSM Method 5, improvements mainly came from C and Z sections which showed 16.5% and 4.6% decreases in V_p respectively, as well as from the L and D modes which had 22.0% and 17.9% decreases in V_p respectively. However, DSM Method 6 produced a slightly lower overall resistance factor ϕ of 0.726 versus that of 0.746 for DSM Method 5, as a result of a lower overall mean P_m (0.993 vs. 1.069). Even for the modes (i.e. L, LG, G and D) that were covered by the current codified DSM, the overall ϕ value of 0.796 was still lower than the prescribed value of 0.85. The only section that was satisfactorily predicted was Z section, as with DSM Method 5.

Fig. 15 and Fig. 16 show that overall, the performance of DSM Method 6 was similar to that of DSM Method 5, with a visibly smaller scatter for C and Z sections failing in the L and D modes.

Table 28: Resistance factors for all columns failing in modes L, LG, G, D, and L+LG+G+D by **DSM Method 6** – Option 4 in (Moen and Schafer 2011), i.e. limit P_{nle} to P_{yn}, transition P_{nd} to P_{yn}, P_{cr} includes the influence of holes by the simplified methods in (Moen and Schafer 2009)

prediction method	Section shape	Failure mode																			
		L				LG				G				D				All L, LG, G, D			
		P_{m}	V_{p}	ϕ	n	P_{m}	V_{p}	ϕ	n	P_{m}	V_{p}	ϕ	n	P_{m}	V_{p}	ϕ	n	P_{m}	V_{p}	ϕ	n
DSM Method 6	C	1.078	0.134	0.866	6923	1.031	0.106	0.855	4245	0.940	0.098	0.786	1651	1.231	0.256	0.815	3678	1.086	0.190	0.807	16497
	Z	1.067	0.111	0.880	3712	1.109	0.087	0.936	784	1.040	0.045	0.903	2548	1.030	0.097	0.862	2444	1.054	0.095	0.883	9488
	Hat	0.852	0.096	0.714	1414	0.952	0.204	0.691	494	1.087	0.044	0.945	137	0.866	0.169	0.664	441	0.887	0.155	0.693	2486
	Rack	0.977	0.093	0.820	461	0.872	0.222	0.614	1065	0.990	0.114	0.814	383	0.913	0.093	0.767	391	0.920	0.172	0.702	2300
	Stiffened C	0.950	0.106	0.787	317	1.018	0.135	0.817	143	1.024	0.067	0.878	196	1.096	0.251	0.733	245	1.016	0.174	0.773	901
	All sections	1.043	0.142	0.830	12827	1.009	0.148	0.796	6731	1.003	0.086	0.847	4915	1.119	0.243	0.759	7199	1.047	0.174	0.796	31672

Table 29: Resistance factors for all columns failing in modes LD, DG, LDG, LD+DG+LDG, and all failure modes by **DSM Method 6** – Option 4 in (Moen and Schafer 2011), i.e. limit P_{nle} to P_{yn}, transition P_{nd} to P_{yn}, P_{cr} includes the influence of holes by the simplified methods in (Moen and Schafer 2009)

| prediction method	Section shape	Failure mode																			
		LD				DG				LDG				All LD, DG, LDG				ALL Failure modes			
		P_{m}	V_{p}	ϕ	n	P_{m}	V_{p}	ϕ	n	P_{m}	V_{p}	ϕ	n	P_{m}	V_{p}	ϕ	n	P_{m}	V_{p}	ϕ	n
DSM Method 6	C	0.881	0.187	0.657	3157	0.836	0.174	0.636	2589	1.060	0.224	0.744	862	0.887	0.206	0.641	6608	1.029	0.213	0.736	23105
	Z	0.999	0.122	0.814	4115	0.998	0.109	0.825	2989	1.064	0.159	0.827	6057	1.029	0.143	0.817	13161	1.039	0.125	0.844	22649
	Hat	0.775	0.176	0.588	585	0.760	0.278	0.483	1927	0.837	0.240	0.572	964	0.784	0.256	0.520	3476	0.827	0.223	0.582	5962
	Rack	0.824	0.101	0.687	137	0.880	0.180	0.663	832	0.895	0.187	0.667	900	0.883	0.181	0.665	1869	0.903	0.177	0.684	4169
	Stiffened C	0.795	0.187	0.593	245	0.775	0.286	0.486	1727	0.854	0.214	0.609	800	0.800	0.260	0.526	2772	0.853	0.260	0.561	3673
	All sections	0.929	0.172	0.708	8239	0.863	0.223	0.606	10064	1.008	0.201	0.735	9583	0.932	0.211	0.669	27886	0.993	0.199	0.726	59558
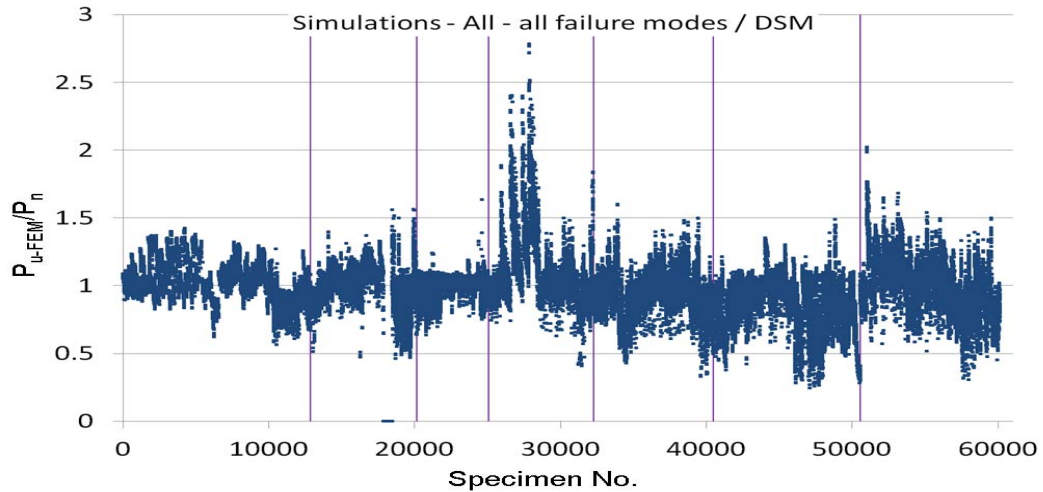
Fig. 15: Simulation-to-predicted ratios for all columns by DSM Method 6 with classified failure modes
(from left to right: L, LG, G, D, LD, DG, and LDG)
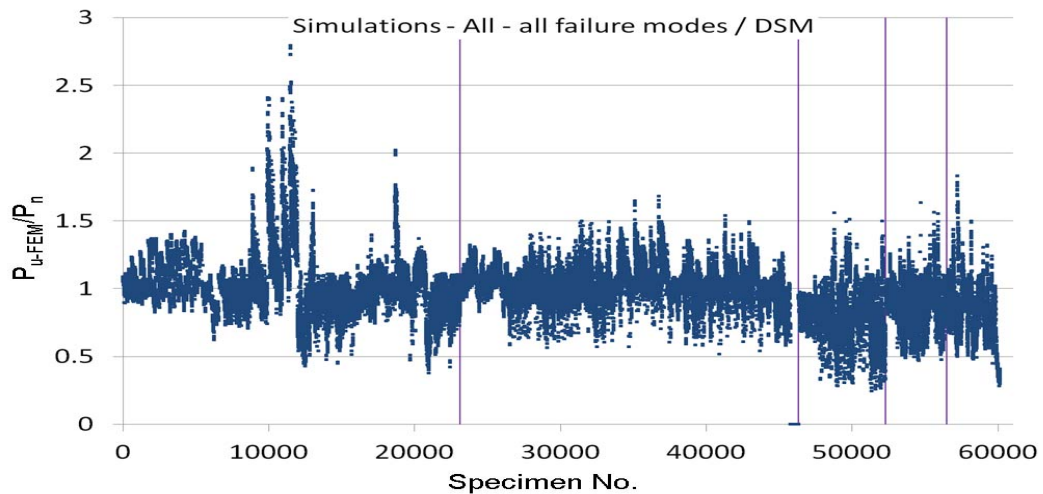
Fig. 16: Simulation-to-predicted ratios for all columns by DSM Method 6 with classified section types
(from left to right: C, Z, Hat, Rack and Stiffened C)

3. Modified DSM

In addition to DSM Method 1 to 6 which have been documented in the literature, this study also experimented with a series of new methods based on the DSM to search for an optimal method which should be able to simultaneously consider the effects of perforation and interactive buckling. Specifically, such a method should produce the smallest scatter (represented by the smallest V_p) and also a resistance factor ϕ higher than 0.85 in most cases.

The methods evaluated in the following sections feature either simple modifications to the AS/NZS 4600 DSM, or simplifications to Option 4 of (Moen and Schafer 2011), or regression analyses based on Option 4 of (Moen and Schafer 2011).

3.1. Modification to AS/NZS 4600 DSM by using P_{yn}

Two methods are presented in this section which were based on the use of P_{yn} in the current codified DSM.

3.1.1. Method 7 – all

DSM Method 7 constitutes replacing P_y by P_{yn} everywhere in Equations (1)-(6) with P_{cr} obtained from the SAFSM or theoretical methods without considering holes.

The performance of DSM Method 7 is shown in Table 30 and Table 31 for the statistics of the predictions and in Fig. 17-Fig. 18 for the simulation-to-predicted ratios for all columns. More detailed figures regarding the simulation-to-predicted ratios for each section are provided in Section G.1.

The results show that, compared with the current DSM (Method 1), Method 7 improved the overall resistant factor ϕ from 0.666 to 0.711, which was mainly attributed to the increase in the overall simulation-to-predicted mean P_m from 0.929 to 1.017 while the overall variation of the predictions V_p increased slightly from 0.212 to 0.226.

A comparison between Method 7 and Method 5 (which considered the effect of holes in P_{cr}) was also made by presenting in Table 32 and Table 33 the differences between their statistics. In general, Method 7 performed slightly worse when comparing its overall ϕ value of 0.711 against 0.746 (4.7% difference) for Method 5, which was mainly due to the fact that Method 7 consistently produced a lower overall mean P_m (4.9% lower). In addition, the difference in the values of ϕ also suggests that the section most adversely affected by ignoring holes in P_{cr} determinations was Rack section (9.4% decrease in ϕ), while the least affected one was C section with a 2.7 % decrease in ϕ. Similarly, the G mode was the most adversely affected failure mode with an 8.4% decrease in ϕ, and more noticeably, a large increase (48.8%) in V_p. On the contrary, the L mode was the least affected mode experiencing only a 0.3% drop in ϕ, while the D mode was moderately influenced with its ϕ value showing a 3% decrease (however, the 12.5% decrease in V_p suggests that considering holes in P_{cr} caused a larger scatter). These data clearly suggest that including holes in the determination of P_{cr} for global buckling was most effective in reducing the scatter and increasing ϕ, while it resulted in hardly any difference in the results when holes were considered in P_{cr} for local buckling, and it was inconclusive regarding the effect of considering holes in P_{cr} for distortional buckling. In other words, determining P_{cr} as per the simplified methods proposed by Moen and Schafer (2009) performed best for global buckling, followed by distortional buckling and then local buckling. The latter result is mainly because in most cases the values of P_{cr} for local buckling as per the simplified methods were the same for non-perforated

and perforated members. It follows that there is no benefit to be gained by determining P_{cr} for local and distortional buckling as per the simplified methods and hence, the simplified methods are not considered for local and distortional buckling hereon in deriving an optimal DSM for perforated columns.

Table 30: Resistance factors for all columns failing in modes L, LG, G, and L+LG+G+D by **DSM Method 7** – AS/NZS 4600 DSM with P_{yn} everywhere and P_{cr} based on gross area (i.e. $P_{cr\text{-}l\text{-}nh}$, $P_{cr\text{-}d\text{-}nh}$, $P_{cr\text{-}e\text{-}nh}$)

prediction method	Section shape	Failure mode																All L, LG, G, D			
		L				LG				G				D							
		P_m	V_p	ϕ	n	P_m	V_p	ϕ	n	P_m	V_p	ϕ	n	P_m	V_p	ϕ	n	P_m	V_p	ϕ	n
DSM Method 7	C	1.229	0.177	0.931	6923	1.015	0.109	0.839	4245	0.872	0.144	0.691	1651	1.242	0.268	0.805	3678	1.141	0.225	0.799	16497
	Z	1.198	0.130	0.968	3712	0.984	0.165	0.758	1358	1.018	0.066	0.874	2548	1.020	0.110	0.842	2444	1.080	0.146	0.855	10062
	Hat	0.896	0.089	0.756	1414	0.955	0.192	0.706	494	1.071	0.057	0.924	137	0.856	0.173	0.652	441	0.910	0.142	0.723	2486
	Rack	1.007	0.095	0.844	461	0.816	0.242	0.555	1065	0.909	0.177	0.688	383	0.880	0.090	0.741	391	0.881	0.198	0.645	2300
	Stiffened C	0.980	0.107	0.812	317	0.970	0.120	0.792	143	0.967	0.102	0.805	196	1.050	0.236	0.722	245	0.995	0.162	0.770	901
	All sections	1.169	0.183	0.877	12827	0.975	0.162	0.755	7305	0.960	0.128	0.777	4915	1.117	0.259	0.737	7199	1.082	0.213	0.774	32246

Table 31: Resistance factors for all columns failing in modes LD, DG, LDG, LD+DG+LDG, and all failure modes by **DSM Method 7** – AS/NZS 4600 DSM with P_{yn} everywhere and P_{cr} based on gross area (i.e. $P_{cr\text{-}l\text{-}nh}$, $P_{cr\text{-}d\text{-}nh}$, $P_{cr\text{-}e\text{-}nh}$)

prediction method	Section shape	Failure mode												All LD, DG, LDG				ALL Failure modes			
		LD				DG				LDG											
		P_m	V_p	ϕ	n	P_m	V_p	ϕ	n	P_m	V_p	ϕ	n	P_m	V_p	ϕ	n	P_m	V_p	ϕ	n
DSM Method 7	C	0.935	0.175	0.710	3157	0.812	0.179	0.614	2589	1.133	0.175	0.860	862	0.913	0.210	0.656	6608	1.076	0.243	0.730	23105
	Z	1.019	0.105	0.845	4115	1.006	0.104	0.836	2989	1.097	0.158	0.854	6057	1.052	0.140	0.839	13161	1.064	0.143	0.845	23223
	Hat	0.773	0.161	0.600	585	0.744	0.278	0.474	1927	0.844	0.243	0.573	964	0.777	0.257	0.514	3476	0.832	0.223	0.585	5962
	Rack	0.758	0.100	0.633	137	0.847	0.183	0.635	832	0.852	0.183	0.640	900	0.843	0.181	0.634	1869	0.864	0.192	0.639	4169
	Stiffened C	0.746	0.186	0.557	245	0.742	0.289	0.463	1727	0.821	0.219	0.581	800	0.765	0.264	0.500	2772	0.821	0.264	0.537	3673
	All sections	0.957	0.163	0.740	8239	0.847	0.231	0.587	10064	1.029	0.208	0.742	9583	0.942	0.219	0.667	27886	1.017	0.226	0.711	60132

Table 32: Difference in resistance factors between **DSM Method 7** and **DSM Method 5** for all columns failing in modes L, LG, G, D, and L+LG+G+D

prediction method	Section shape	Failure mode														
		L			LG			G			D			All L, LG, G, D		
		P_m	V_p	ϕ	P_m	V_p	ϕ	P_m	V_p	ϕ	P_m	V_p	ϕ	P_m	V_p	ϕ
DSM Method 7	C	-0.1%	0.6%	-0.1%	-4.2%	12.4%	-5.3%	-7.2%	46.9%	-12.1%	-11.0%	-12.1%	-4.4%	-4.4%	-7.4%	-1.4%
	Z	-0.1%	0.8%	-0.1%	-11.3%	89.7%	-19.1%	-2.2%	53.5%	-3.4%	-8.3%	-9.8%	-7.2%	-4.2%	17.7%	-6.7%
	Hat	-0.6%	7.2%	-1.0%	-4.4%	-5.0%	-2.9%	-1.5%	29.5%	-2.2%	-4.7%	-1.1%	-4.4%	-2.2%	-3.4%	-1.6%
	Rack	0.0%	0.0%	0.0%	-7.6%	10.5%	-11.3%	-8.2%	55.3%	-15.5%	-7.3%	11.1%	-8.0%	-6.0%	17.2%	-10.2%
	Stiffened C	-0.5%	7.0%	-1.2%	-9.7%	4.3%	-10.2%	-5.6%	52.2%	-8.3%	-8.0%	-4.5%	-6.1%	-5.2%	-5.3%	-4.0%
	All sections	-0.1%	0.5%	-0.3%	-5.6%	13.3%	-8.0%	-4.4%	48.8%	-8.4%	-9.6%	-12.5%	-3.0%	-4.2%	-3.6%	-3.0%

Table 33: Difference in resistance factors between **DSM Method 7** and **DSM Method 5** for all columns failing in modes LD, DG, LDG, LD+DG+LDG, and all

failure modes

prediction method	Section shape	Failure mode														
		LD			DG			LDG			All LD, DG, LDG			ALL Failure modes		
		P_m	V_p	ϕ	P_m	V_p	ϕ	P_m	V_p	ϕ	P_m	V_p	ϕ	P_m	V_p	ϕ
DSM Method 7	C	-6.5%	-5.4%	-5.1%	-5.9%	12.6%	-8.5%	-5.7%	-23.2%	2.5%	-6.1%	-4.1%	-4.7%	-4.8%	-4.7%	-2.7%
	Z	-9.7%	1.0%	-9.8%	-2.1%	9.5%	-3.0%	-3.4%	2.6%	-3.9%	-5.1%	3.7%	-5.7%	-4.7%	9.2%	-6.1%
	Hat	-7.8%	3.2%	-8.3%	-5.3%	5.7%	-7.8%	-5.0%	7.0%	-7.6%	-5.6%	5.8%	-8.1%	-4.1%	5.2%	-5.9%
	Rack	-10.9%	4.2%	-11.1%	-5.9%	8.3%	-8.0%	-7.5%	1.1%	-7.6%	-7.1%	4.6%	-8.2%	-6.4%	12.3%	-9.4%
	Stiffened C	-10.0%	10.1%	-12.3%	-6.3%	3.2%	-7.8%	-5.8%	0.0%	-6.0%	-6.5%	3.1%	-7.7%	-6.2%	2.3%	-7.1%
	All sections	-8.4%	-3.6%	-7.6%	-4.6%	8.5%	-7.6%	-4.3%	1.0%	-4.6%	-5.7%	1.9%	-6.3%	-4.9%	-0.4%	-4.7%
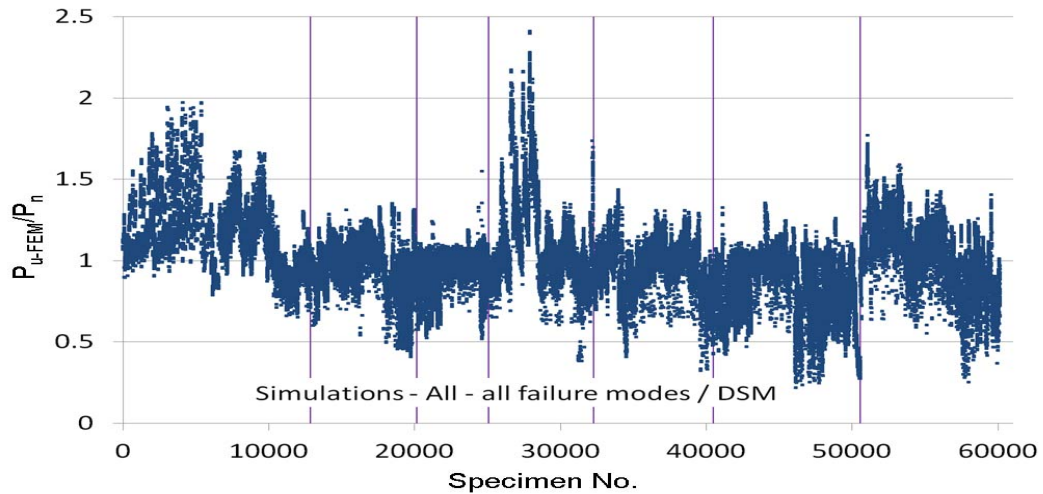
Fig. 17: Simulation-to-predicted ratios for all columns by DSM Method 7 with classified failure modes
(from left to right: L, LG, G, D, LD, DG, and LDG)
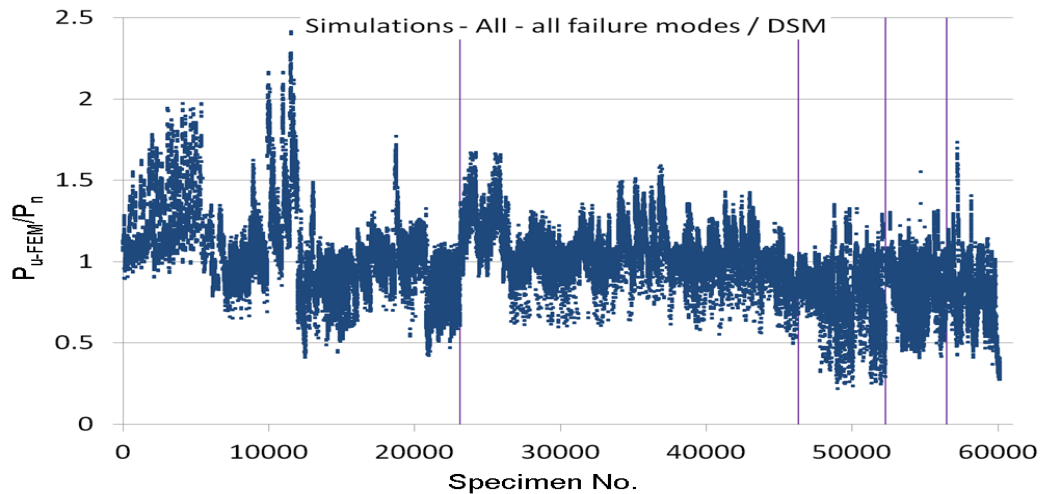
Fig. 18: Simulation-to-predicted ratios for all columns by DSM Method 7 with classified section types
(from left to right: C, Z, Hat, Rack and Stiffened C)

3.1.2. Method 8 – all

DSM Method 8 differed from DSM Method 7 in that P_{yn} did not replace P_y in the slenderness in Equations (1)-(6), therefore $\lambda_c = \sqrt{P_y/P_{cr\text{-}e\text{-}nh}}$ and $\lambda_d = \sqrt{P_y/P_{cr\text{-}d\text{-}nh}}$ were used. Otherwise it was the same as Method 7 such that P_{yn} was used elsewhere and P_{cr} was based on gross area. This option was explored because the figures in Section 4.4.2.5 plotting $P_{u\text{-}FEM}/P_{yn}$ against $(P_{yg}/P_{cr\text{-}FEM})^{0.5}$ showed that this approach could further raise the overall resistance factor of the prediction compared with plotting $P_{u\text{-}FEM}/P_{yn}$ against $(P_{yn}/P_{cr\text{-}FEM})^{0.5}$.

The statistics of the predictions by DSM Method 8 are tabulated in Table 34 and Table 35, while their percentage differences between DSM Method 7 are given in Table 36 and Table 37. In addition, Fig. 19 and

Fig. 20 illustrate the simulation-to-predicted ratios ($P_{\text{u-FEM}}/P_{\text{n}}$) for all columns classified by failure mode and section type respectively.

Comparisons with Method 7 showed that the exclusion of P_{yn} in the calculations of the slenderness (i.e. λ_{c}, λ_{d} and λ_{l}) raised the overall resistance factor ϕ from 0.711 to 0.755 (by 6.2%) due to an increase in the overall simulation-to-predicted mean P_{m} by 11.5%, although the overall scatter of the predictions represented by V_{p} increased by 12.4%. This increase in the value of V_{p} mainly came from C and Z sections which showed 13.2% and 7.7% increases in the values of V_{p} respectively, while the scatter was reduced slightly by 2.7%, 7.8% and 4.2% for Hat, Rack and Stiffened C sections, respectively. Moreover, in terms of failure mode, Method 8, compared with Method 7, seemed to be most beneficial to the G mode which saw a marked increase of 22.8% in the overall value of ϕ, as opposed to the D mode which had a significant increase of 39.4% in the overall value of V_{p} (which was quite noticeable comparing Fig. 19 and Fig. 17) and also a decrease of 5.7% in the overall value of ϕ.

In addition, if the statistics by Method 8 are compared with those (Table 26 and Table 27) for Method 5 (i.e. Option 2 in (Moen and Schafer 2011) that used P_{yn} in all equations and included hole(s) in P_{cr} determinations), one can find that these two methods produced similar resistance factors (0.755 vs. 0.746), although Method 8 resulted in a higher scatter in the predictions as shown by the values of V_{p} (0.254 vs. 0.227).

Table 34: Resistance factors for all columns failing in modes L, LG, G, D, and L+LG+G+D by **DSM Method 8** – AS/NZS 4600 DSM with P_y in the slenderness, P_{yn} elsewhere and P_{cr} based on gross area

prediction method	Section shape	Failure mode																			
		L				LG				G				D				All L, LG, G, D			
		P_m	V_p	ϕ	n	P_m	V_p	ϕ	n	P_m	V_p	ϕ	n	P_m	V_p	ϕ	n	P_m	V_p	ϕ	n
DSM Method 8	C	1.229	0.177	0.931	6923	1.234	0.142	0.981	4245	1.117	0.105	0.927	1651	1.496	0.367	0.795	3678	1.278	0.261	0.840	16497
	Z	1.198	0.130	0.968	3712	1.221	0.206	0.883	1358	1.294	0.109	1.070	2548	1.138	0.159	0.885	2444	1.211	0.151	0.952	10062
	Hat	0.896	0.089	0.756	1414	1.005	0.206	0.726	494	1.183	0.050	1.025	137	0.890	0.172	0.679	441	0.932	0.159	0.725	2486
	Rack	1.007	0.095	0.844	461	0.863	0.221	0.609	1065	0.985	0.144	0.781	383	0.905	0.082	0.767	391	0.919	0.178	0.695	2300
	Stiffened C	0.980	0.107	0.812	317	1.039	0.104	0.863	143	1.044	0.070	0.894	196	1.100	0.239	0.752	245	1.036	0.161	0.803	901
	All sections	1.169	0.183	0.877	12827	1.158	0.206	0.838	7305	1.198	0.140	0.954	4915	1.292	0.361	0.695	7199	1.198	0.246	0.809	32246

Table 35: Resistance factors for all columns failing in modes LD, DG, LDG, LD+DG+LDG, and all failure modes by **DSM Method 8** – AS/NZS 4600 DSM with P_y in the slenderness, P_{yn} elsewhere and P_{cr} based on gross area

prediction method	Section shape	Failure mode																			
		LD				DG				LDG				All LD, DG, LDG				ALL Failure modes			
		P_m	V_p	ϕ	n	P_m	V_p	ϕ	n	P_m	V_p	ϕ	n	P_m	V_p	ϕ	n	P_m	V_p	ϕ	n
DSM Method 8	C	1.011	0.231	0.701	3157	0.953	0.167	0.733	2589	1.282	0.248	0.862	862	1.024	0.239	0.700	6608	1.206	0.275	0.772	23105
	Z	1.157	0.145	0.916	4115	1.194	0.138	0.955	2989	1.265	0.160	0.982	6057	1.215	0.157	0.948	13161	1.214	0.154	0.950	23223
	Hat	0.839	0.160	0.651	585	0.813	0.265	0.530	1927	0.898	0.242	0.611	964	0.841	0.247	0.567	3476	0.879	0.217	0.625	5962
	Rack	0.788	0.097	0.659	137	0.887	0.171	0.678	832	0.880	0.175	0.669	900	0.876	0.172	0.669	1869	0.900	0.177	0.682	4169
	Stiffened C	0.785	0.166	0.604	245	0.789	0.281	0.499	1727	0.870	0.201	0.634	800	0.812	0.253	0.541	2772	0.867	0.253	0.578	3673
	All sections	1.062	0.210	0.763	8239	0.964	0.253	0.642	10064	1.161	0.235	0.800	9583	1.061	0.247	0.715	27886	1.134	0.254	0.755	60132

Table 36: Difference in resistance factors between **DSM Method 8** and **DSM Method 7** for all columns failing in modes L, LG, G, D, and L+LG+G+D

prediction method	Section shape	Failure mode														
		L			LG			G			D			All L, LG, G, D		
		P_m	V_p	ϕ	P_m	V_p	ϕ	P_m	V_p	ϕ	P_m	V_p	ϕ	P_m	V_p	ϕ
DSM Method 8	C	0.0%	0.0%	0.0%	21.6%	30.3%	16.9%	28.1%	-27.1%	34.2%	20.5%	36.9%	-1.2%	12.0%	16.0%	5.1%
	Z	0.0%	0.0%	0.0%	24.1%	24.8%	16.5%	27.1%	65.2%	22.4%	11.6%	44.5%	5.1%	12.1%	3.4%	11.3%
	Hat	0.0%	0.0%	0.0%	5.2%	7.3%	2.8%	10.5%	-12.3%	10.9%	4.0%	-0.6%	4.1%	2.4%	12.0%	0.3%
	Rack	0.0%	0.0%	0.0%	5.8%	-8.7%	9.7%	8.4%	-18.6%	13.5%	2.8%	-8.9%	3.5%	4.3%	-10.1%	7.8%
	Stiffened C	0.0%	0.0%	0.0%	7.1%	-13.3%	9.0%	8.0%	-31.4%	11.1%	4.8%	1.3%	4.2%	4.1%	-0.6%	4.3%
	All sections	0.0%	0.0%	0.0%	18.8%	27.2%	11.0%	24.8%	9.4%	22.8%	15.7%	39.4%	-5.7%	10.7%	15.5%	4.5%

Table 37: Difference in resistance factors between **DSM Method 8** and **DSM Method 7** for all columns failing in modes LD, DG, LDG, LD+DG+LDG, and all

failure modes

prediction method	Section shape	Failure mode														
		LD			DG			LDG			All LD, DG, LDG			ALL Failure modes		
		P_m	V_p	ϕ	P_m	V_p	ϕ	P_m	V_p	ϕ	P_m	V_p	ϕ	P_m	V_p	ϕ
DSM Method 8	C	8.1%	32.0%	-1.3%	17.4%	-6.7%	19.4%	13.2%	41.7%	0.2%	12.2%	13.8%	6.7%	12.1%	13.2%	5.8%
	Z	13.5%	38.1%	8.4%	18.7%	32.7%	14.2%	15.3%	1.3%	15.0%	15.5%	12.1%	13.0%	14.1%	7.7%	12.4%
	Hat	8.5%	-0.6%	8.5%	9.3%	-4.7%	11.8%	6.4%	-0.4%	6.6%	8.2%	-3.9%	10.3%	5.6%	-2.7%	6.8%
	Rack	4.0%	-3.0%	4.1%	4.7%	-6.6%	6.8%	3.3%	-4.4%	4.5%	3.9%	-5.0%	5.5%	4.2%	-7.8%	6.7%
	Stiffened C	5.2%	-10.8%	8.4%	6.3%	-2.8%	7.8%	6.0%	-8.2%	9.1%	6.1%	-4.2%	8.2%	5.6%	-4.2%	7.6%
	All sections	11.0%	28.8%	3.1%	13.8%	9.5%	9.4%	12.8%	13.0%	7.8%	12.6%	12.8%	7.2%	11.5%	12.4%	6.2%
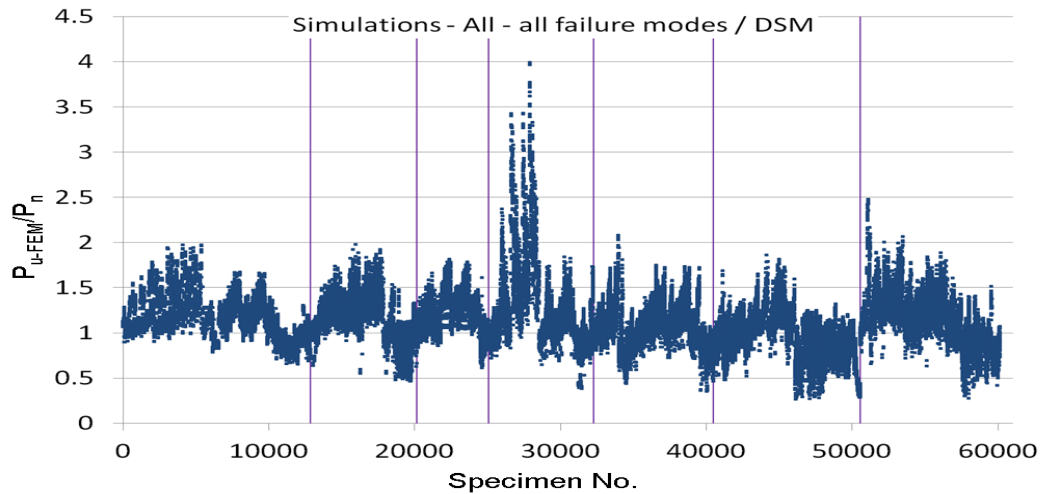
Fig. 19: Simulation-to-predicted ratios for all columns by DSM Method 8 with classified failure modes
(from left to right: L, LG, G, D, LD, DG, and LDG)
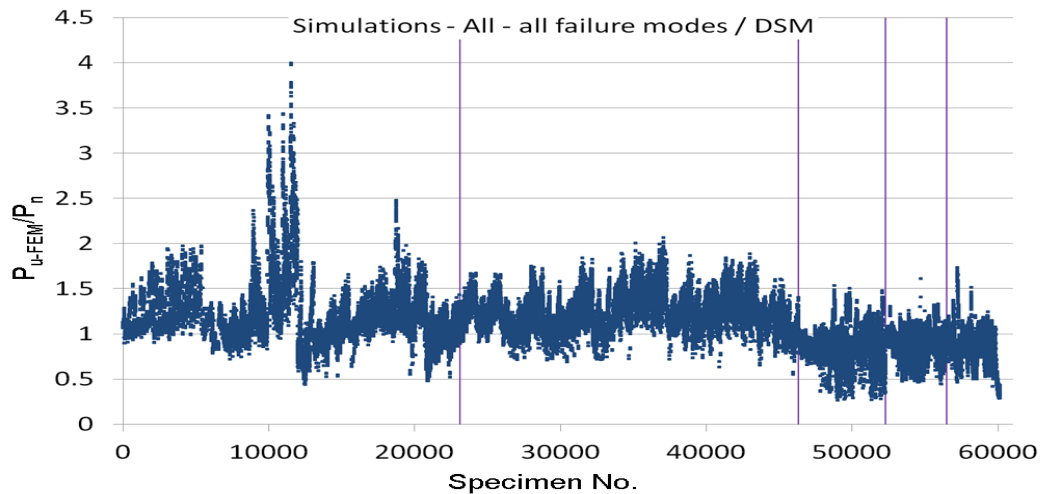
Fig. 20: Simulation-to-predicted ratios for all columns by DSM Method 8 with classified section types
(from left to right: C, Z, Hat, Rack and Stiffened C)

3.2. Modification to the DSM by Moen and Schafer (2011)

Of the previously explored design methods (i.e. DSM Method 1, 5, 6, 7, and 8) which did not consider interactive buckling except LG interaction, Method 6 (i.e. Option 4 in (Moen and Schafer 2011) presented in Section 2.3.2) produced the lowest scatter in the predictions as indicated by its overall V_p value of 0.199, compared to 0.212, 0.227, 0.226 and 0.254 for Methods 1, 5, 7 and 8, respectively. As the primary concern for an accurate design method is its ability to produce small variation in the predictions, Method 6 was chosen as the basis for all subsequent explorations.

3.2.1. Methods 9-12 – simple modifications – all

Options were first sought to simplify DSM Method 6. As shown in Equations (13)-(20), the design expressions employed the elastic buckling properties including the influence of holes in order to calculate the design strength of the column. This requires the designer to spend considerable time in modifying the original cross-section, calculating the weighted cross-sectional properties, performing a series of elastic buckling analyses by the SAFSM, identifying the minimum of buckling loads, before finally obtaining the required elastic buckling loads. This approach could impede the design efficiency especially if the inclusion of such elastic buckling loads would not significantly improve design accuracy. In addition, the modified distortional buckling strength prediction equations, i.e. Equations (17)-(20), also require more calculating time. In view of these considerations, four simple modifications to DSM Method 6, i.e. the Option 4 proposed by Moen and Schafer (2011), were first evaluated as follows:

(i) DSM Method 9 - Modification 1: replacing the $P_{cr\text{-}e\text{-}h}$ in Equations (13)-(14) by $P_{cr\text{-}e\text{-}nh}$ for the gross section.

(ii) DSM Method 10 - Modification 2: replacing the $P_{cr\text{-}l\text{-}h}$ in Equations (15)-(16) by $P_{cr\text{-}l\text{-}nh}$ for the gross section.

(iii) DSM Method 11 - Modification 3: replacing the $P_{cr\text{-}d\text{-}h}$ in Equations (17)-(20) by $P_{cr\text{-}d\text{-}nh}$ for the gross section.

(iv) DSM Method 12 - Modification 4: replacing the Equations (17)-(20) for distortional buckling by the Equations (5)-(6) as in the AS/NZS 4600 DSM, but capping the predicted strength P_{nd} to P_{yn} when $\lambda_d \leq 0.561$ and using $P_{cr\text{-}d\text{-}h}$ which includes the influence of holes.

The statistics of the predictions using DSM Methods 9-12 are tabulated in Table 39 -Table 40, Table 43-Table 44, Table 47-Table 48, and Table 51-Table 52, respectively. The percentage differences between the statistics for DSM Methods 9-12 and DSM Method 6 (i.e. Option 4 proposed by Moen and Schafer (2011)) are given in Table 41-Table 42, Table 45-Table 46, Table 49-Table 50, and Table 53-Table 54, respectively.

The results for DSM Method 9 (Table 39-Table 42) show that replacing $P_{cr\text{-}e\text{-}h}$ by $P_{cr\text{-}e\text{-}nh}$ in Method 6 only slightly adversely affected the predictions, as indicated by a decrease of 1.4% in the overall value of P_m, an increase of 5 % in the overall value of V_p, and a decrease of 3.0% in the overall value of ϕ. In particular, this modification only influenced the predictions for the G, LG, DG and LDG modes, of which the G mode was most adversely affected with a considerable 48.8% increase in V_p and a 8.4% decrease in ϕ. In addition, the section most adversely affected by this method was Rack section as shown by a 6.7% decrease in ϕ, while the least affected section was Z section with a 1.3% decrease in ϕ.

As for Method 10 (Table 43-Table 44), the comparison with Method 6 (Table 45-Table 46) shows that this method virtually made no difference to the strength predictions with a decrease of only 0.1% in the overall

value of ϕ. This was because in most cases the simplified methods produced the same elastic local buckling loads between non-perforated and perforated members.

In addition, the results for Method 11 (Table 47-Table 50) demonstrate that although replacing $P_{\text{cr-d-h}}$ by $P_{\text{cr-d-nh}}$ reduced the overall resistance factor ϕ by 2.1%, the overall value of V_p favourably decreased by 3.5%. This reduced scatter in prediction was observed for a majority of individual sections and failure modes, especially for C section which showed a significant decrease of 10.8% in the overall V_p. In contrast, Z section was most adversely affected in that it had an increase of 8.8% in the overall V_p. However, a close examination revealed that the maximum increase in V_p for each individual mode of Z section was only 2.5% (in the LDG mode), which implied that the higher increase in the overall value of V_p mainly came from differences in the mean values P_m between different modes. In addition, of all modes, the LD mode was most adversely affected in terms of the decrease in ϕ (7.6%), while the D mode benefited most in terms of the decrease in V_p (17.7%).

With regards to Method 12, Table 51-Table 54 clearly show that reverting to using the distortional strength equations (5)-(6) as in the AS/NZS 4600 DSM significantly decreased the accuracy of the predictions concerning members failing in the D mode, as shown by the 11.1% increase in V_p and 7.8% decrease in ϕ. Otherwise, this method had a very slight influence on the LD mode, and almost no influence on the other modes.

Moreover, two figures are also provided for each method to illustrate the simulation-to-predicted ratios ($P_{\text{u-FEM}}/P_n$), as shown in Fig. 21-Fig. 22, Fig. 23-Fig. 24, Fig. 25-Fig. 26, and Fig. 27-Fig. 28 for DSM Methods 9-12 respectively. In comparison with the corresponding figures for DSM Method 6 (Fig. 15 and Fig. 16), very subtle differences are seen in the figures for Methods 9, 10 and 12, whereas it was obvious to see a reduced variation in the $P_{\text{u-FEM}}/P_n$ ratios for the D mode obtained by Method 11.

The overall statistics of the predictions by DSM Methods 9-12 are also summarised in Table 38. The results suggest that if one wishes to use the original design method, i.e. Option 4, proposed by Moen and Schafer (2011), it may not be necessary to calculate (i) the local buckling load as per the simplified methods (Moen and Schafer 2009) because DSM Method 10 has shown that using the local buckling load based on the gross section produced virtually the same results, and (ii) the distortional buckling load as per the simplified methods (Moen and Schafer 2009) because DSM Method 11 has shown that using the distortional buckling load based on the gross section produced a smaller scatter (V_p=0.192) in the predictions.

Table 38: Summary of resistance factors by DSM Methods 9-12

Prediction method	Classification	P_m	V_p	ϕ	n
DSM Method 6 - original (Moen and Schafer 2011)	All columns	0.993	0.199	0.726	59558
DSM Method 9 - modification 1 to (Moen and Schafer 2011)	All columns	0.979	0.209	0.704	59558
DSM Method 10 - modification 2 to (Moen and Schafer 2011)	All columns	0.992	0.200	0.725	59558
DSM Method 11 - modification 3 to (Moen and Schafer 2011)	All columns	0.961	0.192	0.711	59558
DSM Method 12 - modification 4 to (Moen and Schafer 2011)	All columns	0.986	0.203	0.716	59558

Table 39: Resistance factors for all columns failing in modes L, LG, G, and L+LG+G+D by **DSM Method 9** – Modification 1 to Option 4 in (Moen and Schafer 2011) – replace P_{cr-e-h} by $P_{cr-e-nh}$

prediction method	Section shape	Failure mode																				
		L				LG				G				D				All L, LG, G, D			
		P_m	V_p	ϕ	n	P_m	V_p	ϕ	n	P_m	V_p	ϕ	n	P_m	V_p	ϕ	n	P_m	V_p	ϕ	n
DSM Method 9	C	1.078	0.134	0.866	6923	0.991	0.119	0.810	4245	0.872	0.144	0.691	1651	1.231	0.256	0.815	3678	1.069	0.204	0.776	16497
	Z	1.067	0.111	0.880	3712	1.089	0.102	0.907	784	1.017	0.068	0.872	2548	1.030	0.097	0.862	2444	1.046	0.100	0.872	9488
	Hat	0.852	0.096	0.714	1414	0.942	0.213	0.673	494	1.071	0.057	0.924	137	0.866	0.169	0.664	441	0.884	0.156	0.690	2486
	Rack	0.977	0.093	0.820	461	0.823	0.265	0.537	1065	0.909	0.177	0.688	383	0.913	0.093	0.767	391	0.884	0.205	0.640	2300
	Stiffened C	0.950	0.106	0.787	317	1.018	0.135	0.817	143	0.967	0.102	0.805	196	1.096	0.251	0.733	245	1.004	0.181	0.756	901
	All sections	1.043	0.142	0.830	12827	0.973	0.167	0.747	6731	0.959	0.128	0.776	4915	1.119	0.243	0.759	7199	1.032	0.186	0.771	31672

Table 40: Resistance factors for all columns failing in modes LD, DG, LDG, LD+DG+LDG, and all failure modes by **DSM Method 9** – Modification 1 to Option 4 in (Moen and Schafer 2011) – replace P_{cr-e-h} by $P_{cr-e-nh}$

prediction method	Section shape	Failure mode																				
		LD				DG				LDG				All LD, DG, LDG				ALL Failure modes			
		P_m	V_p	ϕ	n	P_m	V_p	ϕ	n	P_m	V_p	ϕ	n	P_m	V_p	ϕ	n	P_m	V_p	ϕ	n
DSM Method 9	C	0.881	0.187	0.657	3157	0.794	0.190	0.589	2589	1.048	0.234	0.723	862	0.869	0.219	0.615	6608	1.012	0.226	0.707	23105
	Z	0.999	0.122	0.814	4115	0.985	0.119	0.805	2989	1.055	0.165	0.813	6057	1.022	0.148	0.806	13161	1.032	0.130	0.833	22649
	Hat	0.775	0.176	0.588	585	0.733	0.283	0.462	1927	0.828	0.246	0.559	964	0.766	0.262	0.503	3476	0.815	0.228	0.568	5962
	Rack	0.824	0.101	0.687	137	0.845	0.204	0.613	832	0.886	0.194	0.654	900	0.863	0.195	0.635	1869	0.874	0.201	0.638	4169
	Stiffened C	0.795	0.187	0.593	245	0.754	0.286	0.472	1727	0.838	0.231	0.581	800	0.782	0.265	0.509	2772	0.836	0.267	0.543	3673
	All sections	0.929	0.172	0.708	8239	0.836	0.236	0.575	10064	0.998	0.208	0.719	9583	0.919	0.220	0.649	27886	0.979	0.209	0.704	59558

Table 41: Difference in resistance factors between **DSM Method 9** and **DSM Method 6** for all columns failing in modes L, LG, G, D, and L+LG+G+D

prediction method	Section shape	Failure mode														
		L			LG			G			D			All L, LG, G, D		
		P_m	V_p	ϕ	P_m	V_p	ϕ	P_m	V_p	ϕ	P_m	V_p	ϕ	P_m	V_p	ϕ
DSM Method 9	C	0.0%	0.0%	0.0%	-3.9%	12.3%	-5.3%	-7.2%	46.9%	-12.1%	0.0%	0.0%	0.0%	-1.6%	7.4%	-3.8%
	Z	0.0%	0.0%	0.0%	-1.8%	17.2%	-3.1%	-2.2%	51.1%	-3.4%	0.0%	0.0%	0.0%	-0.8%	5.3%	-1.2%
	Hat	0.0%	0.0%	0.0%	-1.1%	4.4%	-2.6%	-1.5%	29.5%	-2.2%	0.0%	0.0%	0.0%	-0.3%	0.6%	-0.4%
	Rack	0.0%	0.0%	0.0%	-5.6%	19.4%	-12.5%	-8.2%	55.3%	-15.5%	0.0%	0.0%	0.0%	-3.9%	19.2%	-8.8%
	Stiffened C	0.0%	0.0%	0.0%	0.0%	0.0%	0.0%	-5.6%	52.2%	-8.3%	0.0%	0.0%	0.0%	-1.2%	4.0%	-2.2%
	All sections	0.0%	0.0%	0.0%	-3.6%	12.8%	-6.2%	-4.4%	48.8%	-8.4%	0.0%	0.0%	0.0%	-1.4%	6.9%	-3.1%

Table 42: Difference in resistance factors between **DSM Method 9** and **DSM Method 6** for all columns failing in modes LD, DG, LDG, LD+DG+LDG, and all failure modes

prediction method	Section shape	Failure mode														
		LD			DG			LDG			All LD, DG, LDG			ALL Failure modes		
		P_m	V_p	ϕ	P_m	V_p	ϕ	P_m	V_p	ϕ	P_m	V_p	ϕ	P_m	V_p	ϕ
DSM Method 9	C	0.0%	0.0%	0.0%	-5.0%	9.2%	-7.4%	-1.1%	4.5%	-2.8%	-2.0%	6.3%	-4.1%	-1.7%	6.1%	-3.9%
	Z	0.0%	0.0%	0.0%	-1.3%	9.2%	-2.4%	-0.8%	3.8%	-1.7%	-0.7%	3.5%	-1.3%	-0.7%	4.0%	-1.3%
	Hat	0.0%	0.0%	0.0%	-3.6%	1.8%	-4.3%	-1.1%	2.5%	-2.3%	-2.3%	2.3%	-3.3%	-1.5%	2.2%	-2.4%
	Rack	0.0%	0.0%	0.0%	-4.0%	13.3%	-7.5%	-1.0%	3.7%	-1.9%	-2.3%	7.7%	-4.5%	-3.2%	13.6%	-6.7%
	Stiffened C	0.0%	0.0%	0.0%	-2.7%	0.0%	-2.9%	-1.9%	7.9%	-4.6%	-2.3%	1.9%	-3.2%	-2.0%	2.7%	-3.2%
	All sections	0.0%	0.0%	0.0%	-3.1%	5.8%	-5.1%	-1.0%	3.5%	-2.2%	-1.4%	4.3%	-3.0%	-1.4%	5.0%	-3.0%

Table 43: Resistance factors for all columns failing in modes L, LG, G, D, and L+LG+G+D by **DSM Method 10** – Modification 2 to Option 4 in (Moen and Schafer 2011) – replace P_{cr-l-h} by $P_{cr-l-nh}$

prediction method	Section shape	Failure mode																			
		L				LG				G				D				All L, LG, G, D			
		P_m	V_p	ϕ	n	P_m	V_p	ϕ	n	P_m	V_p	ϕ	n	P_m	V_p	ϕ	n	P_m	V_p	ϕ	n
DSM Method 10	C	1.077	0.135	0.865	6923	1.031	0.106	0.855	4245	0.940	0.098	0.786	1651	1.231	0.256	0.815	3678	1.086	0.190	0.806	16497
	Z	1.066	0.111	0.880	3712	1.109	0.087	0.936	784	1.040	0.045	0.903	2548	1.030	0.097	0.862	2444	1.053	0.094	0.883	9488
	Hat	0.848	0.102	0.706	1414	0.950	0.207	0.686	494	1.087	0.044	0.945	137	0.866	0.169	0.664	441	0.885	0.159	0.688	2486
	Rack	0.977	0.093	0.820	461	0.872	0.222	0.614	1065	0.990	0.114	0.814	383	0.913	0.093	0.767	391	0.920	0.172	0.702	2300
	Stiffened C	0.945	0.113	0.778	317	1.018	0.135	0.817	143	1.024	0.067	0.878	196	1.096	0.251	0.733	245	1.015	0.176	0.769	901
	All sections	1.042	0.143	0.828	12827	1.009	0.149	0.795	6731	1.003	0.086	0.847	4915	1.119	0.243	0.759	7199	1.046	0.175	0.795	31672

Table 44: Resistance factors for all columns failing in modes LD, DG, LDG, LD+DG+LDG, and all failure modes by **DSM Method 10** – Modification 2 to Option 4 in (Moen and Schafer 2011) – replace P_{cr-l-h} by $P_{cr-l-nh}$

prediction method	Section shape	Failure mode																			
		LD				DG				LDG				All LD, DG, LDG				ALL Failure modes			
		P_m	V_p	ϕ	n	P_m	V_p	ϕ	n	P_m	V_p	ϕ	n	P_m	V_p	ϕ	n	P_m	V_p	ϕ	n
DSM Method 10	C	0.881	0.187	0.657	3157	0.836	0.174	0.636	2589	1.060	0.224	0.743	862	0.887	0.206	0.641	6608	1.029	0.213	0.735	23105
	Z	0.999	0.122	0.814	4115	0.998	0.109	0.825	2989	1.064	0.159	0.827	6057	1.029	0.143	0.817	13161	1.039	0.125	0.844	22649
	Hat	0.775	0.177	0.586	585	0.758	0.280	0.480	1927	0.826	0.254	0.550	964	0.780	0.260	0.513	3476	0.823	0.227	0.575	5962
	Rack	0.824	0.101	0.687	137	0.880	0.180	0.663	832	0.894	0.188	0.667	900	0.883	0.181	0.665	1869	0.903	0.177	0.684	4169
	Stiffened C	0.795	0.187	0.593	245	0.774	0.286	0.485	1727	0.854	0.214	0.610	800	0.799	0.260	0.525	2772	0.852	0.260	0.560	3673
	All sections	0.929	0.172	0.708	8239	0.862	0.224	0.605	10064	1.006	0.203	0.732	9583	0.931	0.212	0.667	27886	0.992	0.200	0.725	59558

Table 45: Difference in resistance factors between **DSM Method 10** and **DSM Method 6** for all columns failing in modes L, LG, G, D, and L+LG+G+D

prediction method	Section shape	Failure mode														
		L			LG			G			D			All L, LG, G, D		
		P_m	V_p	ϕ	P_m	V_p	ϕ	P_m	V_p	ϕ	P_m	V_p	ϕ	P_m	V_p	ϕ
DSM Method 10	C	-0.1%	0.7%	-0.1%	0.0%	0.0%	0.0%	0.0%	0.0%	0.0%	0.0%	0.0%	0.0%	0.0%	0.0%	-0.1%
	Z	-0.1%	0.0%	0.0%	0.0%	0.0%	0.0%	0.0%	0.0%	0.0%	0.0%	0.0%	0.0%	-0.1%	-1.1%	0.0%
	Hat	-0.5%	6.2%	-1.1%	-0.2%	1.5%	-0.7%	0.0%	0.0%	0.0%	0.0%	0.0%	0.0%	-0.2%	2.6%	-0.7%
	Rack	0.0%	0.0%	0.0%	0.0%	0.0%	0.0%	0.0%	0.0%	0.0%	0.0%	0.0%	0.0%	0.0%	0.0%	0.0%
	Stiffened C	-0.5%	6.6%	-1.1%	0.0%	0.0%	0.0%	0.0%	0.0%	0.0%	0.0%	0.0%	0.0%	-0.1%	1.1%	-0.5%
	All sections	-0.1%	0.7%	-0.2%	0.0%	0.7%	-0.1%	0.0%	0.0%	0.0%	0.0%	0.0%	0.0%	-0.1%	0.6%	-0.1%

Table 46: Difference in resistance factors between **DSM Method 10** and **DSM Method 6** for all columns failing in modes LD, DG, LDG, LD+DG+LDG, and all

failure modes

prediction method	Section shape	Failure mode														
		LD			DG			LDG			All LD, DG, LDG			ALL Failure modes		
		P_m	V_p	ϕ	P_m	V_p	ϕ	P_m	V_p	ϕ	P_m	V_p	ϕ	P_m	V_p	ϕ
DSM Method 10	C	0.0%	0.0%	0.0%	0.0%	0.0%	0.0%	0.0%	0.0%	-0.1%	0.0%	0.0%	0.0%	0.0%	0.0%	-0.1%
	Z	0.0%	0.0%	0.0%	0.0%	0.0%	0.0%	0.0%	0.0%	0.0%	0.0%	0.0%	0.0%	0.0%	0.0%	0.0%
	Hat	0.0%	0.6%	-0.3%	-0.3%	0.7%	-0.6%	-1.3%	5.8%	-3.8%	-0.5%	1.6%	-1.3%	-0.5%	1.8%	-1.2%
	Rack	0.0%	0.0%	0.0%	0.0%	0.0%	0.0%	-0.1%	0.5%	0.0%	0.0%	0.0%	0.0%	0.0%	0.0%	0.0%
	Stiffened C	0.0%	0.0%	0.0%	-0.1%	0.0%	-0.2%	0.0%	0.0%	0.2%	-0.1%	0.0%	-0.2%	-0.1%	0.0%	-0.2%
	All sections	0.0%	0.0%	0.0%	-0.1%	0.4%	-0.2%	-0.2%	1.0%	-0.4%	-0.1%	0.5%	-0.3%	-0.1%	0.5%	-0.1%

Table 47: Resistance factors for all columns failing in modes L, LG, G, D, and L+LG+G+D by **DSM Method 11** – Modification 3 to Option 4 in (Moen and Schafer 2011) – replace P_{cr-d-h} by $P_{cr-d-nh}$

prediction method	Section shape	Failure mode																				
		L				LG				G				D				All L, LG, G, D			
		P_m	V_p	ϕ	n	P_m	V_p	ϕ	n	P_m	V_p	ϕ	n	P_m	V_p	ϕ	n	P_m	V_p	ϕ	n
DSM Method 11	C	1.078	0.134	0.866	6923	1.026	0.107	0.850	4245	0.940	0.098	0.786	1651	1.108	0.206	0.802	3678	1.058	0.155	0.827	16497
	Z	1.066	0.112	0.879	3712	1.109	0.087	0.936	784	1.040	0.045	0.903	2548	0.957	0.090	0.806	2444	1.034	0.102	0.861	9488
	Hat	0.852	0.096	0.714	1414	0.923	0.181	0.694	494	1.087	0.044	0.945	137	0.831	0.162	0.643	441	0.875	0.146	0.693	2486
	Rack	0.977	0.093	0.820	461	0.854	0.205	0.619	1065	0.990	0.114	0.814	383	0.847	0.104	0.704	391	0.900	0.170	0.689	2300
	Stiffened C	0.950	0.106	0.787	317	0.919	0.138	0.734	143	1.024	0.067	0.878	196	1.009	0.241	0.687	245	0.977	0.161	0.757	901
	All sections	1.043	0.142	0.829	12827	0.999	0.148	0.789	6731	1.003	0.086	0.847	4915	1.022	0.200	0.747	7199	1.023	0.153	0.801	31672

Table 48: Resistance factors for all columns failing in modes LD, DG, LDG, LD+DG+LDG, and all failure modes by **DSM Method 11** – Modification 3 to Option 4 in (Moen and Schafer 2011) – replace P_{cr-d-h} by $P_{cr-d-nh}$

prediction method	Section shape	Failure mode																				
		LD				DG				LDG				All LD, DG, LDG				ALL Failure modes			
		P_m	V_p	ϕ	n	P_m	V_p	ϕ	n	P_m	V_p	ϕ	n	P_m	V_p	ϕ	n	P_m	V_p	ϕ	n
DSM Method 11	C	0.813	0.173	0.620	3157	0.827	0.181	0.623	2589	1.009	0.168	0.774	862	0.844	0.191	0.626	6608	0.997	0.190	0.740	23105
	Z	0.899	0.118	0.736	4115	0.989	0.111	0.816	2989	1.037	0.163	0.801	6057	0.983	0.154	0.769	13161	1.004	0.136	0.805	22649
	Hat	0.716	0.178	0.541	585	0.748	0.286	0.469	1927	0.816	0.235	0.562	964	0.762	0.261	0.500	3476	0.809	0.224	0.567	5962
	Rack	0.734	0.106	0.609	137	0.861	0.172	0.656	832	0.838	0.183	0.629	900	0.840	0.179	0.635	1869	0.873	0.177	0.662	4169
	Stiffened C	0.715	0.203	0.520	245	0.750	0.297	0.460	1727	0.822	0.201	0.600	800	0.768	0.267	0.499	2772	0.819	0.261	0.538	3673
	All sections	0.845	0.162	0.654	8239	0.850	0.229	0.591	10064	0.975	0.199	0.714	9583	0.892	0.212	0.638	27886	0.961	0.192	0.711	59558

Table 49: Difference in resistance factors between **DSM Method 11** and **DSM Method 6** for all columns failing in modes L, LG, G, D, and L+LG+G+D

prediction method	Section shape	Failure mode														
		L			LG			G			D			All L, LG, G, D		
		P_m	V_p	ϕ	P_m	V_p	ϕ	P_m	V_p	ϕ	P_m	V_p	ϕ	P_m	V_p	ϕ
DSM Method 11	C	0.0%	0.0%	0.0%	-0.5%	0.9%	-0.6%	0.0%	0.0%	0.0%	-10.0%	-19.5%	-1.6%	-2.6%	-18.4%	2.5%
	Z	-0.1%	0.9%	-0.1%	0.0%	0.0%	0.0%	0.0%	0.0%	0.0%	-7.1%	-7.2%	-6.5%	-1.9%	7.4%	-2.5%
	Hat	0.0%	0.0%	0.0%	-3.0%	-11.3%	0.4%	0.0%	0.0%	0.0%	-4.0%	-4.1%	-3.2%	-1.4%	-5.8%	0.0%
	Rack	0.0%	0.0%	0.0%	-2.1%	-7.7%	0.8%	0.0%	0.0%	0.0%	-7.2%	11.8%	-8.2%	-2.2%	-1.2%	-1.9%
	Stiffened C	0.0%	0.0%	0.0%	-9.7%	2.2%	-10.2%	0.0%	0.0%	0.0%	-7.9%	-4.0%	-6.3%	-3.8%	-7.5%	-2.1%
	All sections	0.0%	0.0%	-0.1%	-1.0%	0.0%	-0.9%	0.0%	0.0%	0.0%	-8.7%	-17.7%	-1.6%	-2.3%	-12.1%	0.6%

Table 50: Difference in resistance factors between **DSM Method 11** and **DSM Method 6** for all columns failing in modes LD, DG, LDG, LD+DG+LDG, and all failure modes

prediction method	Section shape	Failure mode														
		LD			DG			LDG			All LD, DG, LDG			ALL Failure modes		
		P_m	V_p	ϕ	P_m	V_p	ϕ	P_m	V_p	ϕ	P_m	V_p	ϕ	P_m	V_p	ϕ
DSM Method 11	C	-7.7%	-7.5%	-5.6%	-1.1%	4.0%	-2.0%	-4.8%	-25.0%	4.0%	-4.8%	-7.3%	-2.3%	-3.1%	-10.8%	0.5%
	Z	-10.0%	-3.3%	-9.6%	-0.9%	1.8%	-1.1%	-2.5%	2.5%	-3.1%	-4.5%	7.7%	-5.9%	-3.4%	8.8%	-4.6%
	Hat	-7.6%	1.1%	-8.0%	-1.6%	2.9%	-2.9%	-2.5%	-2.1%	-1.7%	-2.8%	2.0%	-3.8%	-2.2%	0.4%	-2.6%
	Rack	-10.9%	5.0%	-11.4%	-2.2%	-4.4%	-1.1%	-6.4%	-2.1%	-5.7%	-4.9%	-1.1%	-4.5%	-3.3%	0.0%	-3.2%
	Stiffened C	-10.1%	8.6%	-12.3%	-3.2%	3.8%	-5.3%	-3.7%	-6.1%	-1.5%	-4.0%	2.7%	-5.1%	-4.0%	0.4%	-4.1%
	All sections	-9.0%	-5.8%	-7.6%	-1.5%	2.7%	-2.5%	-3.3%	-1.0%	-2.9%	-4.3%	0.5%	-4.6%	-3.2%	-3.5%	-2.1%

Table 51: Resistance factors for all columns failing in modes L, LG, G, D, and L+LG+G+D by **DSM Method 12** – Modification 4 to Option 4 in (Moen and Schafer 2011) – replace the D equation by the AS/NZS 4600 DSM D equation, limit P_{nd} to P_{yn}; use P_{cr-d-h}

prediction method	Section shape	Failure mode																			
		L				LG				G				D				All L, LG, G, D			
		P_m	V_p	ϕ	n	P_m	V_p	ϕ	n	P_m	V_p	ϕ	n	P_m	V_p	ϕ	n	P_m	V_p	ϕ	n
DSM Method 12	C	1.078	0.134	0.866	6923	1.031	0.106	0.855	4245	0.940	0.098	0.786	1651	1.190	0.291	0.738	3678	1.077	0.197	0.791	16497
	Z	1.067	0.111	0.880	3712	1.109	0.087	0.936	784	1.040	0.045	0.903	2548	0.992	0.129	0.802	2444	1.044	0.106	0.865	9488
	Hat	0.852	0.096	0.714	1414	0.947	0.209	0.681	494	1.087	0.044	0.945	137	0.846	0.190	0.627	441	0.883	0.161	0.684	2486
	Rack	0.977	0.093	0.820	461	0.872	0.222	0.614	1065	0.990	0.114	0.814	383	0.912	0.095	0.765	391	0.919	0.172	0.702	2300
	Stiffened C	0.950	0.106	0.787	317	1.018	0.135	0.817	143	1.024	0.067	0.878	196	1.093	0.254	0.728	245	1.016	0.175	0.771	901
	All sections	1.043	0.142	0.830	12827	1.009	0.149	0.795	6731	1.003	0.086	0.847	4915	1.083	0.270	0.700	7199	1.039	0.180	0.783	31672

Table 52: Resistance factors for all columns failing in modes LD, DG, LDG, LD+DG+LDG, and all failure modes by **DSM Method 12** – Modification 4 to Option 4 in (Moen and Schafer 2011) – replace the D equation by the AS/NZS 4600 DSM D equation, limit P_{nd} to P_{yn}; use P_{cr-d-h}

prediction method	Section shape	Failure mode																			
		LD				DG				LDG				All LD, DG, LDG				ALL Failure modes			
		P_m	V_p	ϕ	n	P_m	V_p	ϕ	n	P_m	V_p	ϕ	n	P_m	V_p	ϕ	n	P_m	V_p	ϕ	n
DSM Method 12	C	0.872	0.191	0.646	3157	0.828	0.181	0.623	2589	1.053	0.232	0.729	862	0.878	0.213	0.628	6608	1.020	0.219	0.722	23105
	Z	0.985	0.134	0.792	4115	0.989	0.115	0.813	2989	1.061	0.160	0.823	6057	1.021	0.149	0.805	13161	1.030	0.133	0.829	22649
	Hat	0.775	0.177	0.587	585	0.758	0.281	0.479	1927	0.837	0.240	0.572	964	0.783	0.258	0.517	3476	0.824	0.225	0.577	5962
	Rack	0.824	0.101	0.687	137	0.879	0.181	0.662	832	0.894	0.188	0.667	900	0.883	0.181	0.664	1869	0.903	0.177	0.684	4169
	Stiffened C	0.795	0.187	0.593	245	0.775	0.286	0.486	1727	0.854	0.214	0.609	800	0.800	0.261	0.526	2772	0.853	0.260	0.561	3673
	All sections	0.918	0.177	0.695	8239	0.857	0.225	0.601	10064	1.005	0.202	0.732	9583	0.926	0.214	0.661	27886	0.986	0.203	0.716	59558

Table 53: Difference in resistance factors between **DSM Method 12** and **DSM Method 6** for all columns failing in modes L, LG, G, D, and L+LG+G+D

prediction method	Section shape	Failure mode														
		L			LG			G			D			All L, LG, G, D		
		P_m	V_p	ϕ	P_m	V_p	ϕ	P_m	V_p	ϕ	P_m	V_p	ϕ	P_m	V_p	ϕ
DSM Method 12	C	0.0%	0.0%	0.0%	0.0%	0.0%	0.0%	0.0%	0.0%	0.0%	-3.3%	13.7%	-9.4%	-0.8%	3.7%	-2.0%
	Z	0.0%	0.0%	0.0%	0.0%	0.0%	0.0%	0.0%	0.0%	0.0%	-3.7%	33.0%	-7.0%	-0.9%	11.6%	-2.0%
	Hat	0.0%	0.0%	0.0%	-0.5%	2.5%	-1.4%	0.0%	0.0%	0.0%	-2.3%	12.4%	-5.6%	-0.5%	3.9%	-1.3%
	Rack	0.0%	0.0%	0.0%	0.0%	0.0%	0.0%	0.0%	0.0%	0.0%	-0.1%	2.2%	-0.3%	-0.1%	0.0%	0.0%
	Stiffened C	0.0%	0.0%	0.0%	0.0%	0.0%	0.0%	0.0%	0.0%	0.0%	-0.3%	1.2%	-0.7%	0.0%	0.6%	-0.3%
	All sections	0.0%	0.0%	0.0%	0.0%	0.7%	-0.1%	0.0%	0.0%	0.0%	-3.2%	11.1%	-7.8%	-0.8%	3.4%	-1.6%

Table 54: Difference in resistance factors between **DSM Method 12** and **DSM Method 6** for all columns failing in modes LD, DG, LDG, LD+DG+LDG, and all

failure modes

prediction method	Section shape	Failure mode														
		LD			DG			LDG			All LD, DG, LDG			ALL Failure modes		
		P_m	V_p	ϕ	P_m	V_p	ϕ	P_m	V_p	ϕ	P_m	V_p	ϕ	P_m	V_p	ϕ
DSM Method 12	C	-1.0%	2.1%	-1.7%	-1.0%	4.0%	-2.0%	-0.7%	3.6%	-2.0%	-1.0%	3.4%	-2.0%	-0.9%	2.8%	-1.9%
	Z	-1.4%	9.8%	-2.7%	-0.9%	5.5%	-1.5%	-0.3%	0.6%	-0.5%	-0.8%	4.2%	-1.5%	-0.9%	6.4%	-1.8%
	Hat	0.0%	0.6%	-0.2%	-0.3%	1.1%	-0.8%	0.0%	0.0%	0.0%	-0.1%	0.8%	-0.6%	-0.4%	0.9%	-0.9%
	Rack	0.0%	0.0%	0.0%	-0.1%	0.6%	-0.2%	-0.1%	0.5%	0.0%	0.0%	0.0%	-0.2%	0.0%	0.0%	0.0%
	Stiffened C	0.0%	0.0%	0.0%	0.0%	0.0%	0.0%	0.0%	0.0%	0.0%	0.0%	0.4%	0.0%	0.0%	0.0%	0.0%
	All sections	-1.2%	2.9%	-1.8%	-0.7%	0.9%	-0.8%	-0.3%	0.5%	-0.4%	-0.6%	1.4%	-1.2%	-0.7%	2.0%	-1.4%
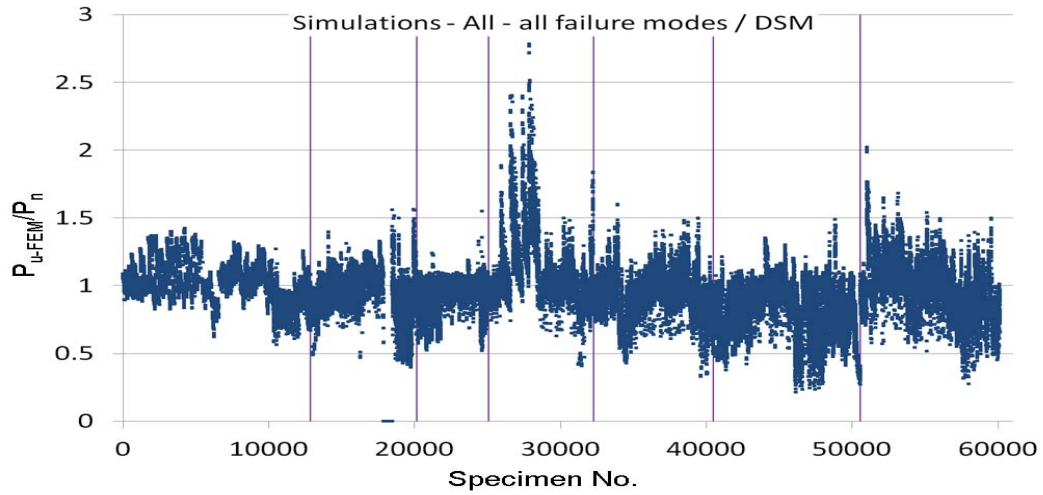
Fig. 21: Simulation-to-predicted ratios for all columns by DSM Method 9 with classified failure modes
(from left to right: L, LG, G, D, LD, DG, and LDG)
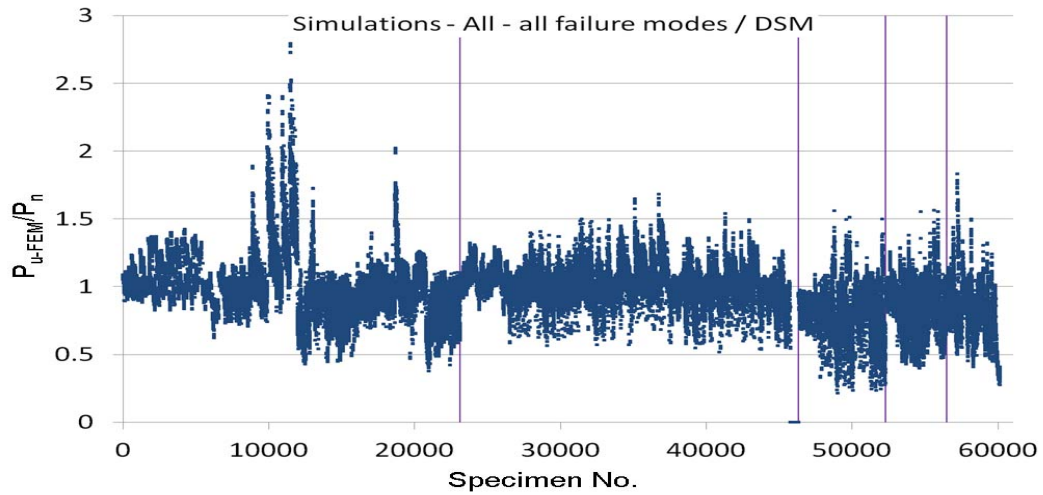
Fig. 22: Simulation-to-predicted ratios for all columns by DSM Method 9 with classified section types
(from left to right: C, Z, Hat, Rack and Stiffened C)
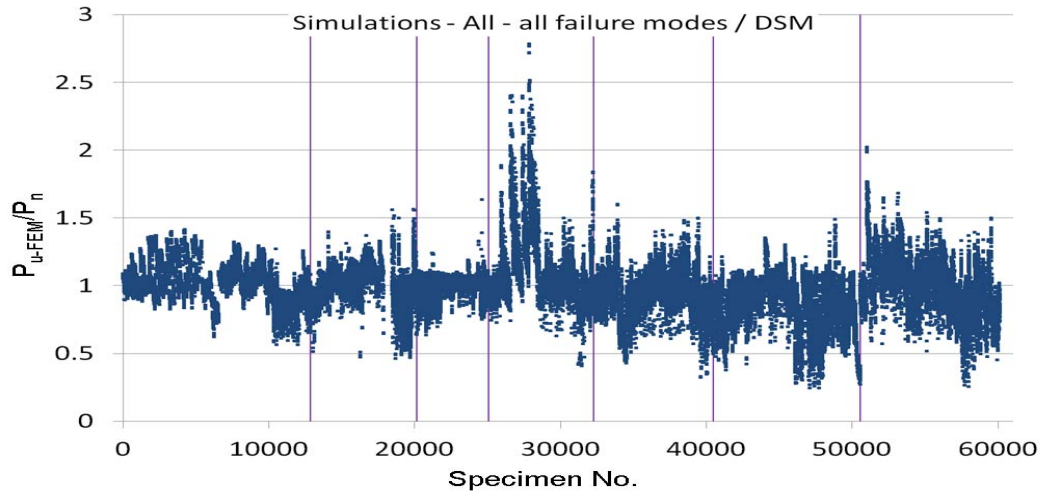
Fig. 23: Simulation-to-predicted ratios for all columns by DSM Method 10 with classified failure modes
(from left to right: L, LG, G, D, LD, DG, and LDG)
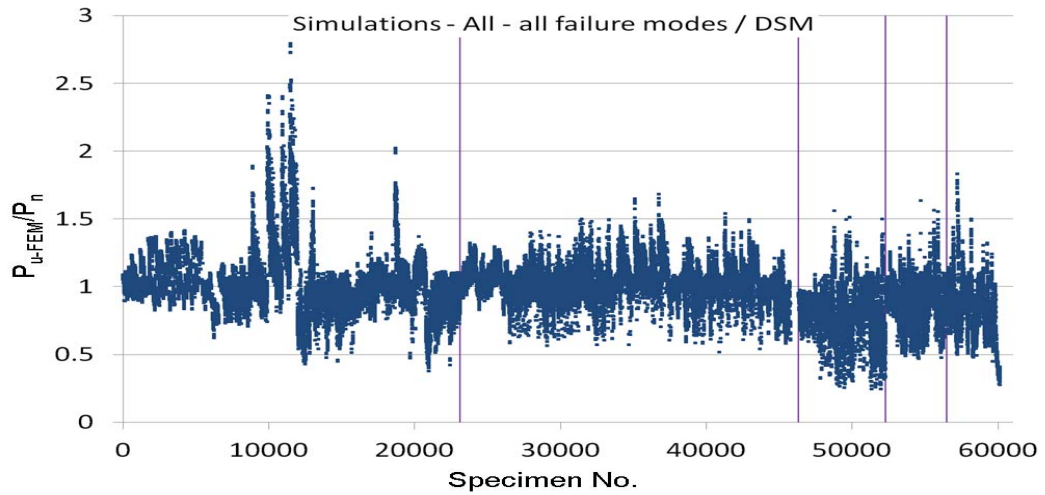
Fig. 24: Simulation-to-predicted ratios for all columns by DSM Method 10 with classified section types
(from left to right: C, Z, Hat, Rack and Stiffened C)
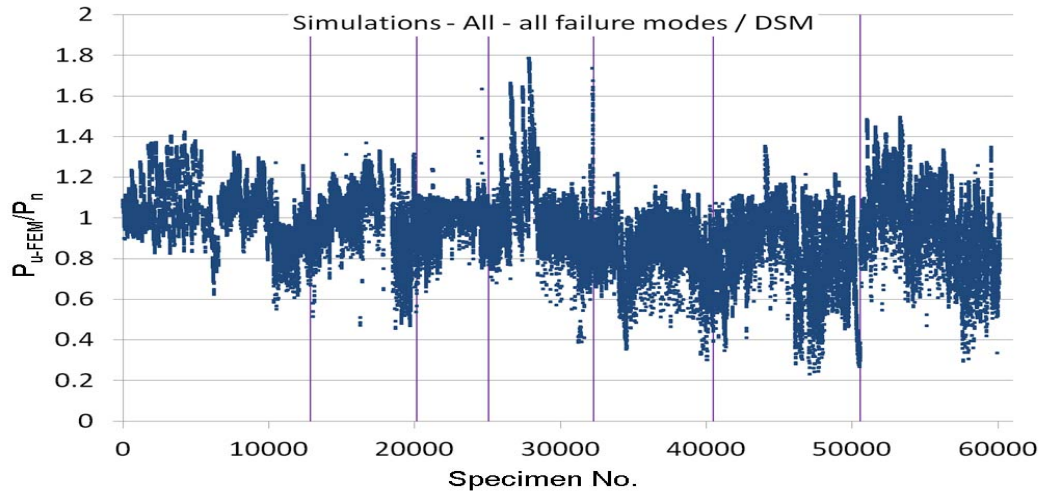
Fig. 25: Simulation-to-predicted ratios for all columns by DSM Method 11 with classified failure modes
(from left to right: L, LG, G, D, LD, DG, and LDG)
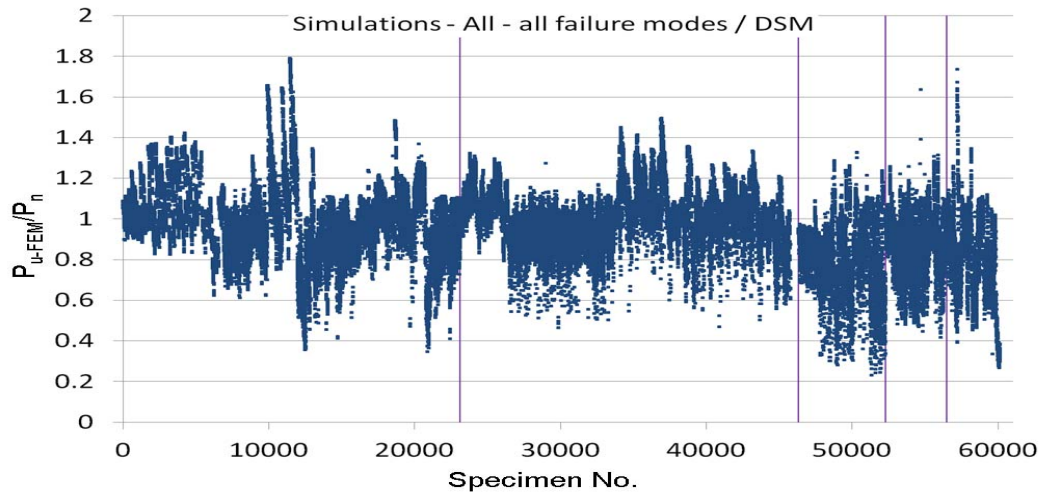
Fig. 26: Simulation-to-predicted ratios for all columns by DSM Method 11 with classified section types
(from left to right: C, Z, Hat, Rack and Stiffened C)
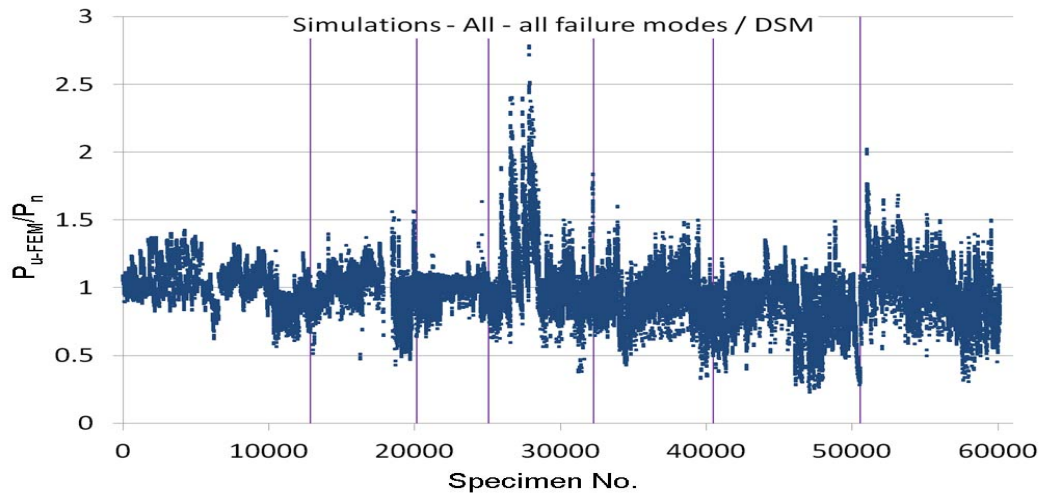
Fig. 27: Simulation-to-predicted ratios for all columns by DSM Method 12 with classified failure modes
(from left to right: L, LG, G, D, LD, DG, and LDG)
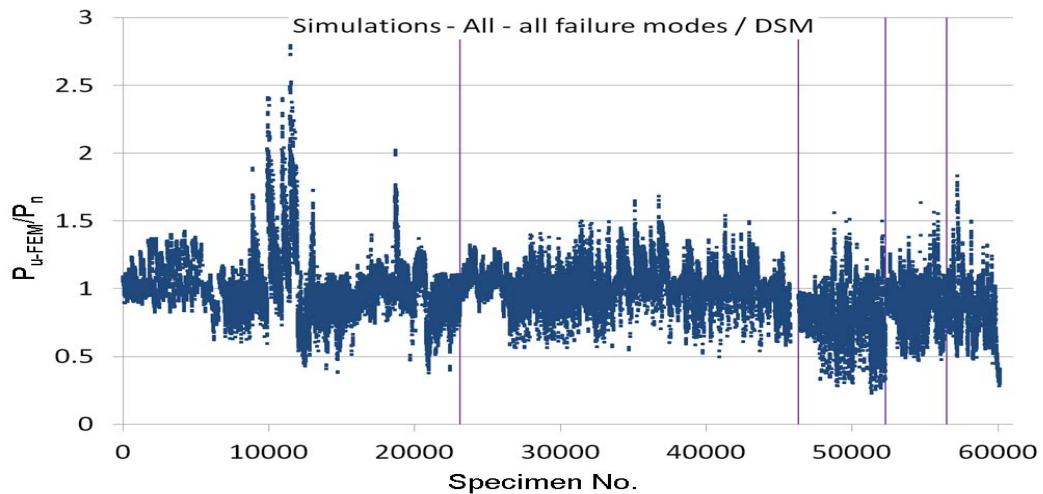
Fig. 28: Simulation-to-predicted ratios for all columns by DSM Method 12 with classified section types
(from left to right: C, Z, Hat, Rack and Stiffened C)

3.2.2. Method 13-15 – regression analyses of LG equations – all

The study in Section 3.2.1 indicates that the local-global Equations (15)-(16) in DSM Method 6 (i.e. Option 4 in (Moen and Schafer 2011)) had poorer performance than the corresponding global and distortional equations. Moreover, Section 2.1.1 showed that even for non-perforated columns, the current codified DSM was unable to predict accurately and safely the strength of certain sections, such as those with wide flanges or small lips. Therefore, regression analyses were resorted to with the aim to (i) improve the performance of the local-global Equations (15)-(16) in DSM Method 6, and (ii) detect the pattern of any variations in the predicted strengths that could not be predicted on the basis of the current DSM.

In particular, DSM Method 13 (i.e. Modification 5 to Option 4 in (Moen and Schafer 2011)) was first explored such that the equations for global buckling and distortional buckling in Option 4 of (Moen and Schafer 2011), i.e. (13)-(14) and (17)-(20) respectively, remained unchanged, while the local buckling strength prediction equations, i.e. (15)-(16) were modified based on a regression analysis of the local buckling strength equations in DSM Method 10 (i.e. replacing the $P_{cr\text{-}l\text{-}h}$ in Equations (15)-(16) by $P_{cr\text{-}l\text{-}nh}$ for the gross section). Therefore, the predicted strength was taken as the minimum of the strength predictions by (i) the regression equations for local-global buckling using $P_{cr\text{-}l\text{-}nh}$, (ii) the distortional buckling equations, and (iii) the global buckling equations.

A nonlinear regression analysis was performed using the software DATAFIT 9.0.59 with rigorous parameter selection process. The significance of each parameter was indicated by the "residual sum of squares" (defined as the sum of squares of the differences between the actual data points and the curve generated by fitted parameters) and the so-called "t-ratio" (defined as the fitted parameter value divided by the standard deviation of the fitted parameter). The proposed strength formulae for local buckling (or local-global buckling interaction) are in the form:

$$\text{For } \lambda_{le} \leq 0.776, \quad P_{nle} = F1 \times P_{ne} \tag{21}$$

$$\text{For } \lambda_{le} > 0.776, \quad P_{nle} = F1 \times \left[1 - 0.15 \left(\frac{P_{cr\text{-}l\text{-}nh}}{P_{ne}} \right)^{0.4} \right] \left(\frac{P_{cr\text{-}l\text{-}nh}}{P_{ne}} \right)^{0.4} P_{ne} \tag{22}$$

where

$$F1 = a + b \times \lambda_{le} + c \times \lambda_d + d \times \lambda_c + e \times HWF + f \times HLF + g \times HSF + h \times \frac{H}{t} + i \times \frac{B}{t} + j \times \frac{D}{t} + k \times \frac{H}{B} + m \times \frac{D}{B} \tag{23}$$

with all the constants defined in Table 55.

Table 55: Constants from regression analysis for DSM Method 13

a	b	c	d	e	f
8.30E-01	1.20E-01	-9.65E-02	1.48E-01	-3.04E-01	-1.81E-02
g	h	i	j	k	m
3.16E-03	1.43E-03	-2.67E-03	-4.06E-03	-1.96E-02	1.49E-01

In Equations (21)-(22), P_{ne} is calculated per Equations (13)-(14), and $\lambda_{le} = \sqrt{P_{ne} / P_{cr\text{-}l\text{-}nh}}$ where $P_{cr\text{-}l\text{-}nh}$ is the elastic local buckling load not considering holes which can be calculate by readily available programs such as THIN-WALL and CUFSM. In Equation (23), λ_d and λ_c are calculated per DSM Method 6 (i.e. Option 4 in (Moen and Schafer 2011)) which consider the influence of holes, while *HWF*=hole width factor=hole width/flat web width, *HLF*=hole length factor=hole length/hole width, *HSF*=hole spacing factor=clear hole spacing/hole width, *H*=overall web width, *B*=overall flange width, *D*=overall lip width, *t*=thickness.

These many variables, 11 in total, were included in the resultant regression equation because the regression analysis suggested that all of them were significant as to reducing the residual sum of squares. Also, the use of a linear regression model for $F1$ as shown in Equation (23) appeared to perform reasonably well and was a compromise between accuracy of prediction and simplicity of calculation.

The statistics of the predictions by means of DSM Method 13 are presented in Table 56-Table 57, along with the percentage differences between Method 13 and Method 6 given in Table 58-Table 59. It should be noted that the constants in Table 55 obtained from the regression analysis had been scaled down in order to raise the P_m value and thus to achieve ϕ=0.85 as prescribed in the current codified DSM. Specifically, in Method 13, the overall value of was adjusted to 0.848.

The results show that, in comparison with DSM Method 6, the additional regression analysis significantly reduced the overall scatter of the predictions, as shown by a decrease in the overall value of V_p from 0.199 to 0.166 (i.e. 16.6% decrease). However, this improvement was not reflected in the statistics for Stiffened C section which showed an increase of 11.2% in the overall value of V_p. This demonstrates that Stiffened C section was distinct from the other sections in that it had a different correlation between the variables in the regression analysis and its member strength, which may be due to the existence of a stiffener in the web. On the contrary, Hat section benefited most from Method 13 as indicated by a substantial increase in its overall value of ϕ from 0.582 to 0.843 (i.e. 44.8% increase) and also a decrease of 17.5% in its overall V_p value. In addition, in terms of failure modes, DSM Method 13 performed best for the D mode which showed a 24.3% decrease in V_p, whereas it was unable to reduce the scatter of the predictions for the LG and G modes which showed 6.1% and 7.0% increases in the V_p values respectively. In particular, Z section failing in the LG mode was worst predicted with a massive 102.3% increase in V_p and also a 17.2% decrease in ϕ. Moreover, DSM Method 13 resulted in acceptable ϕ values (close to or above 0.85) for all the sections failing in combined L, LG, G and D modes (those modes covered by the current codified DSM), whereas it failed to achieve so for C, Hat and Stiffened C sections failing in combined LD, DG and LDG modes (although the overall ϕ value of 0.821 for these modes was still considered to be acceptable).

The simulation-to-predicted ratios for all columns obtained by use of DSM Method 13 are presented in Fig. 29-Fig. 30 classified by failure mode and section type respectively. More detailed figures of the same kind for each section type are provided in Section M.1. Compared with Fig. 15 and Fig. 16 for DSM Method 6, it can be seen that (i) overall, the scatter of the predictions was smaller as shown by the narrower band of the data points, (ii) some substantial discrepancies in accuracy that were inherent in the AS/NZS 4600 DSM (as shown in Fig. 1 and Fig. 2) could not be reduced, (ii) the discrepancy could even increase for some particular members.

Table 56: Resistance factors for all columns failing in modes L, LG, G, D, and L+LG+G+D by **DSM Method 13** – Modification 5 to Option 4 in (Moen and Schafer 2011) – minimum of (i) regression analyses of LG equation using $P_{cr-1-nh}$, (ii) D equation, and (iii) G equation

prediction method	Section shape	Failure mode																			
		L				LG				G				D				All L, LG, G, D			
		P_m	V_p	ϕ	n	P_m	V_p	ϕ	n	P_m	V_p	ϕ	n	P_m	V_p	ϕ	n	P_m	V_p	ϕ	n
DSM Method 13	C	1.086	0.122	0.884	6923	1.052	0.104	0.875	4245	0.963	0.084	0.815	1651	1.283	0.215	0.914	3678	1.109	0.176	0.841	16497
	Z	1.147	0.099	0.958	3712	1.023	0.176	0.775	1358	1.107	0.049	0.960	2548	1.142	0.061	0.983	2444	1.119	0.101	0.932	10062
	Hat	1.115	0.083	0.945	1414	1.321	0.190	0.981	494	1.122	0.062	0.965	137	1.077	0.100	0.898	441	1.150	0.143	0.913	2486
	Rack	1.200	0.062	1.032	461	0.998	0.175	0.758	1065	1.018	0.105	0.845	383	1.066	0.049	0.924	391	1.054	0.146	0.834	2300
	Stiffened C	1.113	0.186	0.832	317	1.018	0.135	0.817	143	1.052	0.047	0.913	196	1.214	0.182	0.912	245	1.112	0.172	0.848	901
	All sections	1.112	0.116	0.912	12827	1.056	0.157	0.823	7305	1.050	0.092	0.883	4915	1.209	0.184	0.905	7199	1.111	0.152	0.872	32246

Table 57: Resistance factors for all columns failing in modes LD, DG, LDG, LD+DG+LDG, and all failure modes by **DSM Method 13** – Modification 5 to Option 4 in (Moen and Schafer 2011) – minimum of (i) regression analyses of LG equation using $P_{cr-1-nh}$, (ii) D equation, and (iii) G equation

prediction method	Section shape	Failure mode																			
		LD				DG				LDG				All LD, DG, LDG				ALL Failure modes			
		P_m	V_p	ϕ	n	P_m	V_p	ϕ	n	P_m	V_p	ϕ	n	P_m	V_p	ϕ	n	P_m	V_p	ϕ	n
DSM Method 13	C	1.057	0.163	0.818	3157	0.943	0.139	0.753	2589	1.033	0.253	0.689	862	1.009	0.179	0.762	6608	1.080	0.182	0.812	23105
	Z	1.127	0.086	0.952	4115	1.143	0.065	0.981	2989	1.198	0.132	0.965	6057	1.163	0.111	0.959	13161	1.144	0.109	0.946	23223
	Hat	1.156	0.154	0.905	585	1.051	0.204	0.763	1927	1.187	0.217	0.843	964	1.107	0.208	0.798	3476	1.125	0.184	0.843	5962
	Rack	0.962	0.126	0.780	137	1.069	0.154	0.837	832	1.114	0.156	0.870	900	1.083	0.158	0.843	1869	1.067	0.152	0.837	4169
	Stiffened C	0.892	0.284	0.561	245	0.918	0.321	0.537	1727	0.996	0.301	0.606	800	0.938	0.314	0.556	2772	0.981	0.289	0.611	3673
	All sections	1.092	0.139	0.872	8239	1.029	0.194	0.759	10064	1.157	0.181	0.872	9583	1.092	0.181	0.821	27886	1.102	0.166	0.848	60132

Table 58: Difference in resistance factors between **DSM Method 13** and **DSM Method 6** for all columns failing in modes L, LG, G, D, and L+LG+G+D

prediction method	Section shape	Failure mode														
		L			LG			G			D			All L, LG, G, D		
		P_m	V_p	ϕ	P_m	V_p	ϕ	P_m	V_p	ϕ	P_m	V_p	ϕ	P_m	V_p	ϕ
DSM Method 13	C	0.7%	-9.0%	2.1%	2.0%	-1.9%	2.3%	2.4%	-14.3%	3.7%	4.2%	-16.0%	12.1%	2.1%	-7.4%	4.2%
	Z	7.5%	-10.8%	8.9%	-7.8%	102.3%	-17.2%	6.4%	8.9%	6.3%	10.9%	-37.1%	14.0%	6.2%	6.3%	5.5%
	Hat	30.9%	-13.5%	32.4%	38.8%	-6.9%	42.0%	3.2%	40.9%	2.1%	24.4%	-40.8%	35.2%	29.7%	-7.7%	31.7%
	Rack	22.8%	-33.3%	25.9%	14.4%	-21.2%	23.5%	2.8%	-7.9%	3.8%	16.8%	-47.3%	20.5%	14.6%	-15.1%	18.8%
	Stiffened C	17.2%	75.5%	5.7%	0.0%	0.0%	0.0%	2.7%	-29.9%	4.0%	10.8%	-27.5%	24.4%	9.4%	-1.1%	9.7%
	All sections	6.6%	-18.3%	9.9%	4.7%	6.1%	3.4%	4.7%	7.0%	4.3%	8.0%	-24.3%	19.2%	6.1%	-12.6%	9.5%

Table 59: Difference in resistance factors between **DSM Method 13** and **DSM Method 6** for all columns failing in modes LD, DG, LDG, LD+DG+LDG, and all

failure modes

prediction method	Section shape	Failure mode														
		LD			DG			LDG			All LD, DG, LDG			ALL Failure modes		
		P_m	V_p	ϕ	P_m	V_p	ϕ	P_m	V_p	ϕ	P_m	V_p	ϕ	P_m	V_p	ϕ
DSM Method 13	C	20.0%	-12.8%	24.5%	12.8%	-20.1%	18.4%	-2.5%	12.9%	-7.4%	13.8%	-13.1%	18.9%	5.0%	-14.6%	10.3%
	Z	12.8%	-29.5%	17.0%	14.5%	-40.4%	18.9%	12.6%	-17.0%	16.7%	13.0%	-22.4%	17.4%	10.1%	-12.8%	12.1%
	Hat	49.2%	-12.5%	53.9%	38.3%	-26.6%	58.0%	41.8%	-9.6%	47.4%	41.2%	-18.8%	53.5%	36.0%	-17.5%	44.8%
	Rack	16.7%	24.8%	13.5%	21.5%	-14.4%	26.2%	24.5%	-16.6%	30.4%	22.7%	-12.7%	26.8%	18.2%	-14.1%	22.4%
	Stiffened C	12.2%	51.9%	-5.4%	18.5%	12.2%	10.5%	16.6%	40.7%	-0.5%	17.3%	20.8%	5.7%	15.0%	11.2%	8.9%
	All sections	17.5%	-19.2%	23.2%	19.2%	-13.0%	25.2%	14.8%	-10.0%	18.6%	17.2%	-14.2%	22.7%	11.0%	-16.6%	16.8%
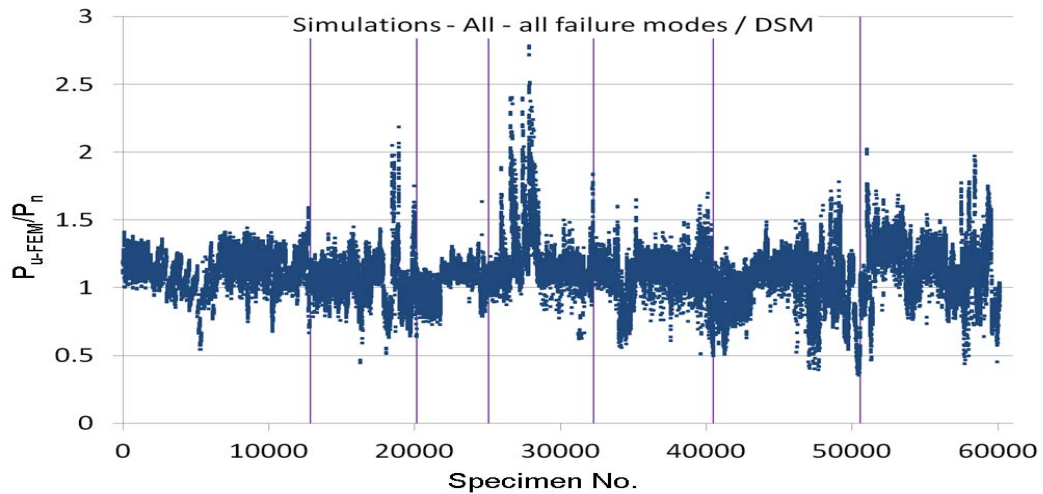
Fig. 29: Simulation-to-predicted ratios for all columns by DSM Method 13 with classified failure modes (from left to right: L, LG, G, D, LD, DG, and LDG)
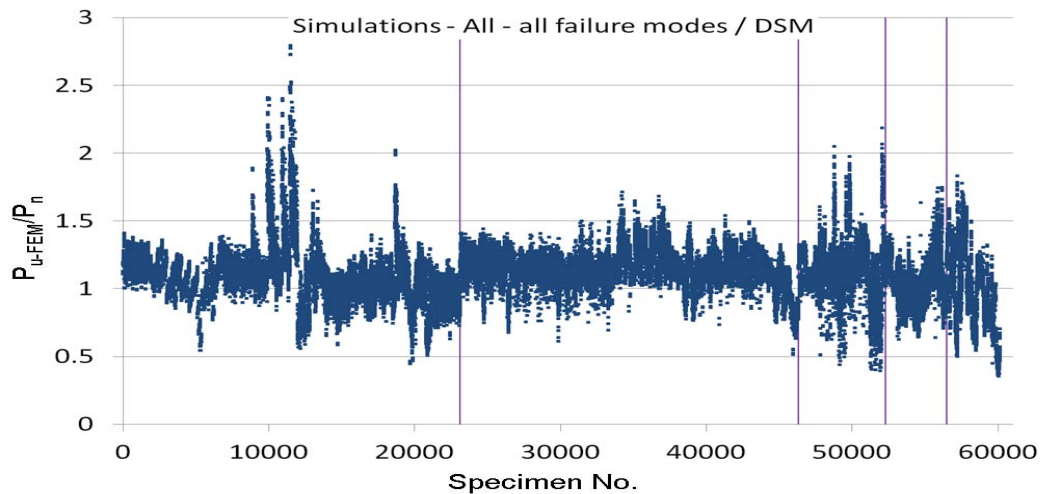
Fig. 30: Simulation-to-predicted ratios for all columns by DSM Method 13 with classified section types (from left to right: C, Z, Hat, Rack and Stiffened C)

Because the regression analysis in DSM Method 13 was performed only for the local (LG) buckling strength P_{nle} and against the "actual" strength data, the local (LG) buckling Equations (21)-(22) controlled the final predicted strength in the majority of cases compared to the global and distortional buckling equations (i.e. (13)-(14) and (17)-(20), respectively). This is verified in Table 60 which shows the number of times each set of strength equations controlled the final predicted strength. In fact, the global and distortional strengths (P_{nd} and P_{ne}) only controlled a significant portion of the final strengths when the column failed in a G or D mode, respectively. This means that in most cases, the use of the global or distortional equations are not necessary.

Table 60: Counts of controlling strength equations

controlling equations	Failure mode									
	L	LG	G	D	LD	DG	LDG	All L, LG, G, D	All LD, DG, LDG	ALL Failure modes
P_{nle} by eqns. (21)-(22)	12799	6490	2805	4659	6515	8726	8361	26749	23602	50355
P_{nd} by eqns. (17)-(20)	28	487	0	2540	1724	592	1221	3055	3537	6592
P_{ne} by eqns. (13)-(14)	0	328	2110	0	0	746	1	2438	747	3185

In view of this, another two design options (i.e. DSM Method 14 and 15) were explored based on DSM Method 13, i.e. Method 14 took the strength as the minimum of the predictions obtained by (i) the regression equations for local-global buckling (i.e. (21)-(23)) and (ii) the distortional equations (i.e. (17)-(20)), while Method 15 predicted the strength as the minimum of the predictions by (i) the regression equations for local-global buckling (i.e. (21)-(23)) and (ii) the global equations (i.e. (13)-(14)). However, the regression constants used in Equation (23) were adjusted accordingly in order to achieve the same overall value of $\phi=0.848$ as for DSM Method 13. These regression constants are tabulated in Table 61 and Table 62 for Method 14 and 15 respectively.

Table 61: Constants from regression analysis for DSM Method 14

a	b	c	d	e	f
8.24E-01	1.19E-01	-9.58E-02	1.47E-01	-3.02E-01	-1.80E-02
g	h	i	j	k	m
3.14E-03	1.42E-03	-2.66E-03	-4.03E-03	-1.94E-02	1.48E-01

Table 62: Constants from regression analysis for DSM Method 15

a	b	c	d	e	f
8.22E-01	1.19E-01	-9.56E-02	1.47E-01	-3.01E-01	-1.80E-02
g	h	i	j	k	m
3.13E-03	1.42E-03	-2.65E-03	-4.02E-03	-1.94E-02	1.47E-01

Table 63-Table 64, and Table 67-Table 68 list the statistics of the predictions for DSM Method 14 and 15 respectively. Meanwhile, Table 65-Table 66, and Table 69-Table 70 present the percentage differences of the statistics between Method 14 and 13, and Method 15 and 13, respectively.

The results shown in these tables suggest that, in comparison with DSM Method 13, the exclusion of using the global buckling equations only caused a minor increase of 1.8% in the overall V_p value. However, a significant scatter existed for the G mode alone, as shown by the overall 14.1% increase in V_p, especially for

the Z and Hat sections whose V_p values increased by 46.9% and 51.6% respectively. Otherwise, it is quite acceptable not to use the global buckling strength equations for the other failure modes.

As for DSM Method 15, although its overall value of V_p decreased by 4.2% compared with that for DSM Method 13, this decrease was mainly due to C section which showed a substantial decrease of 23.6% in V_p. This indicated that the exclusion of the distortional buckling strength equations was substantially beneficial to only C section. In particular, the scatter in the predictions dropped significantly for the D and LDG modes of C section columns, as shown by the corresponding 66% and 49% decreases in the V_p values. Otherwise, DSM Method 15 showed negative influences (indicated by an increase in the value of V_p) on the strength prediction of many individual failure modes and section types. In addition, in terms of the overall performance of a failure mode, the worst affected one was the LD mode which showed a 19.4% increase in the overall value of V_p and also an increased scatter for almost every section type. These observations in general suggested that it was necessary to include the distortional buckling equations in the strength prediction.

Furthermore, Fig. 31-Fig. 32 and Fig. 33-Fig. 34 illustrate the simulation-to-predicted ratios for all columns for DSM Method 14 and 15 respectively. More detailed figures regarding the simulation-to-predicted ratios for each section can be found in Sections N.1 and O.1.

Compared with Fig. 29-Fig. 30 for DSM Method 13, Fig. 31-Fig. 32 for Method 14 are very similar except for a slightly larger scatter for the G mode. However, Fig. 33-Fig. 34 for Method 15 are distinct from those for Method 13 in that the large scatter associated with the D mode of C section columns had been totally eliminated, which suggested that it was the distortional strength equations that significant underestimated the strength of the columns made from such C sections. Apart from this, a slightly larger scatter in the predictions can be seen for the LG and LD modes, which was in line with the statistics.

The above discussions concerning DSM Method 14 and 15 indicate that although the regression analysis in DSM Method 13 was solely based on the value of P_{nle} and performed against the accurate strengths obtained by the FEM, the inclusion of the equations for P_{nd} and P_{ne}, in general, was necessary because they were still useful in reducing the scatter of the prediction related to some particular failure modes and section types as previously discussed. However, the large discrepancies in prediction associated with the D mode of C section columns could not be avoided in this way.

Table 63: Resistance factors for all columns failing in modes L, LG, G, D, and L+LG+G+D by **DSM Method 14** – Modification 6 to Option 4 in (Moen and Schafer 2011) – minimum of (i) regression analyses of LG equation using $P_{cr-1-nh}$ and (ii) D equation

prediction method	Section shape	Failure mode																				
		L				LG				G				D				All L, LG, G, D			
		P_m	V_p	ϕ	n	P_m	V_p	ϕ	n	P_m	V_p	ϕ	n	P_m	V_p	ϕ	n	P_m	V_p	ϕ	n
DSM Method 14	C	1.093	0.122	0.890	6923	1.059	0.104	0.880	4245	0.938	0.085	0.793	1651	1.287	0.213	0.920	3678	1.112	0.177	0.842	16497
	Z	1.155	0.099	0.964	3712	1.015	0.192	0.751	1358	1.091	0.072	0.933	2548	1.149	0.061	0.989	2444	1.118	0.110	0.924	10062
	Hat	1.123	0.083	0.951	1414	1.330	0.190	0.988	494	1.075	0.094	0.902	137	1.084	0.100	0.904	441	1.155	0.145	0.914	2486
	Rack	1.208	0.062	1.040	461	1.003	0.174	0.762	1065	0.979	0.105	0.812	383	1.072	0.049	0.929	391	1.052	0.149	0.829	2300
	Stiffened C	1.121	0.186	0.838	317	1.018	0.135	0.817	143	1.018	0.054	0.880	196	1.218	0.181	0.916	245	1.109	0.177	0.840	901
	All sections	1.119	0.116	0.919	12827	1.060	0.161	0.822	7305	1.028	0.105	0.853	4915	1.213	0.182	0.912	7199	1.113	0.155	0.869	32246

Table 64: Resistance factors for all columns failing in modes LD, DG, LDG, LD+DG+LDG, and all failure modes by **DSM Method 14** – Modification 6 to Option 4 in (Moen and Schafer 2011) – minimum of (i) regression analyses of LG equation using $P_{cr-1-nh}$ and (ii) D equation

prediction method	Section shape	Failure mode																				
		LD				DG				LDG				All LD, DG, LDG				ALL Failure modes			
		P_m	V_p	ϕ	n	P_m	V_p	ϕ	n	P_m	V_p	ϕ	n	P_m	V_p	ϕ	n	P_m	V_p	ϕ	n
DSM Method 14	C	1.063	0.163	0.822	3157	0.937	0.140	0.747	2589	1.038	0.250	0.695	862	1.010	0.181	0.761	6608	1.083	0.183	0.812	23105
	Z	1.132	0.086	0.957	4115	1.148	0.068	0.984	2989	1.205	0.132	0.971	6057	1.170	0.112	0.964	13161	1.147	0.113	0.944	23223
	Hat	1.164	0.154	0.912	585	1.057	0.204	0.767	1927	1.195	0.217	0.849	964	1.114	0.208	0.802	3476	1.131	0.185	0.846	5962
	Rack	0.967	0.127	0.784	137	1.071	0.157	0.835	832	1.121	0.155	0.875	900	1.087	0.159	0.845	1869	1.068	0.155	0.835	4169
	Stiffened C	0.895	0.287	0.560	245	0.922	0.323	0.537	1727	1.001	0.302	0.608	800	0.942	0.316	0.557	2772	0.983	0.290	0.611	3673
	All sections	1.098	0.140	0.876	8239	1.031	0.197	0.757	10064	1.164	0.181	0.877	9583	1.097	0.183	0.823	27886	1.105	0.169	0.848	60132

Table 65: Difference in resistance factors between **DSM Method 14** and **DSM Method 13** for all columns failing in modes L, LG, G, D, and L+LG+G+D

prediction method	Section shape	Failure mode														
		L			LG			G			D			All L, LG, G, D		
		P_m	V_p	ϕ	P_m	V_p	ϕ	P_m	V_p	ϕ	P_m	V_p	ϕ	P_m	V_p	ϕ
DSM Method 14	C	0.6%	0.0%	0.7%	0.7%	0.0%	0.6%	-2.6%	1.2%	-2.7%	0.3%	-0.9%	0.7%	0.3%	0.6%	0.1%
	Z	0.7%	0.0%	0.6%	-0.8%	9.1%	-3.1%	-1.4%	46.9%	-2.8%	0.6%	0.0%	0.6%	-0.1%	8.9%	-0.9%
	Hat	0.7%	0.0%	0.6%	0.7%	0.0%	0.7%	-4.2%	51.6%	-6.5%	0.6%	0.0%	0.7%	0.4%	1.4%	0.1%
	Rack	0.7%	0.0%	0.8%	0.5%	-0.6%	0.5%	-3.8%	0.0%	-3.9%	0.6%	0.0%	0.5%	-0.2%	2.1%	-0.6%
	Stiffened C	0.7%	0.0%	0.7%	0.0%	0.0%	0.0%	-3.2%	14.9%	-3.6%	0.3%	-0.5%	0.4%	-0.3%	2.9%	-0.9%
	All sections	0.6%	0.0%	0.8%	0.4%	2.5%	-0.1%	-2.1%	14.1%	-3.4%	0.3%	-1.1%	0.8%	0.2%	2.0%	-0.3%

Table 66: Difference in resistance factors between **DSM Method 14** and **DSM Method 13** for all columns failing in modes LD, DG, LDG, LD+DG+LDG, and all failure modes

prediction method	Section shape	Failure mode														
		LD			DG			LDG			All LD, DG, LDG			ALL Failure modes		
		P_m	V_p	ϕ	P_m	V_p	ϕ	P_m	V_p	ϕ	P_m	V_p	ϕ	P_m	V_p	ϕ
DSM Method 14	C	0.6%	0.0%	0.5%	-0.6%	0.7%	-0.8%	0.5%	-1.2%	0.9%	0.1%	1.1%	-0.1%	0.3%	0.5%	0.0%
	Z	0.4%	0.0%	0.5%	0.4%	4.6%	0.3%	0.6%	0.0%	0.6%	0.6%	0.9%	0.5%	0.3%	3.7%	-0.2%
	Hat	0.7%	0.0%	0.8%	0.6%	0.0%	0.5%	0.7%	0.0%	0.7%	0.6%	0.0%	0.5%	0.5%	0.5%	0.4%
	Rack	0.5%	0.8%	0.5%	0.2%	1.9%	-0.2%	0.6%	-0.6%	0.6%	0.4%	0.6%	0.2%	0.1%	2.0%	-0.2%
	Stiffened C	0.3%	1.1%	-0.2%	0.4%	0.6%	0.0%	0.5%	0.3%	0.3%	0.4%	0.6%	0.2%	0.2%	0.3%	0.0%
	All sections	0.5%	0.7%	0.5%	0.2%	1.5%	-0.3%	0.6%	0.0%	0.6%	0.5%	1.1%	0.2%	0.3%	1.8%	0.0%

Table 67: Resistance factors for all columns failing in modes L, LG, G, D, and L+LG+G+D by **DSM Method 15** – Modification 7 to Option 4 in (Moen and Schafer 2011) – minimum of (i) regression analyses of LG equation using $P_{cr\text{-}1\text{-}nh}$ and (ii) G equation

prediction method	Section shape	Failure mode																			
		L				LG				G				D				All L, LG, G, D			
		P_m	V_p	ϕ	n	P_m	V_p	ϕ	n	P_m	V_p	ϕ	n	P_m	V_p	ϕ	n	P_m	V_p	ϕ	n
rDSM Method 15	C	1.095	0.123	0.892	6923	1.052	0.117	0.862	4245	0.968	0.083	0.820	1651	1.131	0.073	0.966	3678	1.079	0.116	0.885	16497
	Z	1.158	0.099	0.967	3712	1.030	0.178	0.779	1358	1.114	0.051	0.964	2548	1.138	0.057	0.982	2444	1.125	0.101	0.937	10062
	Hat	1.125	0.083	0.954	1414	1.334	0.190	0.990	494	1.127	0.064	0.968	137	1.083	0.099	0.904	441	1.159	0.144	0.920	2486
	Rack	1.211	0.062	1.042	461	1.005	0.171	0.767	1065	1.022	0.104	0.849	383	1.070	0.052	0.926	391	1.060	0.145	0.840	2300
	Stiffened C	1.123	0.186	0.840	317	0.749	0.134	0.602	143	1.056	0.046	0.917	196	1.054	0.207	0.761	245	1.030	0.208	0.742	901
	All sections	1.122	0.116	0.921	12827	1.054	0.168	0.809	7305	1.056	0.093	0.887	4915	1.124	0.079	0.956	7199	1.097	0.123	0.893	32246

Table 68: Resistance factors for all columns failing in modes LD, DG, LDG, LD+DG+LDG, and all failure modes by **DSM Method 15** – Modification 7 to Option 4 in (Moen and Schafer 2011) – minimum of (i) regression analyses of LG equation using $P_{cr\text{-}1\text{-}nh}$ and (ii) G equation

prediction method	Section shape	Failure mode																			
		LD				DG				LDG				All LD, DG, LDG				ALL Failure modes			
		P_m	V_p	ϕ	n	P_m	V_p	ϕ	n	P_m	V_p	ϕ	n	P_m	V_p	ϕ	n	P_m	V_p	ϕ	n
DSM Method 15	C	1.035	0.192	0.766	3157	0.946	0.141	0.753	2589	0.942	0.129	0.761	862	0.988	0.175	0.751	6608	1.053	0.139	0.841	23105
	Z	1.107	0.098	0.925	4115	1.152	0.066	0.989	2989	1.195	0.144	0.948	6057	1.158	0.122	0.943	13161	1.144	0.115	0.940	23223
	Hat	1.167	0.154	0.914	585	1.059	0.205	0.767	1927	1.198	0.217	0.851	964	1.116	0.209	0.803	3476	1.134	0.184	0.849	5962
	Rack	0.964	0.130	0.778	137	1.077	0.154	0.843	832	1.118	0.155	0.874	900	1.089	0.158	0.848	1869	1.073	0.151	0.843	4169
	Stiffened C	0.782	0.436	0.358	245	0.902	0.350	0.497	1727	0.964	0.323	0.562	800	0.909	0.352	0.499	2772	0.939	0.322	0.548	3673
	All sections	1.072	0.166	0.825	8239	1.032	0.203	0.750	10064	1.146	0.187	0.854	9583	1.083	0.192	0.801	27886	1.090	0.159	0.848	60132

Table 69: Difference in resistance factors between **DSM Method 15** and **DSM Method 13** for all columns failing in modes L, LG, G, D, and L+LG+G+D

prediction method	Section shape	Failure mode															
		L			LG			G			D			All L, LG, G, D		
		P_m	V_p	ϕ	P_m	V_p	ϕ	P_m	V_p	ϕ	P_m	V_p	ϕ	P_m	V_p	ϕ
DSM Method 15	C	0.8%	0.8%	0.9%	0.0%	12.5%	-1.5%	0.5%	-1.2%	0.6%	-11.8%	-66.0%	5.7%	-2.7%	-34.1%	5.2%
	Z	1.0%	0.0%	0.9%	0.7%	1.1%	0.5%	0.6%	4.1%	0.4%	-0.4%	-6.6%	-0.1%	0.5%	0.0%	0.5%
	Hat	0.9%	0.0%	1.0%	1.0%	0.0%	0.9%	0.4%	3.2%	0.3%	0.6%	-1.0%	0.7%	0.8%	0.7%	0.8%
	Rack	0.9%	0.0%	1.0%	0.7%	-2.3%	1.2%	0.4%	-1.0%	0.5%	0.4%	6.1%	0.2%	0.6%	-0.7%	0.7%
	Stiffened C	0.9%	0.0%	1.0%	-26.4%	-0.7%	-26.3%	0.4%	-2.1%	0.4%	-13.2%	13.7%	-16.6%	-7.4%	20.9%	-12.5%
	All sections	0.9%	0.0%	1.0%	-0.2%	7.0%	-1.7%	0.6%	1.1%	0.5%	-7.0%	-57.1%	5.6%	-1.3%	-19.1%	2.4%

Table 70: Difference in resistance factors between **DSM Method 15** and **DSM Method 13** for all columns failing in modes LD, DG, LDG, LD+DG+LDG, and all

failure modes

prediction method	Section shape	Failure mode															
		LD			DG			LDG			All LD, DG, LDG			ALL Failure modes		
		P_m	V_p	ϕ	P_m	V_p	ϕ	P_m	V_p	ϕ	P_m	V_p	ϕ	P_m	V_p	ϕ
DSM Method 15	C	-2.1%	17.8%	-6.4%	0.3%	1.4%	0.0%	-8.8%	-49.0%	10.4%	-2.1%	-2.2%	-1.4%	-2.5%	-23.6%	3.6%
	Z	-1.8%	14.0%	-2.8%	0.8%	1.5%	0.8%	-0.3%	9.1%	-1.8%	-0.4%	9.9%	-1.7%	0.0%	5.5%	-0.6%
	Hat	1.0%	0.0%	1.0%	0.8%	0.5%	0.5%	0.9%	0.0%	0.9%	0.8%	0.5%	0.6%	0.8%	0.0%	0.7%
	Rack	0.2%	3.2%	-0.3%	0.7%	0.0%	0.7%	0.4%	-0.6%	0.5%	0.6%	0.0%	0.6%	0.6%	-0.7%	0.7%
	Stiffened C	-12.3%	53.5%	-36.2%	-1.7%	9.0%	-7.4%	-3.2%	7.3%	-7.3%	-3.1%	12.1%	-10.3%	-4.3%	11.4%	-10.3%
	All sections	-1.8%	19.4%	-5.4%	0.3%	4.6%	-1.2%	-1.0%	3.3%	-2.1%	-0.8%	6.1%	-2.4%	-1.1%	-4.2%	0.0%
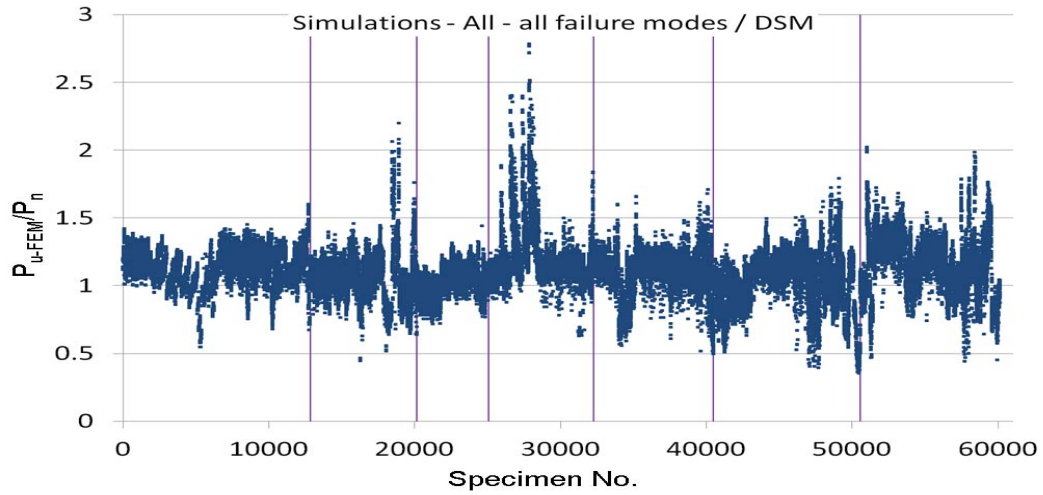
Fig. 31: Simulation-to-predicted ratios for all columns by DSM Method 14 with classified failure modes
(from left to right: L, LG, G, D, LD, DG, and LDG)
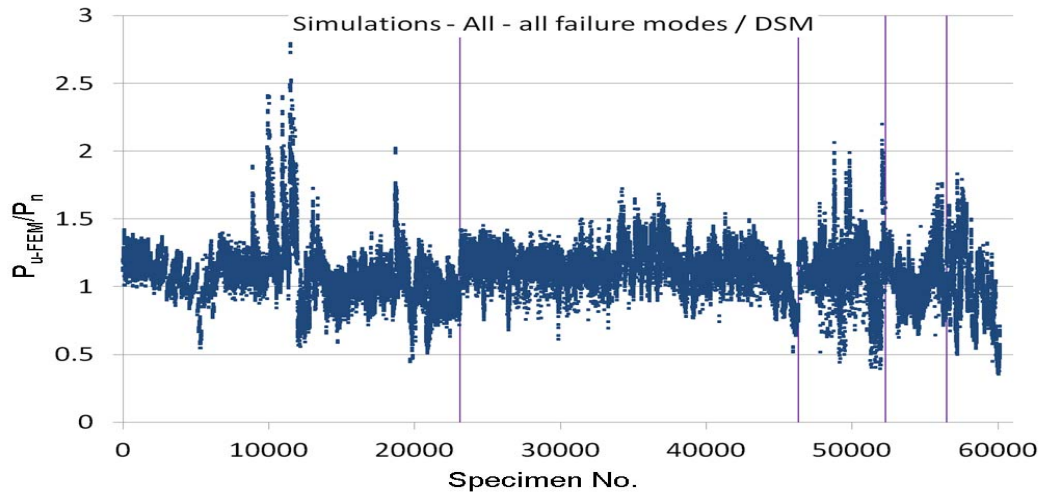
Fig. 32: Simulation-to-predicted ratios for all columns by DSM Method 14 with classified section types
(from left to right: C, Z, Hat, Rack and Stiffened C)
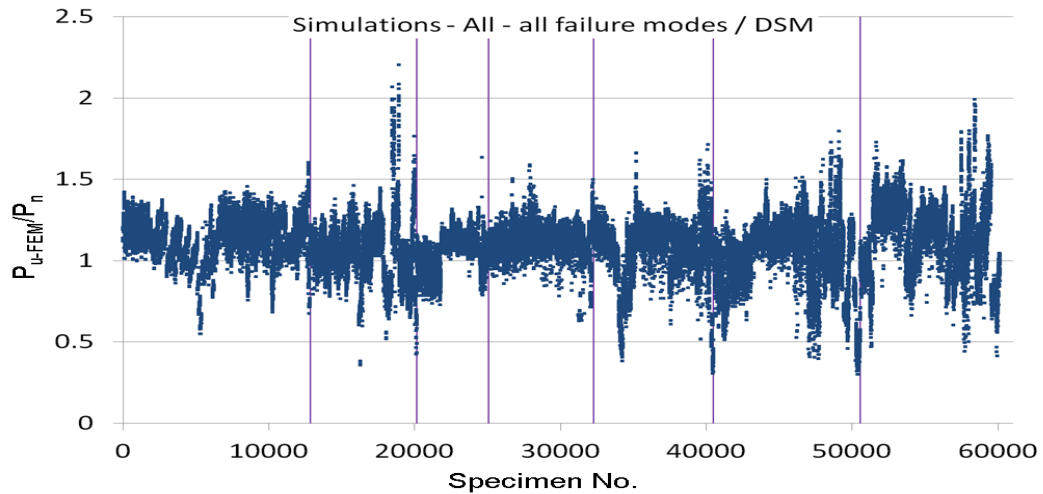
Fig. 33: Simulation-to-predicted ratios for all columns by DSM Method 15 with classified failure modes
(from left to right: L, LG, G, D, LD, DG, and LDG)
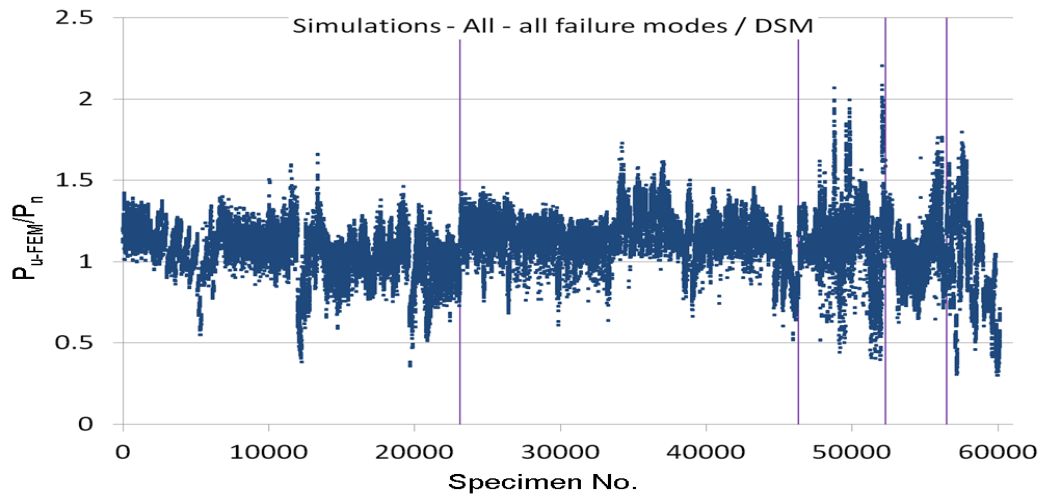
Fig. 34: Simulation-to-predicted ratios for all columns by DSM Method 15 with classified section types
(from left to right: C, Z, Hat, Rack and Stiffened C)

3.3. Method 16-17 – use $P_{cr\text{-}l\text{-}nh}$ and $P_{cr\text{-}d\text{-}nh}$ and/or regression analyses

Another two DSM methods were explored which were based on the observations of the results from DSM Methods 9-12 described in Section 3.2.1, which showed that replacing the $P_{cr\text{-}l\text{-}h}$ in Equations (15)-(16) by $P_{cr\text{-}l\text{-}nh}$ barely made any influence to the predicted strengths, and on the other hand replacing the $P_{cr\text{-}d\text{-}h}$ in Equations (17)-(20) by $P_{cr\text{-}d\text{-}nh}$ could reduce the scatter of the predictions for a majority of individual sections and failure modes. Therefore, in DSM Method 16 and 17, both the $P_{cr\text{-}l\text{-}h}$ and $P_{cr\text{-}d\text{-}h}$ in DSM Method 6 (i.e. Option 4 in (Moen and Schafer 2011)) were replaced by $P_{cr\text{-}l\text{-}nh}$ and $P_{cr\text{-}d\text{-}nh}$. In addition, these two methods differed in that Method 16 simply factored the final predicted strength by a single constant of 0.8 in order to

achieve $\phi{=}0.85$ as prescribed in AS/NZS 4600 DSM, while Method 17 used a regression analysis of the final predicted strength to achieve so.

3.3.1. Method 16 – use P$_{cr-1-nh}$ and P$_{cr-d-nh}$ – all

The statistical results for DSM Method 16 are presented in Table 71-Table 72, along with the simulation-to-predicted ratios for all columns illustrated in Fig. 35-Fig. 36. More detailed figures of the same kind regarding each section are provided in Section P.1.

As expected, DSM Method 16 resulted in almost identical V_p values to those by DSM Method 11 (with only P_{cr-d-h} replaced by $P_{cr-d-nh}$), but the use of an additional penal factor of 0.8 raised the overall resistance factor significantly from 0.711 as in Method 11 to 0.886 (i.e. 24.6% increase), although the ϕ values of 0.70 and 0.67 for Hat and Stiffened C sections were not satisfactory. Furthermore, one the one hand, if the L, LG, G and D modes were considered altogether, the ϕ value for every section type successfully exceeded 0.85, although the ϕ values of 1.033 and 1.050 for C and Z sections were deemed to be overly safe. On the other hand, if the LD, DG and LDG modes were considered altogether, all the sections except Z section failed to reach ϕ values of 0.85, which was mainly due to the large variations (indicated by the value of V_p) in their predictions, as well as the low P_m values for Hat and Stiffened C sections.

Nevertheless, DSM Method 16 was still improved in general over DSM Method 6 (i.e. the original Option 4 in (Moen and Schafer 2011)), and the improvements were threefold: (i) the ϕ values had been increased significantly for many more sections and failure modes, and (ii) the overall scatter of the predictions decreased slightly, especially for the C section which showed a marked decrease of 10.8% in its value of V_p (the increases in the values of V_p for the other sections were not significant), and (iii) the replacement of P_{cr-1-h} and P_{cr-d-h} in the original DSM Method 6 indicated that instead of following the complex procedure set out in (Moen and Schafer 2009) to calculate P_{cr-1-h} and P_{cr-d-h} which involved the choice of a proper buckling halfwavelength and the computation of weighted section properties, etc., one only needs to use a conventional FSM analysis based on the gross section.

Table 71: Resistance factors for all columns failing in modes L, LG, G, D, and L+LG+G+D by **DSM Method 16** – Modification 8 to Option 4 in (Moen and Schafer 2011) – use $P_{cr-l-nh}$ and $P_{cr-d-nh}$, factor final strengths by 0.8

prediction method	Section shape	Failure mode																			
		L				LG				G				D				All L, LG, G, D			
		P_m	V_p	ϕ	n	P_m	V_p	ϕ	n	P_m	V_p	ϕ	n	P_m	V_p	ϕ	n	P_m	V_p	ϕ	n
DSM Method 16	C	1.347	0.135	1.081	6923	1.282	0.107	1.062	4245	1.175	0.098	0.982	1651	1.385	0.206	1.002	3678	1.322	0.155	1.033	16497
	Z	1.333	0.112	1.098	3712	1.230	0.175	0.934	1358	1.299	0.045	1.128	2548	1.196	0.090	1.007	2444	1.277	0.114	1.050	10062
	Hat	1.060	0.102	0.883	1414	1.150	0.185	0.860	494	1.359	0.044	1.181	137	1.039	0.162	0.804	441	1.091	0.149	0.859	2486
	Rack	1.221	0.093	1.025	461	1.068	0.205	0.774	1065	1.238	0.114	1.017	383	1.058	0.104	0.880	391	1.125	0.170	0.862	2300
	Stiffened C	1.181	0.113	0.972	317	1.148	0.138	0.918	143	1.280	0.067	1.098	196	1.262	0.241	0.859	245	1.219	0.163	0.942	901
	All sections	1.302	0.143	1.034	12827	1.230	0.155	0.962	7305	1.254	0.086	1.059	4915	1.278	0.200	0.934	7199	1.273	0.156	0.994	32246

Table 72: Resistance factors for all columns failing in modes LD, DG, LDG, LD+DG+LDG, and all failure modes by **DSM Method 16** – Modification 8 to Option 4 in (Moen and Schafer 2011) – use $P_{cr-l-nh}$ and $P_{cr-d-nh}$, factor final strengths by 0.8

| prediction method	Section shape	Failure mode																			
		LD				DG				LDG				All LD, DG, LDG				ALL Failure modes			
		P_m	V_p	ϕ	n	P_m	V_p	ϕ	n	P_m	V_p	ϕ	n	P_m	V_p	ϕ	n	P_m	V_p	ϕ	n
DSM Method 16	C	1.017	0.173	0.775	3157	1.034	0.181	0.778	2589	1.261	0.168	0.967	862	1.055	0.191	0.782	6608	1.245	0.190	0.924	23105
	Z	1.124	0.118	0.920	4115	1.236	0.111	1.020	2989	1.296	0.163	1.001	6057	1.228	0.154	0.961	13161	1.250	0.139	0.998	23223
	Hat	0.894	0.181	0.673	585	0.933	0.288	0.582	1927	1.005	0.250	0.673	964	0.946	0.266	0.616	3476	1.006	0.229	0.700	5962
	Rack	0.918	0.106	0.762	137	1.076	0.172	0.821	832	1.047	0.183	0.786	900	1.051	0.179	0.794	1869	1.092	0.177	0.827	4169
	Stiffened C	0.893	0.203	0.650	245	0.935	0.298	0.572	1727	1.028	0.200	0.751	800	0.958	0.267	0.622	2772	1.022	0.262	0.670	3673
	All sections	1.056	0.163	0.817	8239	1.061	0.230	0.737	10064	1.218	0.201	0.888	9583	1.113	0.213	0.796	27886	1.199	0.193	0.886	60132
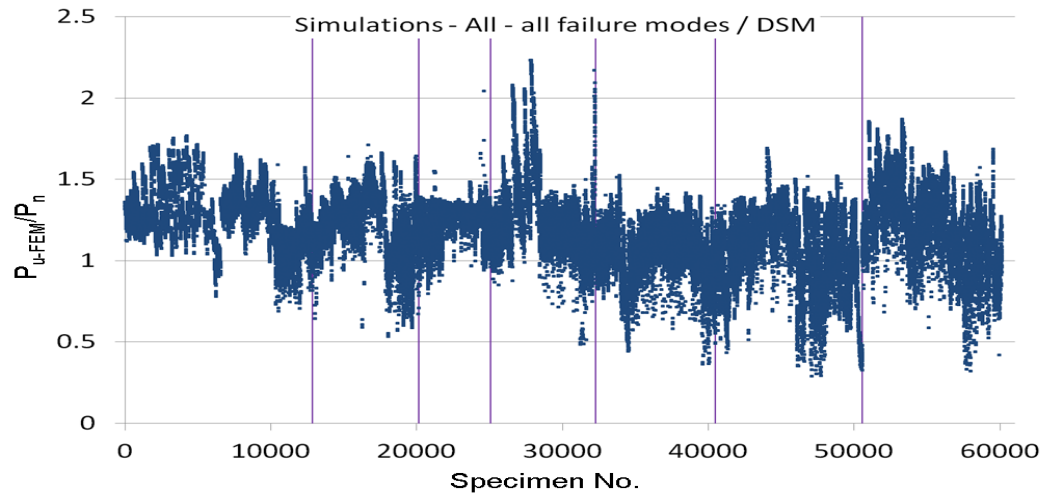
Fig. 35: Simulation-to-predicted ratios for all columns by DSM Method 16 with classified failure modes
(from left to right: L, LG, G, D, LD, DG, and LDG)
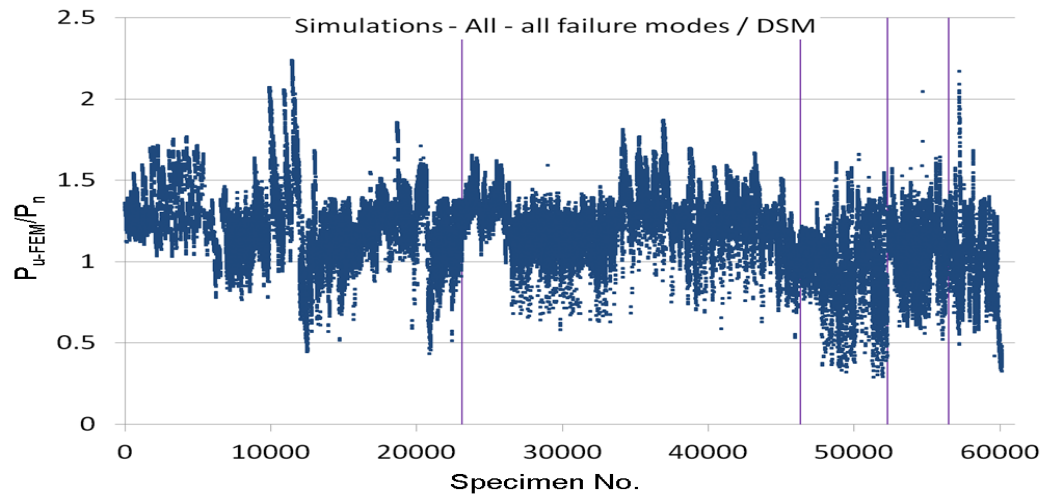
Fig. 36: Simulation-to-predicted ratios for all columns by DSM Method 16 with classified section types
(from left to right: C, Z, Hat, Rack and Stiffened C)

3.3.2. Method 17 – use P$_{cr-l-nh}$ and P$_{cr-d-nh}$ and regression analyses – all

With regards to DSM Method 17, apart from replacing P_{cr-l-h} and P_{cr-d-h} by $P_{cr-l-nh}$ and $P_{cr-d-nh}$ in DSM Method 6, a regression analysis was performed based on the minimum of the local-global buckling strength P_{nle} (i.e. eqns. (15)-(16)), the distortional buckling strength P_{nd} (i.e. eqns. (17)-(20)), and the global buckling strength P_{ne} (i.e. eqns. (13)-(14)). The final predicted strength is defined as:

$$P_n = F1 \times \min(P_{nle},\ P_{nd},\ P_{ne}) \tag{24}$$

where *F*1 is per Equation (23) with all the constants defined as:

Table 73: Constants from regression analysis for DSM Method 17

a	b	c	d	e	f
9.04E-01	5.91E-02	-3.68E-02	4.30E-02	-2.12E-01	-2.38E-02
g	h	i	j	k	m
5.26E-03	1.35E-03	-2.22E-03	-7.02E-03	-7.49E-03	7.73E-02

The performance of DSM Method 17 is shown in Table 75-Table 76 for the statistics of the predictions and in Fig. 37-Fig. 38 for the simulation-to-predicted ratios for all columns. More detailed figures regarding the simulation-to-predicted ratios for each section are provided in Section Q.1. In addition, the percentage differences of the statistics between Method 17 and Method 16 as well as between Method 17 and Method 13 are also given in Table 77-Table 78 and Table 79-Table 80, respectively.

In general, DSM Method 17 performed better than Method 16, as demonstrated by a significant decrease in the overall scatter (indicated by a 15.5% decrease in the value of V_p), and also a marked increase of 20.7% (from 0.700 to 0.845) in the resistance factor ϕ for Hat section. However, the major drawback of Method 17 was that it performed poorly against Stiffened C sections, as shown by the 13.4% increase in the overall value of V_p, which resulted in an overall ϕ value of only 0.628. Also, the method did not perform satisfactorily for C and Hat sections subjected to the collection of LD, DG and LDG modes.

In addition, when the performance of Method 17 was compared to that of Method 13 which also involved the use of regression analysis and all the three sets of strength equations, it was seen that the major difference lay in the value of V_p for C section which decreased substantially under Method 17 by 18.1% in its overall value. In particular, the values of V_p for C section decreased by a massive 40% and 47% for the D and LDG modes. This improvement was clearly reflected in Fig. 37-Fig. 38 where the considerable discrepancies associated with the D mode of C section, as shown in Fig. 29-Fig. 30, almost disappeared. This indicates that those over-predictions by the distortional strength equations had been partially "corrected" by the regression factor $F1$. However, the improvement on C section was accompanied by a slight deterioration in the strength predictions for the other sections, as shown by their slightly larger scatter represented by increases of 2.8%-15.8% in their overall V_p vaules.

As the regression constants listed in Table 73 failed to produce accurate and reliable predictions for Stiffened C section, as demonstrated by its overall V_p value of 0.297 and overall ϕ value of 0.628, a separate regression analysis based on DSM Method 17 was carried out on Stiffened C section only. The resulting regression constants are presented in Table 74.

Table 74: Constants from regression analysis for DSM Method 17 – Stiffened C section only

a	b	c	d	e	f
8.58E-01	1.65E-02	-4.95E-02	0.00E+00	-1.65E-01	-1.65E-02
g	h	i	j	k	m
1.10E-02	5.50E-04	-6.60E-04	-5.50E-03	-2.75E-02	2.20E-01

Table 81-Table 82 present the statistics of the predictions by means of the separate regression analysis for all columns made from Stiffened C section, while Table 83-Table 84 list the percentage differences of the statistics between Table 81-Table 82 and Table 75-Table 76.

The results demonstrate that this separate regression analysis significantly improved the performance of the prediction for Stiffened C section. Not only did the overall ϕ value improve from 0.628 to 0.856, but more importantly, the overall scatter in the predictions represented by the value of V_p was reduced by almost 20% (from 0.297 to 0.238). A close observation of the results for each failure mode showed that the scatter was reduced for all the modes except the D mode which had an 8.9% increase in the value of V_p. In addition, the ϕ value for the DG mode was the only one that did not satisfy the prescribed value of 0.85 as in the current DSM standards, although the ϕ values for the L, LG, G and LDG mode were considered overly conservative. Despite these improvements, the overall scatter in the predictions for Stiffened C section (i.e. V_p=0.238) was still larger than that for the other sections as listed in Table 76. This was mainly attributed to the large scatter associated with the D and DG mode, as shown by their V_p values of 0.293 and 0.264 respectively, which failed to be reduced by the separate regression analysis.

In addition, the simulation-to-predicted ratios for Stiffened C section are also presented in Fig. 39 and Fig. 40 using the regression constants in Table 73 and Table 74 respectively. It is clear that although the scatter had been significantly reduced by the separate regression analysis, it still clearly existed, especially for the D and DG modes. This observation suggests that in addition to LG interaction, DG interaction should also be included in the basis of the DSM.

Table 75: Resistance factors for all columns failing in modes L, LG, G, D, and L+LG+G+D by **DSM Method 17** – Modification 9 to Option 4 in (Moen and Schafer 2011) – use $P_{cr-l-nh}$ and $P_{cr-d-nh}$, regression analyses of final strengths

prediction method	Section shape	Failure mode																			
		L				LG				G				D				All L, LG, G, D			
		P_m	V_p	ϕ	n	P_m	V_p	ϕ	n	P_m	V_p	ϕ	n	P_m	V_p	ϕ	n	P_m	V_p	ϕ	n
DSM Method 17	C	1.158	0.108	0.958	6923	1.115	0.104	0.926	4245	1.084	0.084	0.918	1651	1.287	0.129	1.040	3678	1.168	0.126	0.947	16497
	Z	1.205	0.097	1.008	3712	1.108	0.183	0.832	1358	1.237	0.060	1.065	2548	1.218	0.081	1.034	2444	1.203	0.105	0.999	10062
	Hat	1.165	0.104	0.968	1414	1.456	0.226	1.018	494	1.338	0.077	1.139	137	1.164	0.113	0.959	441	1.232	0.177	0.934	2486
	Rack	1.233	0.077	1.050	461	1.104	0.242	0.751	1065	1.158	0.086	0.978	383	1.117	0.051	0.967	391	1.141	0.174	0.868	2300
	Stiffened C	1.118	0.151	0.879	317	1.015	0.120	0.829	143	1.185	0.064	1.018	196	1.324	0.269	0.856	245	1.172	0.208	0.845	901
	All sections	1.174	0.107	0.973	12827	1.133	0.179	0.855	7305	1.180	0.095	0.990	4915	1.248	0.128	1.010	7199	1.182	0.133	0.951	32246

Table 76: Resistance factors for all columns failing in modes LD, DG, LDG, LD+DG+LDG, and all failure modes by **DSM Method 17** – Modification 9 to Option 4 in (Moen and Schafer 2011) – use $P_{cr-l-nh}$ and $P_{cr-d-nh}$, regression analyses of final strengths

prediction method	Section shape	Failure mode																			
		LD				DG				LDG				All LD, DG, LDG				ALL Failure modes			
		P_m	V_p	ϕ	n	P_m	V_p	ϕ	n	P_m	V_p	ϕ	n	P_m	V_p	ϕ	n	P_m	V_p	ϕ	n
DSM Method 17	C	1.012	0.166	0.779	3157	0.999	0.155	0.781	2589	1.022	0.134	0.821	862	1.008	0.158	0.785	6608	1.122	0.149	0.884	23105
	Z	1.095	0.090	0.922	4115	1.209	0.079	1.028	2989	1.197	0.153	0.938	6057	1.168	0.130	0.943	13161	1.183	0.120	0.966	23223
	Hat	1.181	0.160	0.916	585	1.081	0.217	0.767	1927	1.247	0.260	0.821	964	1.144	0.233	0.790	3476	1.181	0.213	0.845	5962
	Rack	1.108	0.115	0.910	137	1.092	0.155	0.853	832	1.187	0.160	0.921	900	1.139	0.161	0.883	1869	1.140	0.168	0.875	4169
	Stiffened C	0.938	0.323	0.546	245	0.963	0.317	0.568	1727	1.018	0.301	0.619	800	0.977	0.314	0.579	2772	1.025	0.297	0.628	3673
	All sections	1.065	0.146	0.843	8239	1.078	0.200	0.787	10064	1.171	0.190	0.868	9583	1.106	0.188	0.824	27886	1.147	0.163	0.887	60132

Table 77: Difference in resistance factors between **DSM Method 17** and **DSM Method 16** for all columns failing in modes L, LG, G, D, and L+LG+G+D

prediction method	Section shape	Failure mode														
		L			LG			G			D			All L, LG, G, D		
		P_m	V_p	ϕ	P_m	V_p	ϕ	P_m	V_p	ϕ	P_m	V_p	ϕ	P_m	V_p	ϕ
DSM Method 17	C	-14.0%	-20.0%	-11.4%	-13.0%	-2.8%	-12.8%	-7.7%	-14.3%	-6.5%	-7.1%	-37.4%	3.8%	-11.6%	-18.7%	-8.3%
	Z	-9.6%	-13.4%	-8.2%	-9.9%	4.6%	-10.9%	-4.8%	33.3%	-5.6%	1.8%	-10.0%	2.7%	-5.8%	-7.9%	-4.9%
	Hat	9.9%	2.0%	9.6%	26.6%	22.2%	18.4%	-1.5%	75.0%	-3.6%	12.0%	-30.2%	19.3%	12.9%	18.8%	8.7%
	Rack	1.0%	-17.2%	2.4%	3.4%	18.0%	-3.0%	-6.5%	-24.6%	-3.8%	5.6%	-51.0%	9.9%	1.4%	2.4%	0.7%
	Stiffened C	-5.3%	33.6%	-9.6%	-11.6%	-13.0%	-9.7%	-7.4%	-4.5%	-7.3%	4.9%	11.6%	-0.3%	-3.9%	27.6%	-10.3%
	All sections	-9.8%	-25.2%	-5.9%	-7.9%	15.5%	-11.1%	-5.9%	10.5%	-6.5%	-2.3%	-36.0%	8.1%	-7.1%	-14.7%	-4.3%

Table 78: Difference in resistance factors between **DSM Method 17** and **DSM Method 16** for all columns failing in modes LD, DG, LDG, LD+DG+LDG, and all

failure modes

prediction method	Section shape	Failure mode														
		LD			DG			LDG			All LD, DG, LDG			ALL Failure modes		
		P_m	V_p	ϕ	P_m	V_p	ϕ	P_m	V_p	ϕ	P_m	V_p	ϕ	P_m	V_p	ϕ
DSM Method 17	C	-0.5%	-4.0%	0.5%	-3.4%	-14.4%	0.4%	-19.0%	-20.2%	-15.1%	-4.5%	-17.3%	0.4%	-9.9%	-21.6%	-4.3%
	Z	-2.6%	-23.7%	0.2%	-2.2%	-28.8%	0.8%	-7.6%	-6.1%	-6.3%	-4.9%	-15.6%	-1.9%	-5.4%	-13.7%	-3.2%
	Hat	32.1%	-11.6%	36.1%	15.9%	-24.7%	31.8%	24.1%	4.0%	22.0%	20.9%	-12.4%	28.2%	17.4%	-7.0%	20.7%
	Rack	20.7%	8.5%	19.4%	1.5%	-9.9%	3.9%	13.4%	-12.6%	17.2%	8.4%	-10.1%	11.2%	4.4%	-5.1%	5.8%
	Stiffened C	5.0%	59.1%	-16.0%	3.0%	6.4%	-0.7%	-1.0%	50.5%	-17.6%	2.0%	17.6%	-6.9%	0.3%	13.4%	-6.3%
	All sections	0.9%	-10.4%	3.2%	1.6%	-13.0%	6.8%	-3.9%	-5.5%	-2.3%	-0.6%	-11.7%	3.5%	-4.3%	-15.5%	0.1%

Table 79: Difference in resistance factors between **DSM Method 17** and **DSM Method 13** for all columns failing in modes L, LG, G, D, and L+LG+G+D

prediction method	Section shape	Failure mode														
		L			LG			G			D			All L, LG, G, D		
		P_m	V_p	ϕ	P_m	V_p	ϕ	P_m	V_p	ϕ	P_m	V_p	ϕ	P_m	V_p	ϕ
DSM Method 17	C	6.6%	-11.5%	8.4%	6.0%	0.0%	5.8%	12.6%	0.0%	12.6%	0.3%	-40.0%	13.8%	5.3%	-28.4%	12.6%
	Z	5.1%	-2.0%	5.2%	8.3%	4.0%	7.4%	11.7%	22.4%	10.9%	6.7%	32.8%	5.2%	7.5%	4.0%	7.2%
	Hat	4.5%	25.3%	2.4%	10.2%	18.9%	3.8%	19.3%	24.2%	18.0%	8.1%	13.0%	6.8%	7.1%	23.8%	2.3%
	Rack	2.8%	24.2%	1.7%	10.6%	38.3%	-0.9%	13.8%	-18.1%	15.7%	4.8%	4.1%	4.7%	8.3%	19.2%	4.1%
	Stiffened C	0.4%	-18.8%	5.6%	-0.3%	-11.1%	1.5%	12.6%	36.2%	11.5%	9.1%	47.8%	-6.1%	5.4%	20.9%	-0.4%
	All sections	5.6%	-7.8%	6.7%	7.3%	14.0%	3.9%	12.4%	3.3%	12.1%	3.2%	-30.4%	11.6%	6.4%	-12.5%	9.1%

Table 80: Difference in resistance factors between **DSM Method 17** and **DSM Method 13** for all columns failing in modes LD, DG, LDG, LD+DG+LDG, and all

failure modes

prediction method	Section shape	Failure mode														
		LD			DG			LDG			All LD, DG, LDG			ALL Failure modes		
		P_m	V_p	ϕ	P_m	V_p	ϕ	P_m	V_p	ϕ	P_m	V_p	ϕ	P_m	V_p	ϕ
DSM Method 17	C	-4.3%	1.8%	-4.8%	5.9%	11.5%	3.7%	-1.1%	-47.0%	19.2%	-0.1%	-11.7%	3.0%	3.9%	-18.1%	8.9%
	Z	-2.8%	4.7%	-3.2%	5.8%	21.5%	4.8%	-0.1%	15.9%	-2.8%	0.4%	17.1%	-1.7%	3.4%	10.1%	2.1%
	Hat	2.2%	3.9%	1.2%	2.9%	6.4%	0.5%	5.1%	19.8%	-2.6%	3.3%	12.0%	-1.0%	5.0%	15.8%	0.2%
	Rack	15.2%	-8.7%	16.7%	2.2%	0.6%	1.9%	6.6%	2.6%	5.9%	5.2%	1.9%	4.7%	6.8%	10.5%	4.5%
	Stiffened C	5.2%	13.7%	-2.7%	4.9%	-1.2%	5.8%	2.2%	0.0%	2.1%	4.2%	0.0%	4.1%	4.5%	2.8%	2.8%
	All sections	-2.5%	5.0%	-3.3%	4.8%	3.1%	3.7%	1.2%	5.0%	-0.5%	1.3%	3.9%	0.4%	4.1%	-1.8%	4.6%

Table 81: Resistance factors for stiffened C section columns failing in modes L, LG, G, D, and L+LG+G+D by **DSM Method 17** – Modification 9 to Option 4 in (Moen and Schafer 2011) – use $P_{\text{cr-l-nh}}$ and $P_{\text{cr-d-nh}}$, **separate** regression analyses of final strengths

prediction method	Section shape	Failure mode																			
		L				LG				G				D				All L, LG, G, D			
		P_m	V_p	ϕ	n	P_m	V_p	ϕ	n	P_m	V_p	ϕ	n	P_m	V_p	ϕ	n	P_m	V_p	ϕ	n
DSM Method 17	Stiffened C	1.226	0.090	1.032	317	1.505	0.081	1.278	143	1.384	0.050	1.199	196	1.529	0.293	0.944	245	1.387	0.203	1.009	901

Table 82: Resistance factors for stiffened C section columns failing in modes LD, DG, LDG, LD+DG+LDG, and all failure modes by **DSM Method 17** – Modification 9 to Option 4 in (Moen and Schafer 2011) – use $P_{\text{cr-l-nh}}$ and $P_{\text{cr-d-nh}}$, **separate** regression analyses of final strengths

prediction method	Section shape	Failure mode																			
		LD				DG				LDG				All LD, DG, LDG				ALL Failure modes			
		P_m	V_p	ϕ	n	P_m	V_p	ϕ	n	P_m	V_p	ϕ	n	P_m	V_p	ϕ	n	P_m	V_p	ϕ	n
DSM Method 17	Stiffened C	1.135	0.149	0.894	245	1.142	0.264	0.745	1727	1.368	0.162	1.058	800	1.206	0.240	0.823	2772	1.251	0.238	0.856	3673

Table 83: Difference in resistance factors between Table 81 and Table 75 for Stiffened C columns failing in modes L, LG, G, D, and L+LG+G+D

prediction method	Section shape	Failure mode														
		L			LG			G			D			All L, LG, G, D		
		P_m	V_p	ϕ	P_m	V_p	ϕ	P_m	V_p	ϕ	P_m	V_p	ϕ	P_m	V_p	ϕ
DSM Method 17 (for SC)	Stiffened C	9.7%	-40.4%	17.4%	48.3%	-32.5%	54.2%	16.8%	-21.9%	17.8%	15.5%	8.9%	10.3%	18.3%	-2.4%	19.4%

Table 84: Difference in resistance factors between Table 82 and Table 76 for Stiffened C failing in modes LD, DG, LDG, LD+DG+LDG, and all failure modes

prediction method	Section shape	Failure mode														
		LD			DG			LDG			All LD, DG, LDG			ALL Failure modes		
		P_m	V_p	ϕ	P_m	V_p	ϕ	P_m	V_p	ϕ	P_m	V_p	ϕ	P_m	V_p	ϕ
DSM Method 17 (for SC)	Stiffened C	21.0%	-53.9%	63.7%	18.6%	-16.7%	31.2%	34.4%	-46.2%	70.9%	23.4%	-23.6%	42.1%	22.0%	-19.9%	36.3%
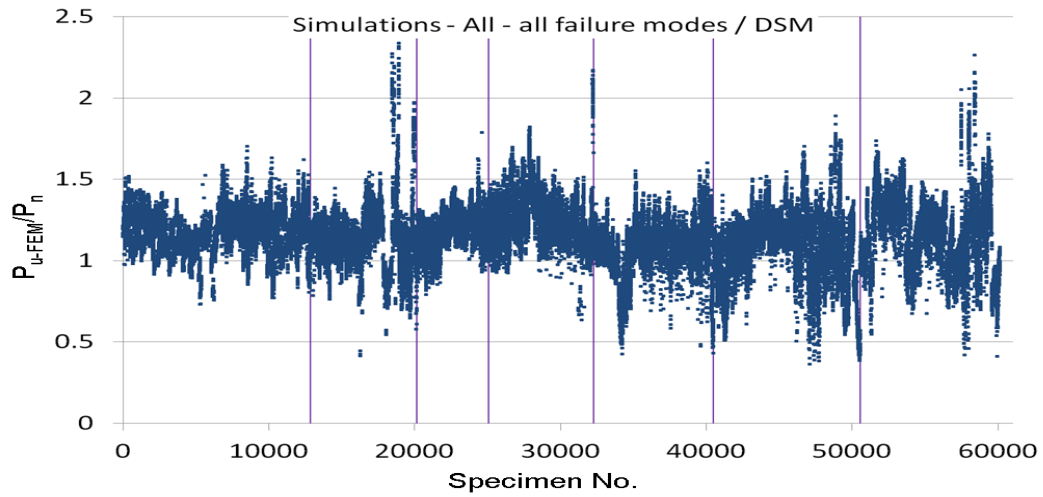
Fig. 37: Simulation-to-predicted ratios for all columns by DSM Method 17 with classified failure modes
(from left to right: L, LG, G, D, LD, DG, and LDG)
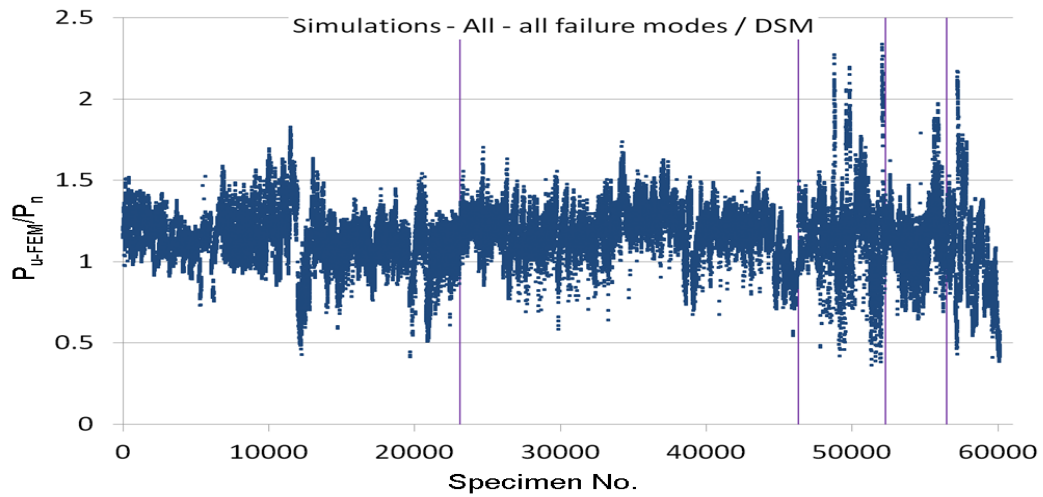
Fig. 38: Simulation-to-predicted ratios for all columns by DSM Method 17 with classified section types
(from left to right: C, Z, Hat, Rack and Stiffened C)
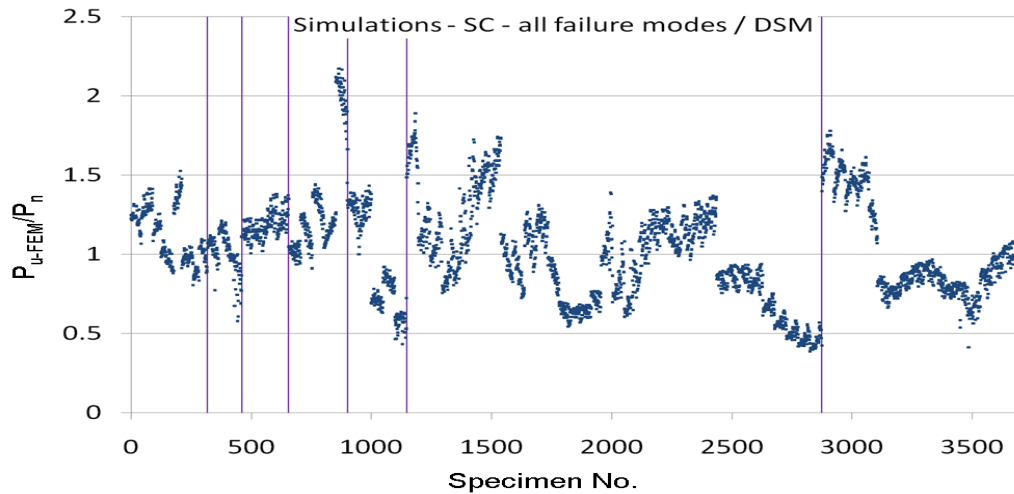
Fig. 39: Simulation-to-predicted ratios for all Stiffened C section columns by DSM Method 17 with classified failure modes (from left to right: L, LG, G, D, LD, DG, and LDG)
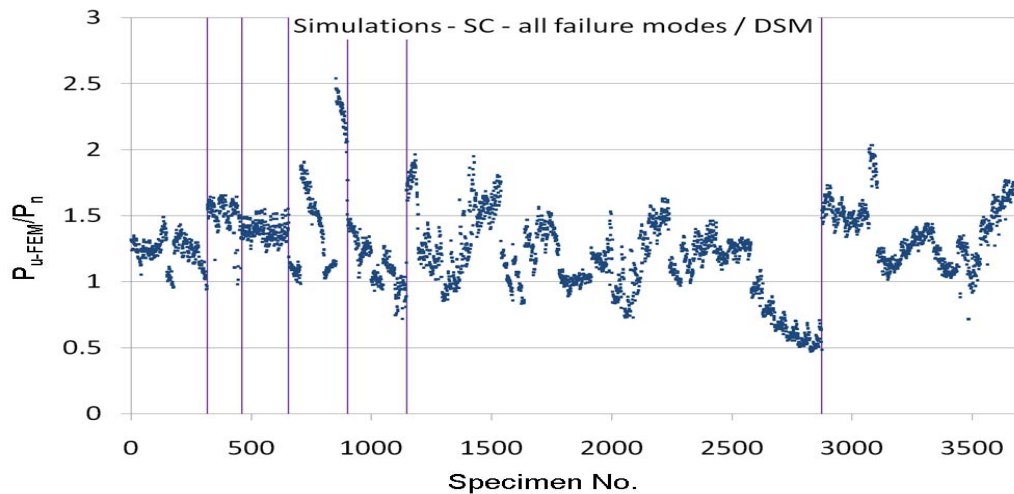
Fig. 40: Simulation-to-predicted ratios for all Stiffened C section columns by DSM Method 17 by separate regression parameters with classified failure modes (from left to right: L, LG, G, D, LD, DG, and LDG)

3.4. Method 18-19 – include DG interaction and/or regression analyses

3.4.1. Method 18 – include DG interaction – all

The studies carried out in Sections 2.1.1, 2.2.1, 2.2.2 and 2.2.3 on non-perforated columns clearly showed that among DSM Methods 1-4, Method 2 which considered LG and DG interactions produced the smallest scatter in the predictions. Therefore, a new method (i.e. DSM Method 18) was explored which modified the distortional strengths equations (17)-(20) in Method 6 (i.e. Option 4 in (Moen and Schafer 2011) to include the interaction with global buckling. Also, following the considerations described at the beginning of

Section 3.3, $P_{cr-l-nh}$ and $P_{cr-d-nh}$ were used instead of P_{cr-l-h} and P_{cr-d-h}. The formulae for calculating the DG interaction strength P_{nde} are given as

$$\text{For } \lambda_{de} \leq \lambda_{d1}, \quad P_{nde} = P_{min} \tag{25}$$

$$\text{For } \lambda_{d1} < \lambda_{de} \leq \lambda_{d2}, \quad P_{nde} = P_{min} - \left(\frac{P_{min} - P_{d2}}{\lambda_{d2} - \lambda_{d1}} \right) \left(\lambda_{d2} - \lambda_{d1} \right) \tag{26}$$

$$\text{For } \lambda_{de} > \lambda_{d2}, \quad P_{nde} = \left[1 - 0.25 \left(\frac{P_{cr-d-nh}}{P_{ne}} \right)^{0.6} \right] \left(\frac{P_{cr-d-nh}}{P_{ne}} \right)^{0.6} P_{ne} \tag{27}$$

where $\lambda_{de} = \sqrt{P_{ne}/P_{cr-d-nh}}$, $P_{min} = \min(P_{ne,} P_{yn})$, $\lambda_{d1} = 0.561 \left(P_{yn} / P_{y} \right)$,

$\lambda_{d2} = 0.561 \left(14 \left(P_{y} / P_{yn} \right)^{0.4} - 13 \right)$, and $P_{d2} = \left(1 - 0.25 \left(1/\lambda_{d2} \right)^{1.2} \right) \left(1/\lambda_{d2} \right)^{1.2} P_{ne}$.

Besides, for completeness, the local buckling (or LG interactive buckling) strength equations are,

$$\text{For } \lambda_{le} \leq 0.776, P_{nle} = P_{ne} \leq P_{yn} \tag{28}$$

$$\text{For } \lambda_{le} > 0.776, P_{nle} = \left[1 - 0.15 \left(\frac{P_{cr-l-nh}}{P_{ne}} \right)^{0.4} \right] \left(\frac{P_{cr-l-nh}}{P_{ne}} \right)^{0.4} P_{ne} \leq P_{yn} \tag{29}$$

where $\lambda_{le} = (P_{ne} / P_{cr-l-nh})^{0.5}$. The global buckling strength equations are,

$$\text{For } \lambda_{c} \leq 1.5: \quad P_{ne} = \left(0.658^{\lambda_{c}^{2}} \right) P_{y} \tag{30}$$

$$\text{For } \lambda_{c} > 1.5: \quad P_{ne} = \left(\frac{0.877}{\lambda_{c}^{2}} \right) P_{y} \tag{31}$$

where $\lambda_{c} = (P_{y}/P_{cr-e-h})^{0.5}$. Therefore, the final strength using DSM Method 18 was taken as

$$P_{n} = \min(P_{nle}, P_{nde}, P_{ne}) \tag{32}$$

The statistics of the predictions by DSM Method 18 are tabulated in Table 85-Table 86, along with the simulation-to-predicted ratios for all columns illustrated in Fig. 41-Fig. 42. More detailed figures of the same kind for each section are provided in Section R.1.

The influence of considering DG interaction in Method 18 can be demonstrated by comparing the statistics to Method 11 (although Method 11 used P_{cr-l-h}, it has been shown that P_{cr-l-h} was the same as $P_{cr-l-nh}$ for the vast majority of cases), as shown in Table 87-Table 88 the percentage differences of the statistics

between Method 18 and 11. Overall, Method 18 performed better than Method 11 in that the overall value of P_m increased by 2.1% from 0.961 to 0.981, the overall value of V_p decreased by 5.7% from 0.192 to 0.181, and the overall value of ϕ increased by 3.9% from 0.711 to 0.739. In particular, improvement in prediction was seen for every section type, especially Stifffened C section whose V_p value decreased by a significant amount of 18.4%, resulting in an increase of 20.1% in the value of ϕ. This improvement mainly came from the DG and LDG modes, which proved the aforementioned assumption that DG interaction should be included in the DSM equations in order to reduce the large scatter associated with Stiffened C section. In addition, among all failure modes, Method 18 performed worst against the LG mode as shown by an overall 6.1% increase in the value of V_p, especially for Z section failing in this mode which experienced a massive 105.7% increase in the value of V_p. Otherwise, Method 18 gave a generally good performance for the DG and LDG modes (although it worked poorly against the LDG mode of C section whose V_p value increased by 27.4%), while making almost no difference to the L, G, D, and LD modes.

In addition, a comparison between Fig. 41-Fig. 42 and Fig. 25-Fig. 26 (for Method 11) can visually demonstrate the slightly reduced scatter related to DG and LDG modes, as well as to Rack and Stiffened C sections.

In addition, in order to achieve an overall resistance factor ϕ of about 0.85 as stipulated in the existing DSM, a penalty factor of 0.85 was applied to the final predicted strength such that,

$$P_n = 0.85 \times \min(P_{nle},\ P_{nde},\ P_{ne}) \qquad (33)$$

The statistics of the resulting predictions are tabulated in Table 89-Table 90, along with the simulation-to-predicted ratios for all columns illustrated in Fig. 43-Fig. 44. More detailed figures of the same kind for each section are provided in Section R.2. The additional 0.85 factor did not change the scatter of the prediction (represented by V_p) but raised the mean P_m and hence the resistance factor ϕ uniformly for all failure modes and section types. However, it failed to raise the overall ϕ values to 0.85 for Hat and Stiffened C sections.

Table 85: Resistance factors for all columns failing in modes L, LG, G, D, and L+LG+G+D by **DSM Method 18** – Modification 10 to Option 4 in (Moen and Schafer 2011) – replace D equation by DG interaction equation, use $P_{cr\text{-}1\text{-}nh}$ and $P_{cr\text{-}d\text{-}nh}$

| prediction method | Section shape | Failure mode | | | | | | | | | | | | | | | | | | | | |
| | | L | | | | LG | | | | G | | | | D | | | | All L, LG, G, D | | | |
		P_m	V_p	ϕ	n	P_m	V_p	ϕ	n	P_m	V_p	ϕ	n	P_m	V_p	ϕ	n	P_m	V_p	ϕ	n
DSM Method 18	C	1.077	0.135	0.865	6923	1.043	0.124	0.848	4245	0.942	0.096	0.789	1651	1.108	0.206	0.802	3678	1.062	0.157	0.828	16497
	Z	1.066	0.112	0.879	3712	0.995	0.179	0.752	1358	1.053	0.043	0.916	2548	0.957	0.090	0.806	2444	1.027	0.115	0.844	10062
	Hat	0.848	0.102	0.706	1414	0.932	0.187	0.695	494	1.087	0.044	0.945	137	0.831	0.162	0.643	441	0.875	0.151	0.688	2486
	Rack	0.977	0.093	0.820	461	0.897	0.182	0.674	1065	0.990	0.114	0.814	383	0.847	0.104	0.704	391	0.920	0.154	0.720	2300
	Stiffened C	0.945	0.113	0.778	317	0.964	0.137	0.771	143	1.024	0.067	0.878	196	1.009	0.241	0.687	245	0.983	0.161	0.762	901
	All sections	1.042	0.143	0.827	12827	1.004	0.157	0.782	7305	1.011	0.087	0.853	4915	1.022	0.200	0.747	7199	1.024	0.155	0.800	32246

Table 86: Resistance factors for all columns failing in modes LD, DG, LDG, LD+DG+LDG, and all failure modes by **DSM Method 18** – Modification 10 to Option 4 in (Moen and Schafer 2011) – replace D equation by DG interaction equation, use $P_{cr\text{-}1\text{-}nh}$ and $P_{cr\text{-}d\text{-}nh}$

| prediction method | Section shape | Failure mode | | | | | | | | | | | | | | | | | | | | |
| | | LD | | | | DG | | | | LDG | | | | All LD, DG, LDG | | | | ALL Failure modes | | | |
		P_m	V_p	ϕ	n	P_m	V_p	ϕ	n	P_m	V_p	ϕ	n	P_m	V_p	ϕ	n	P_m	V_p	ϕ	n
DSM Method 18	C	0.813	0.173	0.620	3157	0.866	0.163	0.670	2589	1.056	0.214	0.754	862	0.866	0.200	0.633	6608	1.006	0.189	0.748	23105
	Z	0.899	0.118	0.736	4115	1.039	0.098	0.868	2989	1.067	0.147	0.842	6057	1.008	0.150	0.794	13161	1.016	0.136	0.815	23223
	Hat	0.715	0.181	0.538	585	0.820	0.240	0.560	1927	0.855	0.232	0.592	964	0.812	0.238	0.556	3476	0.838	0.207	0.606	5962
	Rack	0.734	0.106	0.609	137	0.917	0.179	0.693	832	0.947	0.154	0.741	900	0.918	0.174	0.699	1869	0.919	0.163	0.710	4169
	Stiffened C	0.715	0.203	0.520	245	0.867	0.237	0.594	1727	0.951	0.153	0.745	800	0.877	0.223	0.617	2772	0.903	0.213	0.646	3673
	All sections	0.845	0.163	0.654	8239	0.913	0.197	0.670	10064	1.024	0.178	0.774	9583	0.931	0.198	0.683	27886	0.981	0.181	0.739	60132

Table 87: Difference in resistance factors between **DSM Method 18** and **DSM Method 11** for all columns failing in modes L, LG, G, D, and L+LG+G+D

prediction method	Section shape	Failure mode														
		L			LG			G			D			All L, LG, G, D		
		P_m	V_p	ϕ	P_m	V_p	ϕ	P_m	V_p	ϕ	P_m	V_p	ϕ	P_m	V_p	ϕ
DSM Method 18	C	-0.1%	0.7%	-0.1%	1.7%	15.9%	-0.2%	0.2%	-2.0%	0.4%	0.0%	0.0%	0.0%	0.4%	1.3%	0.1%
	Z	0.0%	0.0%	0.0%	-10.3%	105.7%	-19.7%	1.2%	-4.4%	1.4%	0.0%	0.0%	0.0%	-0.7%	12.7%	-2.0%
	Hat	-0.5%	6.2%	-1.1%	1.0%	3.3%	0.1%	0.0%	0.0%	0.0%	0.0%	0.0%	0.0%	0.0%	3.4%	-0.7%
	Rack	0.0%	0.0%	0.0%	5.0%	-11.2%	8.9%	0.0%	0.0%	0.0%	0.0%	0.0%	0.0%	2.2%	-9.4%	4.5%
	Stiffened C	-0.5%	6.6%	-1.1%	4.9%	-0.7%	5.0%	0.0%	0.0%	0.0%	0.0%	0.0%	0.0%	0.6%	0.0%	0.7%
	All sections	-0.1%	0.7%	-0.2%	0.5%	6.1%	-0.9%	0.8%	1.2%	0.7%	0.0%	0.0%	0.0%	0.1%	1.3%	-0.1%

Table 88: Difference in resistance factors between **DSM Method 18** and **DSM Method 11** for all columns failing in modes LD, DG, LDG, LD+DG+LDG, and all

failure modes

prediction method	Section shape	Failure mode														
		LD			DG			LDG			All LD, DG, LDG			ALL Failure modes		
		P_m	V_p	ϕ	P_m	V_p	ϕ	P_m	V_p	ϕ	P_m	V_p	ϕ	P_m	V_p	ϕ
DSM Method 18	C	0.0%	0.0%	0.0%	4.7%	-9.9%	7.5%	4.7%	27.4%	-2.6%	2.6%	4.7%	1.1%	0.9%	-0.5%	1.1%
	Z	0.0%	0.0%	0.0%	5.1%	-11.7%	6.4%	2.9%	-9.8%	5.1%	2.5%	-2.6%	3.3%	1.2%	0.0%	1.2%
	Hat	-0.1%	1.7%	-0.6%	9.6%	-16.1%	19.4%	4.8%	-1.3%	5.3%	6.6%	-8.8%	11.2%	3.6%	-7.6%	6.9%
	Rack	0.0%	0.0%	0.0%	6.5%	4.1%	5.6%	13.0%	-15.8%	17.8%	9.3%	-2.8%	10.1%	5.3%	-7.9%	7.3%
	Stiffened C	0.0%	0.0%	0.0%	15.6%	-20.2%	29.1%	15.7%	-23.9%	24.2%	14.2%	-16.5%	23.6%	10.3%	-18.4%	20.1%
	All sections	0.0%	0.6%	0.0%	7.4%	-14.0%	13.4%	5.0%	-10.6%	8.4%	4.4%	-6.6%	7.1%	2.1%	-5.7%	3.9%

Table 89: Resistance factors for all columns failing in modes L, LG, G, and L+LG+G+D by **DSM Method 18** – Modification 10 to Option 4 in (Moen and Schafer 2011) – replace D equation by DG interaction equation, use $P_{cr\text{-}l\text{-}nh}$ and $P_{cr\text{-}d\text{-}nh}$, factor final strengths by 0.85

prediction method	Section shape	Failure mode																				
		L				LG				G				D				All L, LG, G, D			
		P_m	V_p	ϕ	n	P_m	V_p	ϕ	n	P_m	V_p	ϕ	n	P_m	V_p	ϕ	n	P_m	V_p	ϕ	n
DSM Method 18	C	1.268	0.135	1.017	6923	1.227	0.124	0.997	4245	1.109	0.096	0.929	1651	1.304	0.206	0.943	3678	1.249	0.157	0.974	16497
	Z	1.254	0.112	1.034	3712	1.171	0.179	0.884	1358	1.239	0.043	1.077	2548	1.126	0.090	0.948	2444	1.208	0.115	0.992	10062
	Hat	0.998	0.102	0.831	1414	1.096	0.187	0.818	494	1.279	0.044	1.112	137	0.978	0.162	0.757	441	1.029	0.151	0.809	2486
	Rack	1.149	0.093	0.965	461	1.056	0.182	0.793	1065	1.165	0.114	0.958	383	0.996	0.104	0.828	391	1.082	0.154	0.847	2300
	Stiffened C	1.112	0.113	0.915	317	1.134	0.137	0.907	143	1.205	0.067	1.033	196	1.187	0.241	0.808	245	1.156	0.161	0.896	901
	All sections	1.226	0.143	0.973	12827	1.181	0.157	0.920	7305	1.189	0.087	1.004	4915	1.203	0.200	0.879	7199	1.205	0.155	0.942	32246

Table 90: Resistance factors for all columns failing in modes LD, DG, LDG, LD+DG+LDG, and all failure modes by **DSM Method 18** – Modification 10 to Option 4 in (Moen and Schafer 2011) – replace D equation by DG interaction equation, use $P_{cr\text{-}l\text{-}nh}$ and $P_{cr\text{-}d\text{-}nh}$, factor final strengths by 0.85

| prediction method	Section shape	Failure mode																				
		LD				DG				LDG				All LD, DG, LDG				ALL Failure modes			
		P_m	V_p	ϕ	n	P_m	V_p	ϕ	n	P_m	V_p	ϕ	n	P_m	V_p	ϕ	n	P_m	V_p	ϕ	n
DSM Method 18	C	0.957	0.173	0.729	3157	1.019	0.163	0.788	2589	1.243	0.214	0.887	862	1.018	0.200	0.744	6608	1.183	0.189	0.879	23105
	Z	1.058	0.118	0.866	4115	1.222	0.098	1.022	2989	1.255	0.147	0.991	6057	1.186	0.150	0.934	13161	1.195	0.136	0.958	23223
	Hat	0.841	0.181	0.633	585	0.965	0.240	0.659	1927	1.006	0.232	0.696	964	0.955	0.238	0.654	3476	0.986	0.207	0.713	5962
	Rack	0.864	0.106	0.717	137	1.079	0.179	0.815	832	1.114	0.154	0.872	900	1.080	0.174	0.822	1869	1.081	0.163	0.836	4169
	Stiffened C	0.841	0.203	0.612	245	1.019	0.237	0.699	1727	1.118	0.153	0.876	800	1.032	0.223	0.726	2772	1.063	0.213	0.760	3673
	All sections	0.994	0.163	0.769	8239	1.074	0.197	0.788	10064	1.204	0.178	0.911	9583	1.095	0.198	0.803	27886	1.154	0.181	0.869	60132
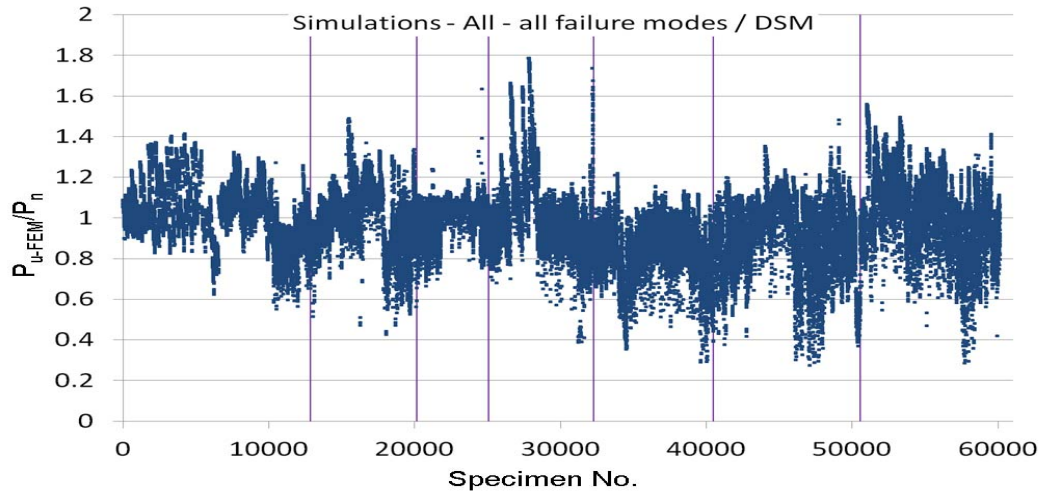
Fig. 41: Simulation-to-predicted ratios for all columns by DSM Method 18 with classified failure modes
(from left to right: L, LG, G, D, LD, DG, and LDG)
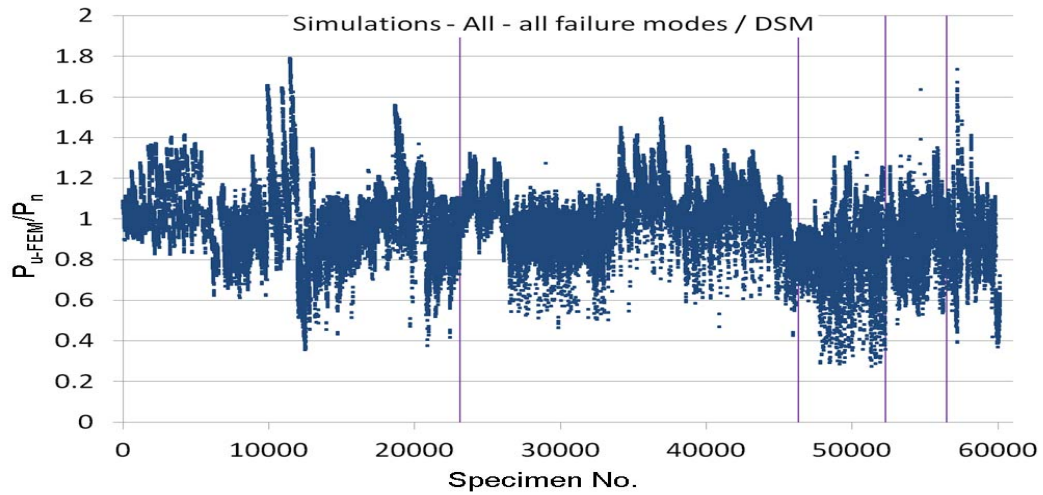
Fig. 42: Simulation-to-predicted ratios for all columns by DSM Method 18 with classified section types
(from left to right: C, Z, Hat, Rack and Stiffened C)
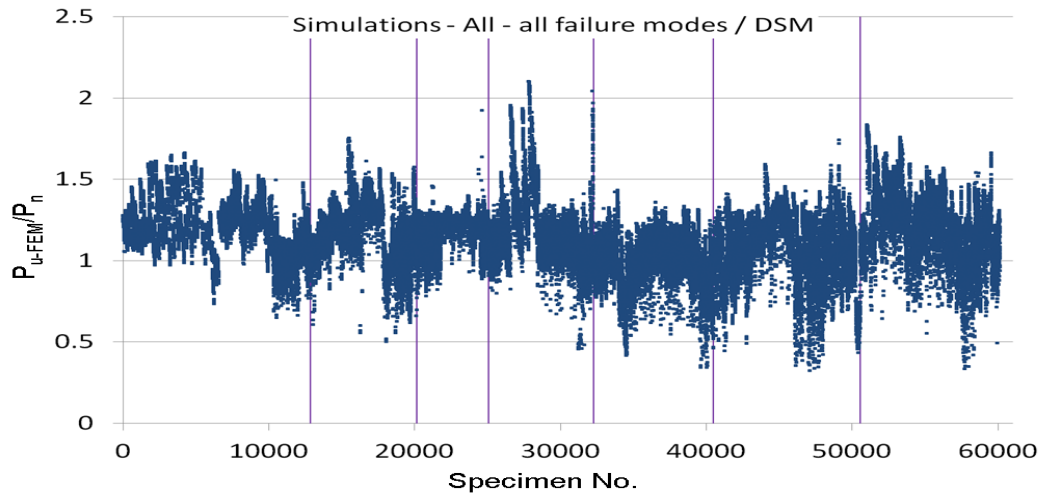
Fig. 43: Simulation-to-predicted ratios for all columns by DSM Method 18 with classified failure modes (from left to right: L, LG, G, D, LD, DG, and LDG), factor final strengths by 0.85
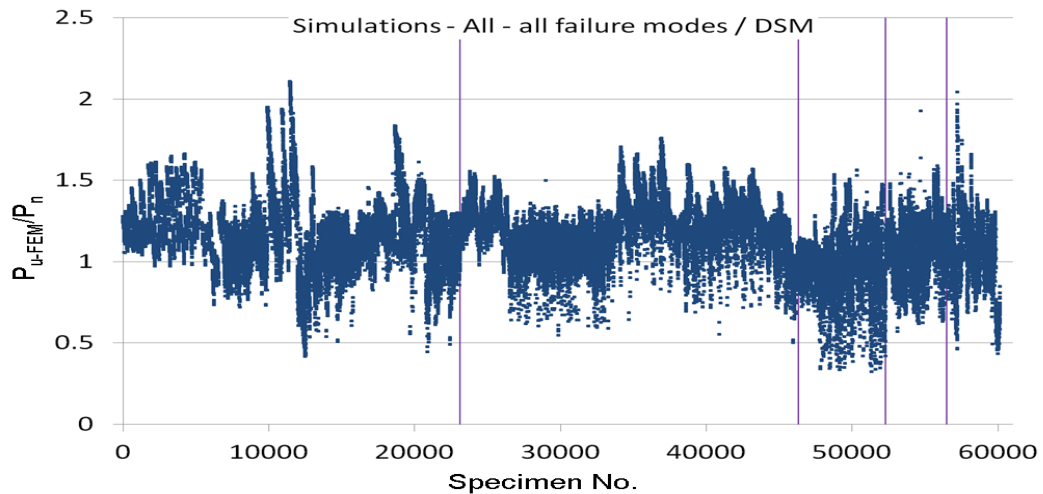
Fig. 44: Simulation-to-predicted ratios for all columns by DSM Method 18 with classified section types (from left to right: C, Z, Hat, Rack and Stiffened C), factor final strengths by 0.85

3.4.2. Method 19 – include DG interaction and use regression analyses – all

In terms of producing a small scatter in prediction (as indicated by the value of V_p), DSM Method 18 was by far the best-performing design scheme among those not using a regression analysis (i.e. DSM Method 1-12, 16, and 18). Therefore, based on Method 18 a regression analysis was carried out to further improve its performance. This new scheme constituted DSM Method 19 which is defined as

$$P_n = F1 \times \min(P_{nle}, P_{nde}, P_{ne}) \tag{34}$$

where (i) $F1$ is obtained from the regression analysis and computed as per Equation (35) with all the constants defined in Table 91, (ii) P_{nle} represents the LG buckling strength via Equations (28)-(29), (iii) P_{nde}

stands for the DG buckling strength per Equations (25)-(27), and (iv) P_{ne} is the global buckling strength according to Equations (30)-(31).

$$F1 = a + b \times \lambda_{le} + c \times \lambda_{de} + d \times \lambda_{c} + e \times HWF + f \times HLF + g \times HSF + h \times \frac{H}{t} + i \times \frac{B}{t} + j \times \frac{D}{t} + k \times \frac{H}{B} + m \times \frac{D}{B} \quad (35)$$

Table 91: Constants from regression analysis for DSM Method 19

a	b	c	d	e	f
9.38E-01	6.89E-02	-3.14E-02	5.76E-02	-2.20E-01	-2.46E-02
g	h	i	j	k	m
5.32E-03	1.10E-03	-2.24E-03	-6.76E-03	-7.98E-03	5.57E-02

Table 93-Table 94 list the statistics of the predictions for all columns using DSM Method 19, along with the percentage differences of the statistics between Method 19 and 18 as well as between Method 19 and 17 given in Table 95-Table 96 and Table 97-Table 98, respectively. In addition, the simulation-to-predicted ratios for all columns are illustrated in Fig. 45-Fig. 46. More detailed figures for each section type can be found in Section S.1.

In comparison with DSM Method 18, the additional regression analysis significantly improved the overall performance of the prediction, as shown by a 15.5% decrease in the overall value of V_p, and a 18.1 % increase in the overall value of ϕ. This improvement mainly came from C, Z and Hat sections, while Method 19 resulted in a larger scatter in the predictions for Rack and particularly Stiffened C sections, as indicated by a 5.5% and 14.6% increase in the values of V_p. In addition, although a considerable larger scatter (i.e. 34.9% and 77.3% increase in V_p) was produced by Method 19 for Z and Hat sections failing in the G mode, the corresponding values of ϕ were still overly safe (i.e. ϕ=0.990 and 1.048 respectively). Moreover, the overall values of ϕ showed that all section types except Stiffened C section satisfied the prescribed value of ϕ=0.85. In particular, when the collection of the L, LG, G and D modes (i.e. those modes covered in the AS/NZS 4600 DSM) were considered in isolation, ϕ=0.85 was satisfied for all section types, whereas it failed to be satisfied for C, Hat and Stiffened C sections when the collection of the LD, DG and LDG modes were concerned.

Moreover, Table 97-Table 98 showed that Method 19 generally performed better than Method 17 which did not consider DG interaction, as implied by a 6.1% decrease in the overall value of V_p. In particular, the scatter related to Hat and Stiffened C sections decreased significantly, as shown by 12.2% and 17.8% decreases in the values of V_p. This result indicated that the phenomenon of DG interaction was significant with these section types. However, considering DG interaction worsened the predictions for occasional cases, such as C and Rack section columns failing in the LDG and DG mode respectively, as indicated by the increases of 31.3% and 22.6% in the values of V_p. Otherwise, it was beneficial to most cases, and therefore should be included in the strength prediction as a general practice, especially for Hat and Stiffened C sections.

Compared with the simulation-to-predicted ratios (Fig. 41-Fig. 42) for DSM Method 18, Fig. 45-Fig. 46 show that the overall scatter in prediction was significantly reduced by the addition of a regression analysis,

especially for C and Z sections, while some large discrepancies from unity in the value of $P_{u\text{-}FEM}/P_n$ appeared in the LG, LD, DG, and LDG modes with Hat, Rack and Stiffened C sections. In addition, in comparison with Fig. 37-Fig. 38 for DSM Method 17, Fig. 45-Fig. 46 demonstrate that the inclusion of DG interaction equations produced largely similar results, except for some slight improvements, particularly the decrease of some large discrepancies in the LG, D, LD, DG, and LDG modes for Hat, Rack, and Stiffened C sections.

In order to improve the performance of DSM Method 19 for Stiffened C section whose overall V_p and ϕ values of 0.244 and 0.726 respectively were unsatisfactory, a separate regression analysis based on DSM Method 19 was carried out on Stiffened C section alone which resulted in a separate set of regression constants defined in Table 92.

Table 92: Constants from regression analysis for DSM Method 19 – Stiffened C section only

a	b	c	d	e	f
7.42E-01	3.65E-02	-1.66E-02	3.01E-02	-2.05E-01	-2.11E-02
g	h	i	j	k	m
8.96E-03	-1.15E-03	1.73E-03	3.20E-03	3.39E-02	1.47E-01

The resulting statistics of the predictions are presented in Table 99-Table 100, while the percentage differences of the statistics between Table 99-Table 100 and Table 93-Table 94 are provided in Table 101-Table 102.

The separate set of regression constants substantially improved the prediction for Stiffened C section. With a 7.9% increase in the overall value of P_m and a 21.3% (from 0.244 to 0.192) decrease in the overall value of V_p, a 17.9% increase in the overall resistance factor ϕ was achieved. Moreover, this improvement, especially in terms of the accuracy of the prediction, was seen for all failure modes, as demonstrated by the decrease in their V_p values which were as high as over 50% for the LD and LDG modes. In addition, the ϕ values for all failure modes satisfied the 0.85 requirement as prescribed in the AS/NZS 4600 DSM except the LD and DG modes whose ϕ values were 0.759 and 0.784 respectively, although the ϕ values for the remaining modes were considered slightly overly conservative. Also, this method performed significantly better than the similar method based on DSM Method 17 presented in Table 81-Table 82, as shown by comparing their overall V_p values, i.e. 0.192 for this method versus 0.238 for Method 17.

Furthermore, Fig. 47 and Fig. 48 illustrate the simulation-to-predicted ratios for Stiffened C section using the regression constants in Table 91 and Table 92 respectively. It is obvious that the separate regression analysis reduced the scatter considerably, while significant discrepancies still existed for a minority of columns subjected to the D and DG modes. In addition, the mean value of the predicted strengths of the columns failing in the LD mode was clearly over-predicted.

Table 93: Resistance factors for all columns failing in modes L, LG, G, and L+LG+G+D by **DSM Method 19** – Modification 11 to Option 4 in (Moen and Schafer 2011) – replace D equation by DG interaction equation, use $P_{cr-l-nh}$ and $P_{cr-d-nh}$, regression analyses of final strengths

prediction method	Section shape	Failure mode																			
		L				LG				G				D				All L, LG, G, D			
		P_m	V_p	ϕ	n	P_m	V_p	ϕ	n	P_m	V_p	ϕ	n	P_m	V_p	ϕ	n	P_m	V_p	ϕ	n
DSM Method 19	C	1.134	0.107	0.940	6923	1.041	0.103	0.866	4245	0.994	0.082	0.842	1651	1.248	0.129	1.009	3678	1.122	0.134	0.901	16497
	Z	1.180	0.098	0.987	3712	1.035	0.171	0.791	1358	1.148	0.058	0.990	2548	1.181	0.081	1.002	2444	1.153	0.106	0.956	10062
	Hat	1.121	0.095	0.940	1414	1.363	0.203	0.991	494	1.233	0.078	1.048	137	1.122	0.110	0.927	441	1.175	0.157	0.916	2486
	Rack	1.206	0.077	1.027	461	1.080	0.214	0.772	1065	1.065	0.088	0.899	383	1.087	0.048	0.943	391	1.104	0.159	0.858	2300
	Stiffened C	1.106	0.136	0.887	317	1.068	0.114	0.879	143	1.092	0.065	0.938	196	1.286	0.255	0.854	245	1.146	0.191	0.849	901
	All sections	1.148	0.105	0.953	12827	1.068	0.168	0.819	7305	1.090	0.097	0.912	4915	1.210	0.127	0.980	7199	1.135	0.133	0.913	32246

Table 94: Resistance factors for all columns failing in modes LD, DG, LDG, LD+DG+LDG, and all failure modes by **DSM Method 19** – Modification 11 to Option 4 in (Moen and Schafer 2011) – replace D equation by DG interaction equation, use $P_{cr-l-nh}$ and $P_{cr-d-nh}$, regression analyses of final strengths

prediction method	Section shape	Failure mode																			
		LD				DG				LDG				All LD, DG, LDG				ALL Failure modes			
		P_m	V_p	ϕ	n	P_m	V_p	ϕ	n	P_m	V_p	ϕ	n	P_m	V_p	ϕ	n	P_m	V_p	ϕ	n
DSM Method 19	C	0.976	0.161	0.757	3157	0.978	0.134	0.785	2589	1.017	0.176	0.772	862	0.982	0.154	0.769	6608	1.082	0.151	0.850	23105
	Z	1.062	0.090	0.894	4115	1.182	0.080	1.004	2989	1.152	0.137	0.922	6057	1.131	0.121	0.923	13161	1.140	0.115	0.937	23223
	Hat	1.100	0.147	0.868	585	1.083	0.185	0.810	1927	1.214	0.237	0.832	964	1.122	0.205	0.813	3476	1.144	0.187	0.853	5962
	Rack	1.053	0.108	0.871	137	1.100	0.190	0.817	832	1.251	0.151	0.983	900	1.169	0.179	0.882	1869	1.133	0.172	0.865	4169
	Stiffened C	0.922	0.294	0.569	245	1.035	0.251	0.693	1727	1.111	0.243	0.753	800	1.047	0.257	0.693	2772	1.071	0.244	0.726	3673
	All sections	1.028	0.140	0.820	8239	1.078	0.176	0.818	10064	1.152	0.173	0.878	9583	1.089	0.172	0.830	27886	1.113	0.153	0.873	60132

Table 95: Difference in resistance factors between **DSM Method 19** and **DSM Method 18** for all columns failing in modes L, LG, G, D, and L+LG+G+D

prediction method	Section shape	Failure mode														
		L			LG			G			D			All L, LG, G, D		
		P_m	V_p	ϕ	P_m	V_p	ϕ	P_m	V_p	ϕ	P_m	V_p	ϕ	P_m	V_p	ϕ
DSM Method 19	C	5.3%	-20.7%	8.7%	-0.2%	-16.9%	2.1%	5.5%	-14.6%	6.7%	12.6%	-37.4%	25.8%	5.6%	-14.6%	8.8%
	Z	10.7%	-12.5%	12.3%	4.0%	-4.5%	5.2%	9.0%	34.9%	8.1%	23.4%	-10.0%	24.3%	12.3%	-7.8%	13.3%
	Hat	32.2%	-6.9%	33.1%	46.2%	8.6%	42.6%	13.4%	77.3%	10.9%	35.0%	-32.1%	44.2%	34.3%	4.0%	33.1%
	Rack	23.4%	-17.2%	25.2%	20.4%	17.6%	14.5%	7.6%	-22.8%	10.4%	28.3%	-53.8%	33.9%	20.0%	3.2%	19.2%
	Stiffened C	17.0%	20.4%	14.0%	10.8%	-16.8%	14.0%	6.6%	-3.0%	6.8%	27.5%	5.8%	24.3%	16.6%	18.6%	11.4%
	All sections	10.2%	-26.6%	15.2%	6.4%	7.0%	4.7%	7.8%	11.5%	6.9%	18.4%	-36.5%	31.2%	10.8%	-14.2%	14.1%

Table 96: Difference in resistance factors between **DSM Method 19** and **DSM Method 18** for all columns failing in modes LD, DG, LDG, LD+DG+LDG, and all

failure modes

prediction method	Section shape	Failure mode														
		LD			DG			LDG			All LD, DG, LDG			ALL Failure modes		
		P_m	V_p	ϕ	P_m	V_p	ϕ	P_m	V_p	ϕ	P_m	V_p	ϕ	P_m	V_p	ϕ
DSM Method 19	C	20.0%	-6.9%	22.1%	12.9%	-17.8%	17.2%	-3.7%	-17.8%	2.4%	13.4%	-23.0%	21.5%	7.6%	-20.1%	13.6%
	Z	18.1%	-23.7%	21.5%	13.8%	-18.4%	15.7%	8.0%	-6.8%	9.5%	12.2%	-19.3%	16.2%	12.2%	-15.4%	15.0%
	Hat	53.8%	-18.8%	61.3%	32.1%	-22.9%	44.6%	42.0%	2.2%	40.5%	38.2%	-13.9%	46.2%	36.5%	-9.7%	40.8%
	Rack	43.5%	1.9%	43.0%	20.0%	6.1%	17.9%	32.1%	-1.9%	32.7%	27.3%	2.9%	26.2%	23.3%	5.5%	21.8%
	Stiffened C	29.0%	44.8%	9.4%	19.4%	5.9%	16.7%	16.8%	58.8%	1.1%	19.4%	15.2%	12.3%	18.6%	14.6%	12.4%
	All sections	21.7%	-14.1%	25.4%	18.1%	-10.7%	22.1%	12.5%	-2.8%	13.4%	17.0%	-13.1%	21.5%	13.5%	-15.5%	18.1%

Table 97: Difference in resistance factors between **DSM Method 19** and **DSM Method 17** for all columns failing in modes L, LG, G, D, and L+LG+G+D

prediction method	Section shape	Failure mode														
		L			LG			G			D			All L, LG, G, D		
		P_m	V_p	ϕ	P_m	V_p	ϕ	P_m	V_p	ϕ	P_m	V_p	ϕ	P_m	V_p	ϕ
DSM Method 19	C	-2.1%	-0.9%	-1.9%	-6.6%	-1.0%	-6.5%	-8.3%	-2.4%	-8.3%	-3.0%	0.0%	-3.0%	-3.9%	6.3%	-4.9%
	Z	-2.1%	1.0%	-2.1%	-6.6%	-6.6%	-4.9%	-7.2%	-3.3%	-7.0%	-3.0%	0.0%	-3.1%	-4.2%	1.0%	-4.3%
	Hat	-3.8%	-8.7%	-2.9%	-6.4%	-10.2%	-2.7%	-7.8%	1.3%	-8.0%	-3.6%	-2.7%	-3.3%	-4.6%	-11.3%	-1.9%
	Rack	-2.2%	0.0%	-2.2%	-2.2%	-11.6%	2.8%	-8.0%	2.3%	-8.1%	-2.7%	-5.9%	-2.5%	-3.2%	-8.6%	-1.2%
	Stiffened C	-1.1%	-9.9%	0.9%	5.2%	-5.0%	6.0%	-7.8%	1.6%	-7.9%	-2.9%	-5.2%	-0.2%	-2.2%	-8.2%	0.5%
	All sections	-2.2%	-1.9%	-2.1%	-5.7%	-6.1%	-4.2%	-7.6%	2.1%	-7.9%	-3.0%	-0.8%	-3.0%	-4.0%	0.0%	-4.0%

Table 98: Difference in resistance factors between **DSM Method 19** and **DSM Method 17** for all columns failing in modes LD, DG, LDG, LD+DG+LDG, and all

failure modes

prediction method	Section shape	Failure mode														
		LD			DG			LDG			All LD, DG, LDG			ALL Failure modes		
		P_m	V_p	ϕ	P_m	V_p	ϕ	P_m	V_p	ϕ	P_m	V_p	ϕ	P_m	V_p	ϕ
DSM Method 19	C	-3.6%	-3.0%	-2.8%	-2.1%	-13.5%	0.5%	-0.5%	31.3%	-6.0%	-2.6%	-2.5%	-2.0%	-3.6%	1.3%	-3.8%
	Z	-3.0%	0.0%	-3.0%	-2.2%	1.3%	-2.3%	-3.8%	-10.5%	-1.7%	-3.2%	-6.9%	-2.1%	-3.6%	-4.2%	-3.0%
	Hat	-6.9%	-8.1%	-5.2%	0.2%	-14.7%	5.6%	-2.6%	-8.8%	1.3%	-1.9%	-12.0%	2.9%	-3.1%	-12.2%	0.9%
	Rack	-5.0%	-6.1%	-4.3%	0.7%	22.6%	-4.2%	5.4%	-5.6%	6.7%	2.6%	11.2%	-0.1%	-0.6%	2.4%	-1.1%
	Stiffened C	-1.7%	-9.0%	4.2%	7.5%	-20.8%	22.0%	9.1%	-19.3%	21.6%	7.2%	-18.2%	19.7%	4.5%	-17.8%	15.6%
	All sections	-3.5%	-4.1%	-2.7%	0.0%	-12.0%	3.9%	-1.6%	-8.9%	1.2%	-1.5%	-8.5%	0.7%	-3.0%	-6.1%	-1.6%

Table 99: Resistance factors for stiffened C section columns failing in modes L, LG, G, and L+LG+G+D by **DSM Method 19** – Modification 11 to Option 4 in (Moen and Schafer 2011) – replace D equation by DG interaction equation, use $P_{cr\text{-}l\text{-}nh}$ and $P_{cr\text{-}d\text{-}nh}$, **separate** regression analyses of final strengths

prediction method	Section shape	Failure mode																		
		L				LG				G				D				All L, LG, G, D			
		P_m	V_p	ϕ	n	P_m	V_p	ϕ	n	P_m	V_p	ϕ	n	P_m	V_p	ϕ	n	P_m	V_p	ϕ	n
DSM Method 19 (for SC)	Stiffened C	1.173	0.100	0.979	317	1.310	0.078	1.115	143	1.210	0.057	1.044	196	1.365	0.231	0.947	245	1.255	0.161	0.972	901

Table 100: Resistance factors for stiffened C section columns failing in modes LD, DG, LDG, LD+DG+LDG, and all failure modes by **DSM Method 19** – Modification 11 to Option 4 in (Moen and Schafer 2011) – replace D equation by DG interaction equation, use $P_{cr\text{-}l\text{-}nh}$ and $P_{cr\text{-}d\text{-}nh}$, **separate** regression analyses of final strengths

Prediction method	Section shape	Failure mode																		
		LD				DG				LDG				All LD, DG, LDG				ALL Failure modes			
		P_m	V_p	ϕ	n	P_m	V_p	ϕ	n	P_m	V_p	ϕ	n	P_m	V_p	ϕ	n	P_m	V_p	ϕ	n
DSM Method 19 (for SC)	Stiffened C	0.942	0.131	0.759	245	1.095	0.212	0.784	1727	1.242	0.106	1.029	800	1.124	0.194	0.829	2772	1.156	0.192	0.856	3673

Table 101: Difference in resistance factors between Table 99 and Table 93 for Stiffened C columns failing in modes L, LG, G, D, and L+LG+G+D

prediction method	Section shape	Failure mode														
		L			LG			G			D			All L, LG, G, D		
		P_m	V_p	ϕ	P_m	V_p	ϕ	P_m	V_p	ϕ	P_m	V_p	ϕ	P_m	V_p	ϕ
DSM Method 19 (for SC)	Stiffened C	6.1%	-26.5%	10.4%	22.7%	-31.6%	26.8%	10.8%	-12.3%	11.3%	6.1%	-9.4%	10.9%	9.5%	-15.7%	14.5%

Table 102: Difference in resistance factors between Table 100 and Table 94 for Stiffened C failing in modes LD, DG, LDG, LD+DG+LDG, and all failure modes

prediction method	Section shape	Failure mode														
		LD			DG			LDG			All LD, DG, LDG			ALL Failure modes		
		P_m	V_p	ϕ	P_m	V_p	ϕ	P_m	V_p	ϕ	P_m	V_p	ϕ	P_m	V_p	ϕ
DSM Method 19 (for SC)	Stiffened C	2.2%	-55.4%	33.4%	5.8%	-15.5%	13.1%	11.8%	-56.4%	36.7%	7.4%	-24.5%	19.6%	7.9%	-21.3%	17.9%
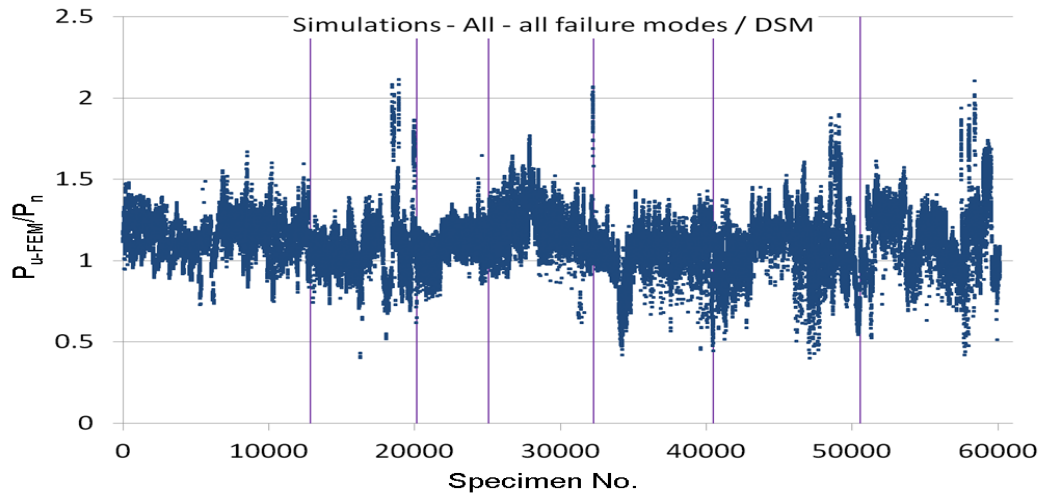
Fig. 45: Simulation-to-predicted ratios for all columns by DSM Method 19 with classified failure modes
(from left to right: L, LG, G, D, LD, DG, and LDG)
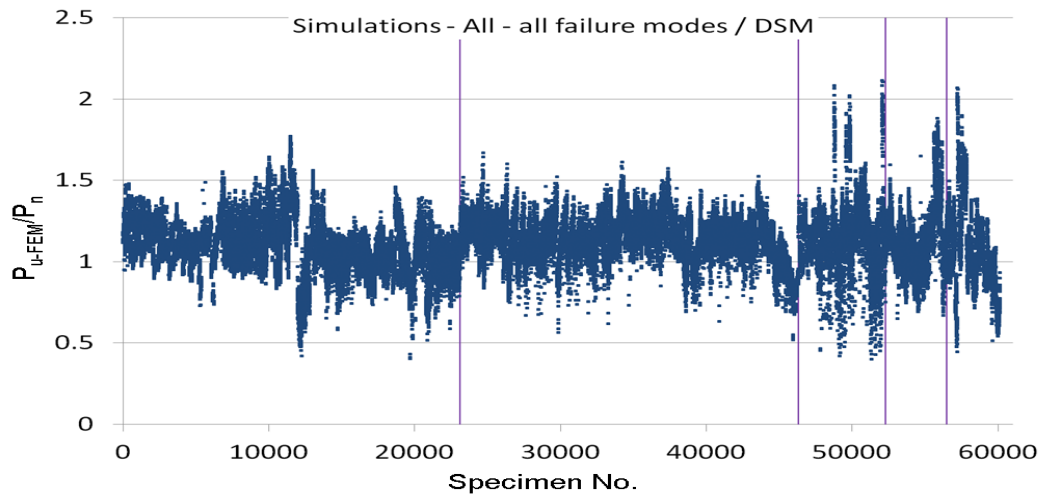
Fig. 46: Simulation-to-predicted ratios for all columns by DSM Method 19 with classified section types
(from left to right: C, Z, Hat, Rack and Stiffened C)
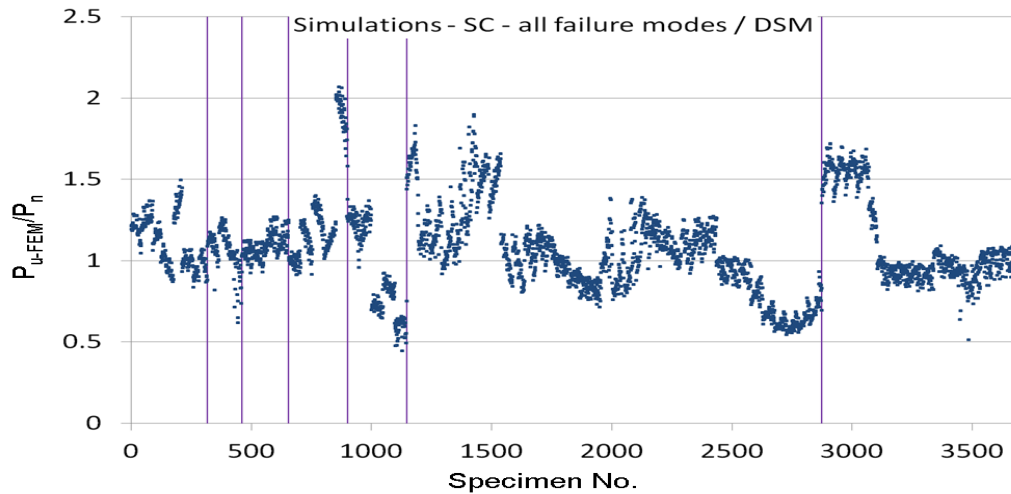
Fig. 47: Simulation-to-predicted ratios for all Stiffened C section columns by DSM Method 19 with classified failure modes (from left to right: L, LG, G, D, LD, DG, and LDG)
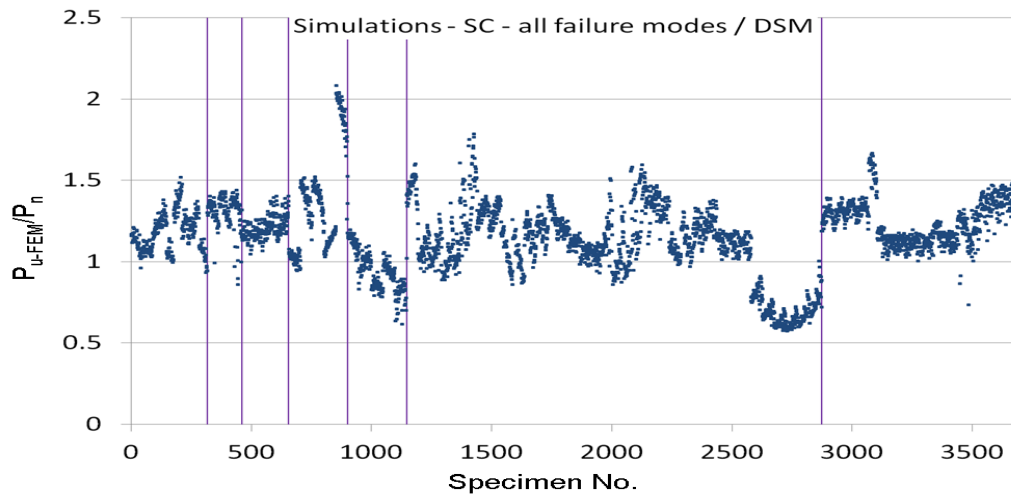
Fig. 48: Simulation-to-predicted ratios for all Stiffened C section columns by DSM Method 19 by separate regression parameters with classified failure modes (from left to right: L, LG, G, D, LD, DG, and LDG)

3.4.3. Method 19 – incl. DG interaction & regression analyses – non-perforated

In the following, DSM Method 19 was applied to only non-perforated columns, with the aim to verify its applicability to this subset of columns, and also to identify its inherent limitations with respect to certain sections.

Table 103-Table 104 list the statistics of the predictions for non-perforated columns using DSM Method 19 (with the constants defined in Table 91). Meanwhile, Table 105-Table 106 and Table 107-Table 108 present the percentage differences of the statistics between Method 19 and Method 1, and between Method 19 and Method 2, respectively.

The comparison with Method 1 demonstrates that Method 19 improved the performance of the prediction considerably, in terms of both a reduced overall scatter and an increased overall reliability, as indicated by a 16.1% decrease in the value of V_p from 0.155 to 0.130 and a 3.5% increase in the value of ϕ from 0.824 to 0.853. In particular, the values of ϕ exceeded (or were close to) 0.85 for all section types except for Stiffened C section which had a ϕ value of 0.708 (despite the fact that it had been improved from 0.609 as per Method 1). However, in terms of an individual failure mode of a particular section type, Method 19 did not always performed better than Method 1. In particular, the poorer performance related to the G, LG, and LDG modes of C section and the LG mode of Z section caused their ϕ values to drop from above (or close to) 0.85 to below it. Besides, in terms of the failure mode, Method 19 had the worst performance against G, LG, and LD modes which showed either a large increase in the scatter of the prediction or a significant decrease in the resistance factors, whereas the DG mode seemed to be the one most improved as shown by a 26.9% decrease in the overall value of V_p and a 17.2% increase in the overall value of ϕ. On the other hand, in terms of section type, the most improved sections were C section (with the largest decrease (22.2%) in the overall V_p value) and Hat section (with the largest increase (22.9%) in the overall ϕ value).

The comparison with Method 2 showed that an additional regression analysis was in general beneficial to the improvement of the prediction, as shown by a 9.7% decrease in the overall value of V_p. Although there was only a slight 0.2% increase in the overall value of ϕ, Method 19 successfully increased the overall ϕ value for Hat section from 0.789 to 0.906 which was well above the prescribed value of 0.85, leaving the Stiffened C section, the only section for which Method 19 performed significantly worse than Method 2, as the only one whose ϕ value failed to reach this value. In terms of failure mode, Method 19 produced a much larger scatter (i.e. larger values of V_p) than Method 2 for the G, LG, and LD modes, especially for Hat, Rack, and Stiffened C sections. This was mainly because in the regression analysis the total numbers of the columns made from these sections were much smaller than those for C and Z sections. Therefore, the results of the regression analysis were predominantly dependent on the data for C and Z sections.

The simulation-to-predicted ratios ($P_{\text{u-FEM}}/P_n$) for all non-perforated columns are also illustrated in Fig. 49-Fig. 50 for Method 19. More detailed figures for each section type can be found in Section S.3. Compared with both Fig. 1-Fig. 2 for Method 1 and Fig. 5-Fig. 6 for Method 2, it is visually clear that Method 19 had a better performance as there was a smaller scatter in the $P_{\text{u-FEM}}/P_n$ ratios. However, there were still some large discrepancies from unity in the $P_{\text{u-FEM}}/P_n$ ratios with almost every failure mode (Fig. 49) and every section type (Fig. 50), which will be investigated closely in the next section.

Table 103: Resistance factors for **non-perforated** columns failing in modes L, LG, G, D, and L+LG+G+D by **DSM Method 19** – Modification 11 to Option 4 in (Moen and Schafer 2011) – replace D equation by DG interaction equation, use $P_{cr-1-nh}$ and $P_{cr-d-nh}$, regression analyses of final strengths (same regression constants as with Table 93 and Table 94)

prediction method	Section shape	Failure mode																			
		L				LG				G				D				All L, LG, G, D			
		P_m	V_p	ϕ	n	P_m	V_p	ϕ	n	P_m	V_p	ϕ	n	P_m	V_p	ϕ	n	P_m	V_p	ϕ	n
DSM Method 19	C	1.044	0.090	0.880	292	0.972	0.098	0.813	94	0.949	0.083	0.804	34	1.129	0.145	0.895	80	1.038	0.115	0.853	500
	Z	1.089	0.084	0.922	147	0.960	0.141	0.764	28	1.014	0.028	0.886	52	1.086	0.061	0.935	50	1.061	0.090	0.894	277
	Hat	1.067	0.071	0.912	42	1.330	0.192	0.984	13	1.069	0.032	0.933	3	1.167	0.096	0.978	9	1.131	0.147	0.894	67
	Rack	1.110	0.064	0.954	11	1.185	0.136	0.949	22	1.048	0.048	0.909	8	1.119	0.058	0.965	8	1.135	0.111	0.936	49
	Stiffened C	1.031	0.129	0.833	10	1.088	0.074	0.929	3	1.023	0.009	0.898	4	1.321	0.314	0.783	5	1.103	0.214	0.787	22
	All sections	1.060	0.089	0.894	502	1.031	0.169	0.789	160	0.997	0.063	0.857	101	1.123	0.134	0.902	152	1.059	0.118	0.867	915

Table 104: Resistance factors for **non-perforated** columns failing in modes LD, DG, LDG, LD+DG+LDG, and all failure modes by **DSM Method 19** – Modification 11 to Option 4 in (Moen and Schafer 2011) – replace D equation by DG interaction equation, use $P_{cr-1-nh}$ and $P_{cr-d-nh}$, regression analyses of final strengths (same regression constants as with Table 93 and Table 94)

prediction method	Section shape	Failure mode																			
		LD				DG				LDG				All LD, DG, LDG				ALL Failure modes			
		P_m	V_p	ϕ	n	P_m	V_p	ϕ	n	P_m	V_p	ϕ	n	P_m	V_p	ϕ	n	P_m	V_p	ϕ	n
DSM Method 19	C	0.956	0.141	0.761	65	0.939	0.128	0.760	54	1.027	0.190	0.763	22	0.961	0.149	0.757	141	1.021	0.126	0.828	641
	Z	1.017	0.062	0.875	84	1.080	0.081	0.917	62	1.132	0.115	0.930	134	1.086	0.106	0.900	280	1.074	0.099	0.896	557
	Hat	1.128	0.086	0.953	12	1.103	0.085	0.933	41	1.199	0.186	0.895	21	1.134	0.130	0.916	74	1.133	0.138	0.906	141
	Rack	1.081	0.118	0.885	3	1.088	0.094	0.913	17	1.186	0.127	0.961	18	1.134	0.119	0.927	38	1.134	0.114	0.933	87
	Stiffened C	0.935	0.335	0.531	5	0.951	0.220	0.672	36	1.059	0.199	0.774	17	0.981	0.225	0.687	58	1.015	0.227	0.708	80
	All sections	1.000	0.120	0.817	169	1.027	0.141	0.818	210	1.126	0.145	0.893	212	1.055	0.147	0.834	591	1.057	0.130	0.853	1506

Table 105: Difference in resistance factors between **DSM Method 19** and **DSM Method 1** for **non-perforated** columns failing in modes L, LG, G, D, and

L+LG+G+D

prediction method	Section shape	Failure mode														
		L			LG			G			D			All L, LG, G, D		
		P_m	V_p	ϕ	P_m	V_p	ϕ	P_m	V_p	ϕ	P_m	V_p	ϕ	P_m	V_p	ϕ
DSM Method 19	C	-5.8%	-33.3%	-1.0%	-9.6%	19.5%	-10.8%	-7.4%	0.0%	-7.5%	-2.6%	-33.2%	8.9%	-6.0%	-21.2%	-2.3%
	Z	-1.6%	-13.4%	-0.5%	-8.8%	-2.8%	-8.4%	-5.2%	-6.7%	-5.2%	5.2%	5.2%	5.1%	-1.7%	-7.2%	-0.9%
	Hat	14.7%	26.6%	13.6%	27.1%	32.5%	18.7%	-2.2%	143.4%	-2.7%	14.3%	4.3%	13.8%	16.4%	41.5%	10.6%
	Rack	6.5%	-23.8%	8.2%	8.9%	67.9%	2.8%	-5.6%	77.8%	-6.4%	9.2%	28.9%	8.4%	6.0%	50.0%	2.4%
	Stiffened C	0.5%	79.2%	-5.0%	0.9%	117.6%	-1.2%	-6.7%	50.0%	-6.7%	8.7%	15.4%	0.1%	1.3%	37.2%	-7.3%
	All sections	-2.8%	-30.5%	1.4%	-3.6%	69.0%	-11.6%	-5.9%	8.6%	-6.2%	1.7%	-28.0%	9.5%	-2.4%	-10.6%	-0.8%

Table 106: Difference in resistance factors between **DSM Method 19** and **DSM Method 1** for **non-perforated** columns failing in modes LD, DG, LDG,

LD+DG+LDG, and all failure modes

prediction method	Section shape	Failure mode														
		LD			DG			LDG			All LD, DG, LDG			ALL Failure modes		
		P_m	V_p	ϕ	P_m	V_p	ϕ	P_m	V_p	ϕ	P_m	V_p	ϕ	P_m	V_p	ϕ
DSM Method 19	C	2.9%	8.5%	1.5%	2.1%	-26.0%	8.4%	-9.1%	15.2%	-12.3%	0.4%	-13.4%	3.7%	-4.8%	-22.2%	-0.2%
	Z	1.7%	3.3%	1.5%	1.4%	-5.8%	1.9%	-2.0%	-12.2%	-0.1%	-0.3%	-15.2%	1.8%	-1.0%	-10.0%	0.0%
	Hat	27.3%	18.1%	25.9%	23.4%	-59.1%	44.6%	27.0%	9.6%	24.0%	25.0%	-28.7%	34.3%	20.8%	-8.7%	22.9%
	Rack	20.1%	68.6%	14.8%	9.2%	1.1%	9.2%	23.9%	-40.7%	40.7%	16.9%	-25.6%	23.1%	10.4%	-8.8%	11.9%
	Stiffened C	9.9%	53.0%	-11.8%	17.6%	-22.8%	32.3%	15.7%	8.2%	13.0%	16.2%	-11.1%	22.0%	11.4%	-9.9%	16.3%
	All sections	4.4%	12.1%	2.9%	8.7%	-26.9%	17.2%	2.7%	-15.2%	6.6%	5.2%	-17.9%	10.2%	0.4%	-16.1%	3.5%

Table 107: Difference in resistance factors between **DSM Method 19** and **DSM Method 2** for **non-perforated** columns failing in modes L, LG, G, D, and

L+LG+G+D

prediction method	Section shape	Failure mode														
		L			LG			G			D			All L, LG, G, D		
		P_m	V_p	ϕ	P_m	V_p	ϕ	P_m	V_p	ϕ	P_m	V_p	ϕ	P_m	V_p	ϕ
DSM Method 19	C	-5.8%	-33.3%	-1.0%	-12.1%	-14.8%	-10.5%	-7.4%	0.0%	-7.5%	-2.6%	-33.2%	8.9%	-6.5%	-22.8%	-2.4%
	Z	-1.6%	-13.4%	-0.5%	-8.8%	-2.8%	-8.4%	-5.3%	-6.7%	-5.2%	5.2%	5.2%	5.1%	-1.9%	-3.2%	-1.5%
	Hat	14.7%	26.6%	13.6%	25.6%	29.8%	17.8%	-2.2%	143.4%	-2.7%	14.3%	4.3%	13.8%	16.1%	37.5%	10.8%
	Rack	6.5%	-23.8%	8.2%	3.8%	86.3%	-2.7%	-5.6%	77.8%	-6.4%	9.2%	28.9%	8.4%	3.7%	38.8%	0.5%
	Stiffened C	0.5%	79.2%	-5.0%	-3.5%	105.6%	-5.5%	-6.7%	50.0%	-6.7%	8.7%	15.4%	0.1%	0.6%	37.2%	-8.0%
	All sections	-2.8%	-30.5%	1.4%	-6.1%	42.0%	-12.1%	-5.9%	8.6%	-6.3%	1.7%	-28.0%	9.5%	-2.8%	-11.3%	-1.1%

Table 108: Difference in resistance factors between **DSM Method 19** and **DSM Method 2** for **non-perforated** columns failing in modes LD, DG, LDG,

LD+DG+LDG, and all failure modes

prediction method	Section shape	Failure mode														
		LD			DG			LDG			All LD, DG, LDG			ALL Failure modes		
		P_m	V_p	ϕ	P_m	V_p	ϕ	P_m	V_p	ϕ	P_m	V_p	ϕ	P_m	V_p	ϕ
DSM Method 19	C	2.9%	8.5%	1.5%	-1.5%	1.6%	-1.7%	-14.3%	-8.2%	-11.8%	-1.9%	-16.3%	2.0%	-5.6%	-22.7%	-1.0%
	Z	1.7%	3.3%	1.5%	-1.4%	3.8%	-1.5%	-5.3%	13.9%	-6.7%	-2.6%	-8.6%	-1.5%	-2.2%	-7.5%	-1.5%
	Hat	27.3%	18.1%	25.9%	12.4%	-40.9%	19.9%	19.9%	24.2%	13.7%	16.8%	-9.2%	18.8%	16.4%	9.4%	14.8%
	Rack	20.1%	68.6%	14.8%	3.2%	54.1%	0.6%	10.7%	-21.1%	15.8%	8.0%	-6.3%	8.9%	5.4%	10.7%	4.4%
	Stiffened C	9.9%	53.0%	-11.8%	2.1%	-0.5%	2.3%	0.3%	59.2%	-9.8%	2.1%	11.4%	-1.9%	1.7%	15.2%	-3.4%
	All sections	4.4%	12.1%	2.9%	2.2%	-2.8%	2.9%	-2.5%	3.6%	-3.0%	1.0%	-6.4%	2.3%	-1.5%	-9.7%	0.2%
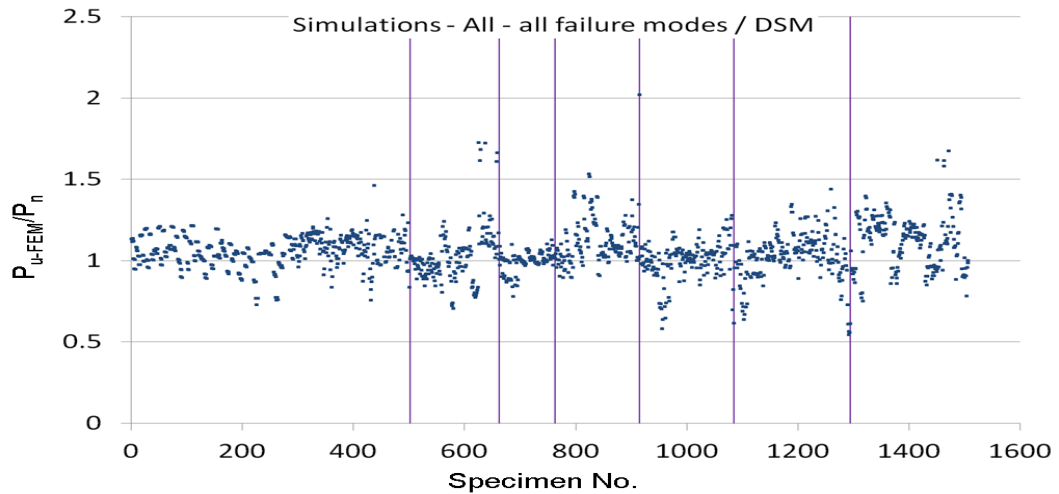
Fig. 49: Simulation-to-predicted ratios for all non-perforated columns by DSM Method 19 with classified failure modes (from left to right: L, LG, G, D, LD, DG, and LDG)
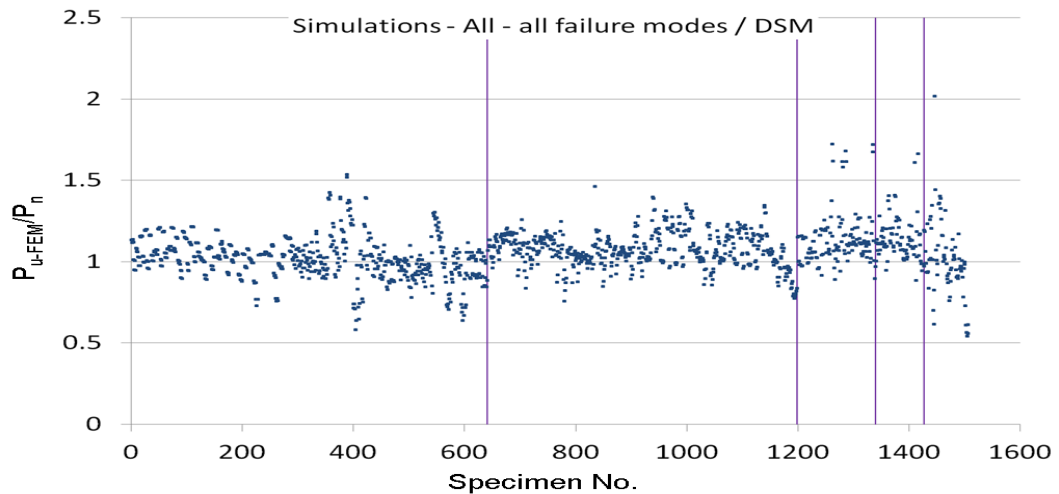
Fig. 50: Simulation-to-predicted ratios for all non-perforated columns by DSM Method 19 with classified section types (from left to right: C, Z, Hat, Rack and Stiffened C)

In the following, DSM Method 19 with separate regression constants listed in Table 92 was applied to non-perforated Stiffened C section columns. Its statistical performance is presented in Table 109-Table 110, with the percentage differences of the statistics between Method 19 and Method 1, as well as between Method 19 and Method 2 given in Table 111-Table 112 and Table 113-Table 114, respectively.

The separate regression analysis based on Method 19 raised the overall value of ϕ for Stiffened C section to 0.824 which was deemed acceptable as it was close to 0.85. Among all the failure modes, $\phi=0.85$ was not satisfied for only the LD and DG modes whose ϕ values were 0.751 and 0.748 respectively. In addition, the comparison with the current codified DSM (i.e. Method 1) demonstrates that the improvement in prediction was substantial, as shown by the 21.8% decrease in the overall value of V_p and 35.3% increase in the overall value of ϕ. A significant increase in the prediction accuracy was seen for the LG, LD, DG, and LDG modes whose V_p values all decreased by more than 20%. On the other hand, compared to Method 2 which also

included DG interaction, the additional regression analysis in Method 19 raised the overall value of ϕ by 12.4%, although it did not change the overall value of V_p. Of all the modes, the LG and LD modes experienced the most marked decrease in the scatter of the prediction, as shown by over 20% decreases in their values of V_p. In addition, the comparisons with both Method 1 and 2 demonstrate that Method 19 increased the scatter of the prediction for both the G and D modes, as shown by a 66.7% and 7.7% increase in their values of V_p, although the resulting ϕ values (i.e. 1.005 and 0.885) were both well above 0.85.

In addition, Fig. 51 illustrates the simulation-to-predicted ratios by Method 19 with separate regression constants for non-perforated Stiffened C section columns. Compared with the corresponding figures for Method 1 and Method 2, the improvement in prediction was obvious in terms of producing a smaller scatter. However, this method still failed to reduce some large discrepancies related to the D and DG modes.

Table 109: Resistance factors for non-perforated stiffened C section columns failing in modes L, LG, G, D, and L+LG+G+D by **DSM Method 19** – Modification 11 to Option 4 in (Moen and Schafer 2011) – replace D equation by DG interaction equation, use $P_{cr-l-nh}$ and $P_{cr-d-nh}$, **separate** regression analyses of final strengths (same regression constants as with Table 99 and Table 100)

prediction method	Section shape	Failure mode																			
		L				LG				G				D				All L, LG, G, D			
		P_m	V_p	ϕ	n	P_m	V_p	ϕ	n	P_m	V_p	ϕ	n	P_m	V_p	ϕ	n	P_m	V_p	ϕ	n
DSM Method 19 (for SC)	Stiffened C	1.143	0.062	0.983	10	1.336	0.022	1.170	3	1.145	0.010	1.005	4	1.431	0.293	0.885	5	1.235	0.184	0.925	22

Table 110: Resistance factors for non-perforated stiffened C section columns failing in modes LD, DG, LDG, LD+DG+LDG, and all failure modes by **DSM Method 19** – Modification 11 to Option 4 in (Moen and Schafer 2011) – replace D equation by DG interaction equation, use $P_{cr-l-nh}$ and $P_{cr-d-nh}$, **separate** regression analyses of final strengths (same regression constants as with Table 99 and Table 100)

prediction method	Section shape	Failure mode																			
		LD				DG				LDG				All LD, DG, LDG				ALL Failure modes			
		P_m	V_p	ϕ	n	P_m	V_p	ϕ	n	P_m	V_p	ϕ	n	P_m	V_p	ϕ	n	P_m	V_p	ϕ	n
DSM Method 19 (for SC)	Stiffened C	0.976	0.166	0.751	5	1.031	0.204	0.748	36	1.209	0.111	0.997	17	1.079	0.189	0.802	58	1.122	0.197	0.824	80

Table 111: Difference in resistance factors between **DSM Method 19 (for SC only)** and **DSM Method 1** for Stiffened C columns failing in modes L, LG, G, D, and L+LG+G+D

prediction method	Section shape	Failure mode														
		L			LG			G			D			All L, LG, G, D		
		P_m	V_p	ϕ	P_m	V_p	ϕ	P_m	V_p	ϕ	P_m	V_p	ϕ	P_m	V_p	ϕ
DSM Method 19 (for SC)	Stiffened C	11.4%	-13.9%	12.1%	23.9%	-35.3%	24.5%	4.4%	66.7%	4.4%	17.8%	7.7%	13.2%	13.4%	17.9%	9.0%

Table 112: Difference in resistance factors between **DSM Method 19 (for SC only)** and **DSM Method 1** for Stiffened C failing in modes LD, DG, LDG, LD+DG+LDG, and all failure modes

prediction method	Section shape	Failure mode														
		LD			DG			LDG			All LD, DG, LDG			ALL Failure modes		
		P_m	V_p	ϕ	P_m	V_p	ϕ	P_m	V_p	ϕ	P_m	V_p	ϕ	P_m	V_p	ϕ
DSM Method 19 (for SC)	Stiffened C	14.7%	-24.2%	24.8%	27.4%	-28.4%	47.2%	32.1%	-39.7%	45.5%	27.8%	-25.3%	42.5%	23.2%	-21.8%	35.3%

Table 113: Difference in resistance factors between **DSM Method 19 (for SC only)** and **DSM Method 2** for Stiffened C columns failing in modes L, LG, G, D, and L+LG+G+D

prediction method	Section shape	Failure mode														
		L			LG			G			D			All L, LG, G, D		
		P_m	V_p	ϕ	P_m	V_p	ϕ	P_m	V_p	ϕ	P_m	V_p	ϕ	P_m	V_p	ϕ
DSM Method 19 (for SC)	Stiffened C	11.4%	-13.9%	12.1%	18.5%	-38.9%	19.0%	4.4%	66.7%	4.4%	17.8%	7.7%	13.2%	12.7%	17.9%	8.2%

Table 114: Difference in resistance factors between **DSM Method 19 (for SC only)** and **DSM Method 2** for Stiffened C failing in modes LD, DG, LDG, LD+DG+LDG, and all failure modes

prediction method	Section shape	Failure mode														
		LD			DG			LDG			All LD, DG, LDG			ALL Failure modes		
		P_m	V_p	ϕ	P_m	V_p	ϕ	P_m	V_p	ϕ	P_m	V_p	ϕ	P_m	V_p	ϕ
DSM Method 19 (for SC)	Stiffened C	14.7%	-24.2%	24.8%	10.7%	-7.7%	13.9%	14.5%	-11.2%	16.2%	12.3%	-6.4%	14.6%	12.4%	0.0%	12.4%
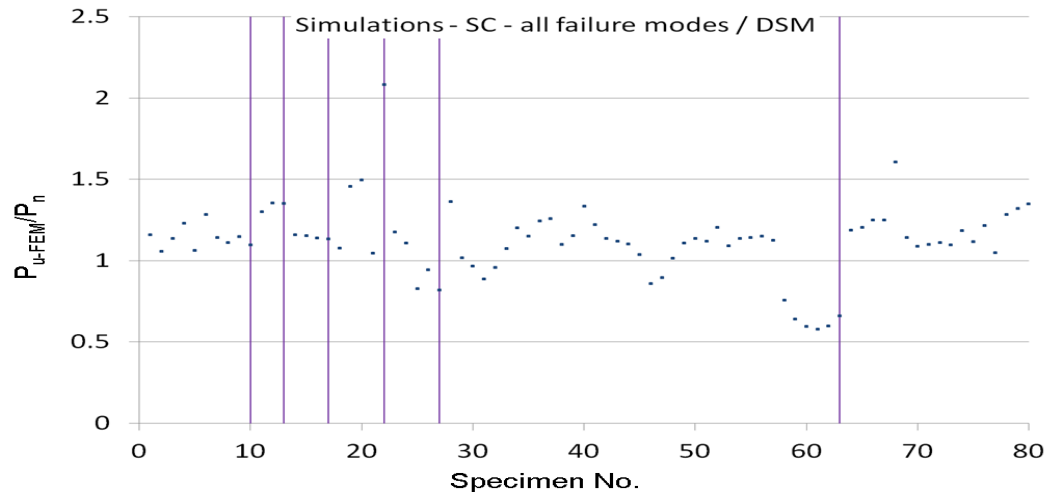
Fig. 51: Simulation-to-predicted ratios for non-perforated Stiffened C section columns by DSM Method 19 by separate regression parameters with classified failure modes (from left to right: L, LG, G, D, LD, DG, and LDG)

3.4.4. Method 19 – applicability

The limitations and hence the applicability of the best-performing method, i.e. DSM Method 19, are presented in this section. First of all, any large discrepancies in the simulation-to-predicted ratios by Method 19 for non-perforated columns are highlighted in the figures in Section T.1 for each section type. Data points for clearly over-predicted and under-predicted strengths are marked red and blue, respectively. These data points are numbered and further described in Table 115, where the ID corresponds to each mark in the figures. Take "D_C1" for example, "D" represents discrepancy, "C" stands for C section, while "1" denotes the corresponding mark numbered in Fig. T.1. For each group of columns whose strengths were not accurately predicted, Table 115 provides information such as the failure mode, section No., column length, whether the current codified DSM produced similar predictions, whether Method 19 produced safer or unsafer predictions compared to the current DSM, and any special features possibly related to the inaccurate predictions. Users of Method 19 should be aware of these discrepancies and avoid using these sections and column lengths that were identified here as leading to inferior strength predictions. Further research is needed to verify the specific limits of parameters within which DSM Method 19 is considered to be adequately accurate.

Table 115: Large discrepancies in predicted strengths by Method 19 for non-perforated columns

ID of discrepancy	Over- or under-predicted	Failure mode	Section No.	Column length	Similar prediction by AS/NZS 4600 DSM?	safer or unsafer compared to AS/NZS 4600 DSM?
D_C1	over	L	C57	3 local half-waves	no	unsafer
	Notes: C57 was an extremely slender section with the highest web/thickness ratio of 478.7						
D_C2	over	L	C66	3 local half-waves	yes	slightly unsafer
	Notes: C66 had very small lips (i.e. lip width to flange width ratio of 0.047) which made it susceptible to distortional deformations even the column was restrained to fail in 3 local half-waves.						
D_C3	over	LG	C56	$\lambda_c=0.52$	no	unsafer
	Notes: C56 was an extremely slender section with a high web/thickness ratio of 372.3.						
D_C4	over	G	C19	$\lambda_c=3.14$	no	unsafer
	Notes: this column had global geometric imperfection bowing towards the flanges, which resulted in more pronounced compression in the web, and hence slight LG mode interaction.						
D_C5	over	LD	C55-C57, C59, C60, C63	4 distortional half-waves	yes	overall similar
	Notes: these sections featured $\lambda_1 \gg \lambda_d$ (λ_1 was at least 1.84 higher than λ_d), and therefore failed in strong LD interaction.						
D_C6	over	DG	C65	$\lambda_c=0.79-2.61$	yes	safer
	Notes: C65 featured small lips (i.e. lip width to flange width ratio of 0.094) and hence $\lambda_d=2.05 > \lambda_1=1.81$, so it was subjected to strong DG interaction.						
D_C7	over	LDG	C56	$\lambda_c=1.05$	yes	safer
	Notes: C56 was an extremely slender section with a high web/thickness ratio of 372.3.						
D_C8	under	LG	C41, C43	$\lambda_c=3.15$ for C41, $\lambda_c=1.57$ and 2.09 for C43	no	inaccurately safer
	Notes: for the long columns made from C41, toward-web geometric imperfection resulted in more than 30% increase in the ultimate strength when compared to toward-flange imperfection; C43 featured a high ratio of web width to flange width of 6.15.						
D_C9	under	D	C32, C32, C36, C43-C46,C49-C54, C65-C66	4 distortional half-waves	yes	unsafer, but more accurate
	Notes: C65 and C66 featured very small lips (lip width/ flange width ratios=0.094 and 0.047 respectively), while the remaining sections listed here featured high web width/thickness ratios of 98.3-231.2 and high web width/flange width ratios of 4.8-7.4.						
D_C10	under	LDG	C43	$\lambda_c=0.52-1.05$	yes	unsafer, but more accurate
	Notes: C43 featured a high ratio of web width to flange width of 6.15.						
D_Z1	over	L	Z34, Z35, Z69, Z70	3 local half-waves	no	unsafer
	Notes: these were slender sections with $\lambda_1=4.14$ and web width/thickness ratio of 203.						
D_Z2	over	LG	Z71	all lengths, i.e. $\lambda_c=0.46-3.14$	yes	slightly unsafer
	Notes: Z71 was a section without lips.						
D_Z3	over	LD	Z6, Z11, Z34, Z59, Z60, Z69	4 distortional half-waves	no	overall similar
	Notes: these are slender sections featured $\lambda_1 > 3.0$ and $\lambda_1 > \lambda_d$.						

D_Z4	over	LDG	Z34, Z35, Z69, Z70	λ_c=0.46-1.05	yes	overall similar
	Notes: see notes for D_Z1.					
D_Z5	under	L	Z26	4 distortional half-waves	yes	inaccurately much safer
	Notes: no special pattern found.					
D_Z6	under	LDG	Z6, Z16, Z19, Z21, Z22, Z30	λ_c=0.46-2.09	yes	overall similar
	Notes: these sections featured lips perpendicular to flanges, no other special pattern was found.					
D_H1	slightly over	LD	H2	4 distortional half-waves	no	unsafer
	Notes: H2 featured the widest web of 304.8 mm, and hence the highest ratio of web width to thickness of 114.3.					
D_H2	slightly over	DG	H1	λ_c=1.38	yes	safer
	Notes: H1 was a slender section with λ_1=2.96 and λ_d=2.73, and also had the lowest ratio of web width to flange width of 0.5, and lip width to flange width of 0.105.					
D_H3	slightly over	DG	H21	λ_c=1.38	yes	safer
	Notes: H21 was the most slender section with λ_1=3.53 and λ_d=3.00, and also had the lowest ratio of web width to flange width of 0.5, and lip width to flange width of 0.105.					
D_H4	under	LG	H1, H4, H8, H21	λ_c=0.27	yes	inaccurately much safer
	Notes: these sections featured high ratios of flange width to thickness between 106.7 and 158.8, and also the lowest ratio of web width to flange width of 0.5.					
D_H5	under	D	H20	4 distortional half-waves	yes	inaccurately safer
	Notes: among all the sections failed in the D mode, H20 had the highest ratios of web width to thickness of 46.2 and also flange width to thickness of 46.2, otherwise no special pattern found.					
D_H6	under	LDG	H1, H4, H8, H21	λ_c=0.55	yes	inaccurately much safer
	Notes: see notes for D_H4					
D_R1	over	LDG	R9	λ_c=0.92	yes	safer
	Notes: no special pattern found.					
D_R2	under	LG	R9, R10	λ_c=0.31	yes	inaccurately much safer
	Notes: These sections featured the widest flange width of 85 mm (i.e. lowest web width to flange width ratio of 1.06)					
D_R3	under	LDG	R1, R3	λ_c=0.36-1.09	yes	inaccurately safer
	Notes: no special pattern found.					
D_SC1	over	LD	SC7, SC9	4 distortional half-waves	yes	safer
	Notes: these were the most slender SC sections with λ_1=3.18 and λ_d=3.01 for SC7 and λ_1=4.67 and λ_d=4.06 for SC9.					
D_SC2	over	DG	SC10	λ_c=0.28-1.75	yes	safer
	Notes: SC10 had very small lips (i.e. lip width to flange width ratio of 0.05) and hence its λ_d=3.26>>λ_1=1.78, therefore was subject to strong interaction with the D mode.					
D_SC3	under	D	SC4, SC5, SC10	4 distortional half-waves	yes	inaccurately much safer

	Notes: these sections featured moderate to high cross-sectional slenderness with λ_1=0.92-2.10 and λ_d=1.71-3.26, and also λ_d was at least 0.79 higher than the corresponding λ_1.					
D_SC4	under	LDG	SC4	λ_c=0.50	yes	inaccurately much safer
	Notes: SC4 featured the highest ratio of web width to flange width of 6.15.					

Further, the strength predictions between the non-perforated and perforated columns were also compared. Taking the simulation-to-predicted ratios for non-perforated columns as a benchmark, any large discrepancies due to perforation are highlighted in the figures presented in Section T.2 where blue and red circles represent the relatively over- and under-predictions, respectively. The results suggest that discrepancies due to the presence of perforations were more obvious for Hat and Rack sections and whether the strength was over- or under-predicted partly correlated with the failure mode. These observations indicate that the influence of holes varied between different section types and failure modes, and thus it may require more than a linear equation (as expressed in *F*1 in Method 19) to provide accurate predictions for different scenarios. For example, different sets of nonlinear equations may be required for different section types which warrants further research.

Simulation-to-predicted ratios are plotted in Fig. 52-Fig. 56 as a function of $(A_g-A_n)/A_g$ (i.e. perforation area ratio of the cross-section). Systematic error in the accuracy of the strength prediction with respect to the size (width) of the perforation can be visually identified for large perforations. In particular, the column strength tended to be over-predicted for Z, Rack, and especially Hat sections with large perforations. The accuracy of the predictions deteriorated quickly with an increase in the hole size of Hat section columns, which indicates that Hat section was influenced more by the presence of perforations. This may be related to the fact that Hat section is the only one that had holes located in the flanges.
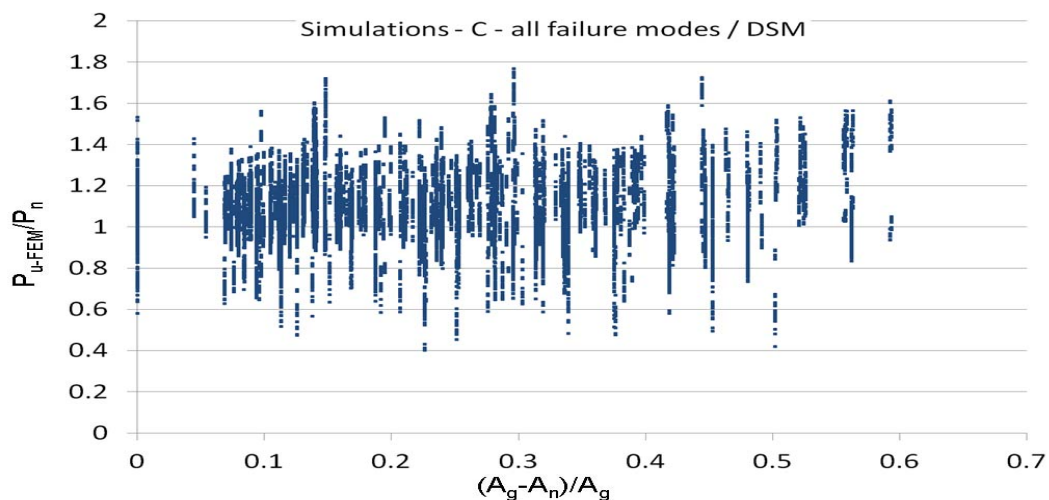
Fig. 52: Simulation-to-predicted ratios for all C section columns by DSM Method 19 as a function of perforated cross-sectional area to gross cross-sectional area
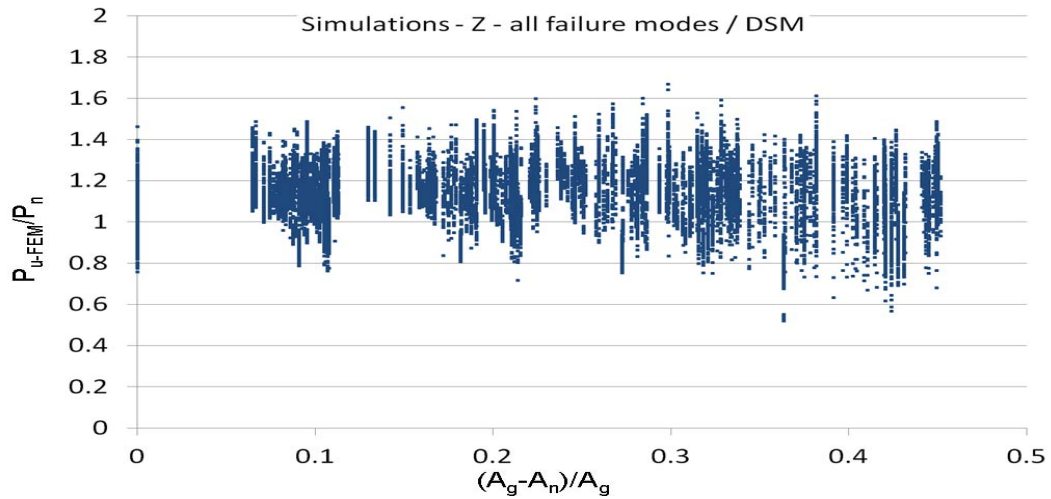
Fig. 53: Simulation-to-predicted ratios for all Z section columns by DSM Method 19 as a function of perforated cross-sectional area to gross cross-sectional area
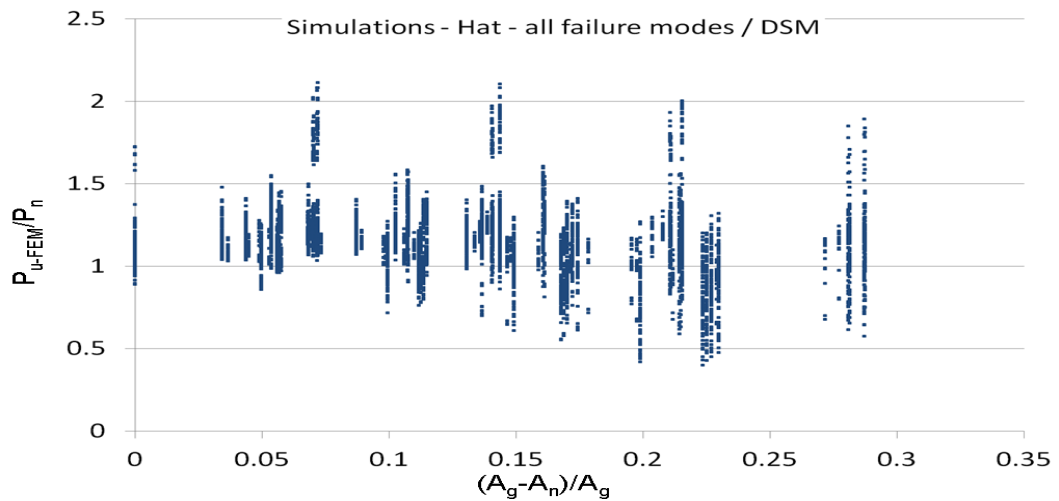
Fig. 54: Simulation-to-predicted ratios for all Hat section columns by DSM Method 19 as a function of perforated cross-sectional area to gross cross-sectional area
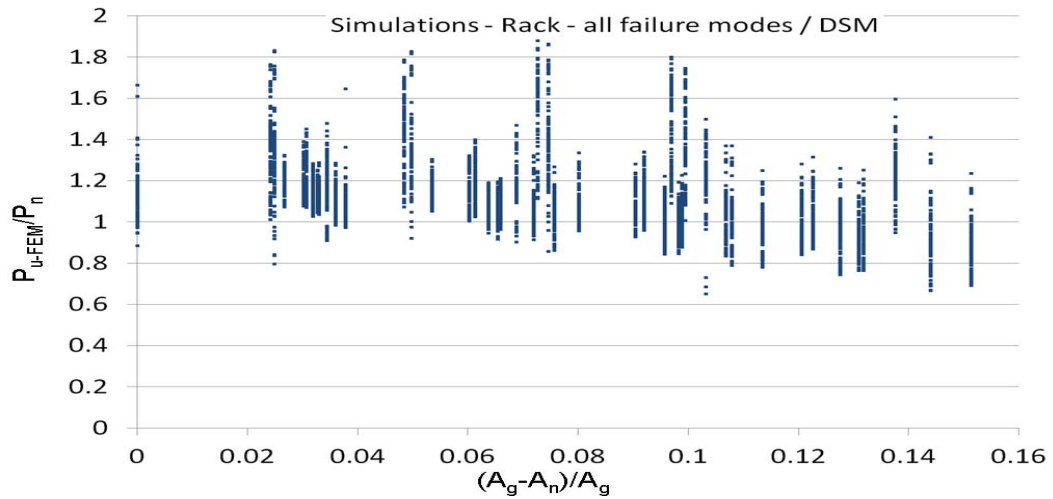
Fig. 55: Simulation-to-predicted ratios for all Rack section columns by DSM Method 19 as a function of perforated cross-sectional area to gross cross-sectional area
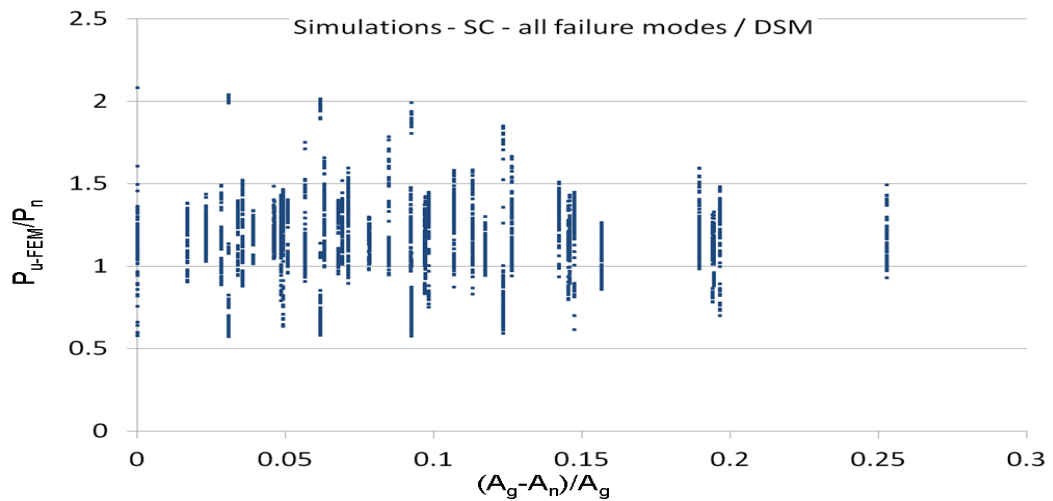
Fig. 56: Simulation-to-predicted ratios for all Stiffened C section columns by DSM Method 19 (with separate regression constants) as a function of perforated cross-sectional area to gross cross-sectional area

In view of this, in order to achieve better results, columns with large holes were excluded from the statistics of the predictions by means of DSM Method 19. Table 116-Table 119 list the statistics of the predictions for all columns with Hole Width Factor (*HWF)* of 0, 0.2, 0.4, and 0.6, while the figures in Section U.1 illustrate the corresponding simulation-to-predicted ratios for each section type. The corresponding statistics and figures for all columns with *HWF*=0, 0.2, and 0.4 are presented in Table 120-Table 123 and in Section V.1.

Overall, the results show that excluding the columns with *HWF*=0.8 results in a decrease in the V_p value from 0.153 to 0.144 (-5.88%) and an increase in the overall ϕ value from 0.873 to 0.888 (1.72%). In terms of section type, Hat and Rack sections benefited most by showing 6.10% (from 0.853 to 0.905) and 4.74% (from

0.865 to 0.906) increases in the values of ϕ, respectively. Besides, in terms of failure mode, the G, LD, DG and LDG modes benefited significantly by showing 7.14%-10.31% decreases in the values of V_p.

When the columns with *HWF*=0.6 were also excluded from the statistics, the overall V_p value further decreased by 3.47% (from 0.144 to 0.139), and the overall ϕ value increased slightly by another 0.34% (from 0.888 to 0.891). Distinctively, the 14.57% (from 0.151 to 0.129) decrease in V_p and 4.30% (from 0.906 to 0.945) increase in ϕ demonstrate that Rack section continued to show significant benefit from excluding larger holes from statistics. In terms of failure mode, the G mode still shows the most decrease in V_p (-8.05% from 0.087 to 0.080), while the LDG mode has the most increase in ϕ (1.54% from 0.907 to 0.921).

In addition, the results for Stiffened C section, whether obtained by the separate regression analysis or not, were minimally affected by excluding from the statistics the columns with large holes. This indicates that the linear formula with respect to the perforation in the regression factor *F*1 (via Equation (35)) was accurate enough to describe the influence of holes on Stiffened C section columns. Furthermore, Section 2.1.2 also showed that the strength of Stiffened C section columns was least affected by the presence of holes compared to the other section types.

Table 116: Resistance factors for columns with **Hole Width Factor=0, 0.2, 0.4, and 0.6** failing in modes L, LG, G, D, and L+LG+G+D by **DSM Method 19** – Modification 11 to Option 4 in (Moen and Schafer 2011) – replace D equation by DG interaction equation, use $P_{cr-l-nh}$ and $P_{cr-d-nh}$, regression analyses of final strengths

prediction method	Section shape	Failure mode																			
		L				LG				G				D				All L, LG, G, D			
		P_m	V_p	ϕ	n	P_m	V_p	ϕ	n	P_m	V_p	ϕ	n	P_m	V_p	ϕ	n	P_m	V_p	ϕ	n
DSM Method 19	C	1.128	0.104	0.938	6331	1.041	0.101	0.868	3333	1.007	0.076	0.857	1253	1.231	0.137	0.985	2870	1.117	0.129	0.904	13787
	Z	1.177	0.093	0.989	3349	1.037	0.160	0.806	1032	1.134	0.057	0.979	1924	1.164	0.068	0.998	1850	1.146	0.099	0.958	8155
	Hat	1.130	0.093	0.949	1212	1.396	0.197	1.025	403	1.213	0.081	1.030	101	1.155	0.073	0.986	333	1.191	0.154	0.932	2049
	Rack	1.197	0.074	1.021	380	1.114	0.195	0.821	807	1.091	0.078	0.927	288	1.091	0.047	0.947	295	1.124	0.144	0.891	1770
	Stiffened C	1.105	0.130	0.892	272	1.087	0.112	0.896	110	1.092	0.058	0.941	148	1.308	0.264	0.854	185	1.152	0.194	0.849	715
	All sections	1.144	0.102	0.953	11544	1.077	0.167	0.828	5685	1.088	0.087	0.919	3714	1.199	0.128	0.971	5533	1.133	0.127	0.918	26476

Table 117: Resistance factors for columns with **Hole Width Factor=0, 0.2, 0.4, and 0.6** failing in modes LD, DG, LDG, LD+DG+LDG, and all failure modes by **DSM Method 19** – Modification 11 to Option 4 in (Moen and Schafer 2011) – replace D equation by DG interaction equation, use $P_{cr-l-nh}$ and $P_{cr-d-nh}$, regression analyses of final strengths

prediction method	Section shape	Failure mode																			
		LD				DG				LDG				All LD, DG, LDG				ALL Failure modes			
		P_m	V_p	ϕ	n	P_m	V_p	ϕ	n	P_m	V_p	ϕ	n	P_m	V_p	ϕ	n	P_m	V_p	ϕ	n
DSM Method 19	C	0.977	0.156	0.763	2384	0.999	0.123	0.813	1979	1.043	0.178	0.789	706	0.995	0.149	0.784	5069	1.085	0.143	0.862	18853
	Z	1.065	0.069	0.912	3107	1.182	0.073	1.010	2273	1.165	0.123	0.948	4732	1.138	0.109	0.941	10112	1.142	0.104	0.948	18267
	Hat	1.137	0.115	0.934	441	1.121	0.147	0.886	1468	1.269	0.209	0.914	743	1.165	0.175	0.885	2652	1.176	0.167	0.905	4701
	Rack	1.039	0.116	0.853	104	1.131	0.155	0.884	628	1.267	0.126	1.027	678	1.190	0.153	0.932	1410	1.153	0.151	0.906	3180
	Stiffened C	0.928	0.292	0.575	185	1.028	0.247	0.693	1320	1.113	0.238	0.762	617	1.044	0.253	0.697	2122	1.071	0.241	0.729	2837
	All sections	1.032	0.130	0.833	6221	1.093	0.160	0.848	7668	1.169	0.160	0.907	7476	1.102	0.161	0.854	21365	1.119	0.144	0.888	47838

Table 118: Resistance factors for stiffened C section columns with **Hole Width Factor=0, 0.2, 0.4, and 0.6** failing in modes L, LG, G, D, and L+LG+G+D by **DSM Method 19** – Modification 11 to Option 4 in (Moen and Schafer 2011) – replace D equation by DG interaction equation, use $P_{cr-l-nh}$ and $P_{cr-d-nh}$, **separate** regression analyses of final strengths

prediction method	Section shape	Failure mode																			
		L				LG				G				D				All L, LG, G, D			
		P_m	V_p	ϕ	n	P_m	V_p	ϕ	n	P_m	V_p	ϕ	n	P_m	V_p	ϕ	n	P_m	V_p	ϕ	n
DSM Method 19 (for SC)	Stiffened C	1.180	0.092	0.992	272	1.328	0.078	1.130	110	1.208	0.052	1.046	148	1.389	0.240	0.947	185	1.263	0.165	0.973	715

Table 119: Resistance factors for stiffened C section columns with **Hole Width Factor=0, 0.2, 0.4, and 0.6** failing in modes LD, DG, LDG, LD+DG+LDG, and all failure modes by **DSM Method 19** – Modification 11 to Option 4 in (Moen and Schafer 2011) – replace D equation by DG interaction equation, use $P_{cr-l-nh}$ and $P_{cr-d-nh}$, **separate** regression analyses of final strengths

Prediction method	Section shape	Failure mode																			
		LD				DG				LDG				All LD, DG, LDG				ALL Failure modes			
		P_m	V_p	ϕ	n	P_m	V_p	ϕ	n	P_m	V_p	ϕ	n	P_m	V_p	ϕ	n	P_m	V_p	ϕ	n
DSM Method 19 (for SC)	Stiffened C	0.950	0.135	0.762	185	1.091	0.214	0.779	1320	1.247	0.107	1.032	617	1.124	0.195	0.828	2122	1.159	0.194	0.855	2837

Table 120: Resistance factors for columns with **Hole Width Factor=0, 0.2, and 0.4** failing in modes L, LG, G, D, and L+LG+G+D by **DSM Method 19** – Modification 11 to Option 4 in (Moen and Schafer 2011) – replace D equation by DG interaction equation, use $P_{cr-l-nh}$ and $P_{cr-d-nh}$, regression analyses of final strengths

prediction method	Section shape	Failure mode																All L, LG, G, D			
		L				LG				G				D							
		P_m	V_p	ϕ	n	P_m	V_p	ϕ	n	P_m	V_p	ϕ	n	P_m	V_p	ϕ	n	P_m	V_p	ϕ	n
DSM Method 19	C	1.119	0.102	0.932	5157	1.035	0.103	0.862	2307	1.006	0.079	0.855	847	1.207	0.149	0.950	1976	1.108	0.127	0.898	10287
	Z	1.171	0.092	0.984	2703	1.026	0.148	0.809	700	1.111	0.051	0.962	1300	1.141	0.059	0.984	1250	1.134	0.095	0.951	5953
	Hat	1.131	0.094	0.949	944	1.414	0.201	1.031	291	1.185	0.076	1.009	66	1.166	0.080	0.990	225	1.193	0.159	0.928	1526
	Rack	1.186	0.073	1.012	273	1.146	0.172	0.874	548	1.111	0.076	0.947	192	1.099	0.045	0.955	199	1.142	0.129	0.923	1212
	Stiffened C	1.099	0.126	0.892	210	1.109	0.090	0.934	74	1.086	0.051	0.940	100	1.320	0.268	0.856	125	1.152	0.193	0.851	509
	All sections	1.137	0.100	0.948	9287	1.079	0.168	0.827	3920	1.076	0.080	0.914	2505	1.181	0.134	0.948	3775	1.126	0.126	0.914	19487

Table 121: Resistance factors for columns with **Hole Width Factor=0, 0.2, and 0.4** failing in modes LD, DG, LDG, LD+DG+LDG, and all failure modes by **DSM Method 19** – Modification 11 to Option 4 in (Moen and Schafer 2011) – replace D equation by DG interaction equation, use $P_{cr-l-nh}$ and $P_{cr-d-nh}$, regression analyses of final strengths

prediction method	Section shape	Failure mode																ALL Failure modes			
		LD				DG				LDG				All LD, DG, LDG							
		P_m	V_p	ϕ	n	P_m	V_p	ϕ	n	P_m	V_p	ϕ	n	P_m	V_p	ϕ	n	P_m	V_p	ϕ	n
DSM Method 19	C	0.976	0.156	0.762	1619	1.003	0.120	0.819	1347	1.053	0.185	0.788	504	0.998	0.151	0.784	3470	1.080	0.139	0.862	13754
	Z	1.064	0.063	0.915	2099	1.166	0.072	0.997	1539	1.171	0.117	0.960	3289	1.137	0.105	0.944	6927	1.136	0.100	0.947	12880
	Hat	1.143	0.106	0.948	298	1.142	0.121	0.932	991	1.294	0.196	0.951	506	1.185	0.160	0.920	1795	1.188	0.159	0.924	3321
	Rack	1.026	0.097	0.859	71	1.154	0.108	0.955	424	1.276	0.104	1.061	455	1.203	0.123	0.979	950	1.169	0.129	0.945	2162
	Stiffened C	0.927	0.290	0.576	125	1.014	0.237	0.696	900	1.111	0.227	0.775	421	1.035	0.244	0.701	1446	1.065	0.235	0.734	1955
	All sections	1.031	0.128	0.834	4212	1.092	0.148	0.861	5201	1.176	0.154	0.921	5175	1.104	0.155	0.863	14588	1.117	0.139	0.891	34072

Table 122: Resistance factors for stiffened C section columns with **Hole Width Factor=0, 0.2, and 0.4** failing in modes L, LG, G, D, and L+LG+G+D by **DSM Method 19** – Modification 11 to Option 4 in (Moen and Schafer 2011) – replace D equation by DG interaction equation, use $P_{cr-l-nh}$ and $P_{cr-d-nh}$, **separate** regression analyses of final strengths

prediction method	Section shape	Failure mode																				
		L				LG				G				D				All L, LG, G, D			
		P_m	V_p	ϕ	n	P_m	V_p	ϕ	n	P_m	V_p	ϕ	n	P_m	V_p	ϕ	n	P_m	V_p	ϕ	n
DSM Method 19 (for SC)	Stiffened C	1.184	0.086	1.000	210	1.351	0.051	1.170	74	1.200	0.047	1.042	100	1.403	0.246	0.947	125	1.265	0.166	0.974	509

Table 123: Resistance factors for stiffened C section columns with **Hole Width Factor=0, 0.2, and 0.4** failing in modes LD, DG, LDG, LD+DG+LDG, and all failure modes by **DSM Method 19** – Modification 11 to Option 4 in (Moen and Schafer 2011) – replace D equation by DG interaction equation, use $P_{cr-l-nh}$ and $P_{cr-d-nh}$, **separate** regression analyses of final strengths

Prediction method	Section shape	Failure mode																				
		LD				DG				LDG				All LD, DG, LDG				ALL Failure modes			
		P_m	V_p	ϕ	n	P_m	V_p	ϕ	n	P_m	V_p	ϕ	n	P_m	V_p	ϕ	n	P_m	V_p	ϕ	n
DSM Method 19 (for SC)	Stiffened C	0.951	0.141	0.757	125	1.079	0.210	0.776	900	1.246	0.109	1.030	421	1.117	0.194	0.823	1446	1.155	0.194	0.852	1955

4. Conclusions

The best-performing, and hence the proposed design method (i.e. DSM Method 19) was based on modifying the Option 4 method in (Moen and Schafer 2011) such that (i) DG interaction was included, (ii) $P_{\text{cr-l-nh}}$ and $P_{\text{cr-d-nh}}$ based on gross section were used, and (iii) a factor based on a regression analysis was added to improve the final design strength. Its expressions are recapitulated as follows:

The nominal member capacity of a perforated member in compression (P_{n}) shall be

$$P_{\text{n}} = F1 \times \min(P_{\text{nle}}, \ P_{\text{nde}}, \ P_{\text{ne}}) \tag{36}$$

(i) The nominal member capacity of a perforated member in compression (P_{ne}) for flexural, torsional or flexural-torsional buckling shall be calculated as follows:

$$\text{For } \lambda_{\text{c}} \leq 1.5: \ \ P_{\text{ne}} = \left(0.658^{\lambda_{\text{c}}^2}\right) P_{\text{y}} \tag{37}$$

$$\text{For } \lambda_{\text{c}} > 1.5: \ \ P_{\text{ne}} = \left(\frac{0.877}{\lambda_{\text{c}}^2}\right) P_{\text{y}} \tag{38}$$

where $\lambda_{\text{c}} = (P_{\text{y}}/P_{\text{cr-e-h}})^{0.5}$, $P_{\text{cr-e-h}}$ includes the influence of hole(s), and may be calculated as per the simplified methods proposed by Moen and Schafer (2009).

(ii) The nominal member capacity of a perforated member in compression (P_{nle}) for local buckling (including local-global interaction) shall be calculated as follows:

$$\text{For } \lambda_{\text{le}} \leq 0.776, P_{\text{nle}} = P_{\text{ne}} \leq P_{\text{yn}} \tag{39}$$

$$\text{For } \lambda_{\text{le}} > 0.776, P_{\text{nle}} = \left[1 - 0.15 \left(\frac{P_{\text{cr-l-nh}}}{P_{\text{ne}}}\right)^{0.4}\right] \left(\frac{P_{\text{cr-l-nh}}}{P_{\text{ne}}}\right)^{0.4} P_{\text{ne}} \leq P_{\text{yn}} \tag{40}$$

where $\lambda_{\text{le}} = (P_{\text{ne}} / P_{\text{cr-l-nh}})^{0.5}$, $P_{\text{cr-l-nh}}$ does not include the influence of hole(s) and may be calculated by means of SAFSM.

(iii) The nominal member capacity of a perforated member in compression (P_{nde}) for distortional buckling (including distortional-global interaction) shall be calculated as follows:

$$\text{For } \lambda_{\text{de}} \leq \lambda_{\text{d1}}, \ \ P_{\text{nde}} = P_{\text{min}} \tag{41}$$

$$\text{For } \lambda_{d1} < \lambda_{de} \leq \lambda_{d2}, \quad P_{nde} = P_{min} - \left(\frac{P_{min} - P_{d2}}{\lambda_{d2} - \lambda_{d1}} \right) \left(\lambda_{d2} - \lambda_{d1} \right) \tag{42}$$

$$\text{For } \lambda_{de} > \lambda_{d2}, \quad P_{nde} = \left[1 - 0.25 \left(\frac{P_{cr\text{-}d\text{-}nh}}{P_{ne}} \right)^{0.6} \right] \left(\frac{P_{cr\text{-}d\text{-}nh}}{P_{ne}} \right)^{0.6} P_{ne} \tag{43}$$

where $\lambda_{de} = \sqrt{P_{ne}/P_{cr\text{-}d\text{-}nh}}$, $P_{min} = \min(P_{ne}, P_{yn})$, $\lambda_{d1} = 0.561 \left(P_{yn}/P_y \right)$,

$\lambda_{d2} = 0.561 \left(14 \left(P_y/P_{yn} \right)^{0.4} - 13 \right)$, $P_{d2} = \left(1 - 0.25 \left(1/\lambda_{d2} \right)^{1.2} \right) \left(1/\lambda_{d2} \right)^{1.2} P_{ne}$, and $P_{cr\text{-}d\text{-}nh}$ does not includes the influence of hole(s) and may be calculated by means of SAFSM.

The factor $F1$ in Equation (36) is calculated as per Equation (44) where HWF=hole width factor=hole width/flat web width, HLF=hole length factor=hole length/hole width, HSF=hole spacing factor=clear hole spacing/hole width, H=overall web width, B=overall flange width, D=overall lip width, t=thickness. The constants in Equation (44) are defined in Table 124.

$$F1 = a + b \times \lambda_{le} + c \times \lambda_{de} + d \times \lambda_c + e \times HWF + f \times HLF + g \times HSF + h \times \frac{H}{t} + i \times \frac{B}{t} + j \times \frac{D}{t} + k \times \frac{H}{B} + m \times \frac{D}{B} \tag{44}$$

Table 124: Constants from regression analysis for DSM Method 19

a	b	c	d	e	f
9.38E-01	6.89E-02	-3.14E-02	5.76E-02	-2.20E-01	-2.46E-02
g	h	i	j	k	m
5.32E-03	1.10E-03	-2.24E-03	-6.76E-03	-7.98E-03	5.57E-02

For improved reliability, constants defined in Table 125 are recommended for Stiffened C section columns.

Table 125: Constants from regression analysis for DSM Method 19 – Stiffened C section only

a	b	c	d	e	f
7.42E-01	3.65E-02	-1.66E-02	3.01E-02	-2.05E-01	-2.11E-02
g	h	i	j	k	m
8.96E-03	-1.15E-03	1.73E-03	3.20E-03	3.39E-02	1.47E-01

Besides, the study presented in this report also prompts the following remarks:

(i)   The proposed design method, i.e. DSM Method 19, can be used not only for perforated columns but also non-perforated columns. Compared to the current DSM, the accuracy

and reliability of the strength prediction for non-perforated columns in general can be improved significantly by means of Method 19.

(ii)   It is generally true that the variation in the predictions was largely caused by interaction of buckling modes rather than the presence of holes, although it is noticed that the influence of holes to some extent depends on the section type, section dimensions, and failure modes.

(iii)   Design methods generally performed worse for failure modes involving the D mode (i.e. D, LD, DG and LDG) as shown by their higher values of V_p. It has been shown that including DG interaction in the DSM distortional equations contributed significantly to the reduction of scatter in prediction related to the DG and LDG modes, and an additional regression analysis could further reduce the scatter associated with the D, LD, DG and LDG modes. In addition, it has been demonstrated that it is unfavourable to include LD or LDG interaction equations in the DSM because they generally resulted in a considerable increase in the prediction scatter and thus a decrease in the resistance factor. Future research is warranted regarding the interaction with the D mode.

(iv)   Although it remains sound to base the column strength on a slenderness that relates elastic buckling and yield (or strength), the statistics of the predictions by the DSM can vary significantly depending on the section type and failure mode. It is virtually impossible to achieve a uniform ϕ value for all section types and failure modes using a particular set of strength equations. From a design viewpoint, it may be preferable to select the accurate ϕ value for a specific section type and failure mode; alternatively, one may use a more conservative approach by adopting the minimum ϕ value of all failure modes for a particular section, or a less conservative approach by adopting the average ϕ value of all failure modes for a particular section.

(v)   It is not recommended to use the local and distortional elastic buckling loads P_{cr-1-h} and P_{cr-d-h} including the influence of holes as per the simplified methods proposed by Moen and Schafer (2009), because for the great majority of columns, P_{cr-1-h} produced the same buckling loads for non-perforated and perforated members, while replacing P_{cr-d-h} by P_{cr-d} based on gross section reduced the overall value of V_p favourably.

5. References

AS/NZS:4600 (2005). Cold-formed steel structures. Sydney, Australia, Standards Australia.

Casafont, M., M. Magdalena Pastor, et al. (2011). "An experimental investigation of distortional buckling of steel storage rack columns." Thin-Walled Structures 49(8): 933-946.`

Kwon, Y. B., B. S. Kim, et al. (2009). "Compression tests of high strength cold-formed steel channels with buckling interaction." Journal of Constructional Steel Research 65(2): 278-289.

Moen, C. D. (2008). Direct strength design of cold-formed steel members with perforations. Baltimore, Maryland, Johns Hopkins university. Ph.D.

Moen, C. D. and B. W. Schafer (2009). "Elastic buckling of cold-formed steel columns and beams with holes." Engineering Structures 31(12): 2812-2824.

Moen, C. D. and B. W. Schafer (2011). "Direct Strength Method for Design of Cold-Formed Steel Columns with Holes." ASCE Journal of Structural Engineering 137(5): 559-570.

NAS (2004). North American specification for the design of cold-formed steel structural members. Washington, D.C, American Iron and Steel Institute (AISI).

NAS (2007). North American specification for the design of cold-formed steel structural members. Washington, D.C, American Iron and Steel Institute (AISI).

Rossi, B., J. Jaspart, et al. (2010). "Combined Distortional and Overall Flexural-Torsional Buckling of Cold-Formed Stainless Steel Sections: Design." Journal of Structural Engineering 136(4): 361-369.

Schafer, B. (2002). "Local, Distortional, and Euler Buckling of Thin-Walled Columns." Journal of Structural Engineering 128(3): 289-299.

Silvestre, N., D. Camotim, et al. (2012). "Post-buckling behaviour and direct strength design of lipped channel columns experiencing local/distortional interaction." Journal of Constructional Steel Research 73: 12-30.

Yang, D. and G. J. Hancock (2004). "Compression tests of high strength steel columns with interaction between local and distortional buckling." Journal of Structural Engineering ASCE 130(12): 1954-1963.

Yao, Z. (2013). Nonlinear analysis and design of perforated thin-walled steel columns. Sydney, University of Sydney. Ph.D thesis.

Yao, Z. and K. J. R. Rasmussen (2014). Finite Element Modelling and Parametric Studies of Perforated Thin-walled Steel Columns. Reserch Report R948. Sydney, University of Sydney.

Yap, D. and G. Hancock (2008). "Experimental Study of Complex High-Strength Cold-Formed Cross-Shaped Steel Section." Journal of Structural Engineering 134(8): 1322-1333.

Yap, D. and G. Hancock (2011). "Experimental Study of High-Strength Cold-Formed Stiffened-Web C-Sections in Compression." Journal of Structural Engineering 137(2): 162-172.

<div align="center">

APPENDIX A

# SIMULATION-TO-PREDICTED RATIOS BY DSM METHOD 1 – AS/NZS 4600 DSM

</div>

A.1 non-perforated columns
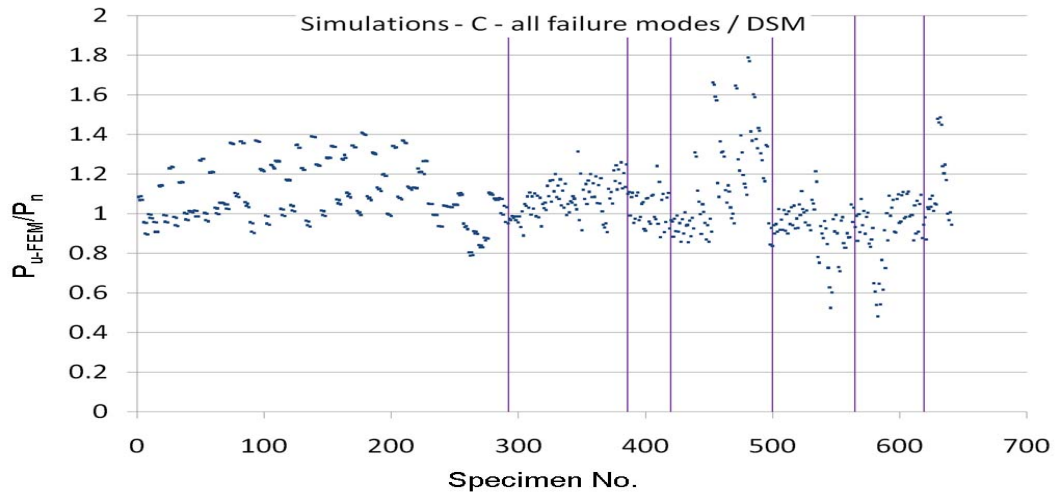
Fig. A.1: Simulation-to-predicted ratios for non-perforated C section columns by DSM Method 1 with classified failure modes (from left to right: L, LG, G, D, LD, DG, and LDG)
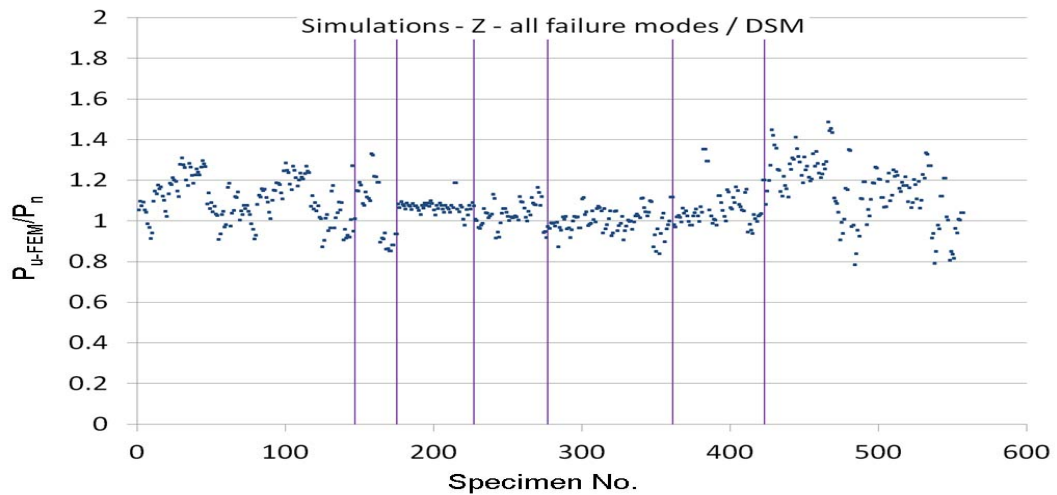

Fig. A.2: Simulation-to-predicted ratios for non-perforated Z section columns by DSM Method 1 with classified failure modes (from left to right: L, LG, G, D, LD, DG, and LDG)
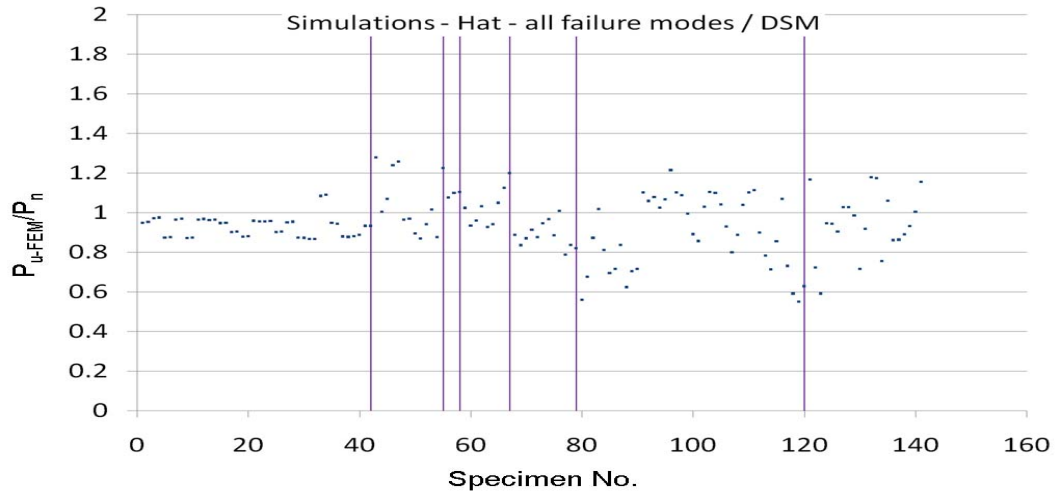
Fig. A.3: Simulation-to-predicted ratios for non-perforated Hat section columns by DSM Method 1 with classified failure modes (from left to right: L, LG, G, D, LD, DG, and LDG)
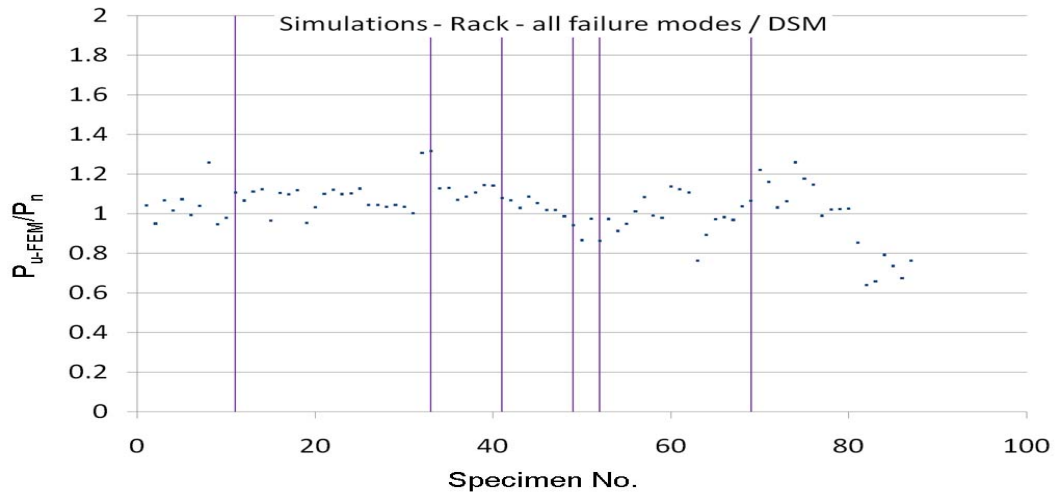

Fig. A.4: Simulation-to-predicted ratios for non-perforated Rack section columns by DSM Method 1 with classified failure modes (from left to right: L, LG, G, D, LD, DG, and LDG)
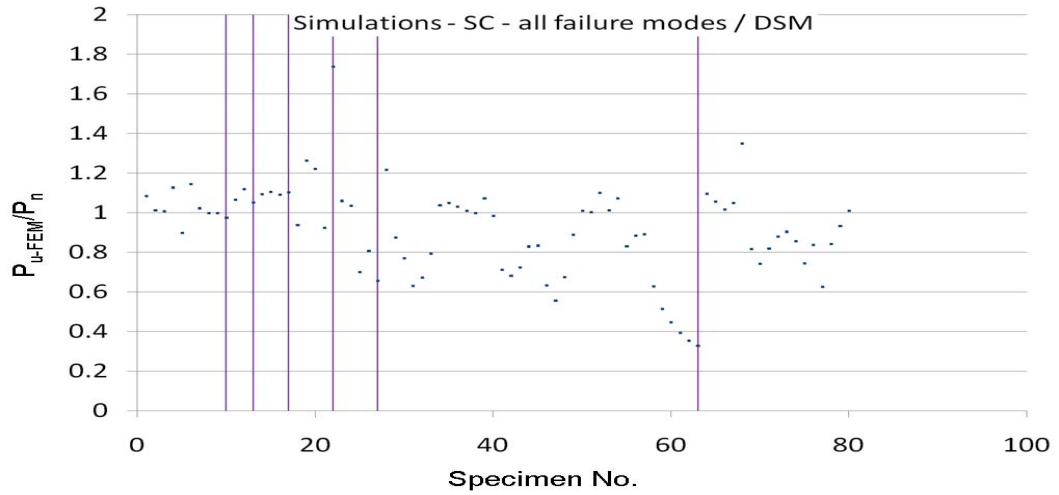
Fig. A.5: Simulation-to-predicted ratios for non-perforated Stiffened C section columns by DSM Method 1 with classified failure modes (from left to right: L, LG, G, D, LD, DG, and LDG)

A.2 perforated columns
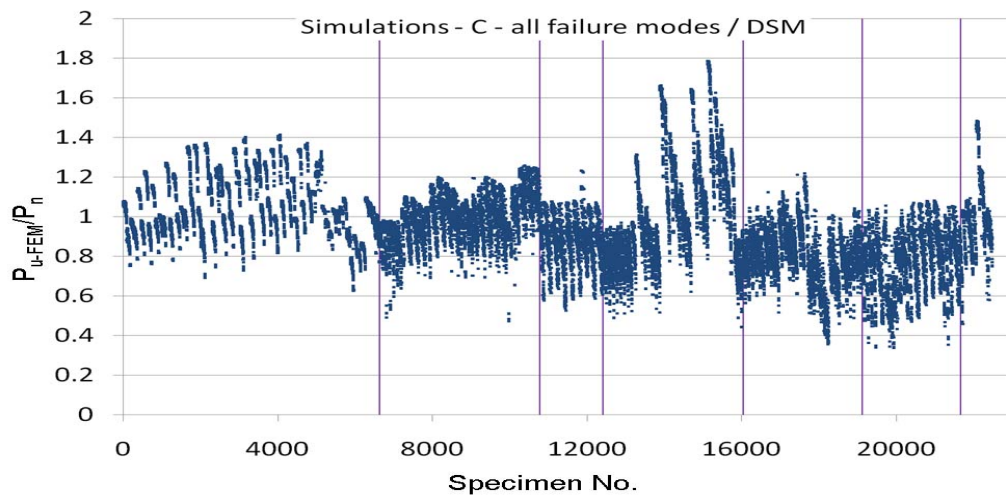
Fig. A.6: Simulation-to-predicted ratios for perforated C section columns by DSM Method 1 with classified failure modes (from left to right: L, LG, G, D, LD, DG, and LDG)
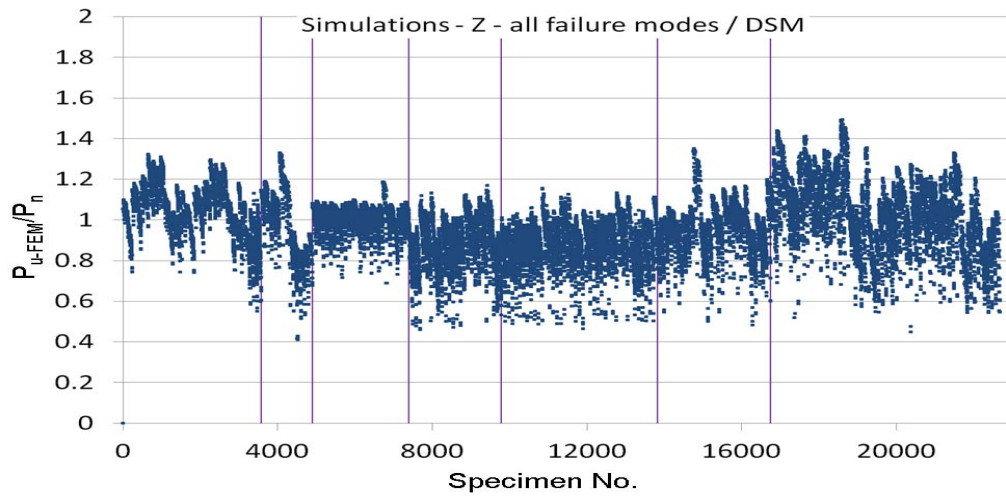
Fig. A.7: Simulation-to-predicted ratios for perforated Z section columns by DSM Method 1 with classified failure modes (from left to right: L, LG, G, D, LD, DG, and LDG)
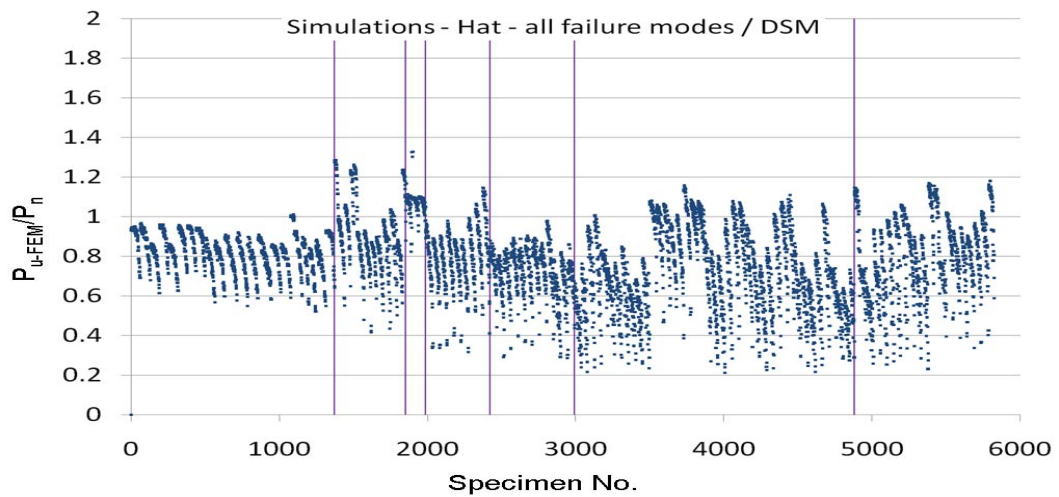

Fig. A.8: Simulation-to-predicted ratios for perforated Hat section columns by DSM Method 1 with classified failure modes (from left to right: L, LG, G, D, LD, DG, and LDG)
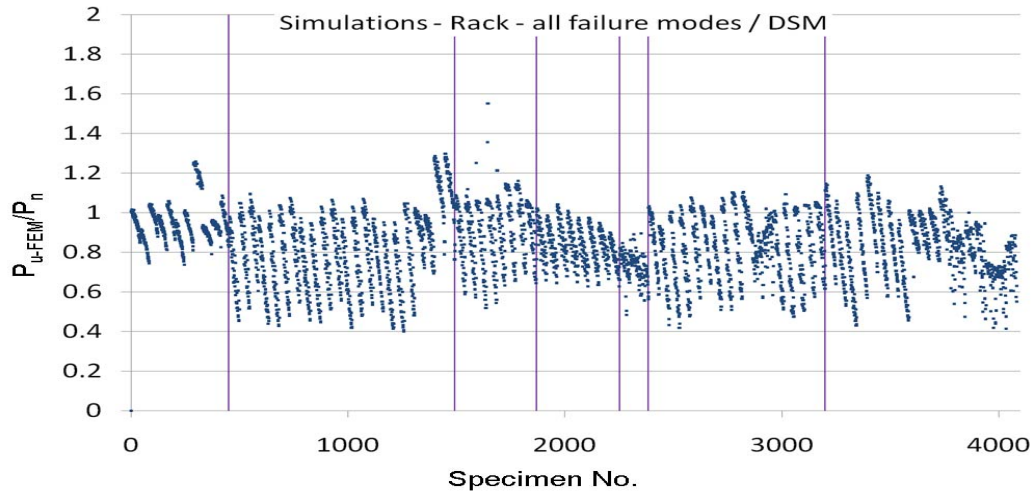
Fig. A.9: Simulation-to-predicted ratios for perforated Rack section columns by DSM Method 1 with classified failure modes (from left to right: L, LG, G, D, LD, DG, and LDG)
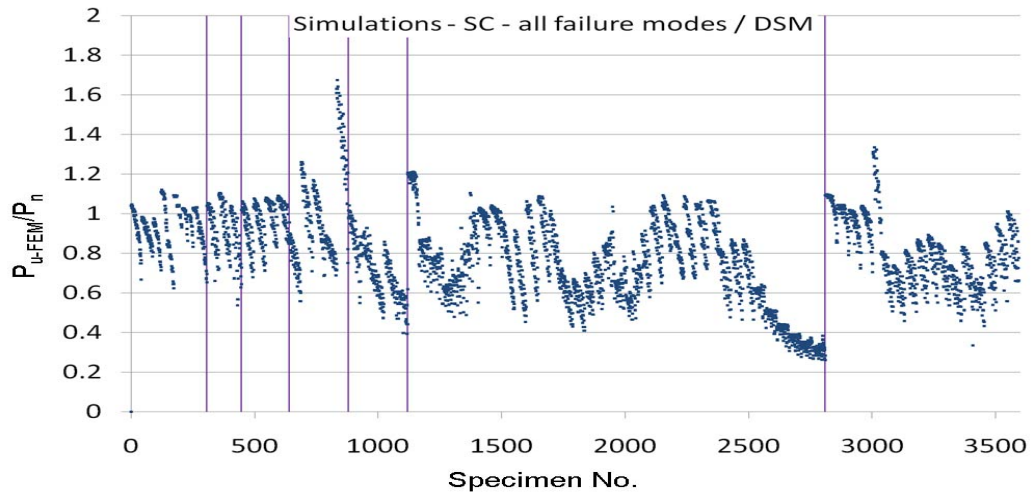
Fig. A.10: Simulation-to-predicted ratios for perforated Stiffened C section columns by DSM Method 1 with classified failure modes (from left to right: L, LG, G, D, LD, DG, and LDG)

A.3 non-perforated and perforated columns
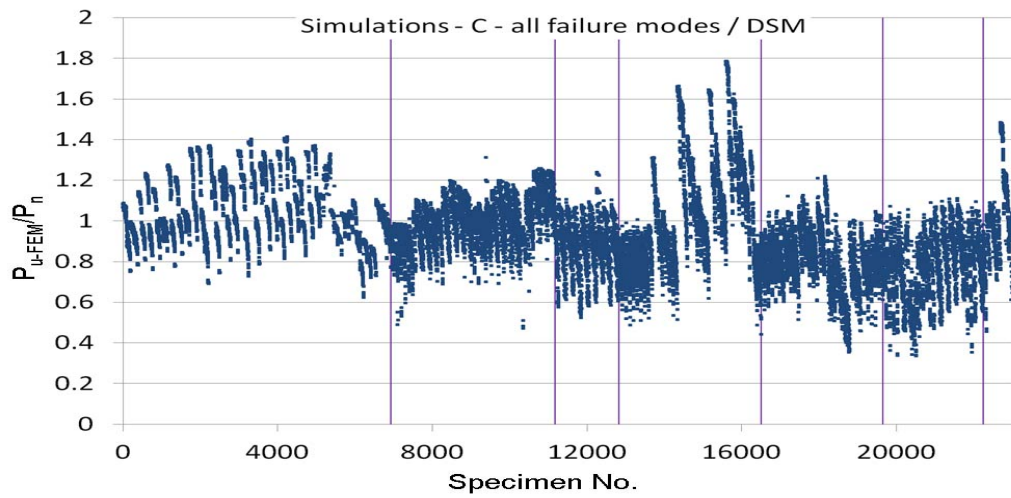
Fig. A.11: Simulation-to-predicted ratios for all C section columns by DSM Method 1 with classified failure modes (from left to right: L, LG, G, D, LD, DG, and LDG)
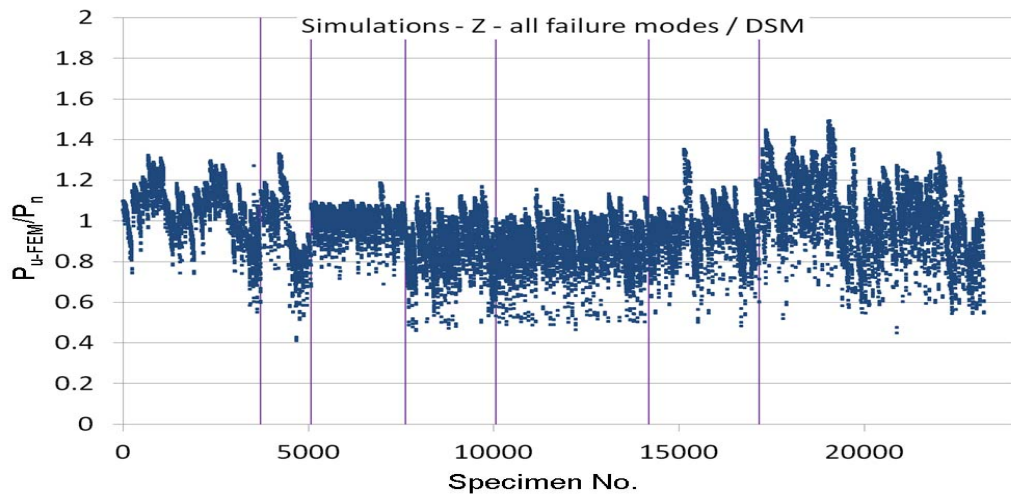
Fig. A.12: Simulation-to-predicted ratios for all Z section columns by DSM Method 1 with classified failure modes (from left to right: L, LG, G, D, LD, DG, and LDG)
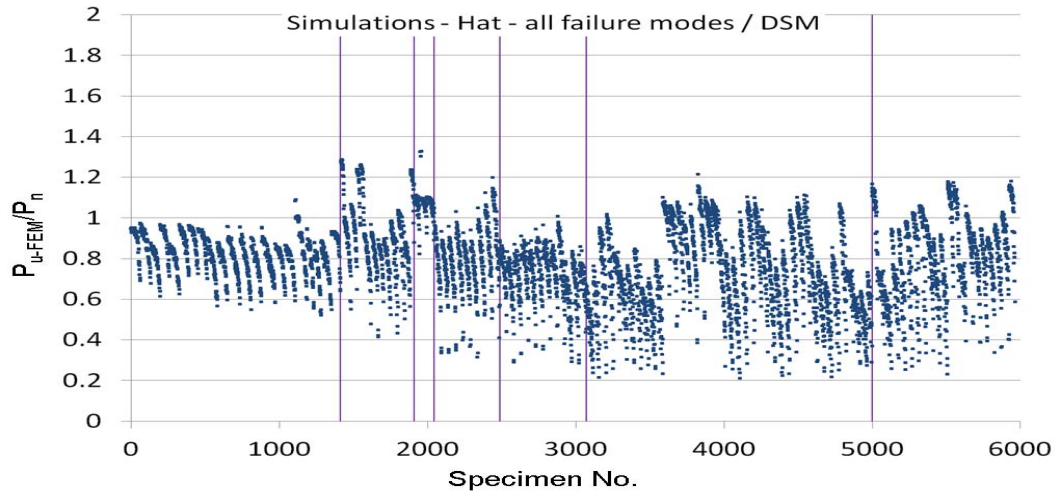
Fig. A.13: Simulation-to-predicted ratios for all Hat section columns by DSM Method 1 with classified failure modes (from left to right: L, LG, G, D, LD, DG, and LDG)
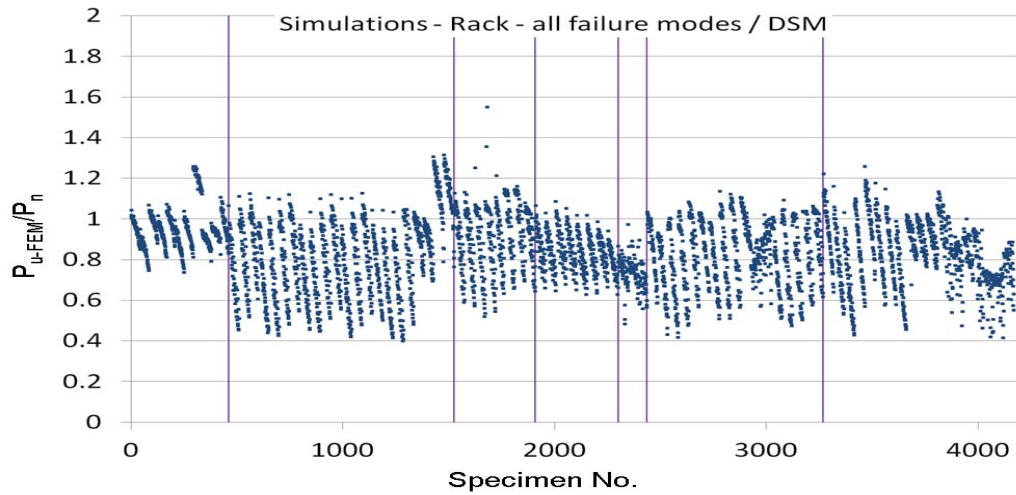
Fig. A.14: Simulation-to-predicted ratios for all Rack section columns by DSM Method 1 with classified failure modes (from left to right: L, LG, G, D, LD, DG, and LDG)
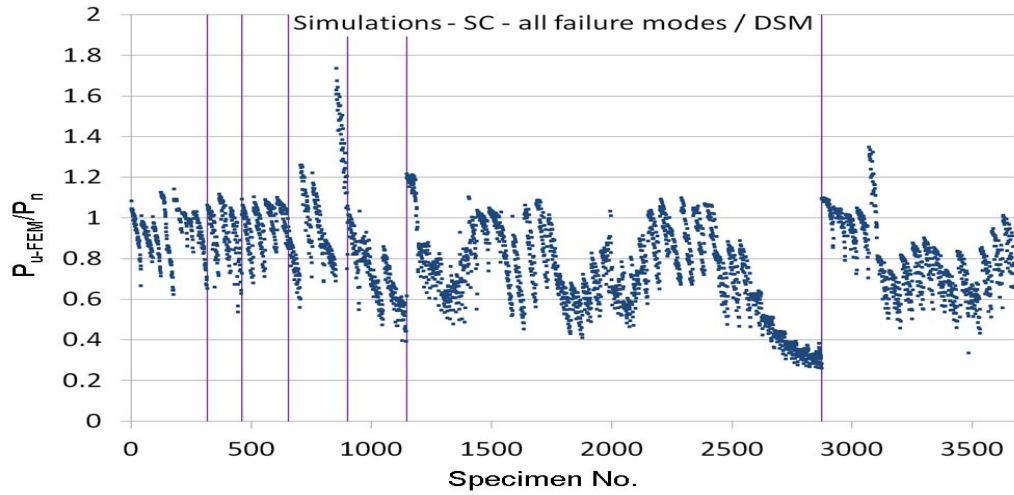
Fig. A.15: Simulation-to-predicted ratios for all Stiffened C section columns by DSM Method 1 with classified failure modes (from left to right: L, LG, G, D, LD, DG, and LDG)
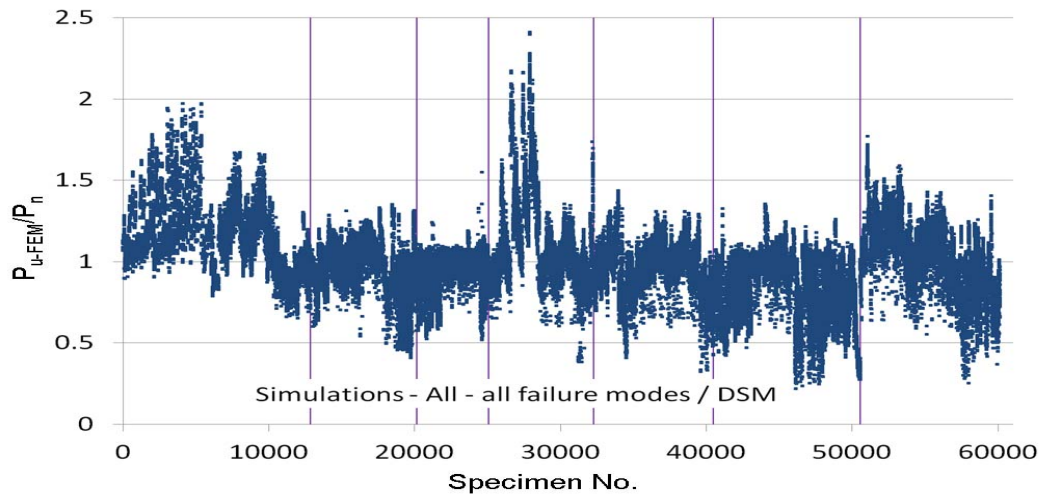
Fig. A.16: Simulation-to-predicted ratios for all columns by DSM Method 1 with classified failure modes (from left to right: L, LG, G, D, LD, DG, and LDG)
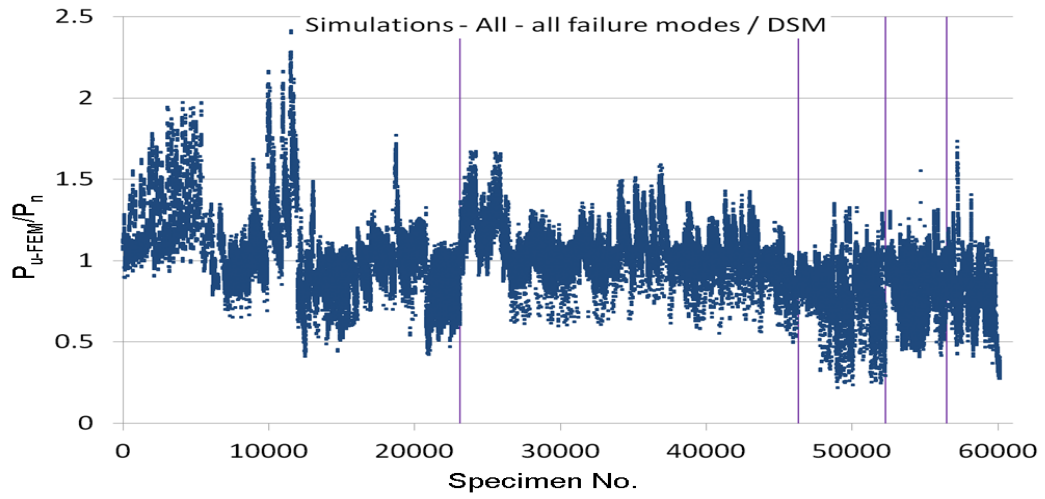
Fig. A.17: Simulation-to-predicted ratios for all columns by DSM Method 1 with classified section types
(from left to right: C, Z, Hat, Rack and Stiffened C)

<div align="center">

APPENDIX B

SIMULATION-TO-PREDICTED RATIOS BY DSM METHOD 2 – minimum of LG and DG interaction equations based on AS/NZS 4600 DSM

</div>

**B.1   non-perforated columns**
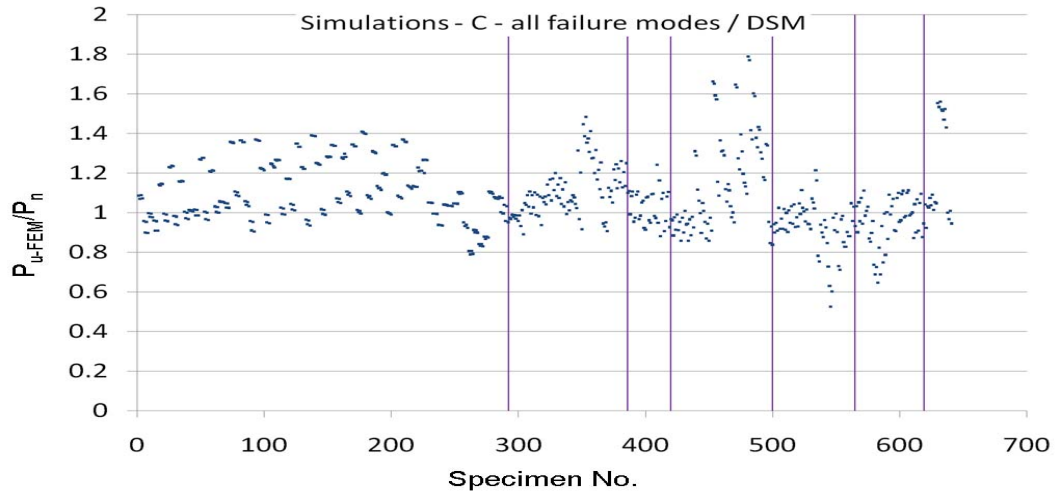
Fig. B.1: Simulation-to-predicted ratios for non-perforated C section columns by DSM Method 2 with classified failure modes (from left to right: L, LG, G, D, LD, DG, and LDG)
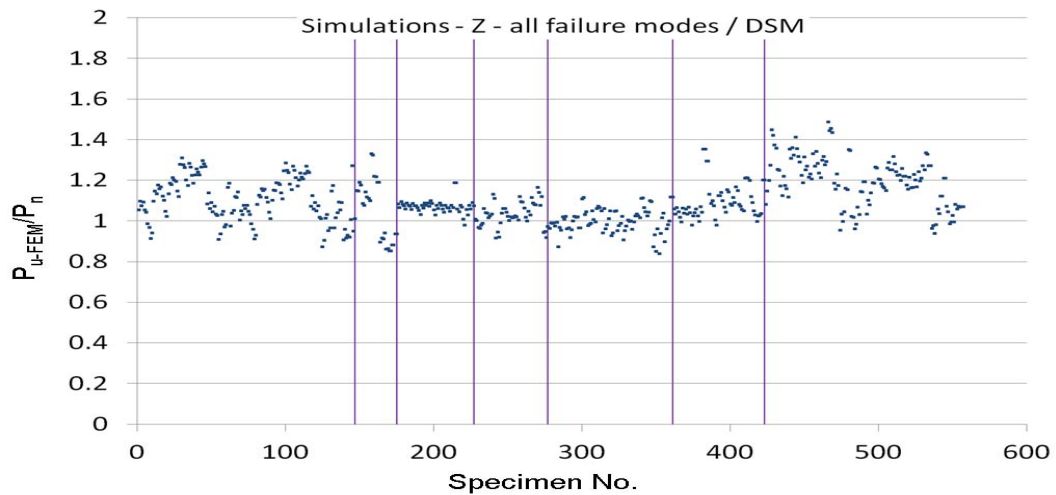
Fig. B.2: Simulation-to-predicted ratios for non-perforated Z section columns by DSM Method 2 with classified failure modes (from left to right: L, LG, G, D, LD, DG, and LDG)
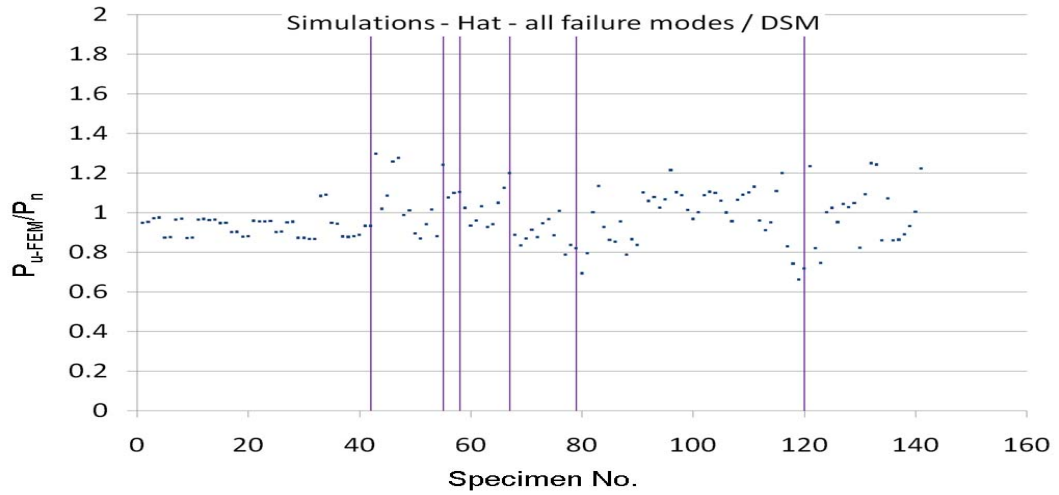
Fig. B.3: Simulation-to-predicted ratios for non-perforated Hat section columns by DSM Method 2 with classified failure modes (from left to right: L, LG, G, D, LD, DG, and LDG)
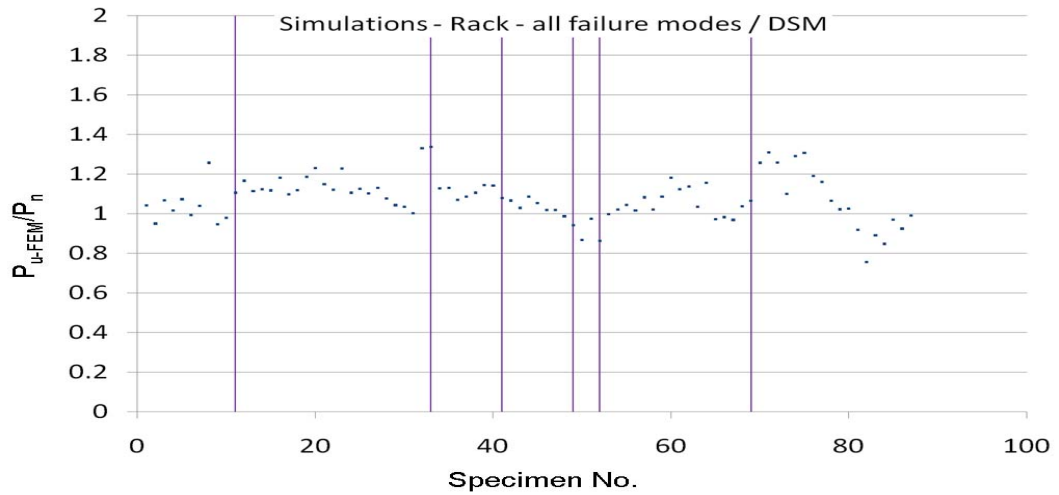
Fig. B.4: Simulation-to-predicted ratios for non-perforated Rack section columns by DSM Method 2 with classified failure modes (from left to right: L, LG, G, D, LD, DG, and LDG)
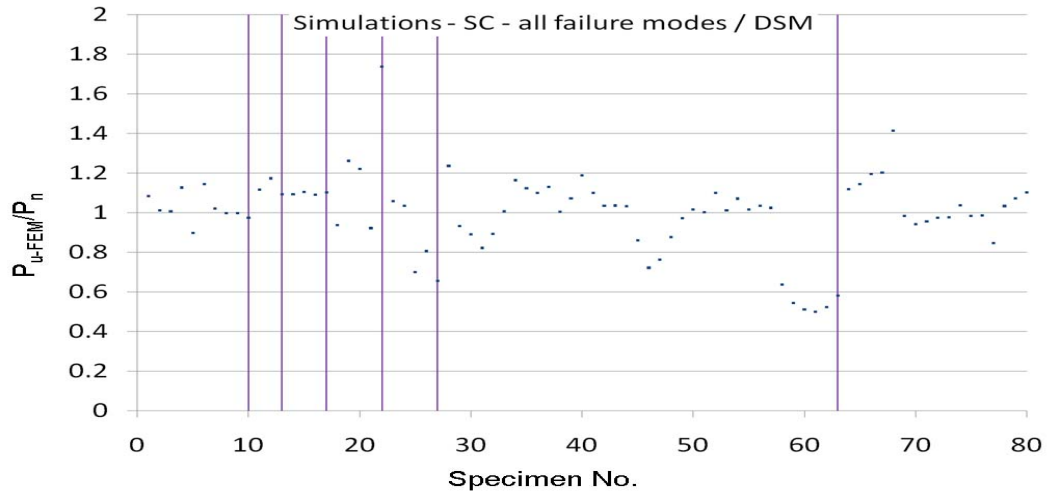
Fig. B.5: Simulation-to-predicted ratios for non-perforated Stiffened C section columns by DSM Method 2 with classified failure modes (from left to right: L, LG, G, D, LD, DG, and LDG)

B.2 non-perforated and perforated columns
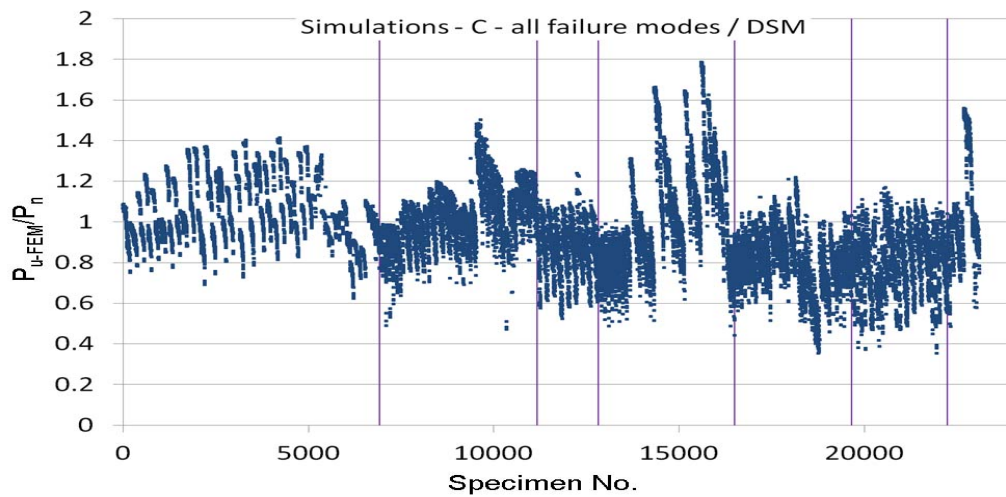
Fig. B.6: Simulation-to-predicted ratios for all C section columns by DSM Method 2 with classified failure modes (from left to right: L, LG, G, D, LD, DG, and LDG)
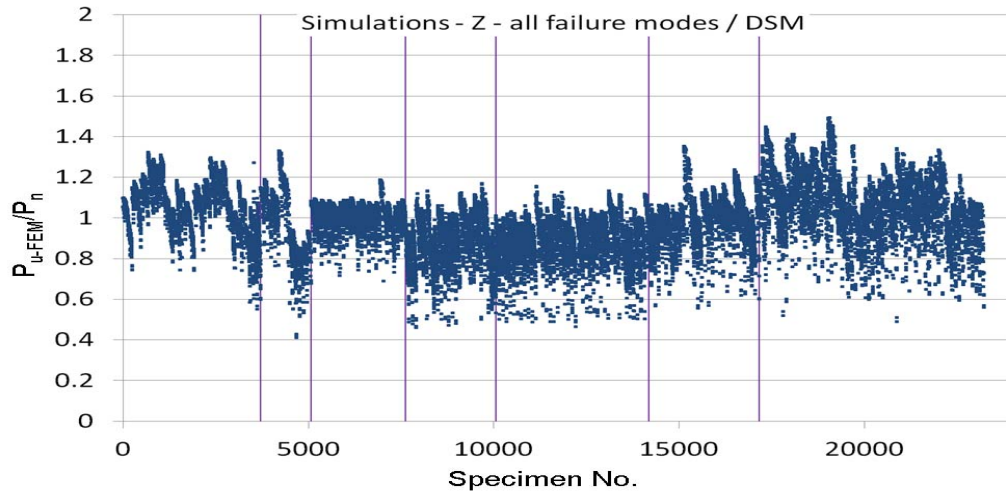
Fig. B.7: Simulation-to-predicted ratios for all Z section columns by DSM Method 2 with classified failure modes (from left to right: L, LG, G, D, LD, DG, and LDG)
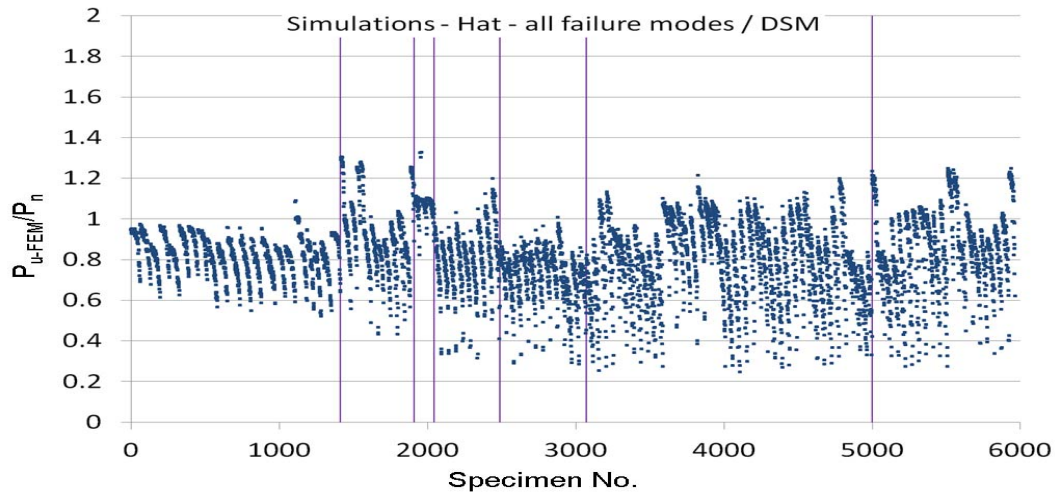

Fig. B.8: Simulation-to-predicted ratios for all Hat section columns by DSM Method 2 with classified failure modes (from left to right: L, LG, G, D, LD, DG, and LDG)
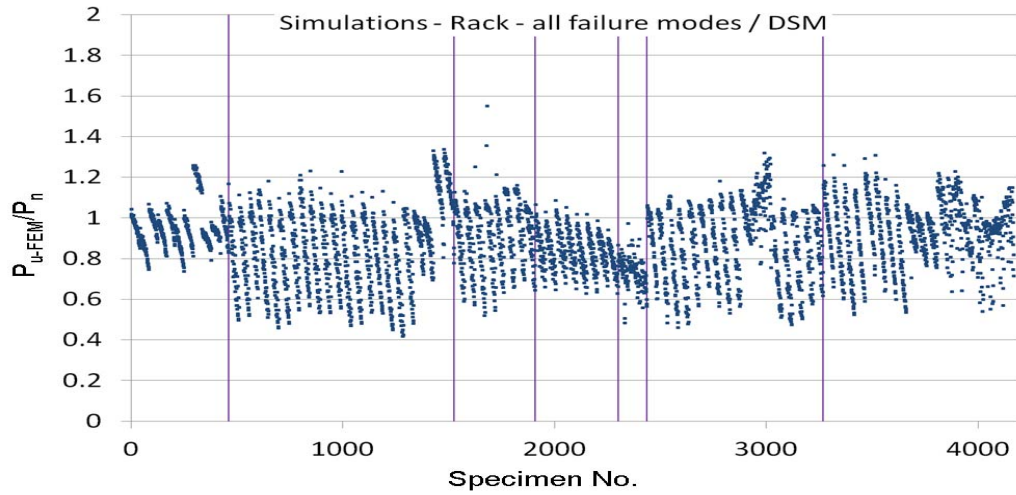
Fig. B.9: Simulation-to-predicted ratios for all Rack section columns by DSM Method 2 with classified failure modes (from left to right: L, LG, G, D, LD, DG, and LDG)
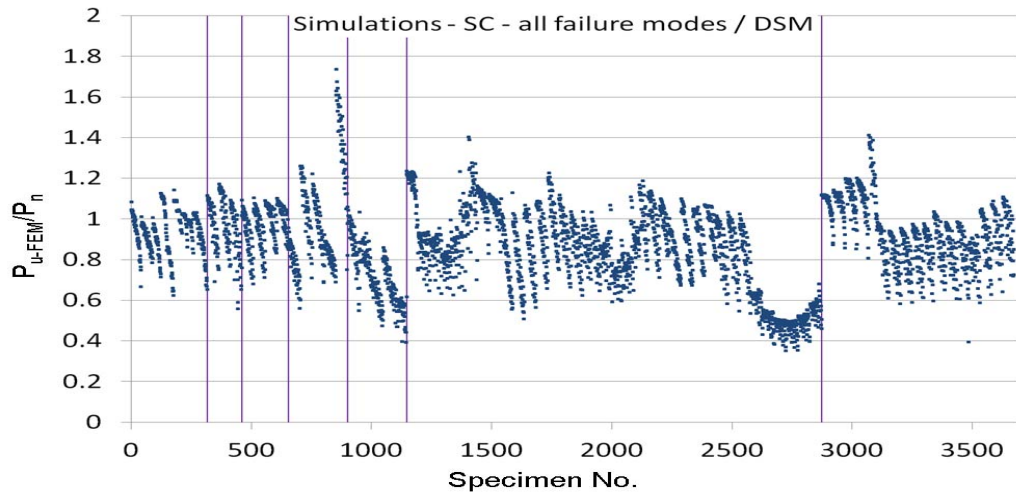

Fig. B.10: Simulation-to-predicted ratios for all Stiffened C section columns by DSM Method 2 with classified failure modes (from left to right: L, LG, G, D, LD, DG, and LDG)

APPENDIX C

Simulation-to-predicted ratios by DSM Method 3 – minimum of LG, DG, and LD interaction equations based on AS/NZS 4600 DSM

C.1   non-perforated columns
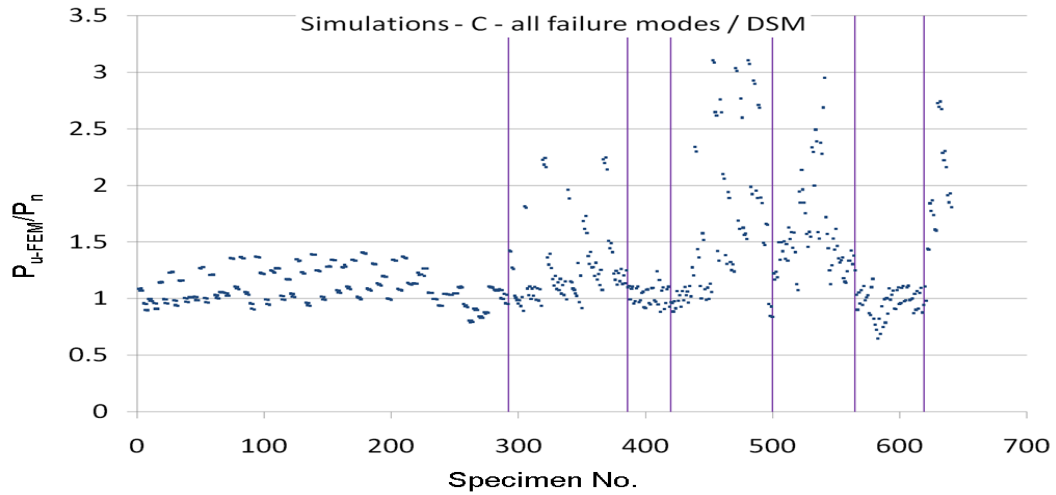
Fig. C.1: Simulation-to-predicted ratios for non-perforated C section columns by DSM Method 3 with classified failure modes (from left to right: L, LG, G, D, LD, DG, and LDG)
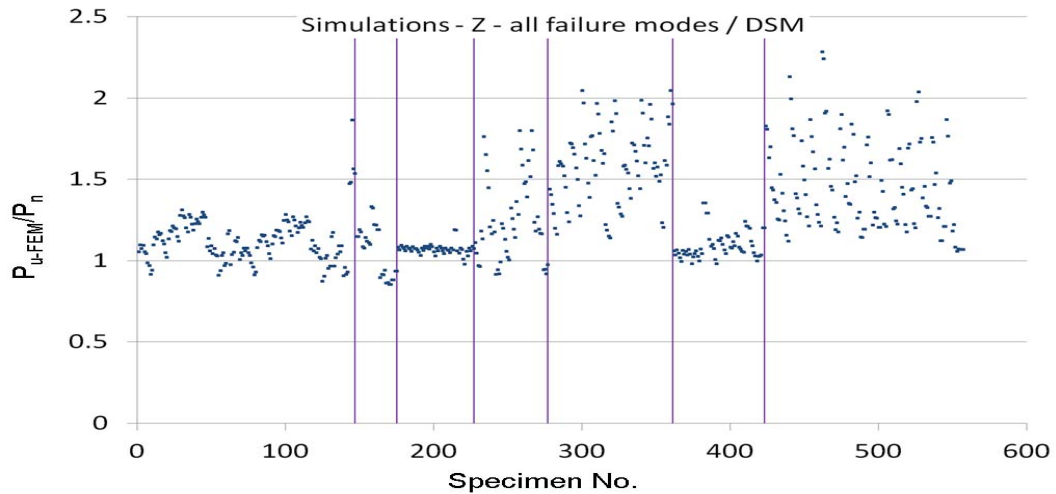
Fig. C.2: Simulation-to-predicted ratios for non-perforated Z section columns by DSM Method 3 with classified failure modes (from left to right: L, LG, G, D, LD, DG, and LDG)
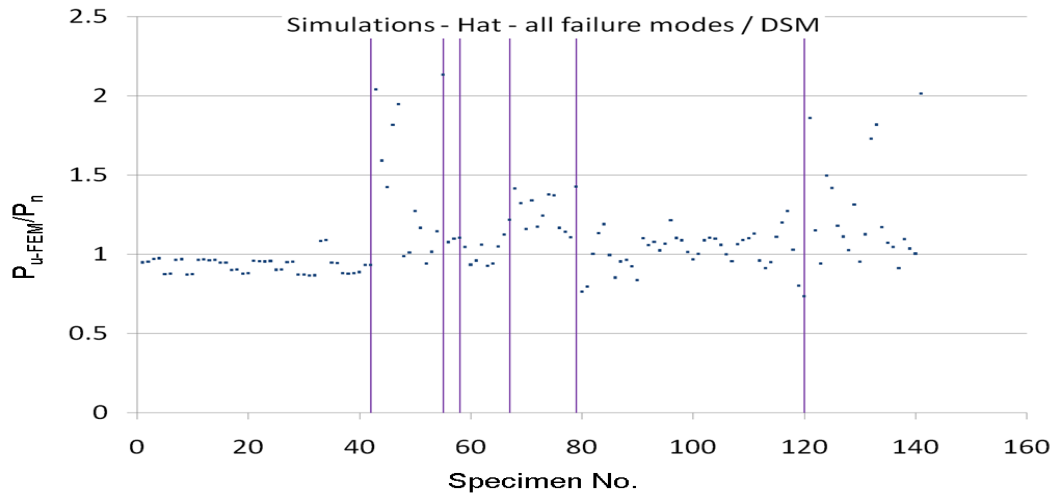
Fig. C.3: Simulation-to-predicted ratios for non-perforated Hat section columns by DSM Method 3 with classified failure modes (from left to right: L, LG, G, D, LD, DG, and LDG)
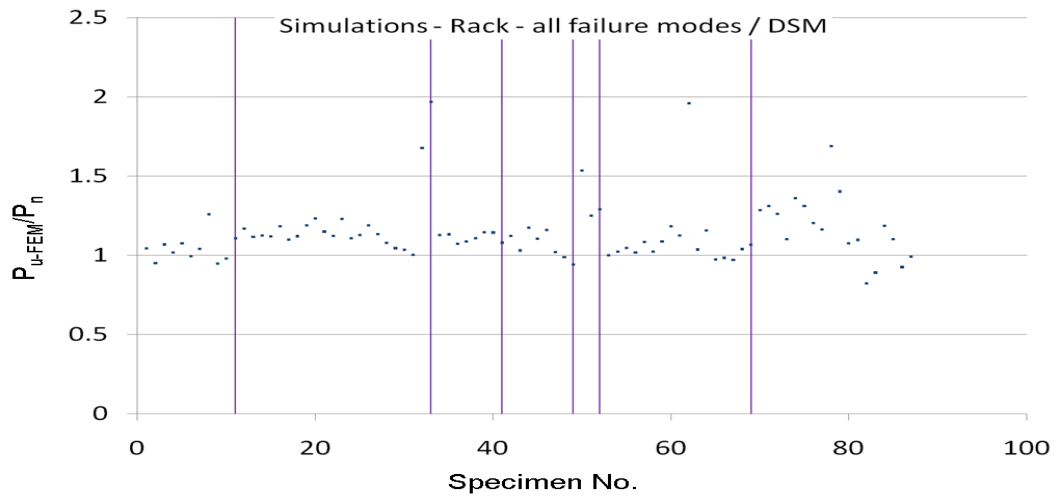

Fig. C.4: Simulation-to-predicted ratios for non-perforated Rack section columns by DSM Method 3 with classified failure modes (from left to right: L, LG, G, D, LD, DG, and LDG)
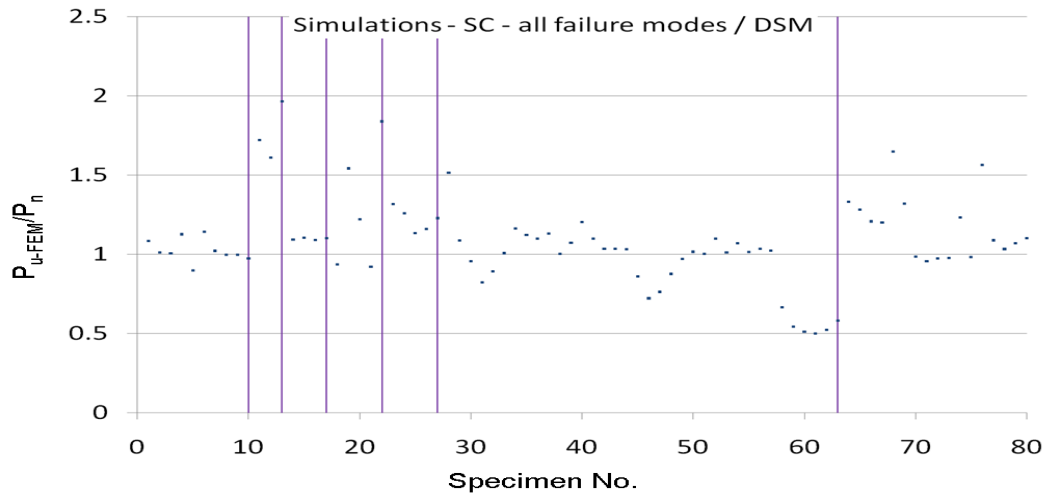
Fig. C.5: Simulation-to-predicted ratios for non-perforated Stiffened C section columns by DSM Method 3 with classified failure modes (from left to right: L, LG, G, D, LD, DG, and LDG)

APPENDIX D

SIMULATION-TO-PREDICTED RATIOS BY DSM METHOD 4 – LDG interaction equation based on AS/NZS 4600 DSM

D.1   non-perforated columns
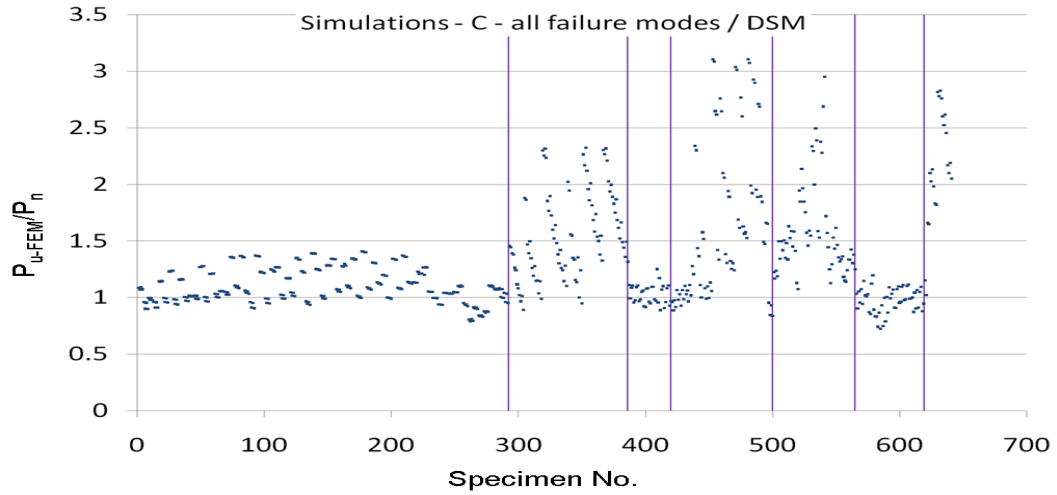
Fig. D.1: Simulation-to-predicted ratios for non-perforated C section columns by DSM Method 4 with classified failure modes (from left to right: L, LG, G, D, LD, DG, and LDG)
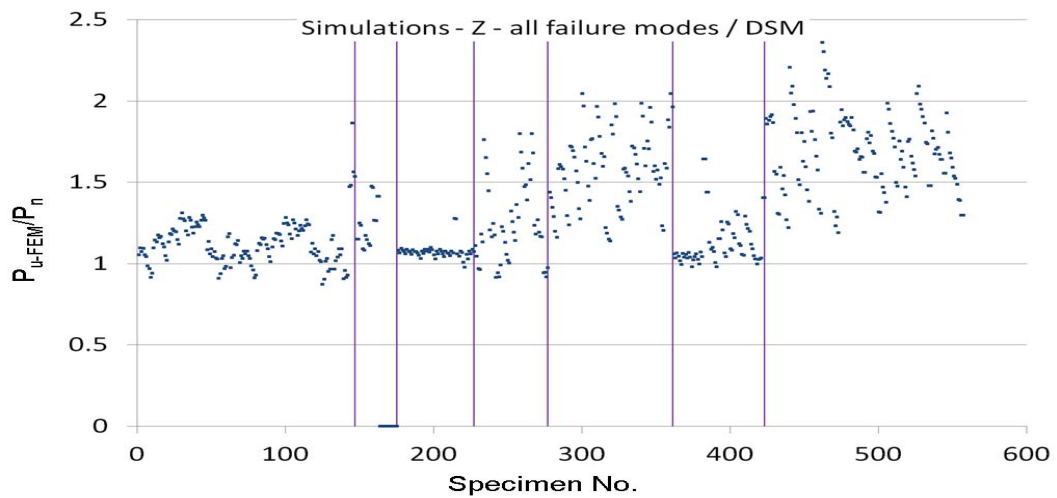

Fig. D.2: Simulation-to-predicted ratios for non-perforated Z section columns by DSM Method 4 with classified failure modes (from left to right: L, LG, G, D, LD, DG, and LDG)
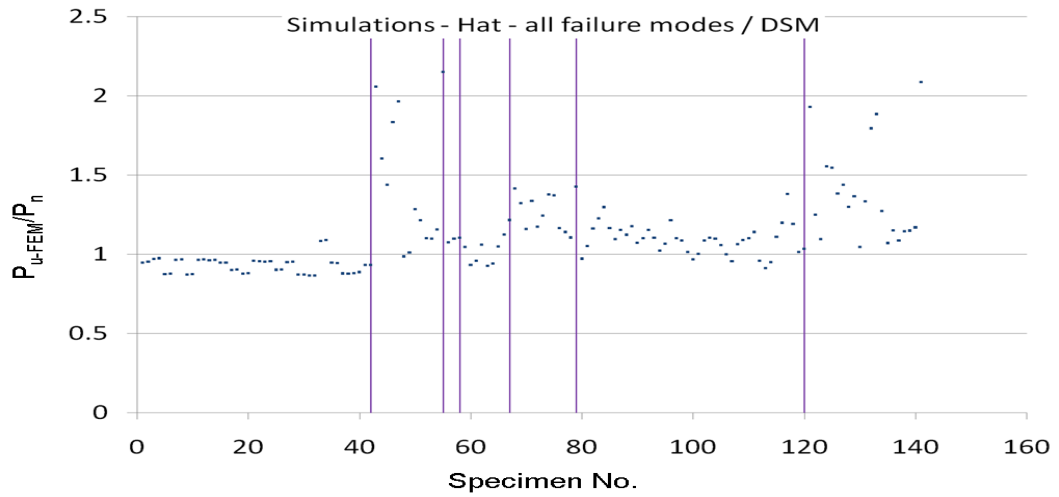
Fig. D.3: Simulation-to-predicted ratios for non-perforated Hat section columns by DSM Method 4 with classified failure modes (from left to right: L, LG, G, D, LD, DG, and LDG)
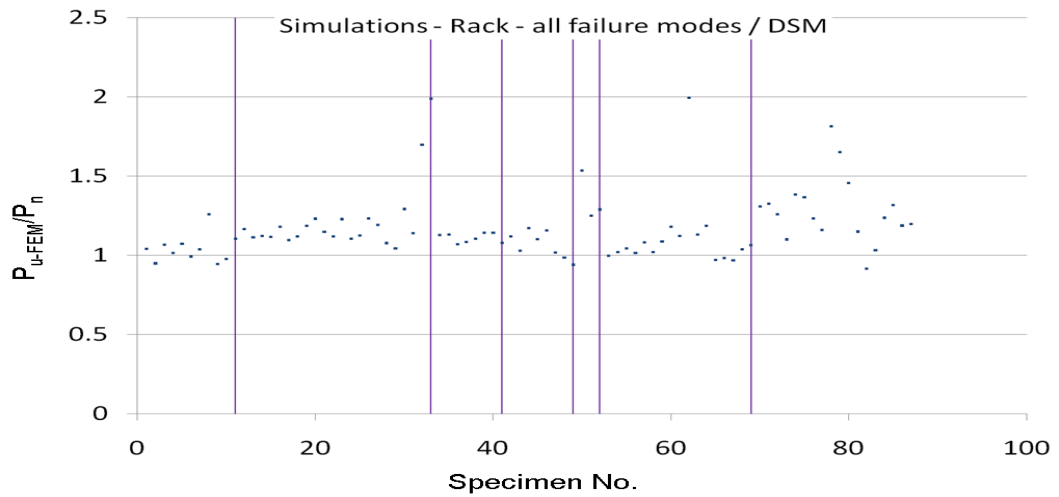

Fig. D.4: Simulation-to-predicted ratios for non-perforated Rack section columns by DSM Method 4 with classified failure modes (from left to right: L, LG, G, D, LD, DG, and LDG)
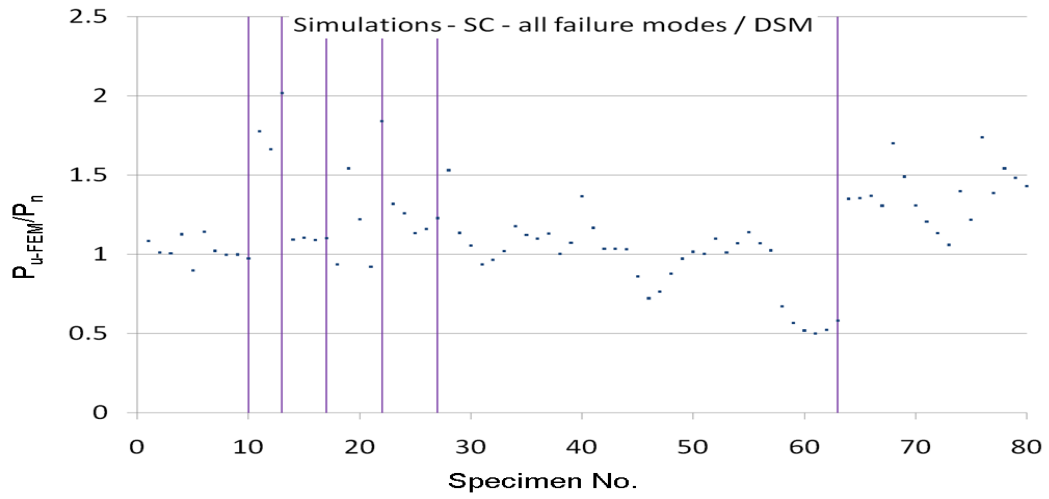
Fig. D.5: Simulation-to-predicted ratios for non-perforated Stiffened C section columns by DSM Method 4 with classified failure modes (from left to right: L, LG, G, D, LD, DG, and LDG)

APPENDIX E

SIMULATION-TO-PREDICTED RATIOS BY DSM METHOD 5 –

Option 2 in (Moen and Schafer 2011) (i.e. P_{yn} everywhere, P_{cr} (i.e. $P_{cr\text{-}l\text{-}h}$, $P_{cr\text{-}d\text{-}h}$, $P_{cr\text{-}e\text{-}h}$) by the simplified methods in (Moen and Schafer 2009))

E.1 non-perforated and perforated columns
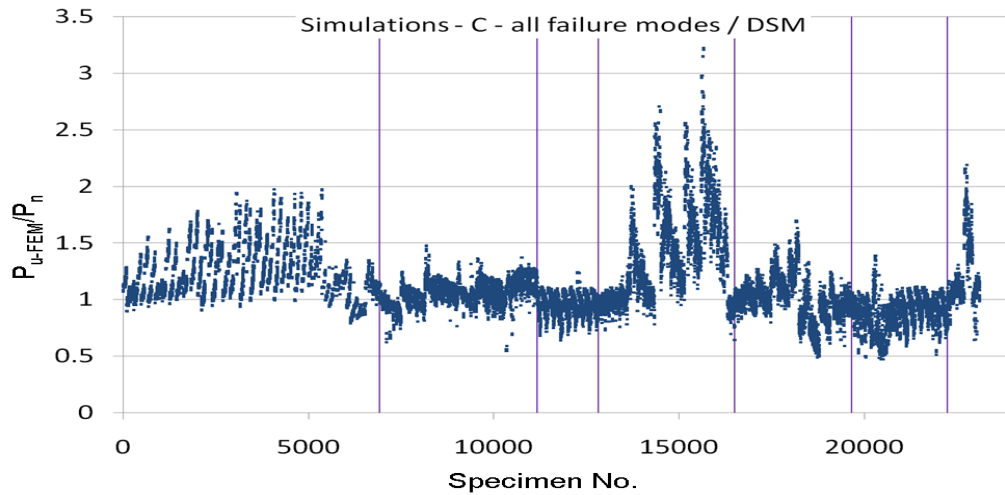
Fig. E.1: Simulation-to-predicted ratios for all C section columns by DSM Method 5 with classified failure modes (from left to right: L, LG, G, D, LD, DG, and LDG)
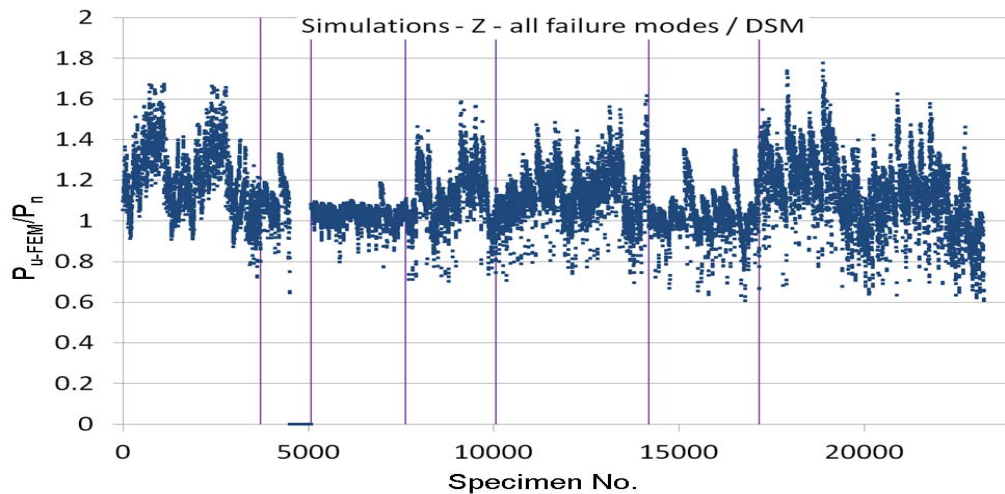

Fig. E.2: Simulation-to-predicted ratios for all Z section columns by DSM Method 5 with classified failure modes (from left to right: L, LG, G, D, LD, DG, and LDG)
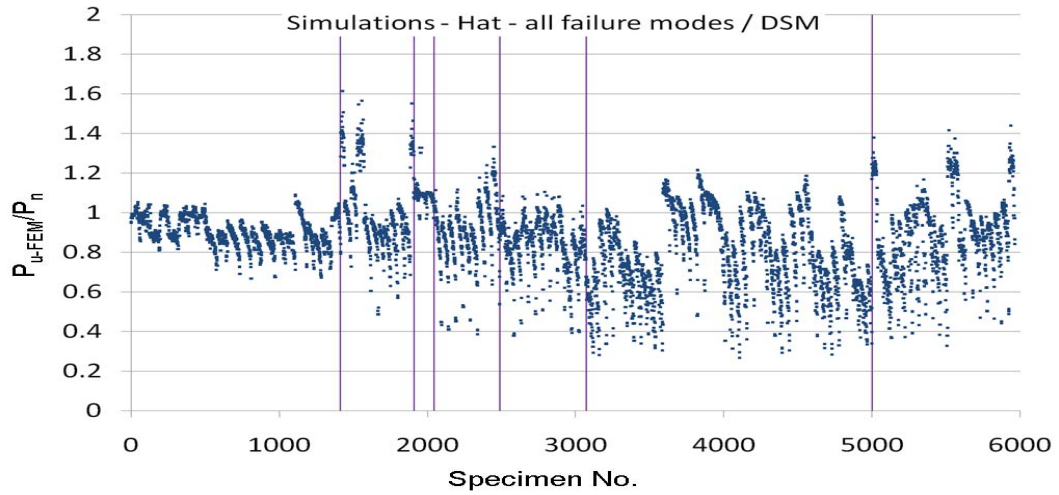
Fig. E.3: Simulation-to-predicted ratios for all Hat section columns by DSM Method 5 with classified failure modes (from left to right: L, LG, G, D, LD, DG, and LDG)
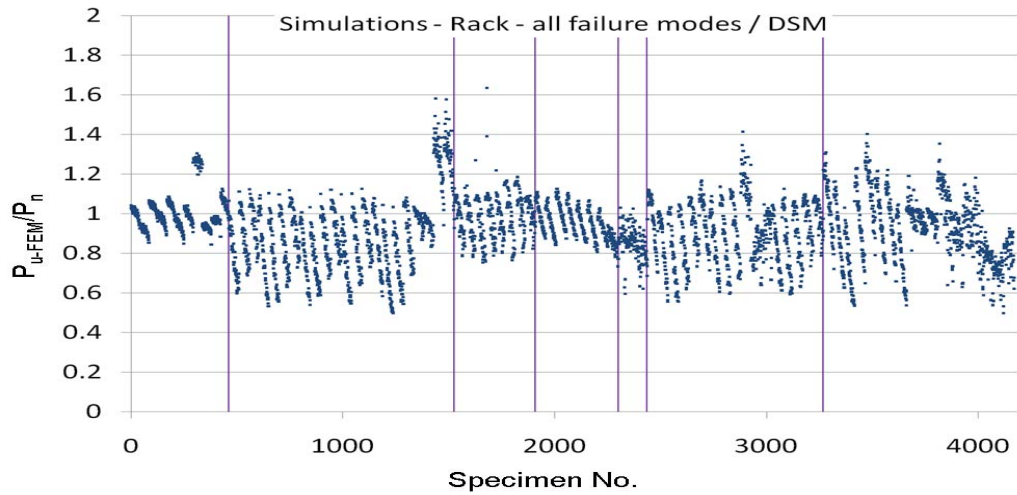
Fig. E.4: Simulation-to-predicted ratios for all Rack section columns by DSM Method 5 with classified failure modes (from left to right: L, LG, G, D, LD, DG, and LDG)
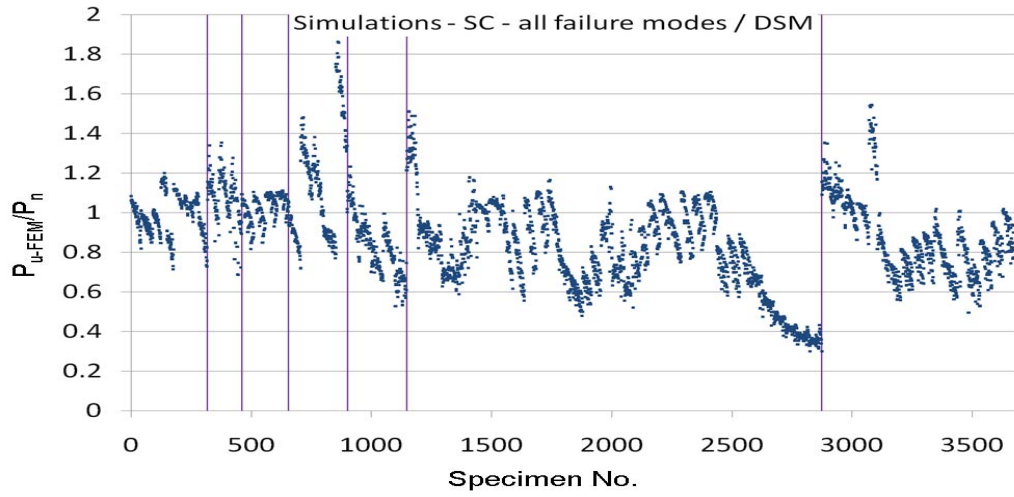
Fig. E.5: Simulation-to-predicted ratios for all Stiffened C section columns by DSM Method 5 with classified failure modes (from left to right: L, LG, G, D, LD, DG, and LDG)

APPENDIX F

SIMULATION-TO-PREDICTED RATIOS BY DSM METHOD 6 –

Option 4 in (Moen and Schafer 2011) (i.e. limit P_{n1} to P_{yn}, transition P_{nd} to P_{yn}, P_{cr} by the simplified methods in (Moen and Schafer 2009))

F.1   non-perforated and perforated columns
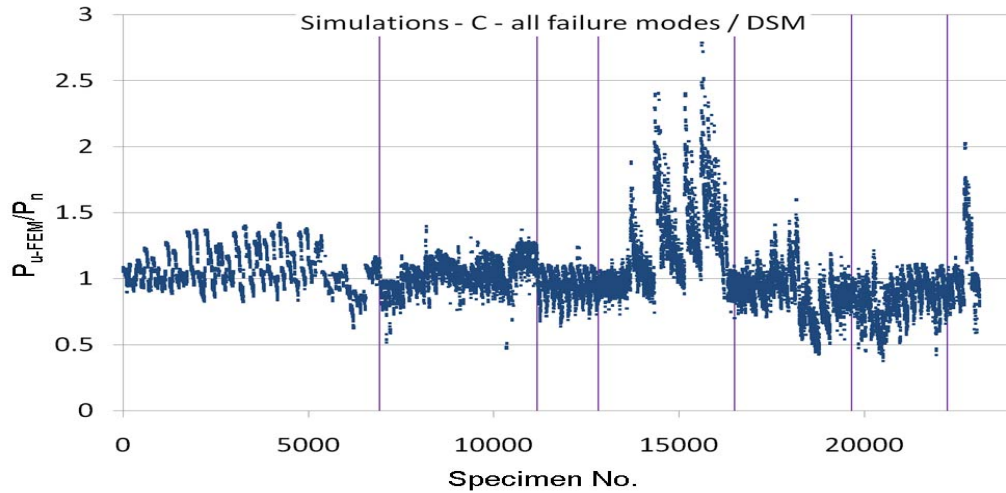
Fig. F.1: Simulation-to-predicted ratios for all C section columns by DSM Method 6 with classified failure modes (from left to right: L, LG, G, D, LD, DG, and LDG)
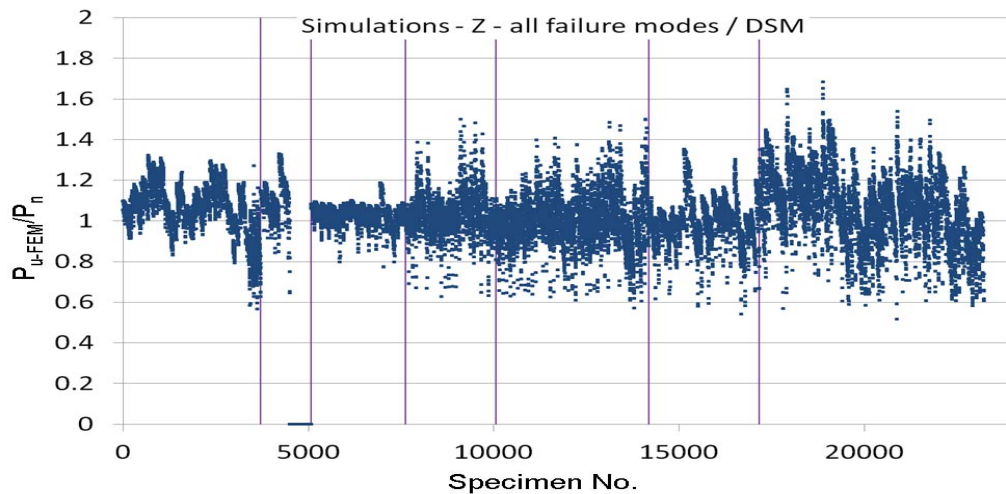

Fig. F.2: Simulation-to-predicted ratios for all Z section columns by DSM Method 6 with classified failure modes (from left to right: L, LG, G, D, LD, DG, and LDG)
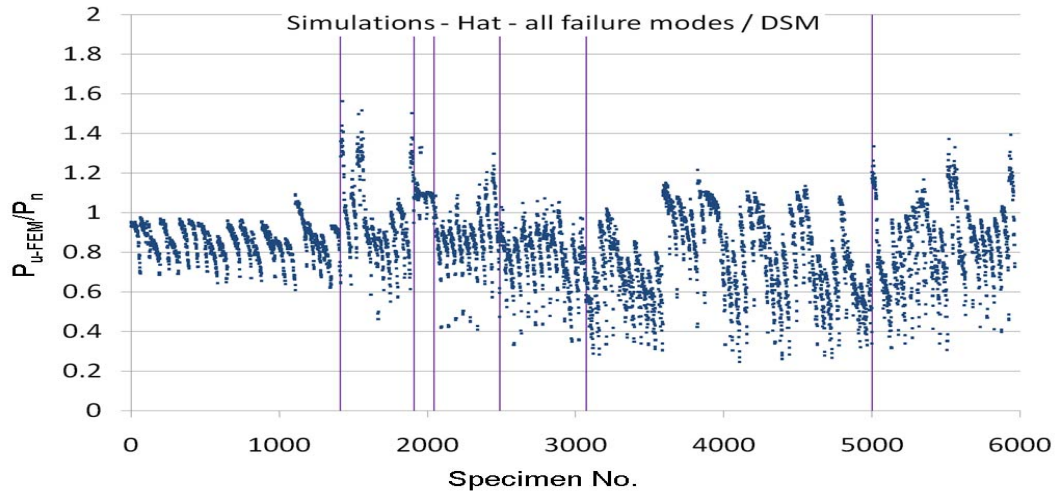
Fig. F.3: Simulation-to-predicted ratios for all Hat section columns by DSM Method 6 with classified failure modes (from left to right: L, LG, G, D, LD, DG, and LDG)
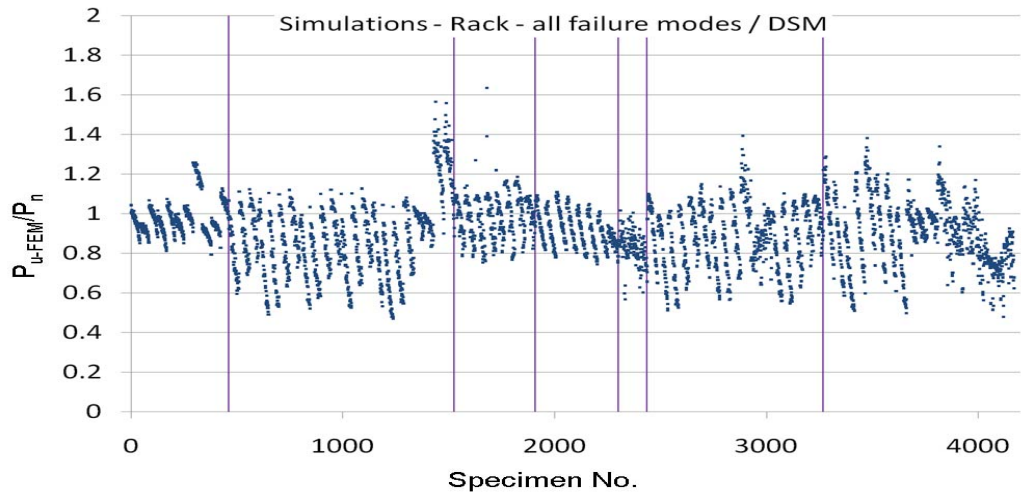

Fig. F.4: Simulation-to-predicted ratios for all Rack section columns by DSM Method 6 with classified failure modes (from left to right: L, LG, G, D, LD, DG, and LDG)
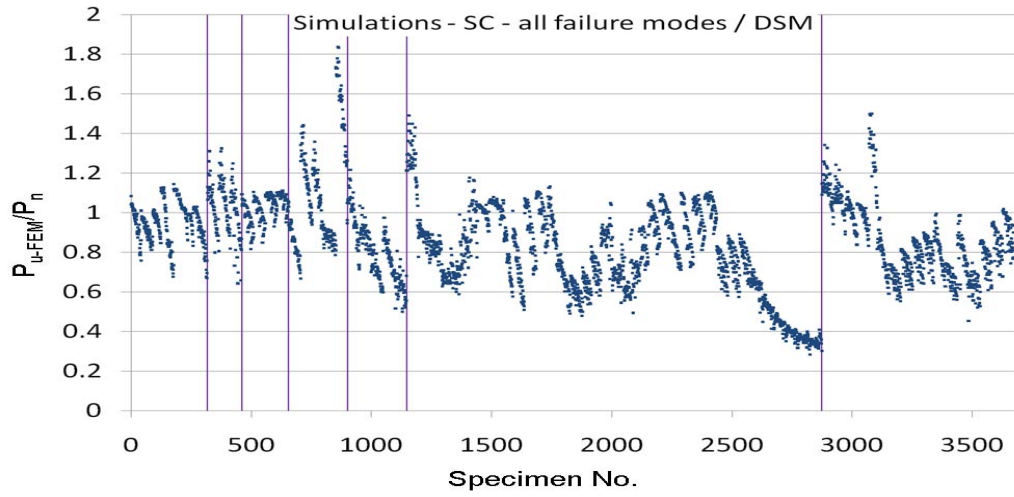
Fig. F.5: Simulation-to-predicted ratios for all Stiffened C section columns by DSM Method 6 with classified failure modes (from left to right: L, LG, G, D, LD, DG, and LDG)

APPENDIX G

SIMULATION-TO-PREDICTED RATIOS BY DSM METHOD 7 – AS/NZS 4600 DSM with P_{yn} everywhere and P_{cr} based on gross area (i.e. $P_{cr\text{-}l\text{-}nh}$, $P_{cr\text{-}d\text{-}nh}$, $P_{cr\text{-}e\text{-}nh}$)

G.1   non-perforated and perforated columns
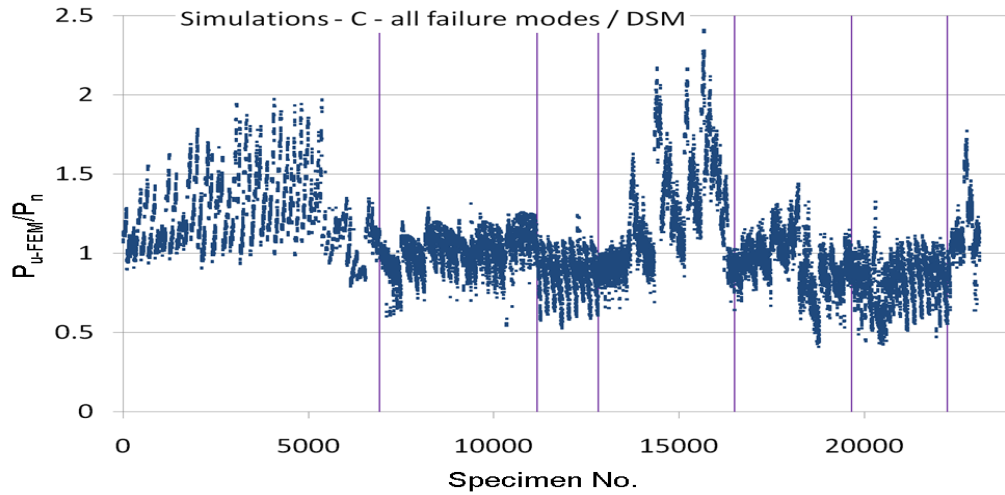
Fig. G.1: Simulation-to-predicted ratios for all C section columns by DSM Method 7 with classified failure modes (from left to right: L, LG, G, D, LD, DG, and LDG)
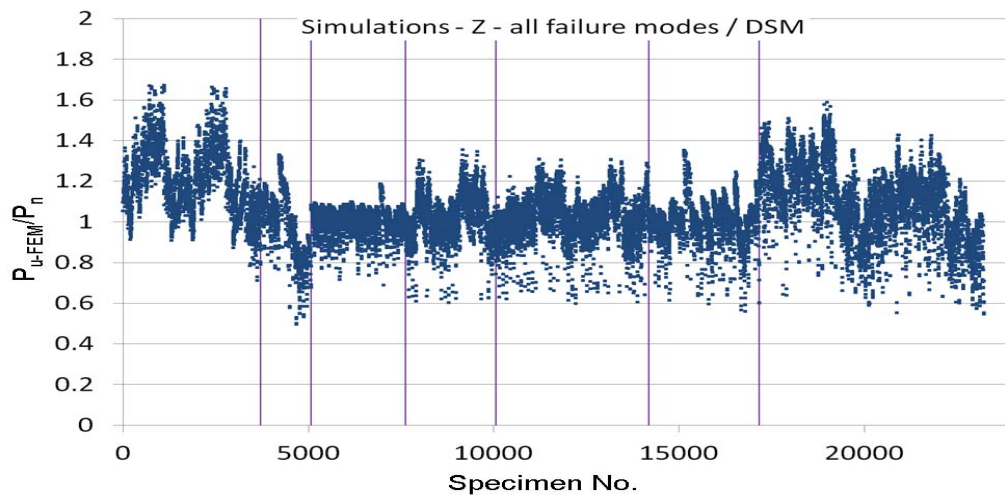
Fig. G.2: Simulation-to-predicted ratios for all Z section columns by DSM Method 7 with classified failure modes (from left to right: L, LG, G, D, LD, DG, and LDG)
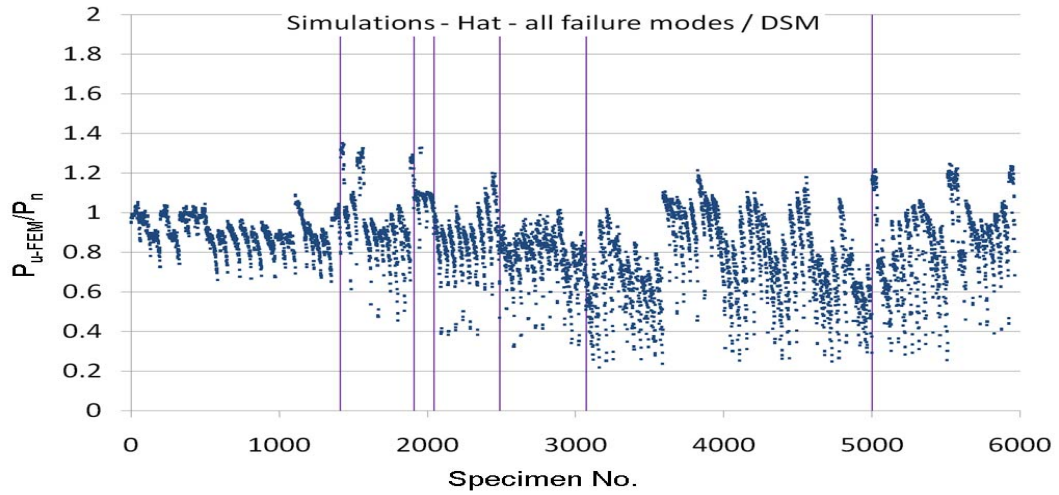
Fig. G.3: Simulation-to-predicted ratios for all Hat section columns by DSM Method 7 with classified

failure modes (from left to right: L, LG, G, D, LD, DG, and LDG)
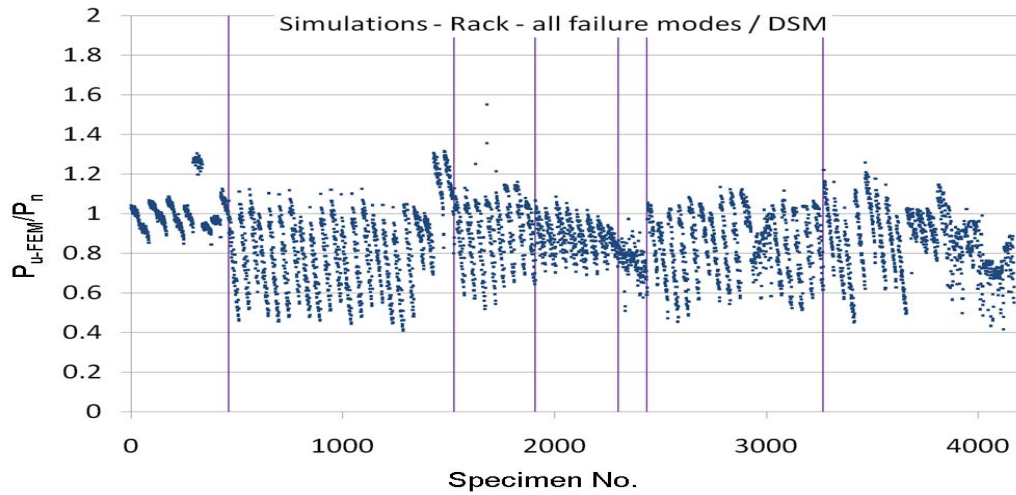
Fig. G.4: Simulation-to-predicted ratios for all Rack section columns by DSM Method 7 with classified

failure modes (from left to right: L, LG, G, D, LD, DG, and LDG)
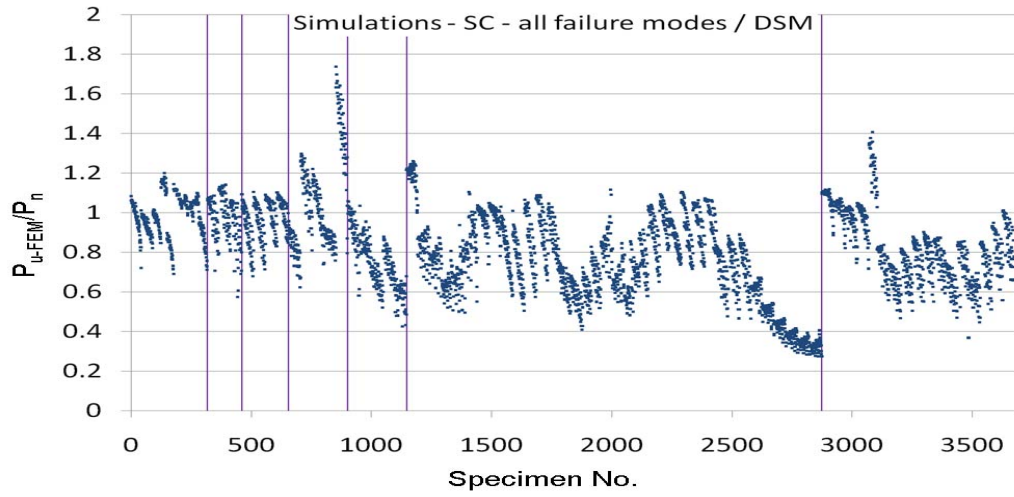
Fig. G.5: Simulation-to-predicted ratios for all Stiffened C section columns by DSM Method 7 with classified failure modes (from left to right: L, LG, G, D, LD, DG, and LDG)

APPENDIX H

SIMULATION-TO-PREDICTED RATIOS BY DSM METHOD 8 – AS/NZS 4600 DSM with P_y in the slenderness, P_{yn} elsewhere and P_{cr} based on gross area

H.1   non-perforated and perforated columns
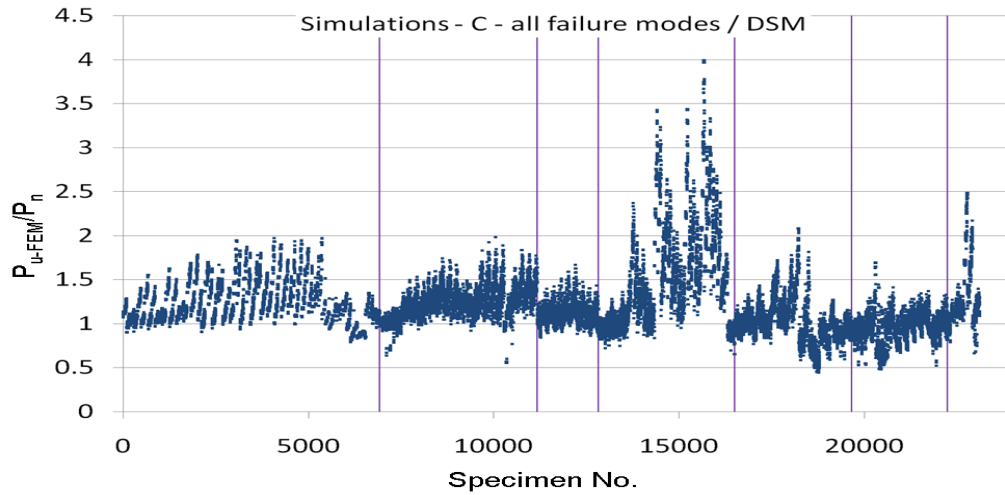
Fig. H.1: Simulation-to-predicted ratios for all C section columns by DSM Method 8 with classified failure modes (from left to right: L, LG, G, D, LD, DG, and LDG)
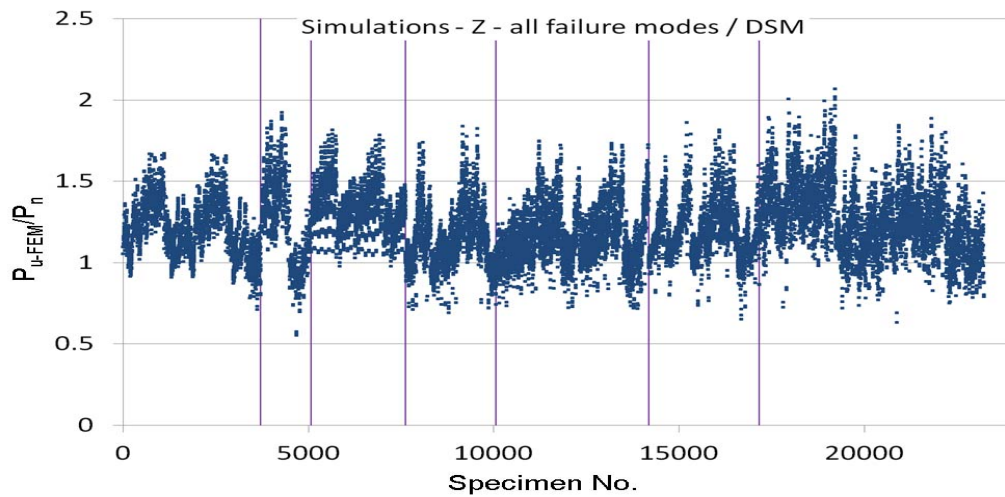
Fig. H.2: Simulation-to-predicted ratios for all Z section columns by DSM Method 8 with classified failure modes (from left to right: L, LG, G, D, LD, DG, and LDG)
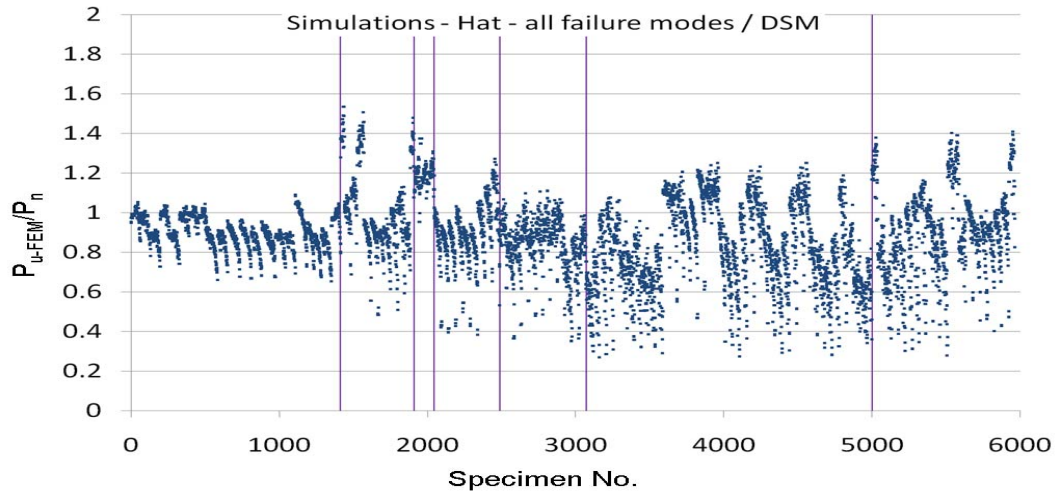
Fig. H.3: Simulation-to-predicted ratios for all Hat section columns by DSM Method 8 with classified failure modes (from left to right: L, LG, G, D, LD, DG, and LDG)
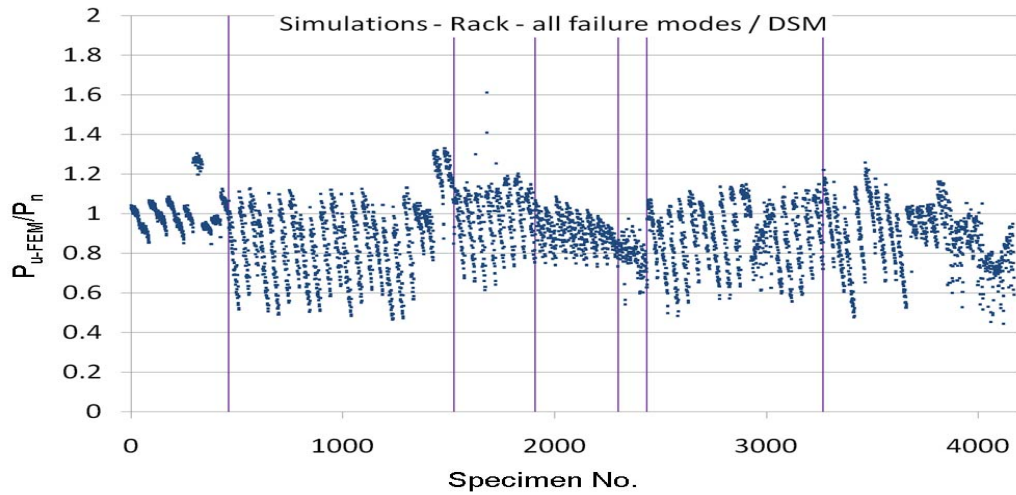

Fig. H.4: Simulation-to-predicted ratios for all Rack section columns by DSM Method 8 with classified failure modes (from left to right: L, LG, G, D, LD, DG, and LDG)
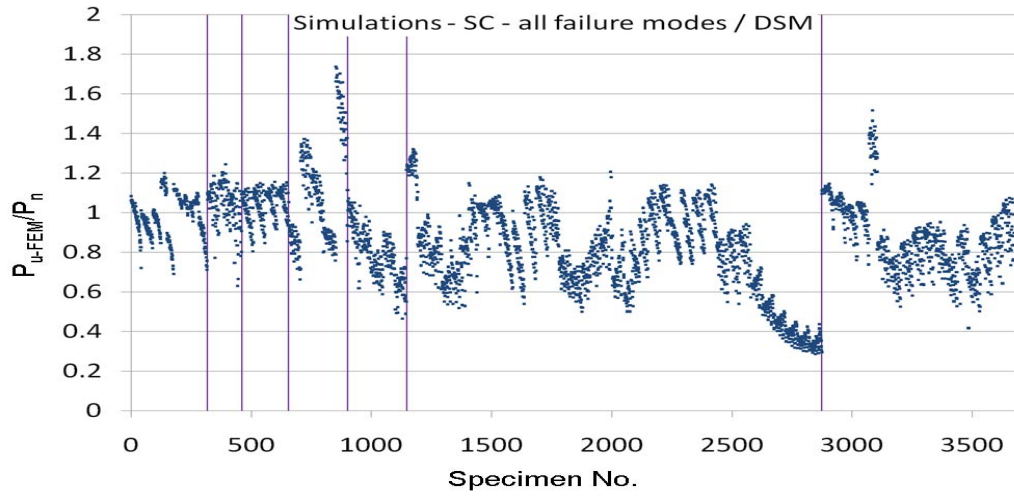
Fig. H.5: Simulation-to-predicted ratios for all Stiffened C section columns by DSM Method 8 with classified failure modes (from left to right: L, LG, G, D, LD, DG, and LDG)

<div align="center">

APPENDIX I

**SIMULATION-TO-PREDICTED RATIOS BY DSM METHOD 9 –
Modification 1 to Option 4 in (Moen and Schafer 2011) – replace $P_{cr\text{-}e\text{-}h}$
by $P_{cr\text{-}e\text{-}nh}$**

</div>

I.1 non-perforated and perforated columns
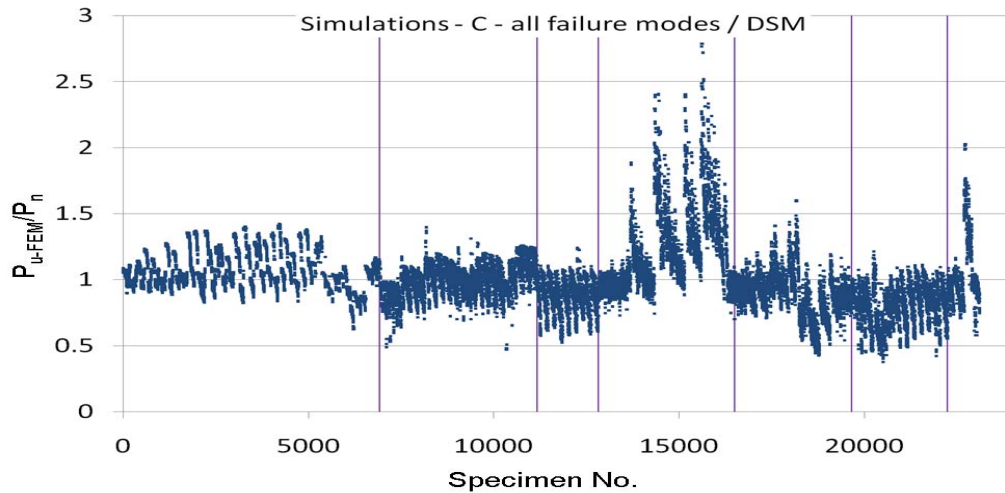
Fig. I.1: Simulation-to-predicted ratios for all C section columns by DSM Method 9 with classified failure modes (from left to right: L, LG, G, D, LD, DG, and LDG)
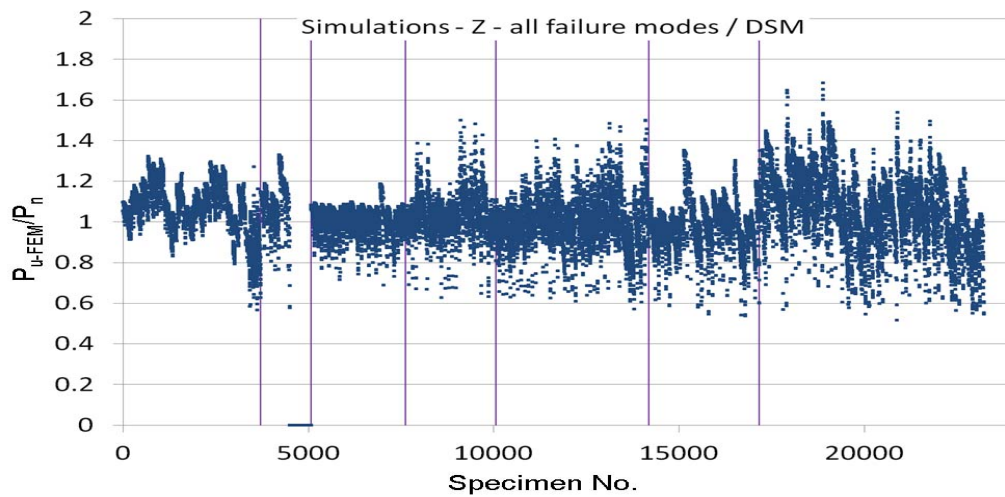
Fig. I.2: Simulation-to-predicted ratios for all Z section columns by DSM Method 9 with classified failure modes (from left to right: L, LG, G, D, LD, DG, and LDG)
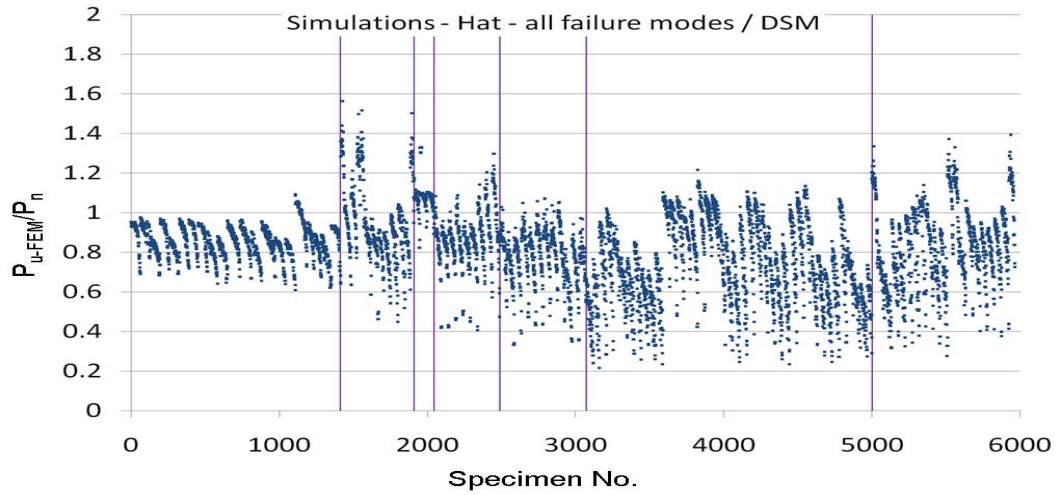
Fig. I.3: Simulation-to-predicted ratios for all Hat section columns by DSM Method 9 with classified failure modes (from left to right: L, LG, G, D, LD, DG, and LDG)
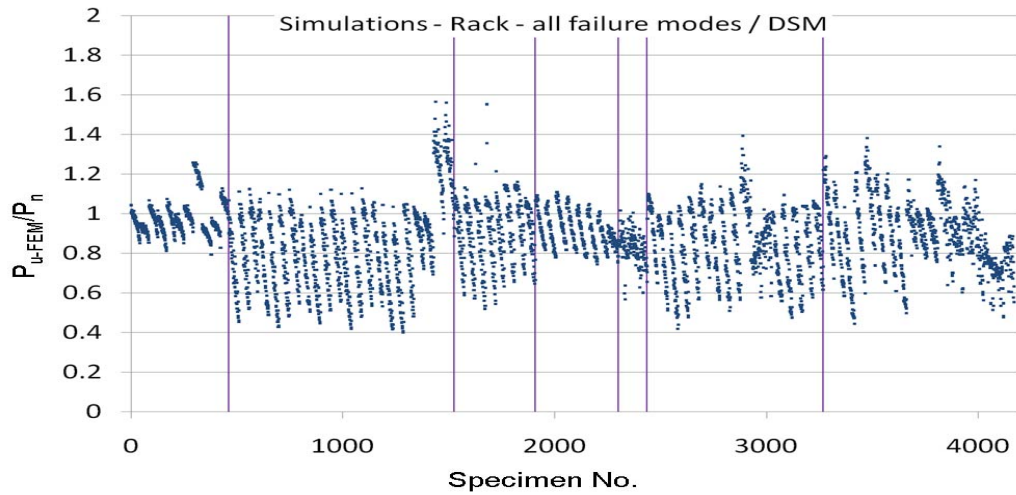
Fig. I.4: Simulation-to-predicted ratios for all Rack section columns by DSM Method 9 with classified failure modes (from left to right: L, LG, G, D, LD, DG, and LDG)
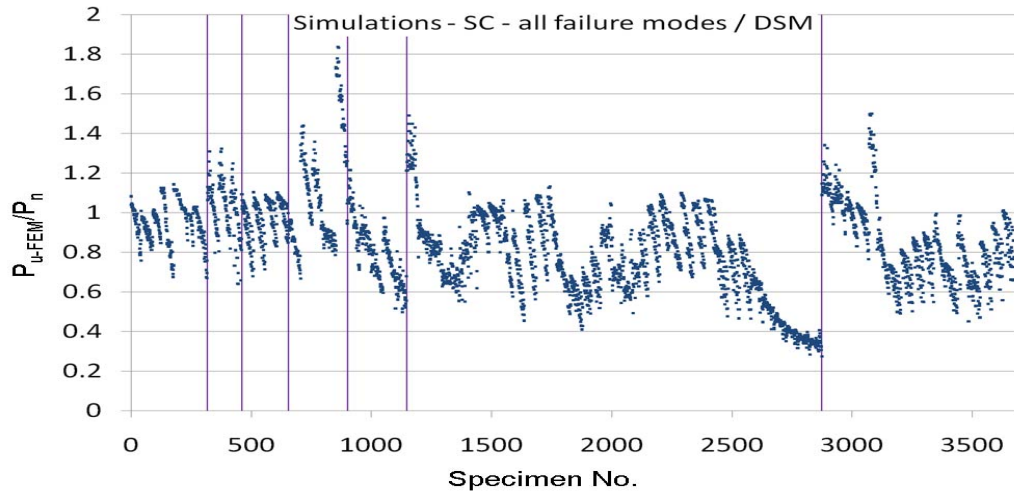
Fig. I.5: Simulation-to-predicted ratios for all Stiffened C section columns by DSM Method 9 with classified failure modes (from left to right: L, LG, G, D, LD, DG, and LDG)

<div align="center">

APPENDIX J

SIMULATION-TO-PREDICTED RATIOS BY DSM METHOD 10 – Modification 2 to Option 4 in (Moen and Schafer 2011) – replace $P_{cr\text{-}\ell\text{-}h}$ by $P_{cr\text{-}\ell\text{-}nh}$

</div>

J.1 non-perforated and perforated columns
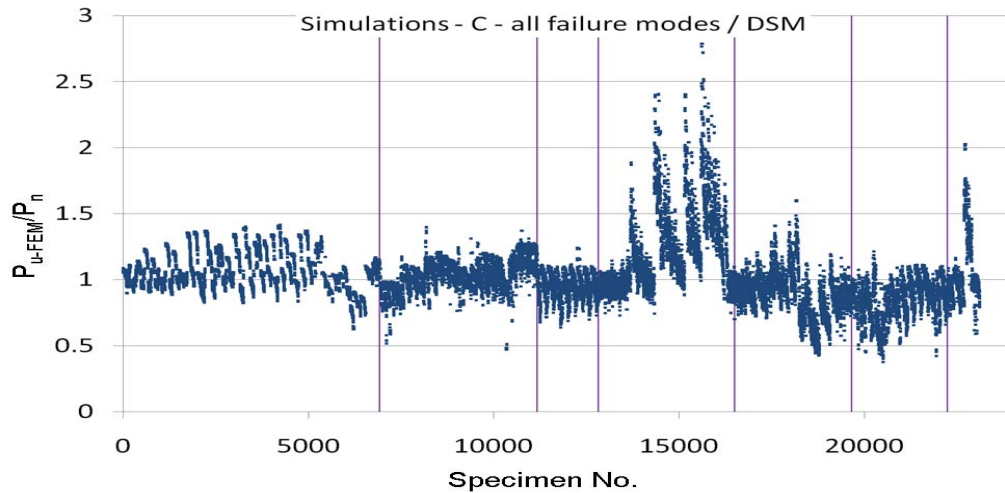
Fig. J.1: Simulation-to-predicted ratios for all C section columns by DSM Method 10 with classified failure modes (from left to right: L, LG, G, D, LD, DG, and LDG)
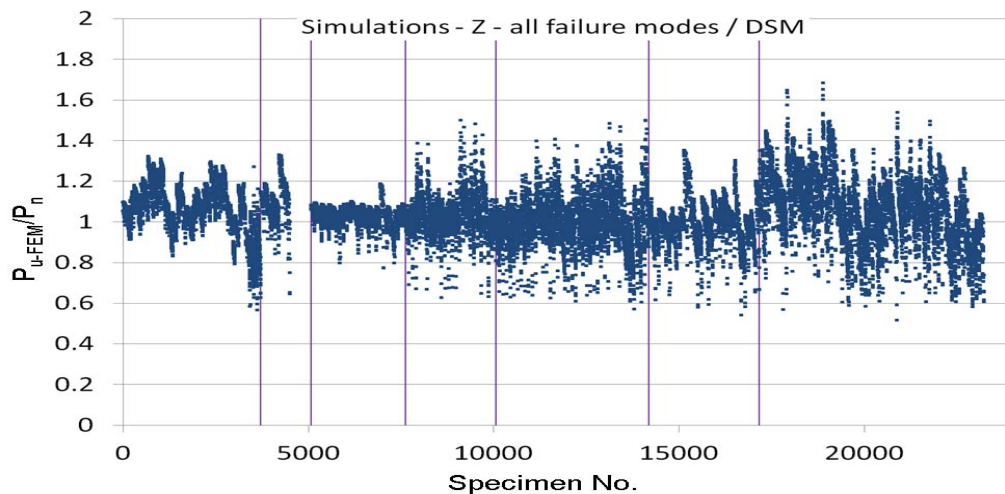

Fig. J.2: Simulation-to-predicted ratios for all Z section columns by DSM Method 10 with classified failure modes (from left to right: L, LG, G, D, LD, DG, and LDG)
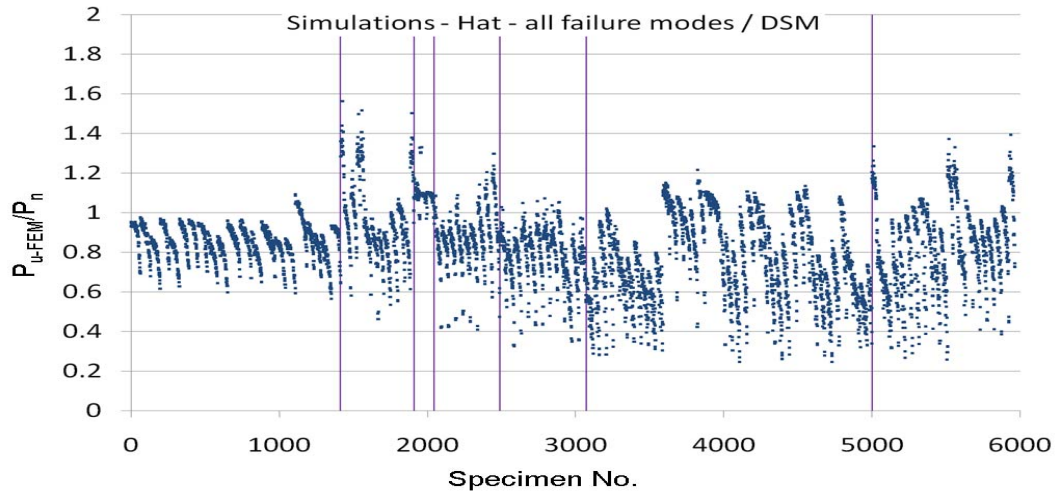
Fig. J.3: Simulation-to-predicted ratios for all Hat section columns by DSM Method 10 with classified failure modes (from left to right: L, LG, G, D, LD, DG, and LDG)
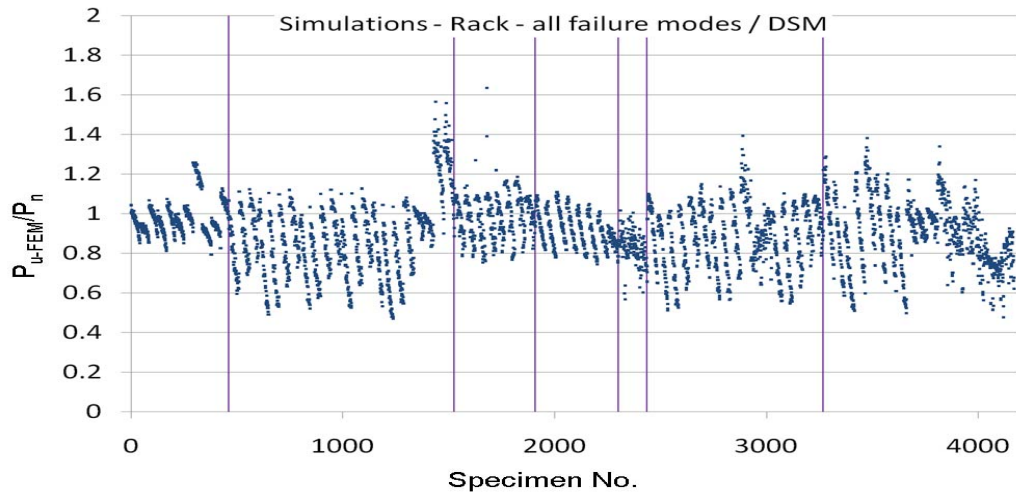
Fig. J.4: Simulation-to-predicted ratios for all Rack section columns by DSM Method 10 with classified failure modes (from left to right: L, LG, G, D, LD, DG, and LDG)
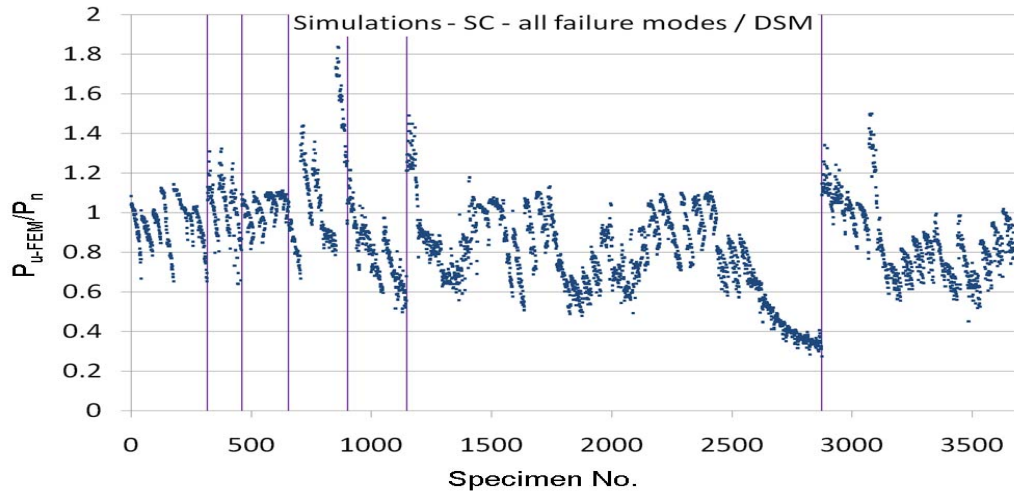
Fig. J.5: Simulation-to-predicted ratios for all Stiffened C section columns by DSM Method 10 with classified failure modes (from left to right: L, LG, G, D, LD, DG, and LDG)

APPENDIX K

SIMULATION-TO-PREDICTED RATIOS BY DSM METHOD 11 – Modification 3 to Option 4 in (Moen and Schafer 2011) – replace $P_{cr\text{-}d\text{-}h}$ by $P_{cr\text{-}d\text{-}nh}$

K.1   non-perforated and perforated columns
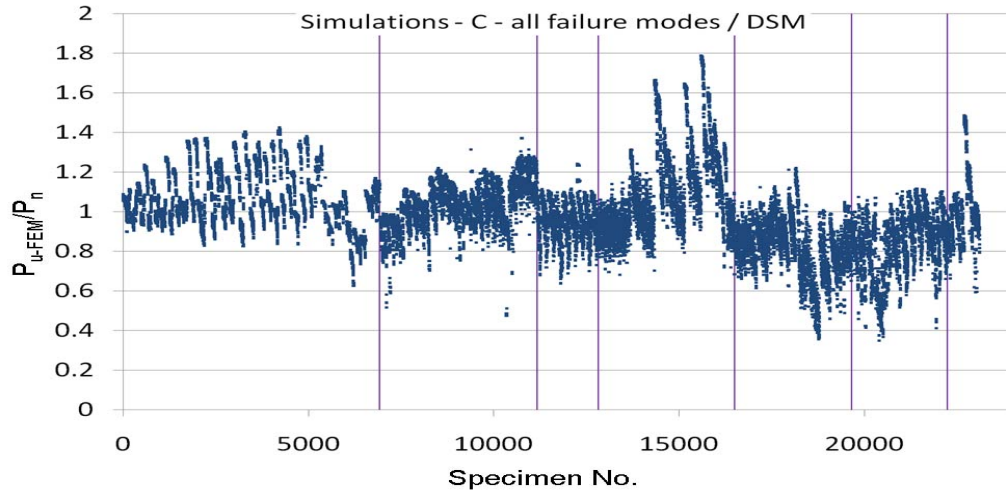
Fig. K.1: Simulation-to-predicted ratios for all C section columns by DSM Method 11 with classified failure modes (from left to right: L, LG, G, D, LD, DG, and LDG)
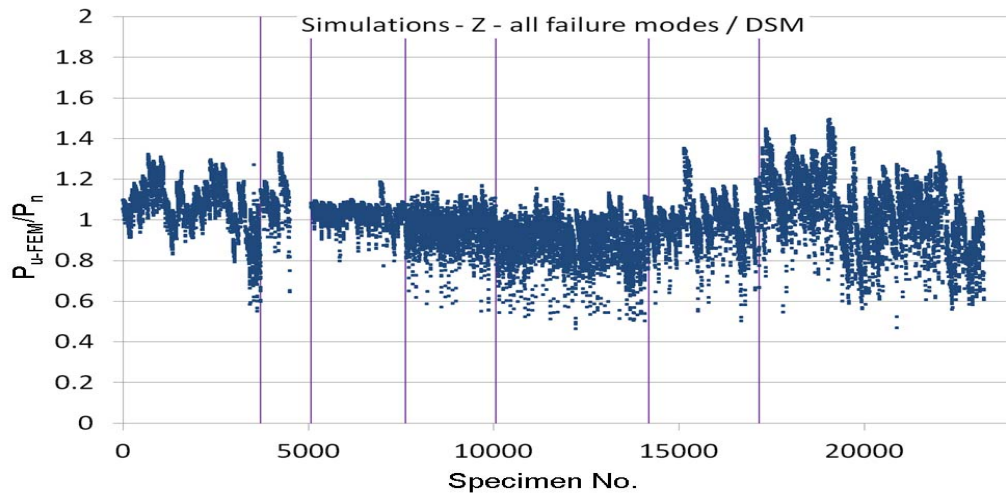
Fig. K.2: Simulation-to-predicted ratios for all Z section columns by DSM Method 11 with classified failure modes (from left to right: L, LG, G, D, LD, DG, and LDG)
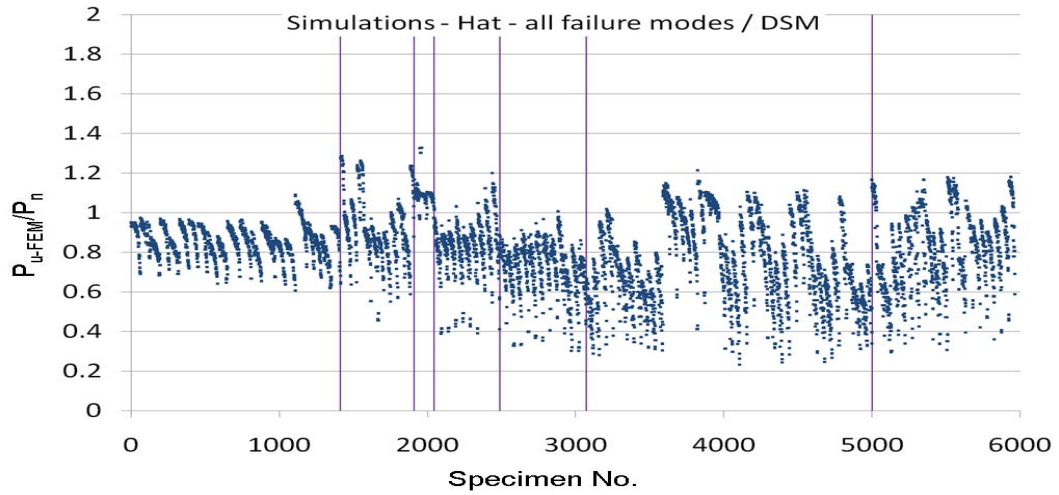
Fig. K.3: Simulation-to-predicted ratios for all Hat section columns by DSM Method 11 with classified failure modes (from left to right: L, LG, G, D, LD, DG, and LDG)
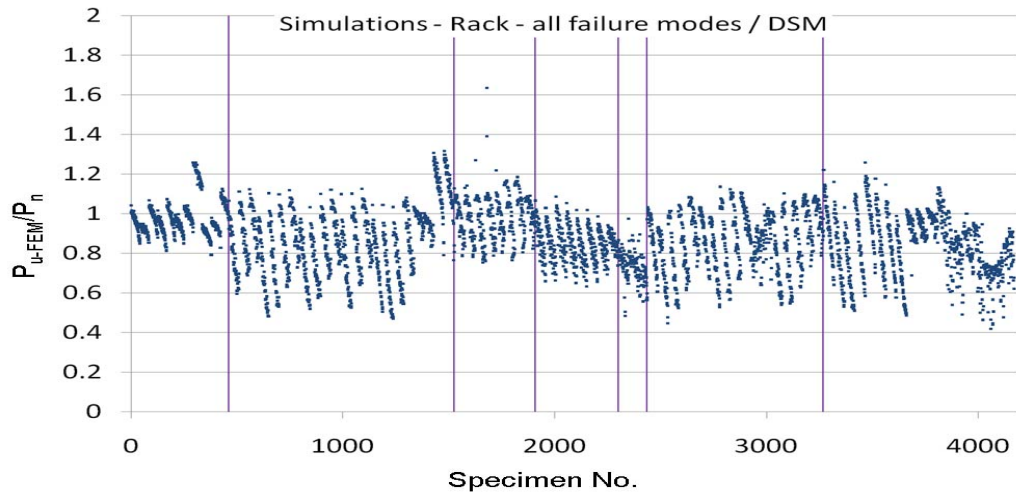
Fig. K.4: Simulation-to-predicted ratios for all Rack section columns by DSM Method 11 with classified failure modes (from left to right: L, LG, G, D, LD, DG, and LDG)
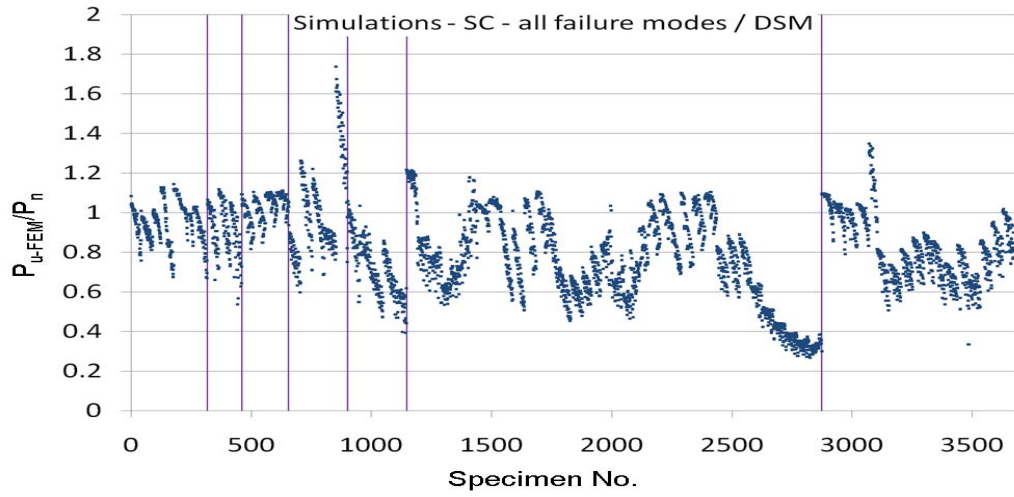
Fig. K.5: Simulation-to-predicted ratios for all Stiffened C section columns by DSM Method 11 with classified failure modes (from left to right: L, LG, G, D, LD, DG, and LDG)

APPENDIX L

SIMULATION-TO-PREDICTED RATIOS BY DSM METHOD 12 – Modification 4 to Option 4 in (Moen and Schafer 2011) – replace the D equation by the AS/NZS 4600 DSM D equation, limit P_{nd} to P_{yn}; use $P_{cr\text{-}d\text{-}h}$

L.1 non-perforated and perforated columns
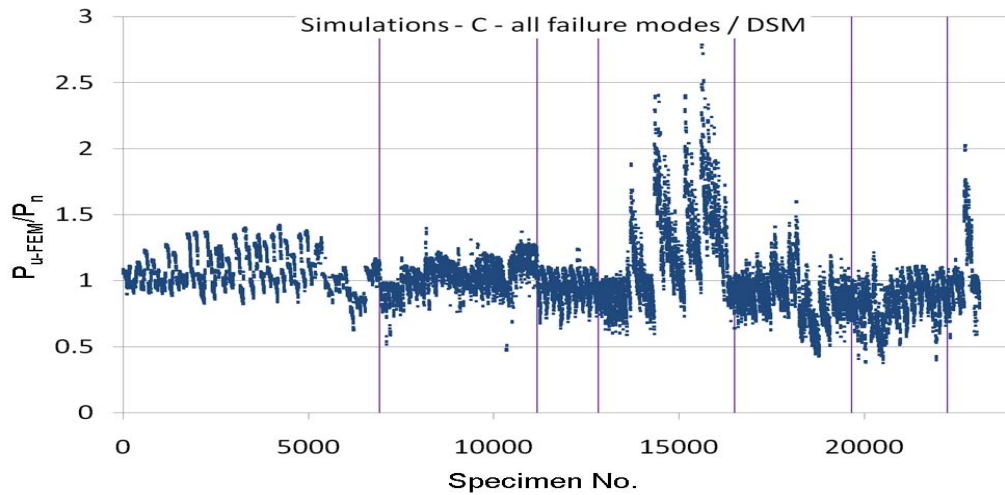
Fig. L.1: Simulation-to-predicted ratios for all C section columns by DSM Method 12 with classified failure modes (from left to right: L, LG, G, D, LD, DG, and LDG)
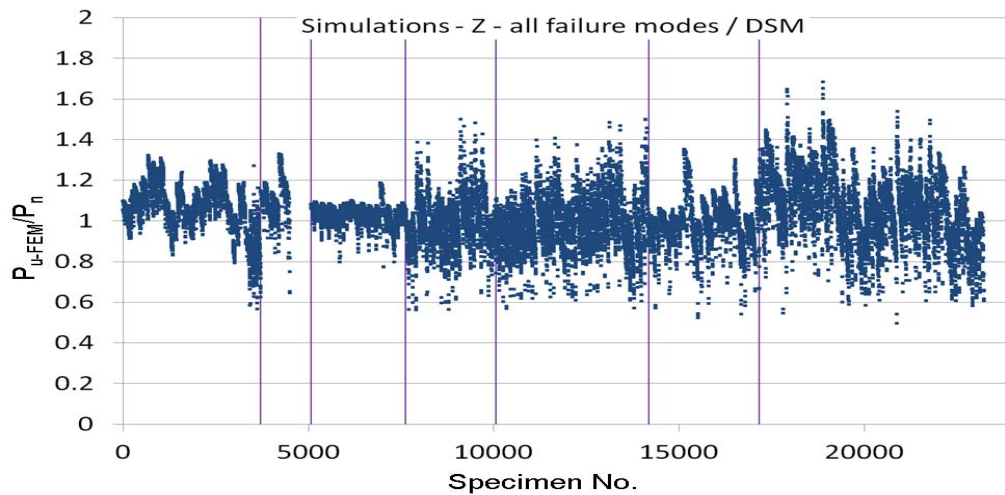
Fig. L.2: Simulation-to-predicted ratios for all Z section columns by DSM Method 12 with classified failure modes (from left to right: L, LG, G, D, LD, DG, and LDG)
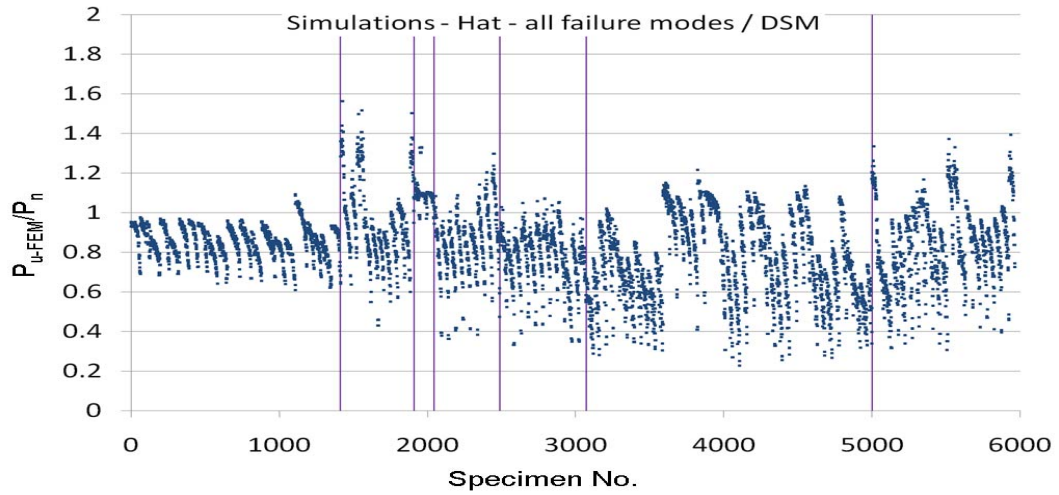
Fig. L.3: Simulation-to-predicted ratios for all Hat section columns by DSM Method 12 with classified failure modes (from left to right: L, LG, G, D, LD, DG, and LDG)
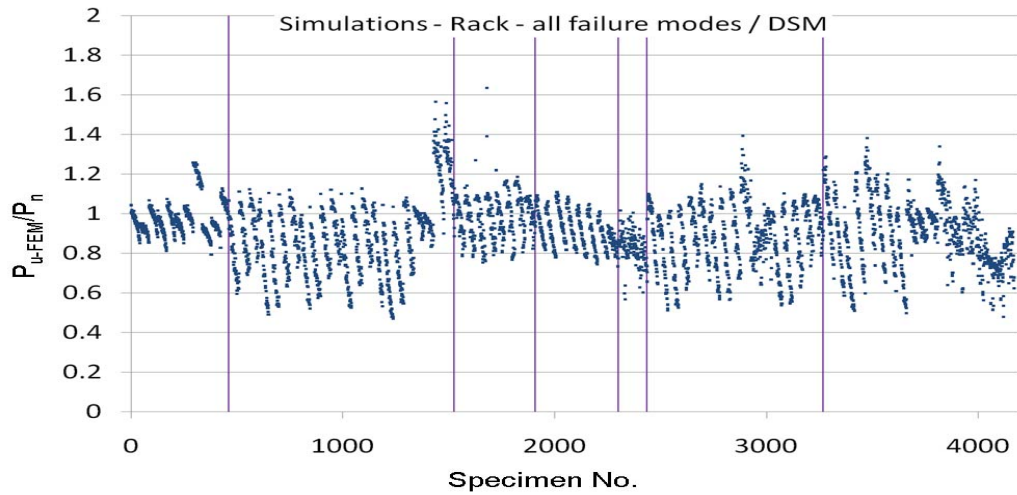

Fig. L.4: Simulation-to-predicted ratios for all Rack section columns by DSM Method 12 with classified failure modes (from left to right: L, LG, G, D, LD, DG, and LDG)
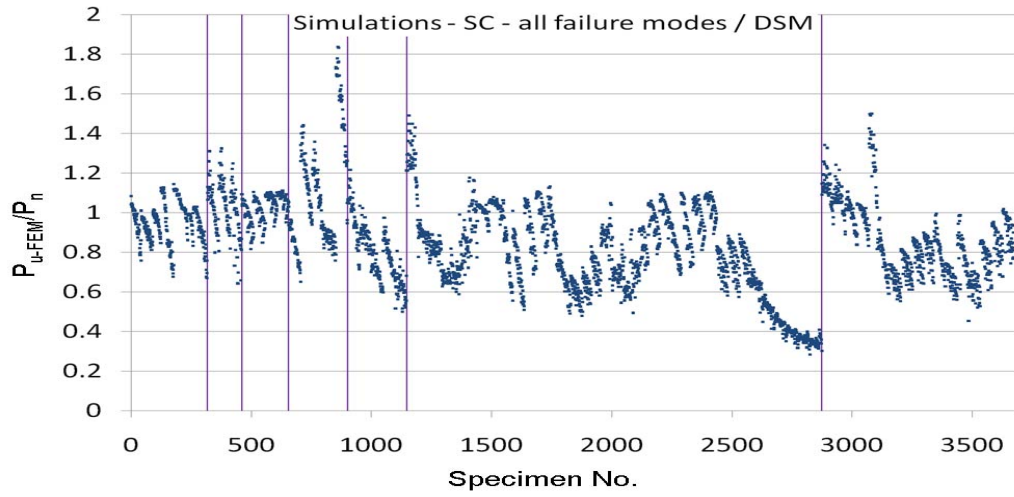
Fig. L.5: Simulation-to-predicted ratios for all Stiffened C section columns by DSM Method 12 with classified failure modes (from left to right: L, LG, G, D, LD, DG, and LDG)

APPENDIX M

SIMULATION-TO-PREDICTED RATIOS BY DSM METHOD 13 – Modification 5 to Option 4 in (Moen and Schafer 2011) – minimum of (i) regression analyses of LG equation using $P_{cr\text{-}1\text{-}nh}$, (ii) D equation, and (iii) G equation

## M.1 non-perforated and perforated columns
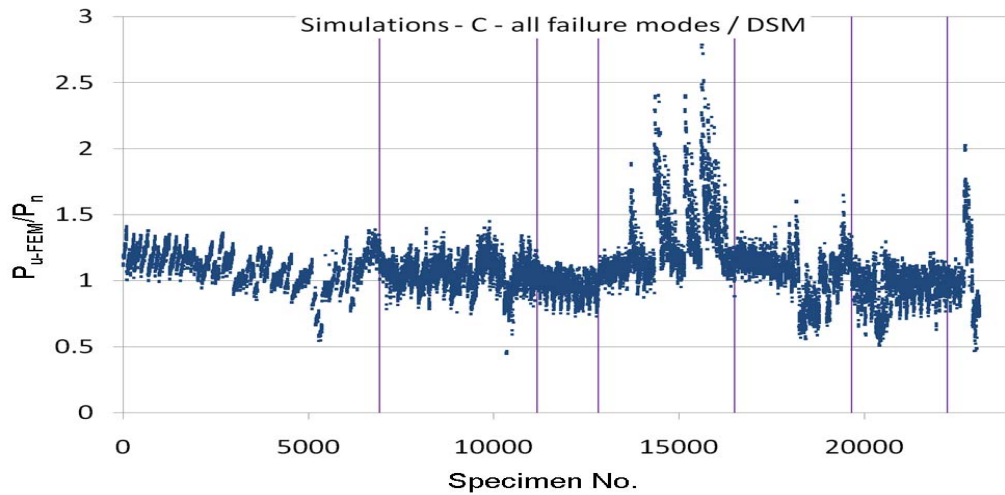
Fig. M.1: Simulation-to-predicted ratios for all C section columns by DSM Method 13 with classified failure modes (from left to right: L, LG, G, D, LD, DG, and LDG)
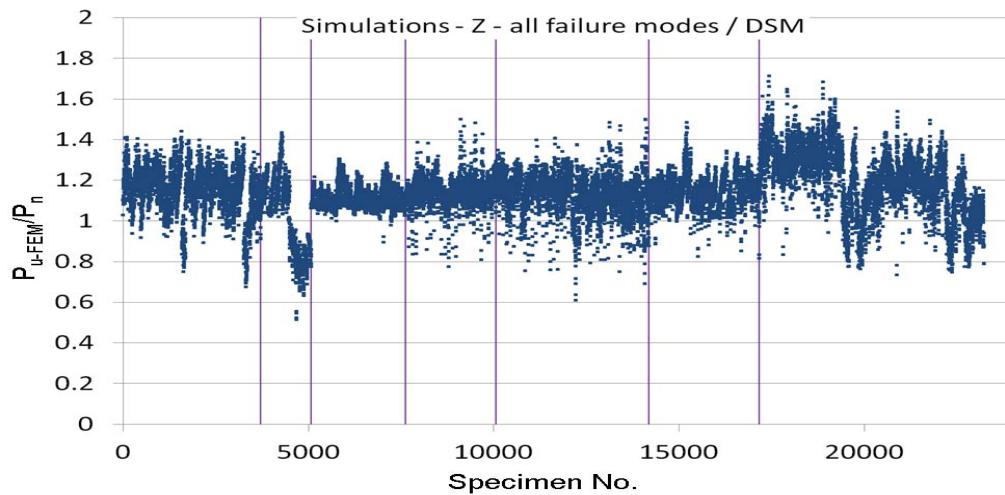
Fig. M.2: Simulation-to-predicted ratios for all Z section columns by DSM Method 13 with classified failure modes (from left to right: L, LG, G, D, LD, DG, and LDG)
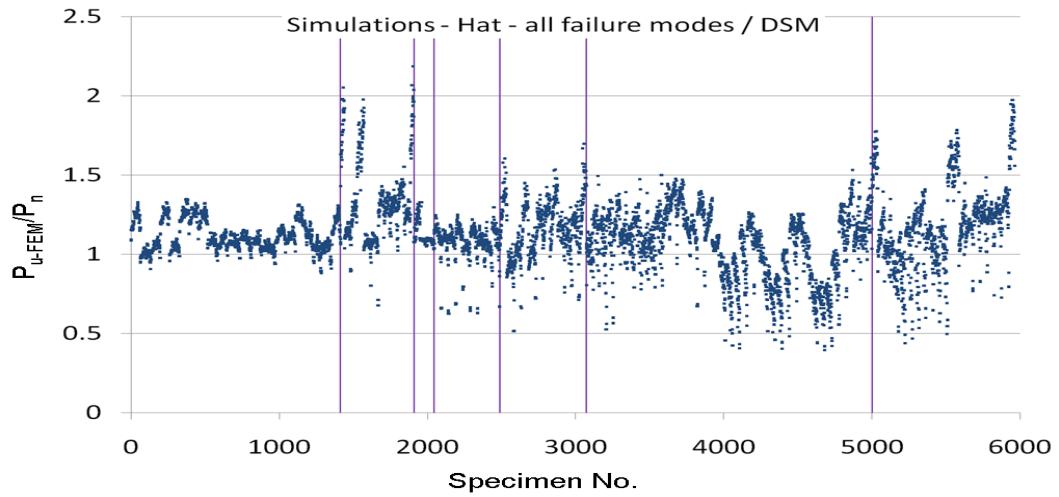
Fig. M.3: Simulation-to-predicted ratios for all Hat section columns by DSM Method 13 with classified failure modes (from left to right: L, LG, G, D, LD, DG, and LDG)
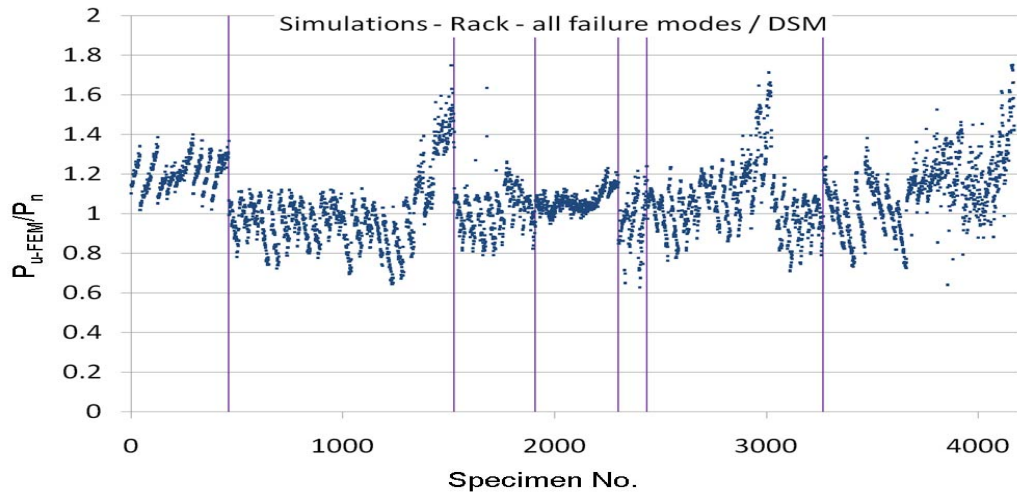
Fig. M.4: Simulation-to-predicted ratios for all Rack section columns by DSM Method 13 with classified failure modes (from left to right: L, LG, G, D, LD, DG, and LDG)
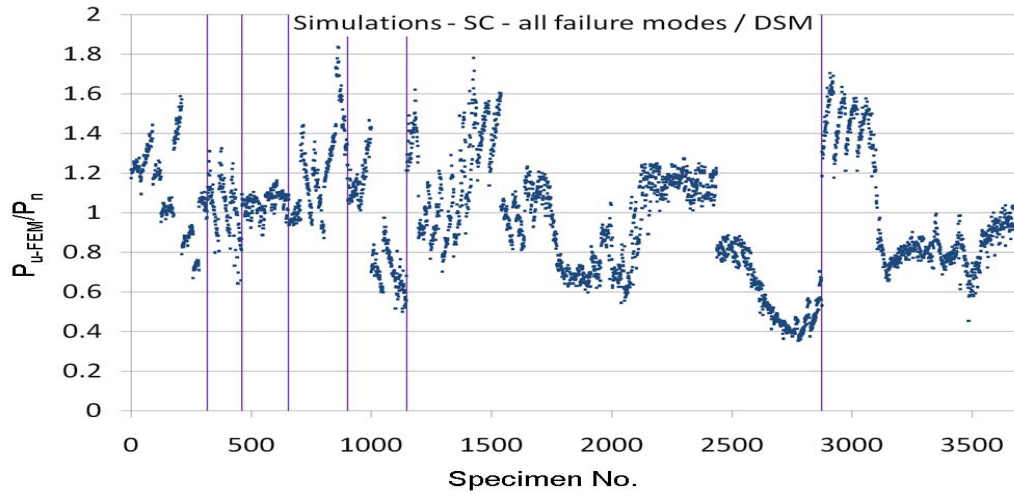
Fig. M.5: Simulation-to-predicted ratios for all Stiffened C section columns by DSM Method 13 with classified failure modes (from left to right: L, LG, G, D, LD, DG, and LDG)

APPENDIX N

SIMULATION-TO-PREDICTED RATIOS BY DSM METHOD 14 – Modification 6 to Option 4 in (Moen and Schafer 2011) – minimum of (i) regression analyses of LG equation using $P_{cr\text{-}1\text{-}nh}$ and (ii) D equation

N.1   non-perforated and perforated columns
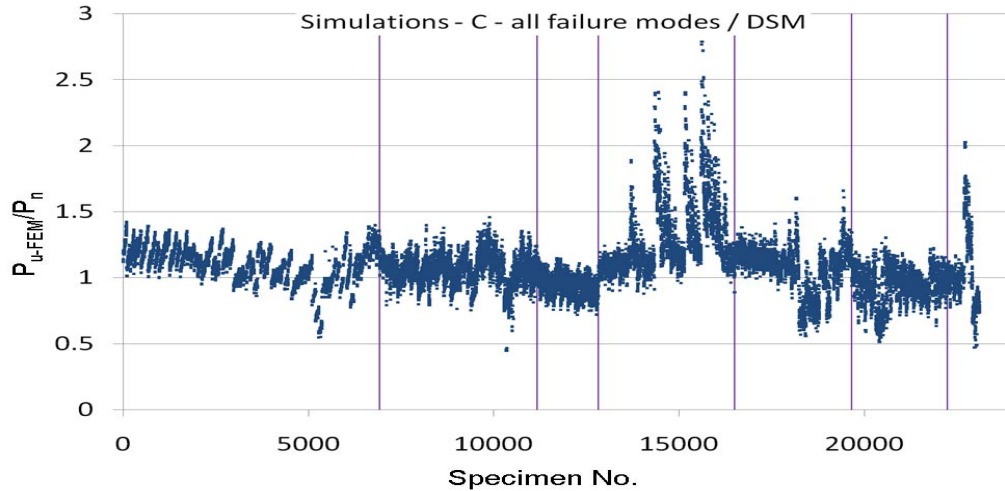
Fig. N.1: Simulation-to-predicted ratios for all C section columns by DSM Method 14 with classified failure modes (from left to right: L, LG, G, D, LD, DG, and LDG)
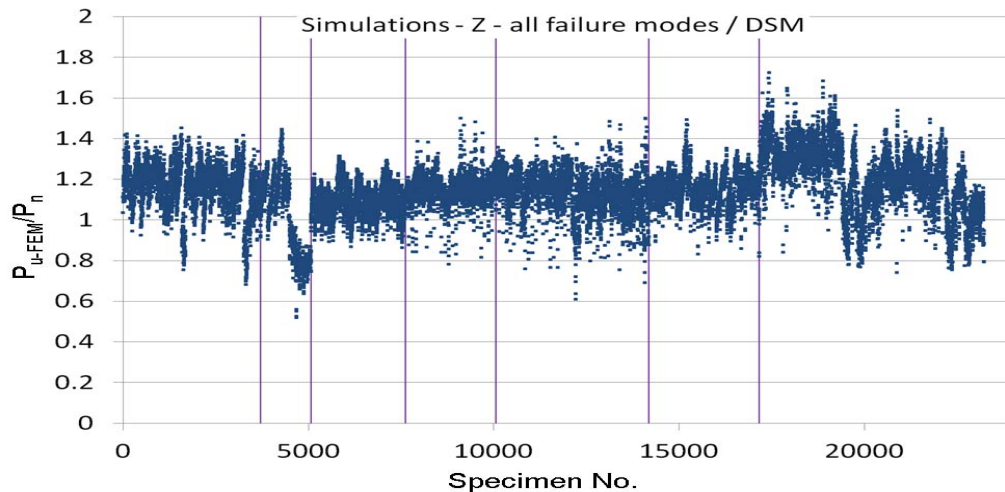

Fig. N.2: Simulation-to-predicted ratios for all Z section columns by DSM Method 14 with classified failure modes (from left to right: L, LG, G, D, LD, DG, and LDG)
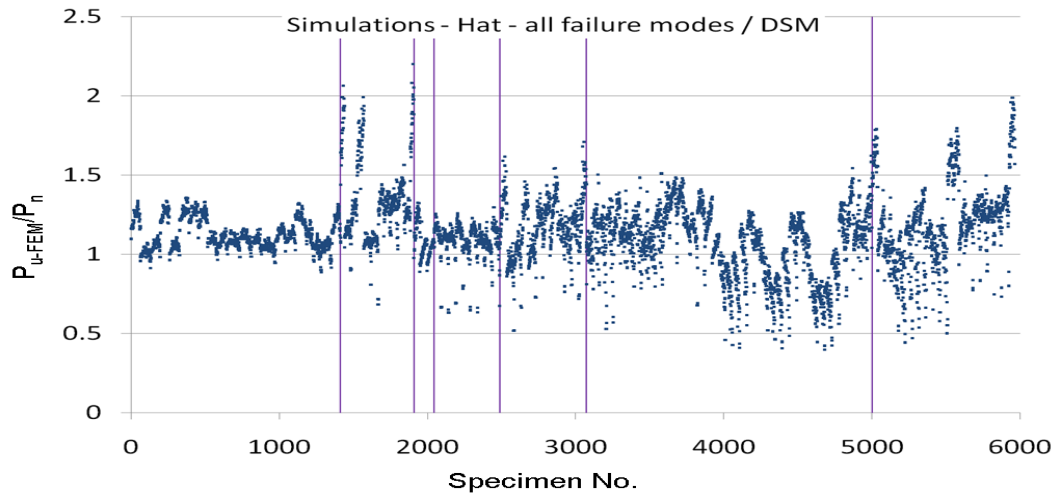
Fig. N.3: Simulation-to-predicted ratios for all Hat section columns by DSM Method 14 with classified failure modes (from left to right: L, LG, G, D, LD, DG, and LDG)
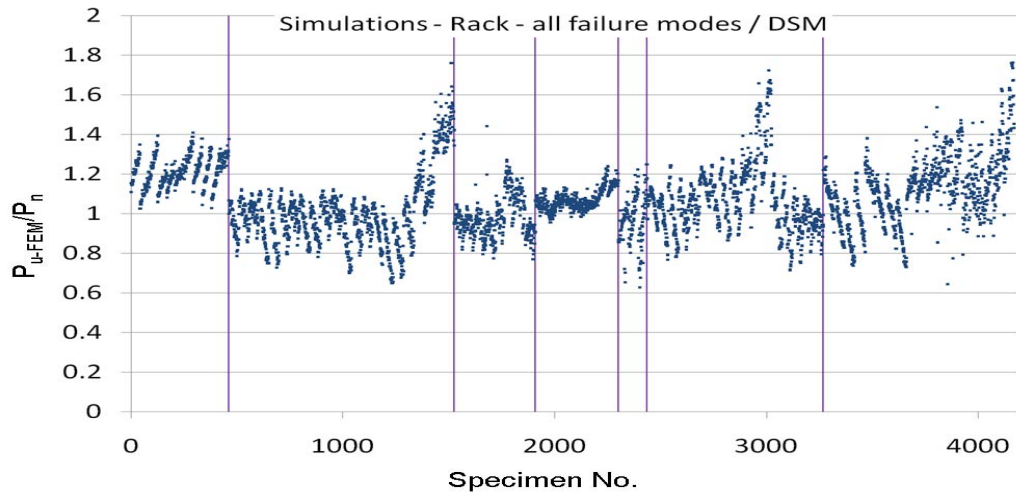
Fig. N.4: Simulation-to-predicted ratios for all Rack section columns by DSM Method 14 with classified failure modes (from left to right: L, LG, G, D, LD, DG, and LDG)
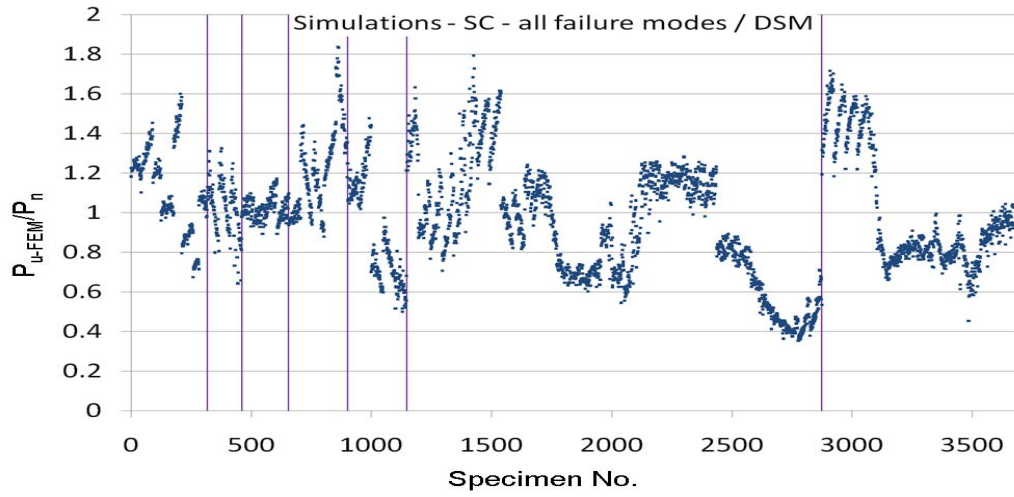
Fig. N.5: Simulation-to-predicted ratios for all Stiffened C section columns by DSM Method 14 with classified failure modes (from left to right: L, LG, G, D, LD, DG, and LDG)

<div align="center">

APPENDIX O

SIMULATION-TO-PREDICTED RATIOS BY DSM METHOD 15 – Modification 7 to Option 4 in (Moen and Schafer 2011) – minimum of (i) regression analyses of LG equation using $P_{\text{cr-1-nh}}$ and (ii) G equation

</div>

O.1   non-perforated and perforated columns
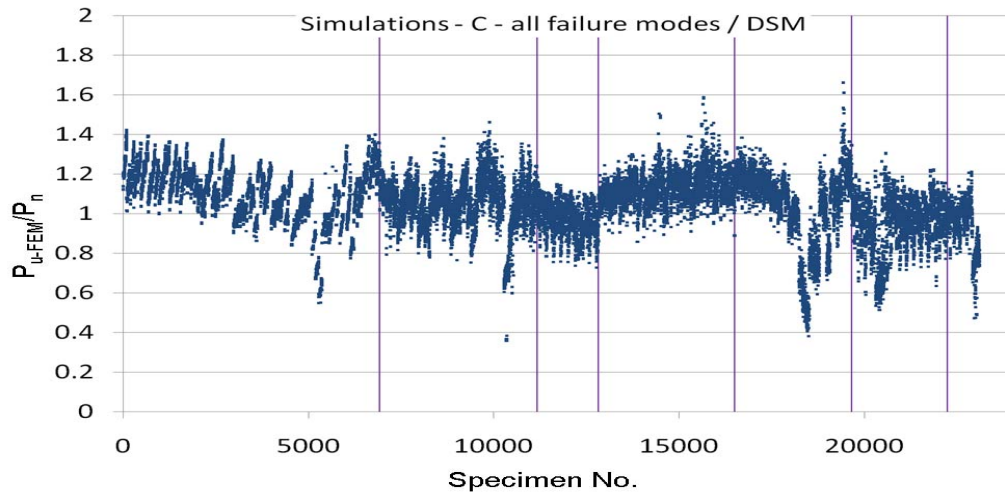
Fig. O.1: Simulation-to-predicted ratios for all C section columns by DSM Method 15 with classified failure modes (from left to right: L, LG, G, D, LD, DG, and LDG)
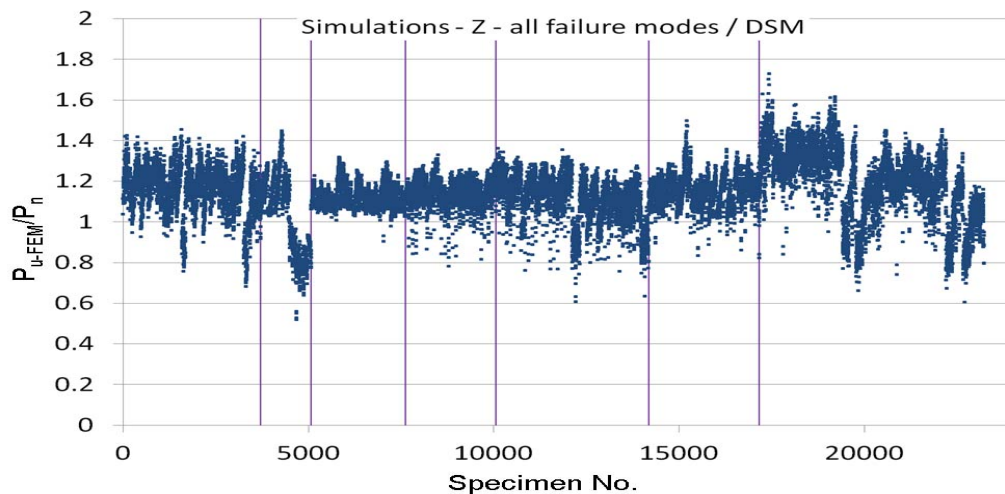

Fig. O.2: Simulation-to-predicted ratios for all Z section columns by DSM Method 15 with classified failure modes (from left to right: L, LG, G, D, LD, DG, and LDG)
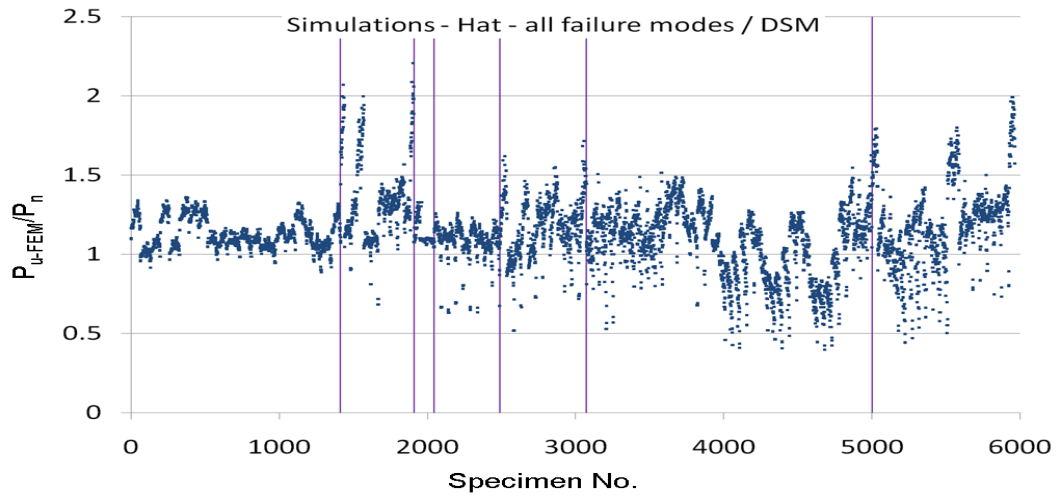
Fig. O.3: Simulation-to-predicted ratios for all Hat section columns by DSM Method 15 with classified failure modes (from left to right: L, LG, G, D, LD, DG, and LDG)
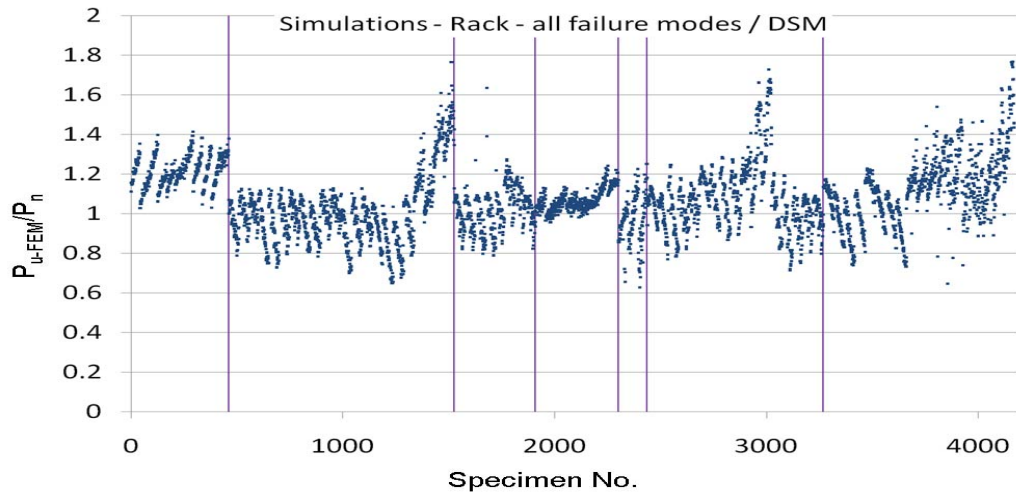
Fig. O.4: Simulation-to-predicted ratios for all Rack section columns by DSM Method 15 with classified failure modes (from left to right: L, LG, G, D, LD, DG, and LDG)
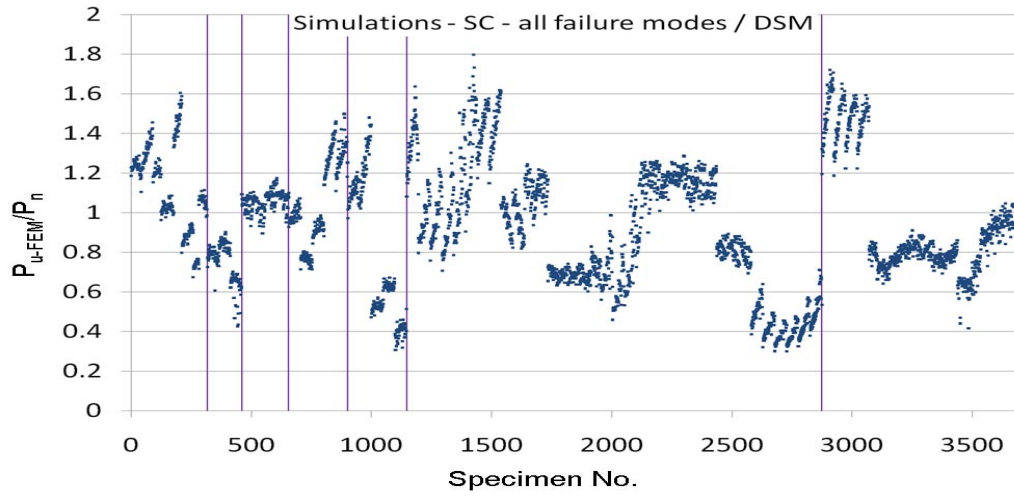
Fig. O.5: Simulation-to-predicted ratios for all Stiffened C section columns by DSM Method 15 with classified failure modes (from left to right: L, LG, G, D, LD, DG, and LDG)

APPENDIX P

SIMULATION-TO-PREDICTED RATIOS BY DSM METHOD 16 – Modification 8 to Option 4 in (Moen and Schafer 2011) – use $P_{cr-l-nh}$ and $P_{cr-d-nh}$, factor final strengths

P.1 non-perforated and perforated columns
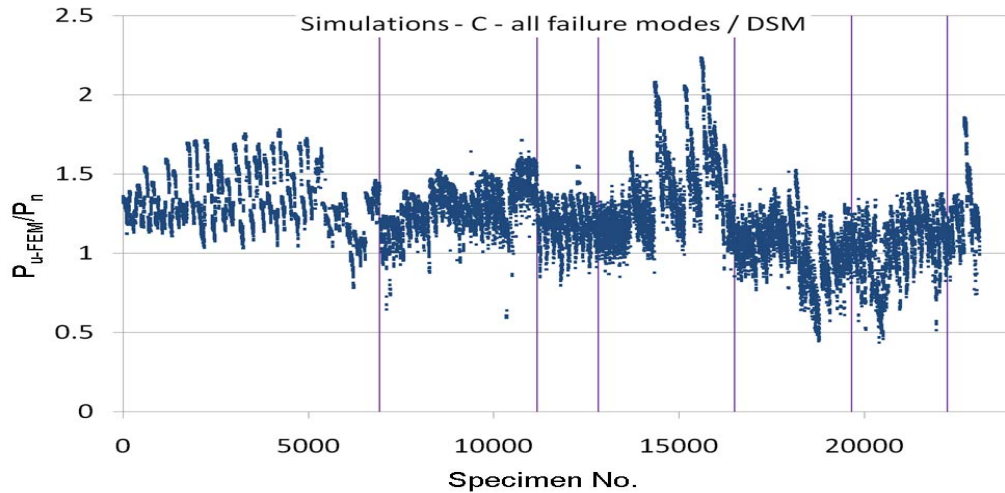
Fig. P.1: Simulation-to-predicted ratios for all C section columns by DSM Method 16 with classified failure modes (from left to right: L, LG, G, D, LD, DG, and LDG)
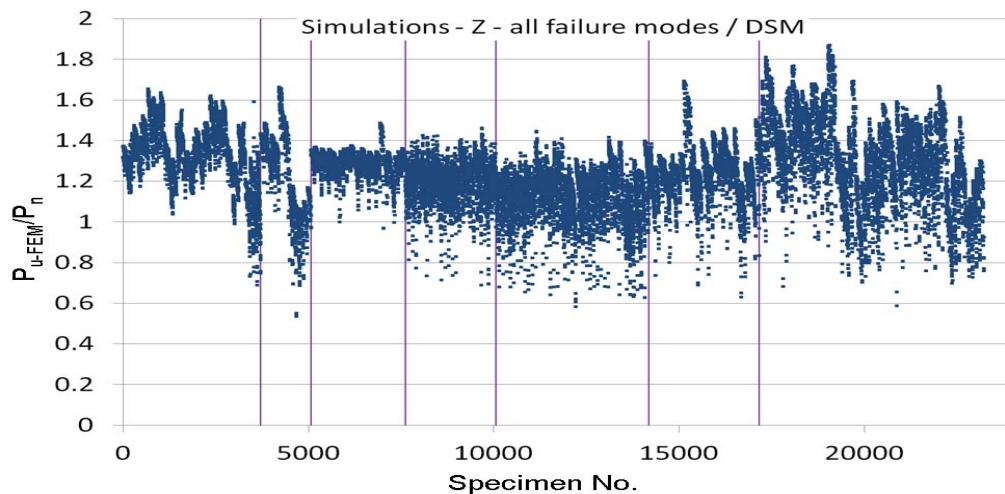

Fig. P.2: Simulation-to-predicted ratios for all Z section columns by DSM Method 16 with classified failure modes (from left to right: L, LG, G, D, LD, DG, and LDG)
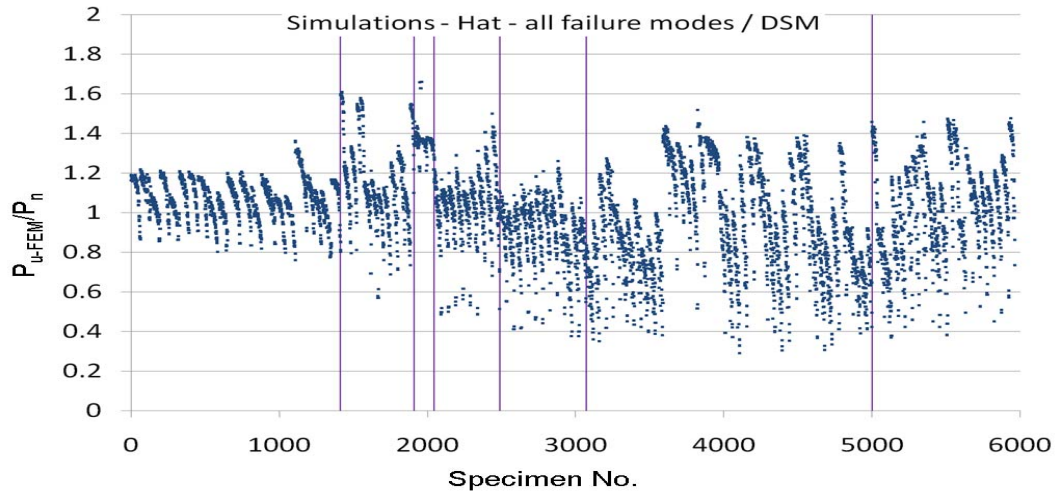
Fig. P.3: Simulation-to-predicted ratios for all Hat section columns by DSM Method 16 with classified failure modes (from left to right: L, LG, G, D, LD, DG, and LDG)
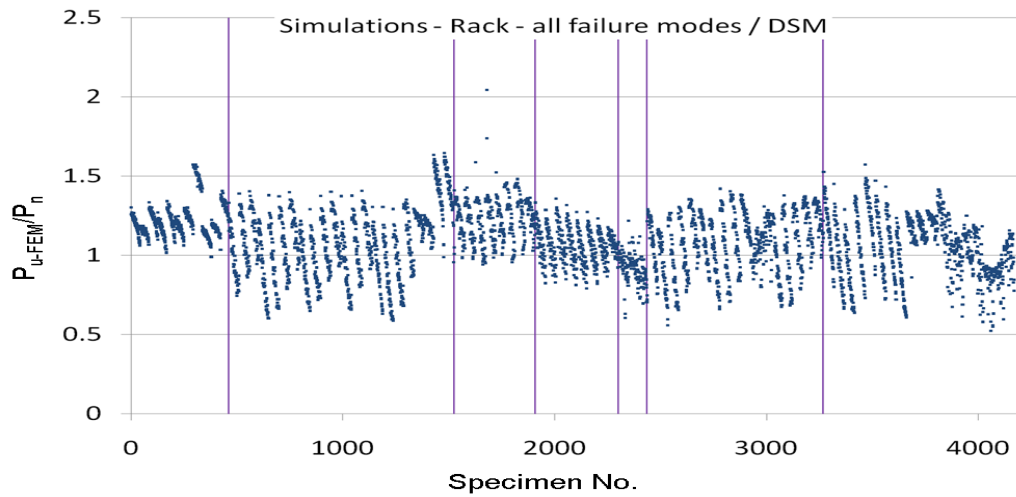
Fig. P.4: Simulation-to-predicted ratios for all Rack section columns by DSM Method 16 with classified failure modes (from left to right: L, LG, G, D, LD, DG, and LDG)
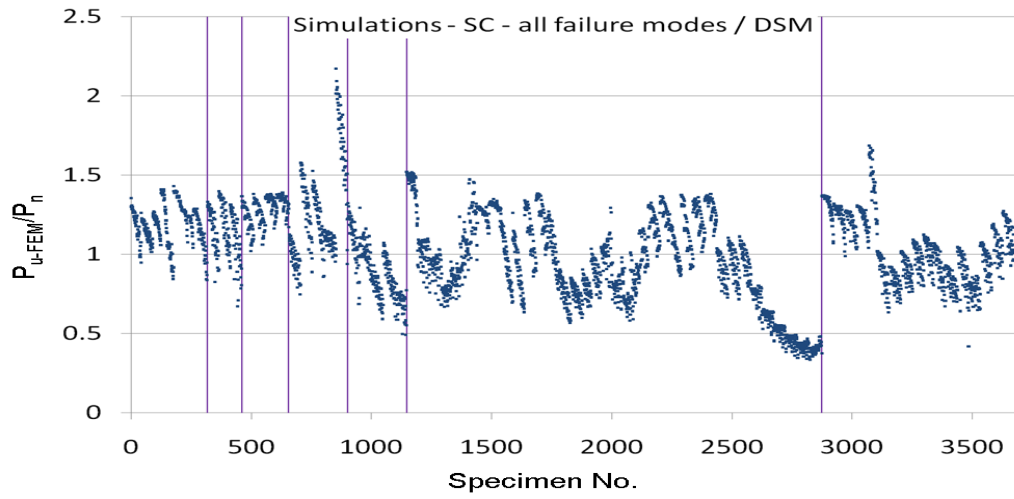
Fig. P.5: Simulation-to-predicted ratios for all Stiffened C section columns by DSM Method 16 with classified failure modes (from left to right: L, LG, G, D, LD, DG, and LDG)

APPENDIX Q

SIMULATION-TO-PREDICTED RATIOS BY DSM METHOD 17 – Modification 9 to Option 4 in (Moen and Schafer 2011) – use $P_{cr\text{-}l\text{-}nh}$ and $P_{cr\text{-}d\text{-}nh}$, regression analyses of final strengths

Q.1   non-perforated and perforated columns
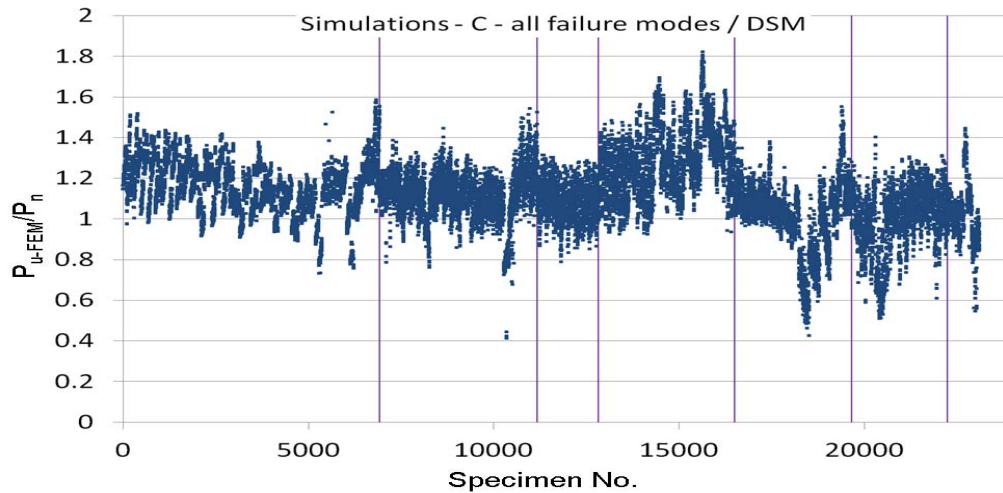
Fig. Q.1: Simulation-to-predicted ratios for all C section columns by DSM Method 17 with classified failure modes (from left to right: L, LG, G, D, LD, DG, and LDG)
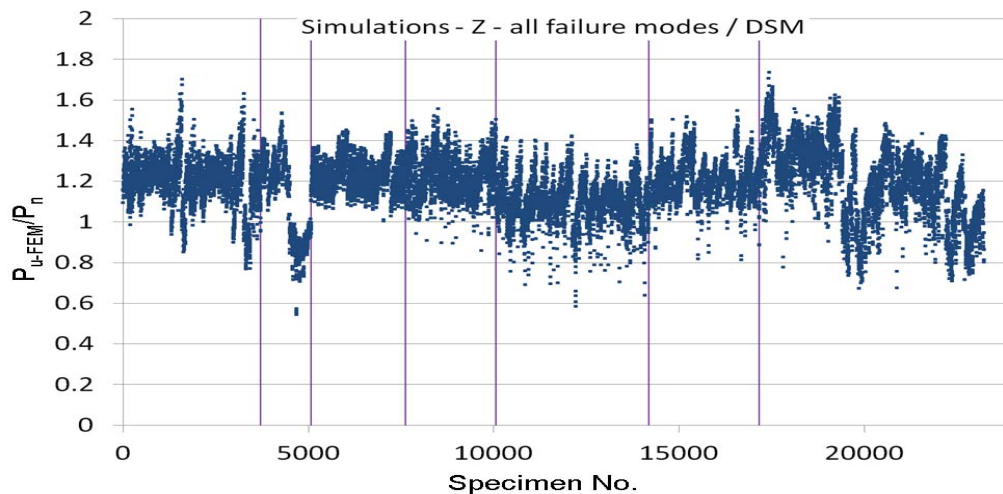

Fig. Q.2: Simulation-to-predicted ratios for all Z section columns by DSM Method 17 with classified failure modes (from left to right: L, LG, G, D, LD, DG, and LDG)
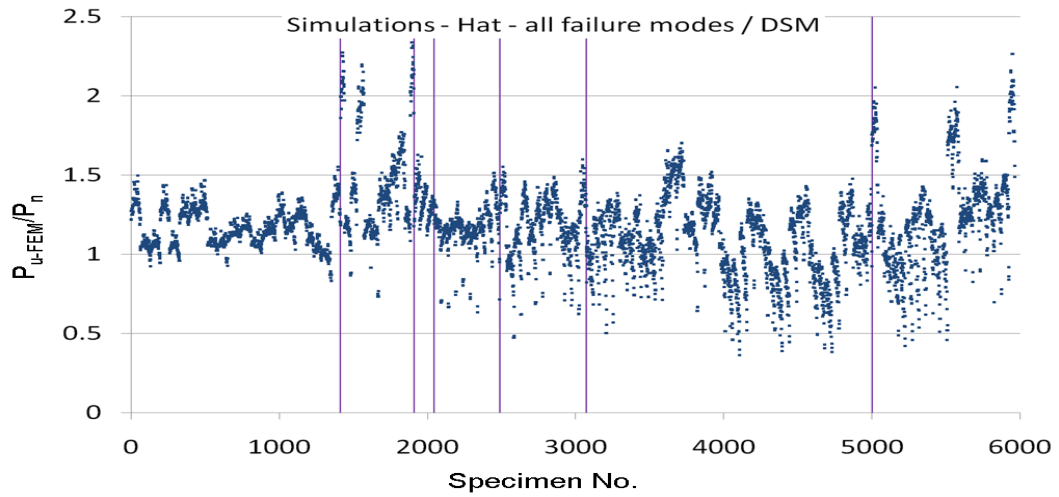
Fig. Q.3: Simulation-to-predicted ratios for all Hat section columns by DSM Method 17 with classified failure modes (from left to right: L, LG, G, D, LD, DG, and LDG)
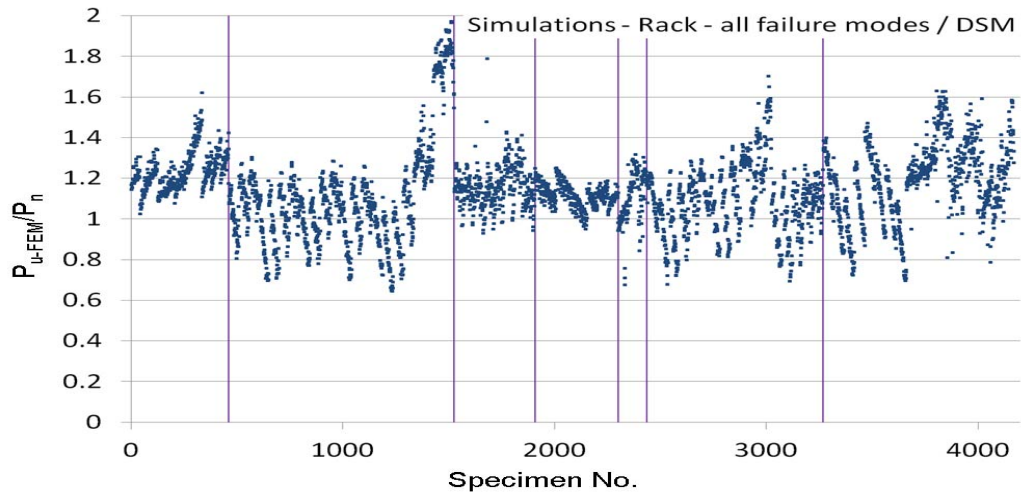
Fig. Q.4: Simulation-to-predicted ratios for all Rack section columns by DSM Method 17 with classified failure modes (from left to right: L, LG, G, D, LD, DG, and LDG)
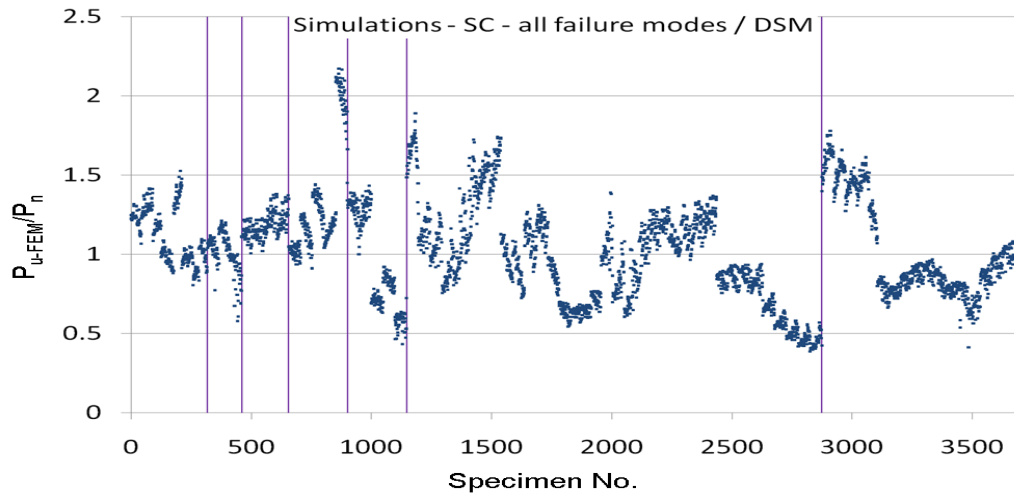
Fig. Q.5: Simulation-to-predicted ratios for all Stiffened C section columns by DSM Method 17 with classified failure modes (from left to right: L, LG, G, D, LD, DG, and LDG)

Q.2 non-perforated and perforated stiffened C section columns with separate regression parameters
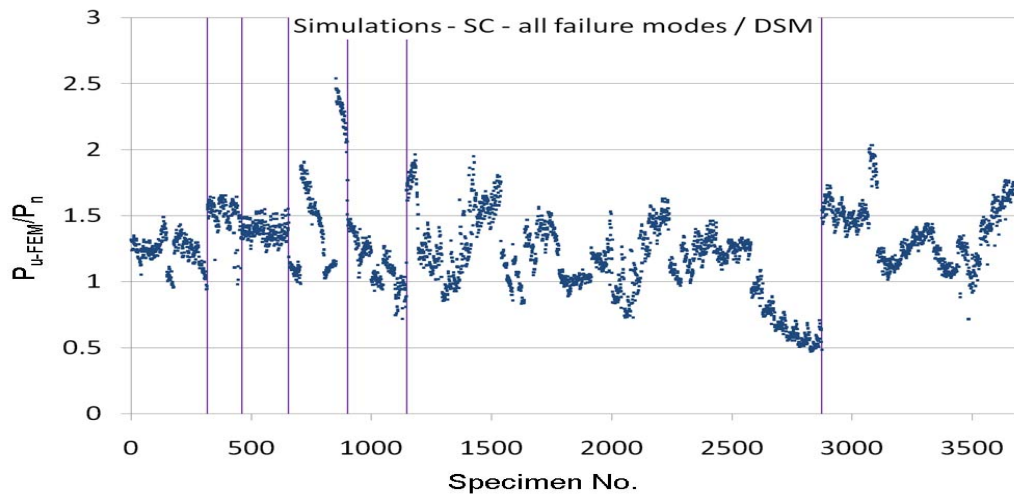
Fig. Q.6: Simulation-to-predicted ratios for all Stiffened C section columns by DSM Method 17 by separate regression parameters with classified failure modes (from left to right: L, LG, G, D, LD, DG, and LDG)

APPENDIX R

SIMULATION-TO-PREDICTED RATIOS BY DSM METHOD 18 – Modification 10 to Option 4 in (Moen and Schafer 2011) – replace D equation by DG interaction equation, use $P_{cr-\ell-nh}$ and $P_{cr-d-nh}$, factor final strengths

R.1   non-perforated and perforated columns, not factor final strengths
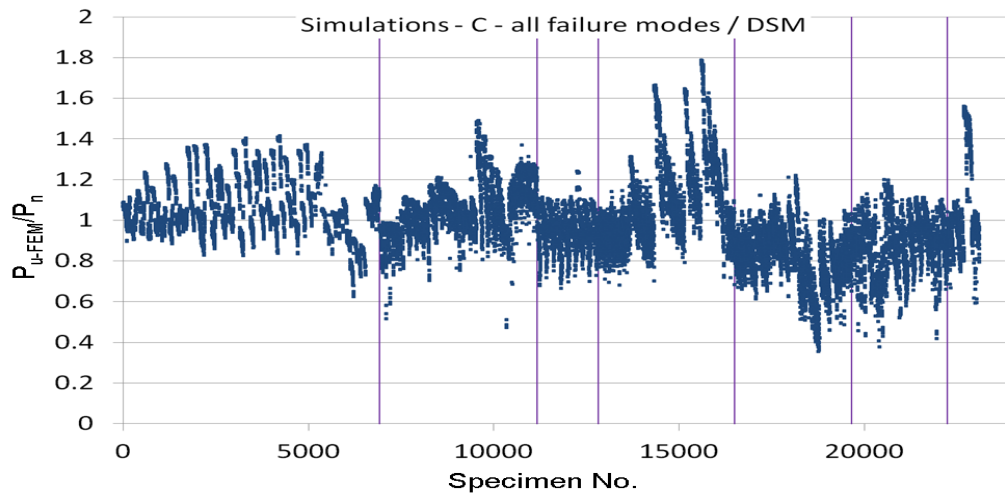
Fig. R.1: Simulation-to-predicted ratios for all C section columns by DSM Method 18 with classified failure modes (from left to right: L, LG, G, D, LD, DG, and LDG)
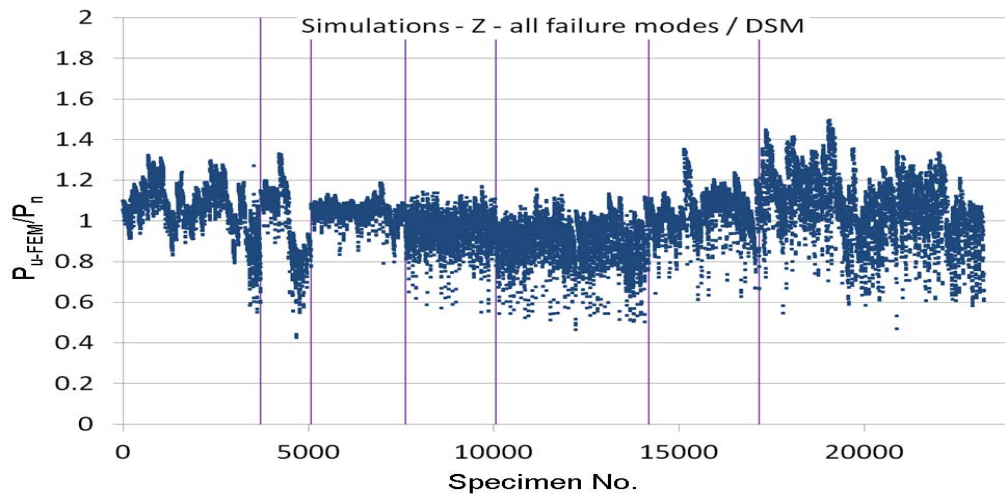
Fig. R.2: Simulation-to-predicted ratios for all Z section columns by DSM Method 18 with classified failure modes (from left to right: L, LG, G, D, LD, DG, and LDG)
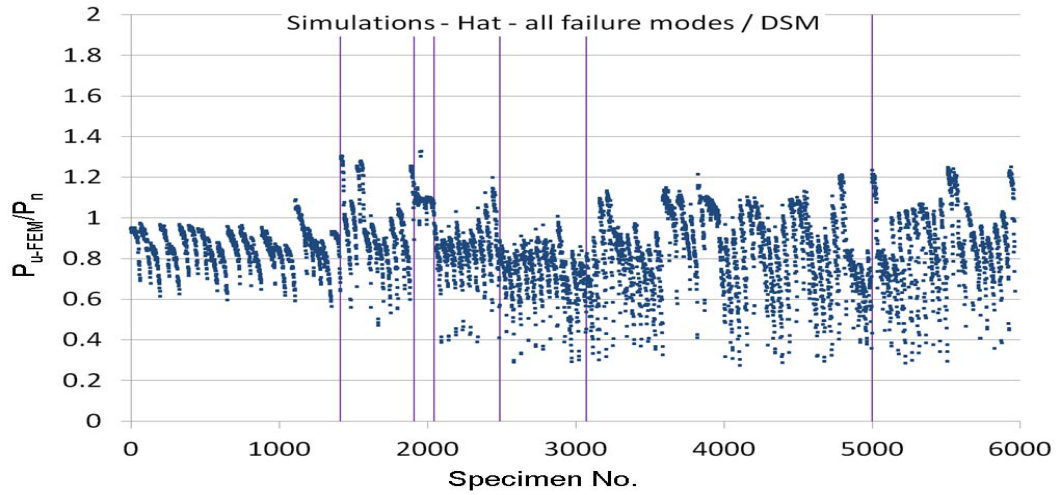
Fig. R.3: Simulation-to-predicted ratios for all Hat section columns by DSM Method 18 with classified
failure modes (from left to right: L, LG, G, D, LD, DG, and LDG)
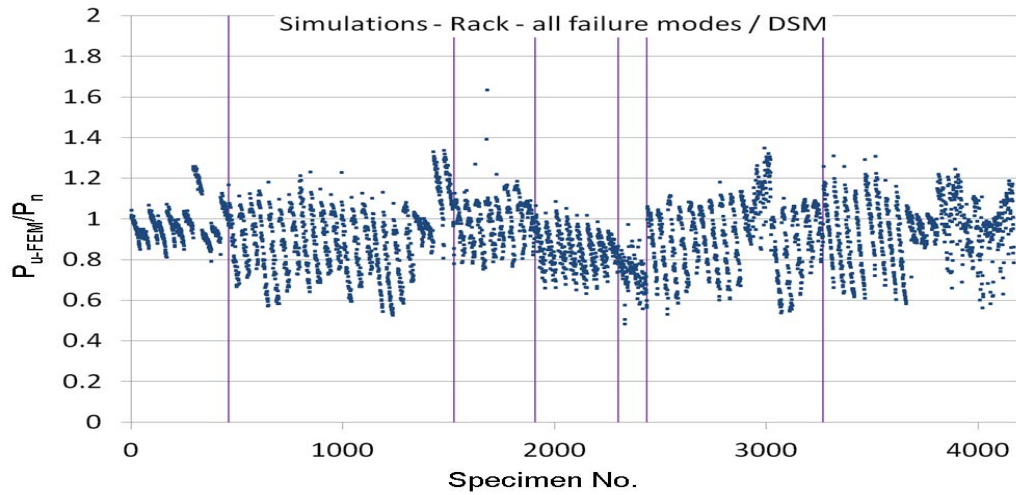
Fig. R.4: Simulation-to-predicted ratios for all Rack section columns by DSM Method 18 with classified
failure modes (from left to right: L, LG, G, D, LD, DG, and LDG)
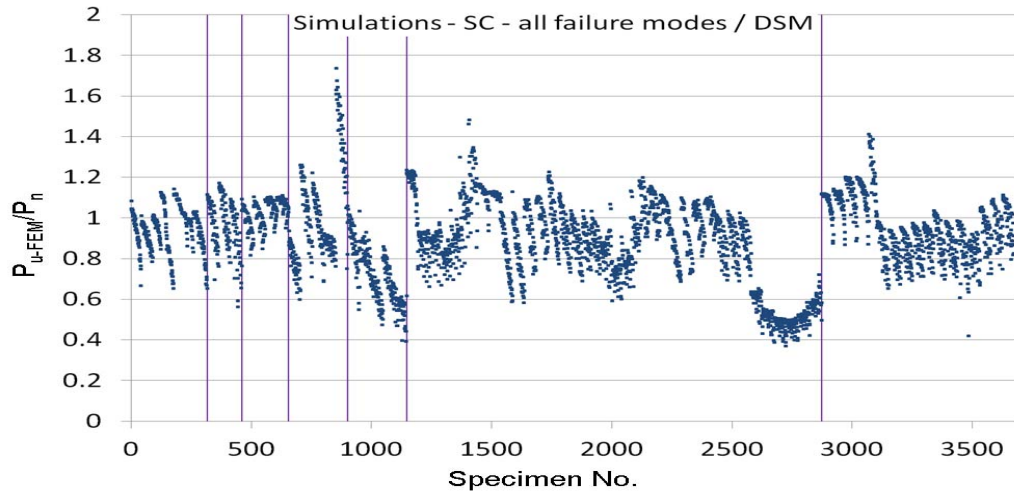
Fig. R.5: Simulation-to-predicted ratios for all Stiffened C section columns by DSM Method 18 with classified failure modes (from left to right: L, LG, G, D, LD, DG, and LDG)

R.2 non-perforated and perforated columns, factor final strengths by 0.85
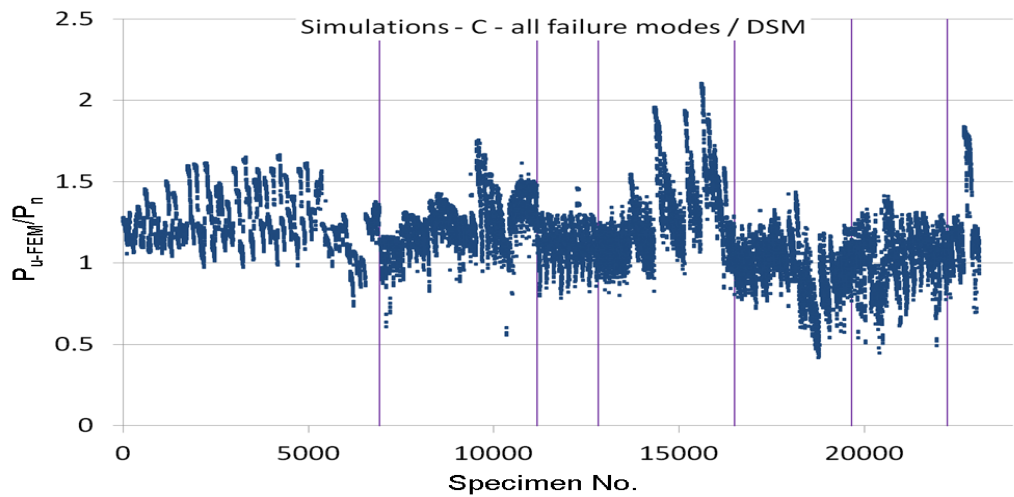
Fig. R.6: Simulation-to-predicted ratios for all C section columns by DSM Method 18 with classified failure modes (from left to right: L, LG, G, D, LD, DG, and LDG
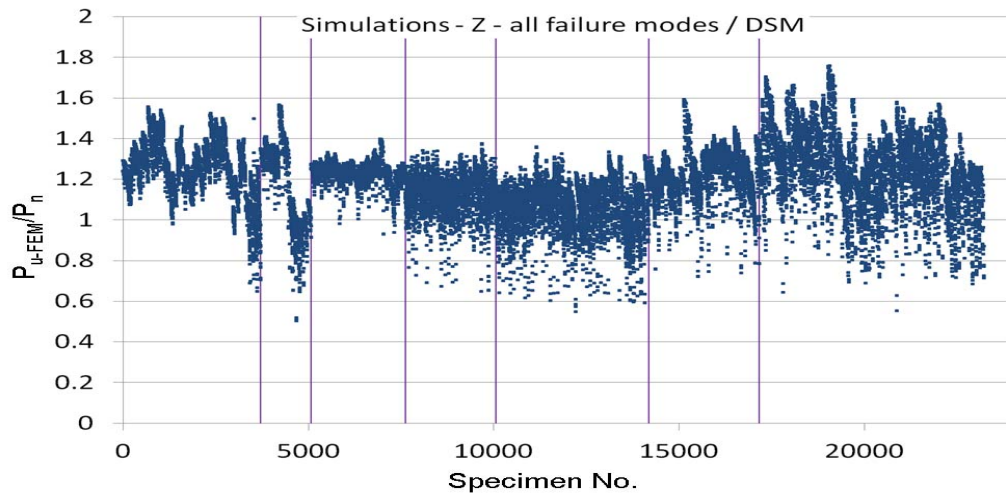
Fig. R.7: Simulation-to-predicted ratios for all Z section columns by DSM Method 18 with classified failure modes (from left to right: L, LG, G, D, LD, DG, and LDG)
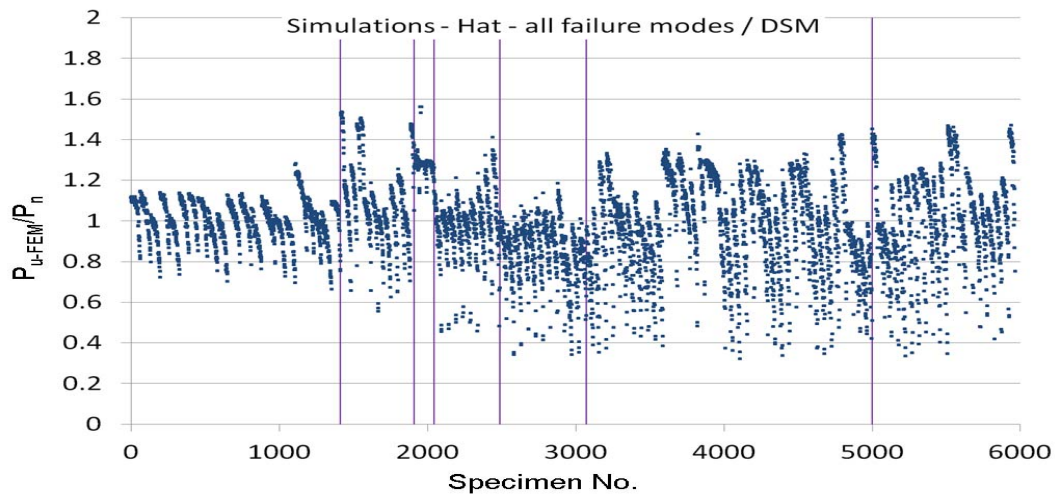

Fig. R.8: Simulation-to-predicted ratios for all Hat section columns by DSM Method 18 with classified failure modes (from left to right: L, LG, G, D, LD, DG, and LDG)
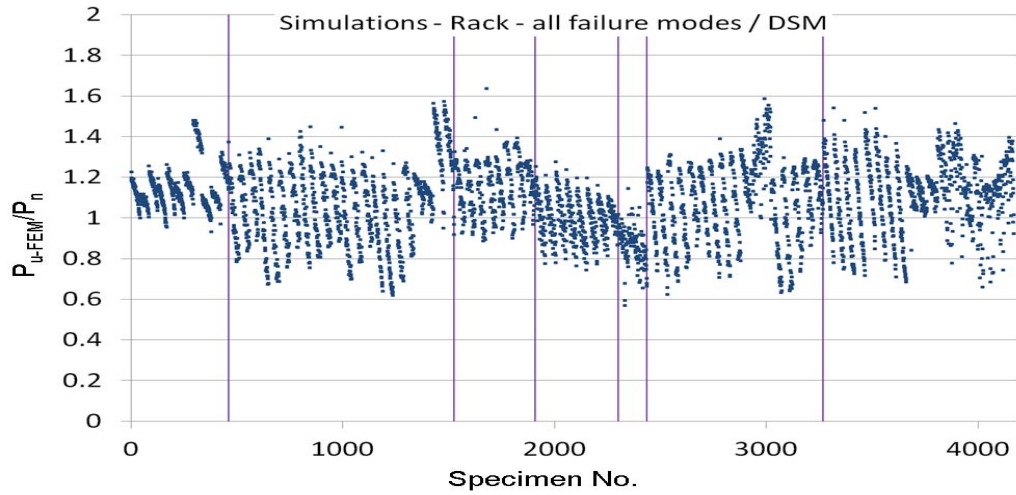
Fig. R.9: Simulation-to-predicted ratios for all Rack section columns by DSM Method 18 with classified failure modes (from left to right: L, LG, G, D, LD, DG, and LDG)
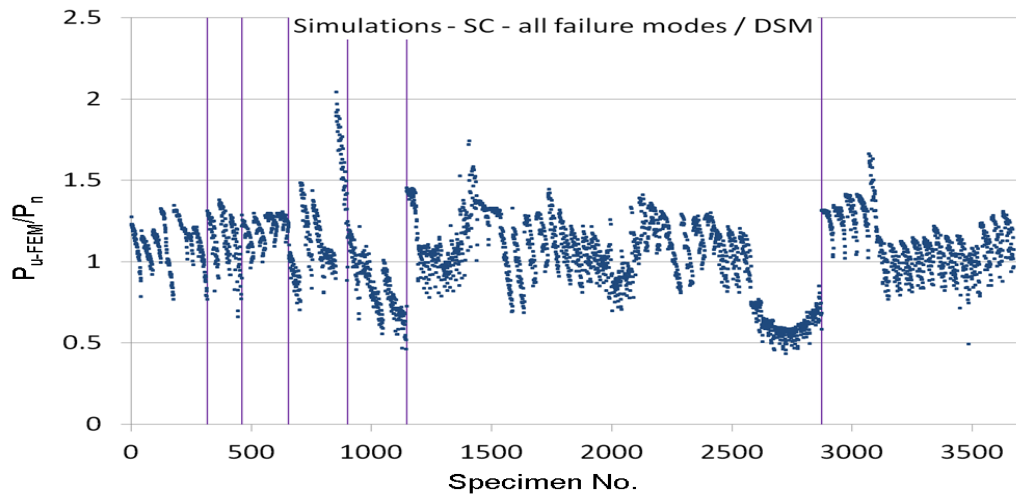
Fig. R.10: Simulation-to-predicted ratios for all Stiffened C section columns by DSM Method 18 with classified failure modes (from left to right: L, LG, G, D, LD, DG, and LDG)

**APPENDIX S**

SIMULATION-TO-PREDICTED RATIOS BY DSM METHOD 19 – Modification 11 to Option 4 in (Moen and Schafer 2011) – replace D equation by DG interaction equation, use $P_{cr-1-nh}$ and $P_{cr-d-nh}$, regression analyses of final strengths

S.1   non-perforated and perforated columns
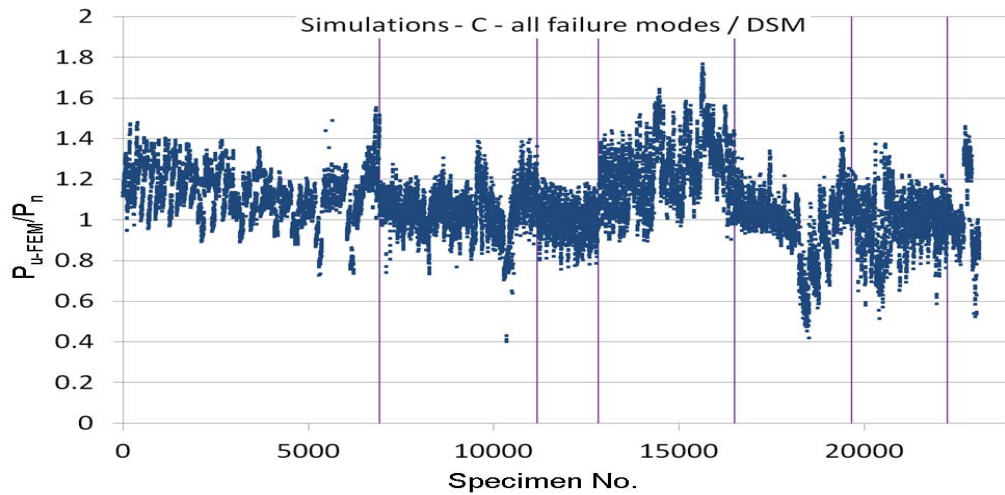
Fig. S.1: Simulation-to-predicted ratios for all C section columns by DSM Method 19 with classified failure modes (from left to right: L, LG, G, D, LD, DG, and LDG)
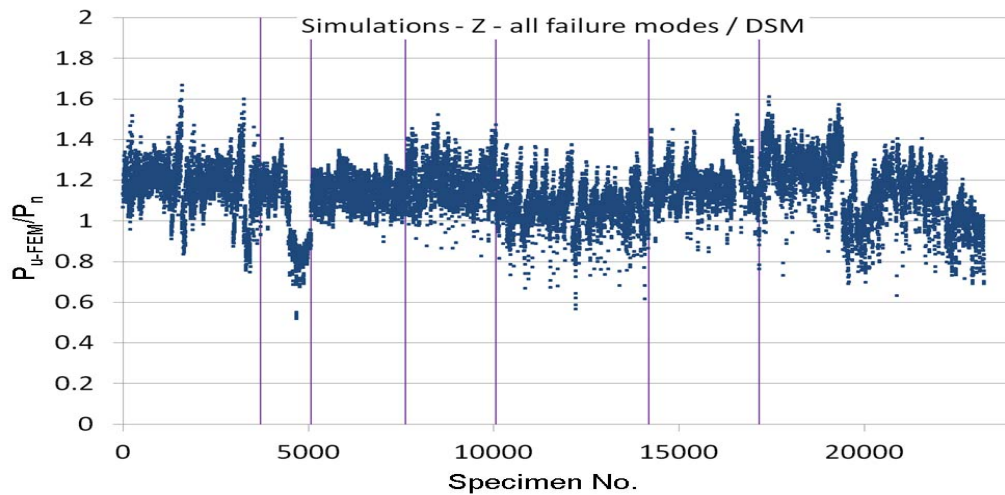

Fig. S.2: Simulation-to-predicted ratios for all Z section columns by DSM Method 19 with classified failure modes (from left to right: L, LG, G, D, LD, DG, and LDG)
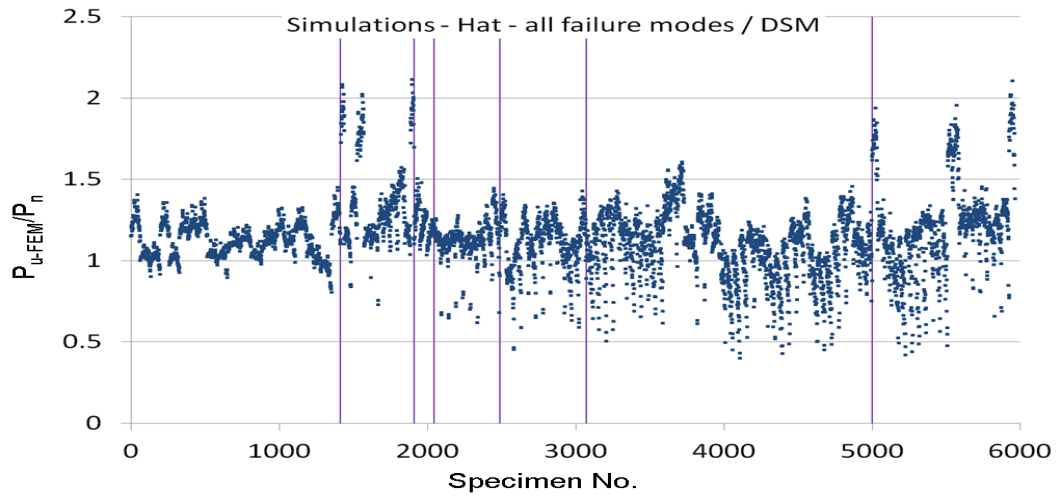
Fig. S.3: Simulation-to-predicted ratios for all Hat section columns by DSM Method 19 with classified

failure modes (from left to right: L, LG, G, D, LD, DG, and LDG)
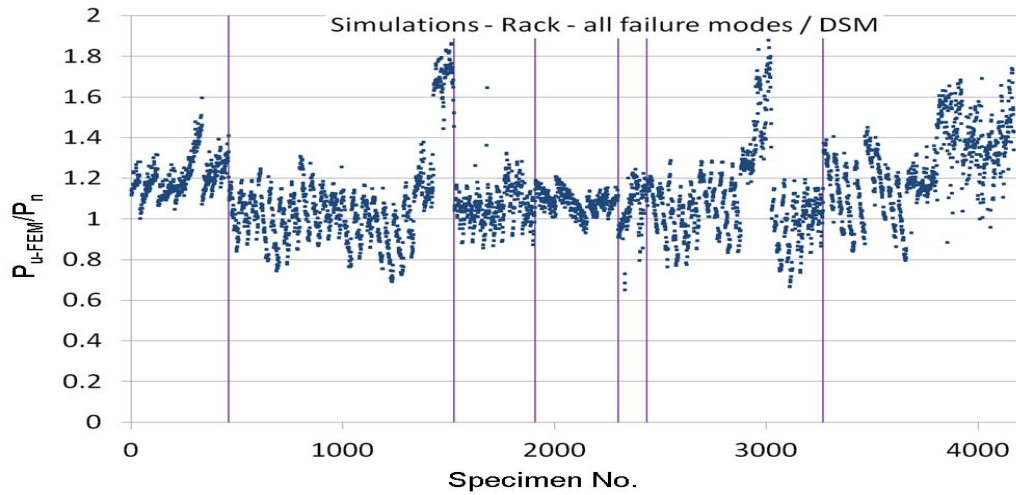
Fig. S.4: Simulation-to-predicted ratios for all Rack section columns by DSM Method 19 with classified

failure modes (from left to right: L, LG, G, D, LD, DG, and LDG)
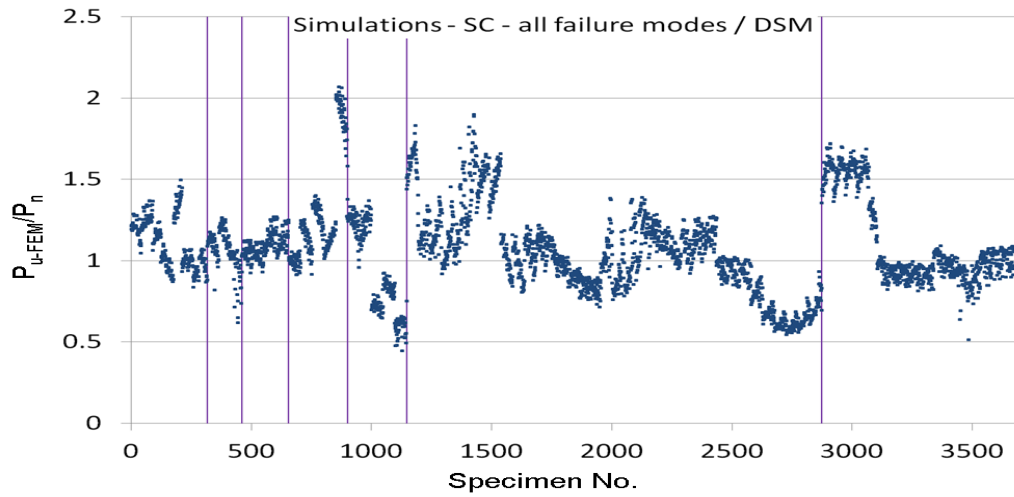
Fig. S.5: Simulation-to-predicted ratios for all Stiffened C section columns by DSM Method 19 with classified failure modes (from left to right: L, LG, G, D, LD, DG, and LDG)

S.2 non-perforated and perforated stiffened C section columns with separate regression parameters
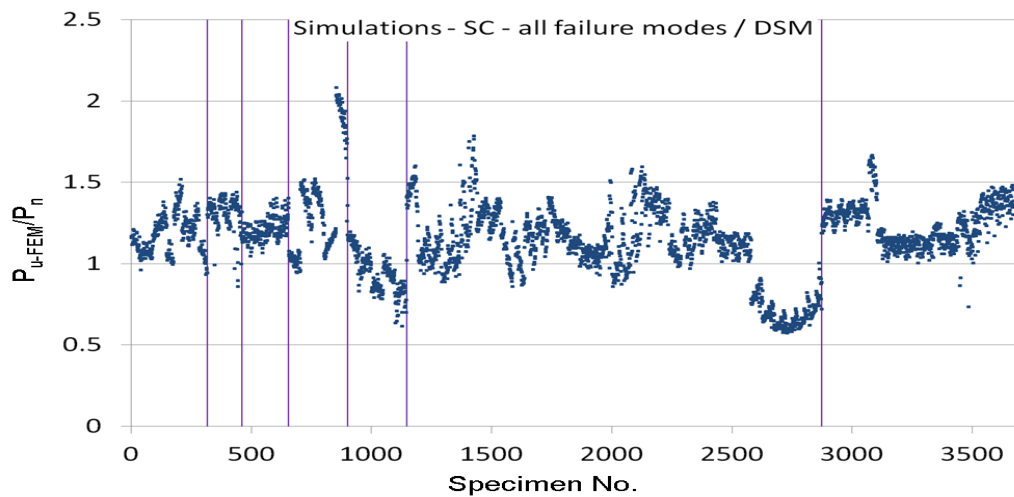
Fig. S.6: Simulation-to-predicted ratios for all Stiffened C section columns by DSM Method 19 by separate regression parameters with classified failure modes (from left to right: L, LG, G, D, LD, DG, and LDG)

S.3 non-perforated columns
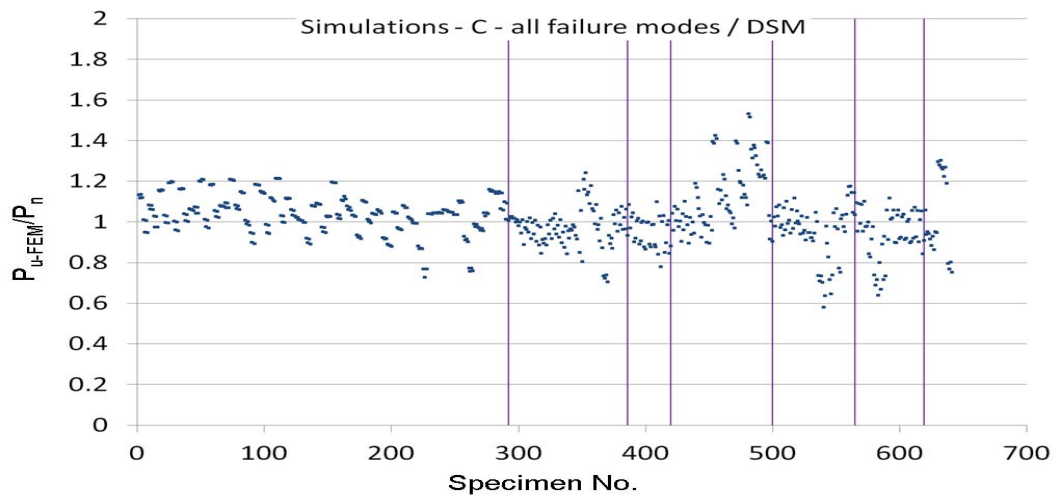
Fig. S.7: Simulation-to-predicted ratios for non-perforated C section columns by DSM Method 19 with classified failure modes (from left to right: L, LG, G, D, LD, DG, and LDG)
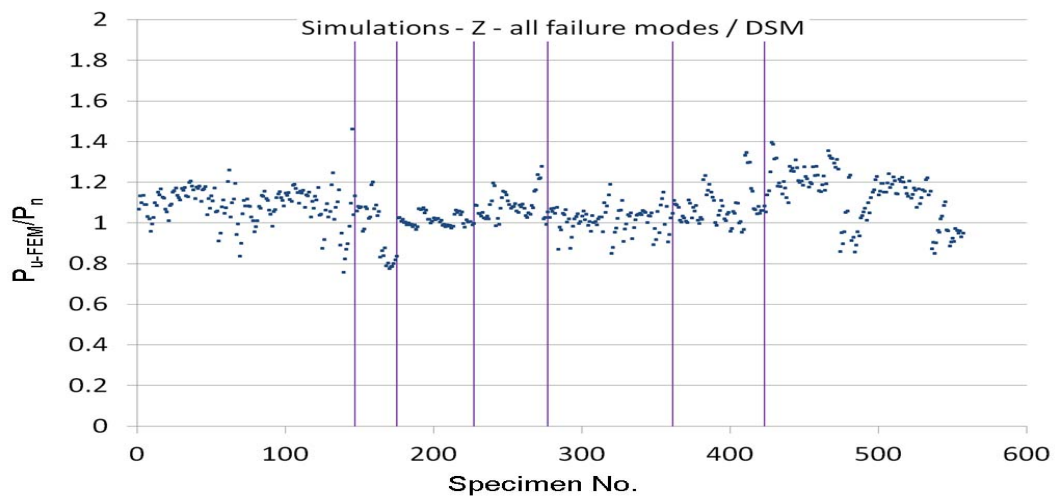
Fig. S.8: Simulation-to-predicted ratios for non-perforated Z section columns by DSM Method 19 with classified failure modes (from left to right: L, LG, G, D, LD, DG, and LDG)
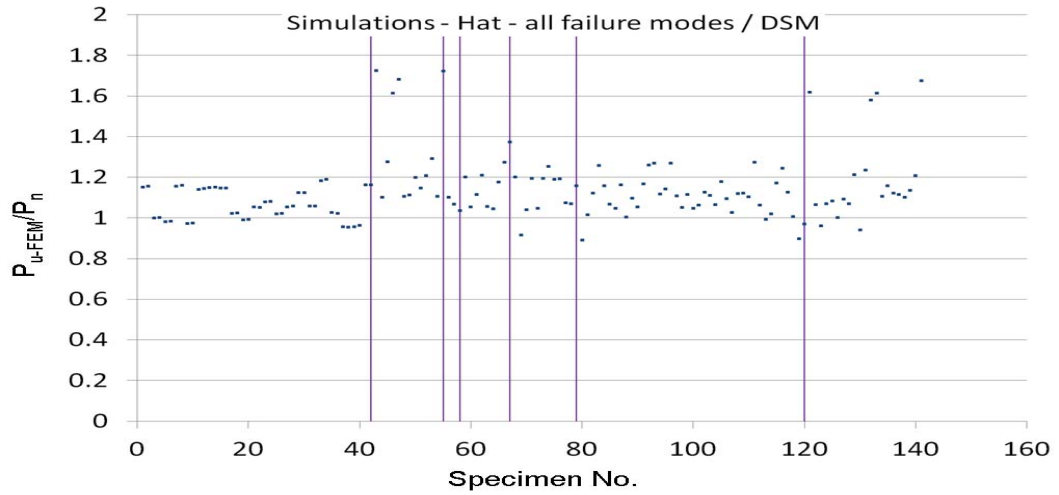
Fig. S.9: Simulation-to-predicted ratios for non-perforated Hat section columns by DSM Method 19 with classified failure modes (from left to right: L, LG, G, D, LD, DG, and LDG)
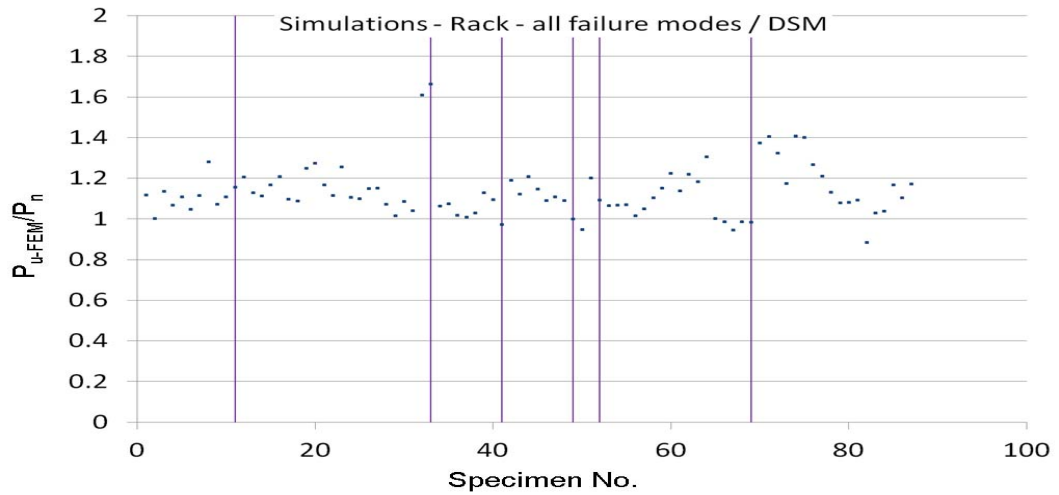
Fig. S.10: Simulation-to-predicted ratios for non-perforated Rack section columns by DSM Method 19 with classified failure modes (from left to right: L, LG, G, D, LD, DG, and LDG)
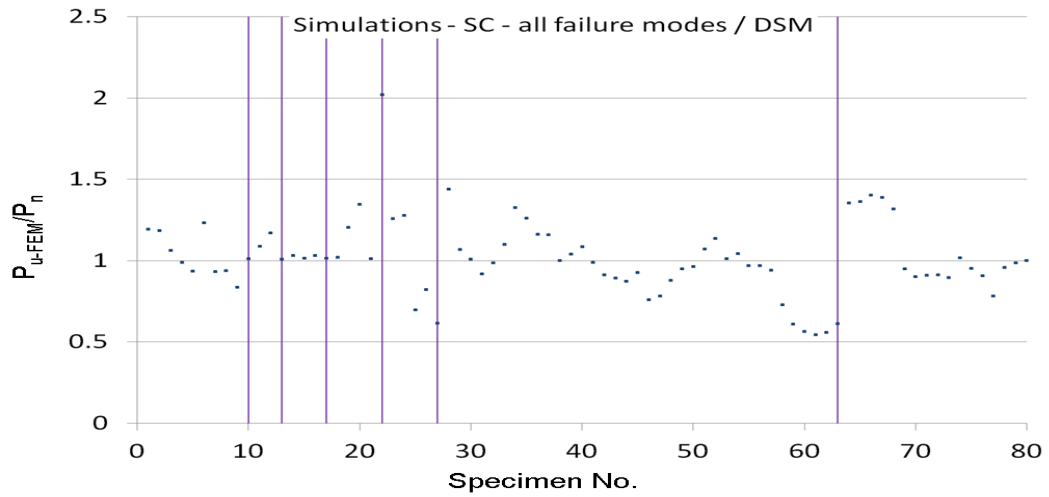
Fig. S.11: Simulation-to-predicted ratios for non-perforated Stiffened C section columns by DSM Method 19 with classified failure modes (from left to right: L, LG, G, D, LD, DG, and LDG)

S.4   non-perforated stiffened C section columns with separate regression parameters
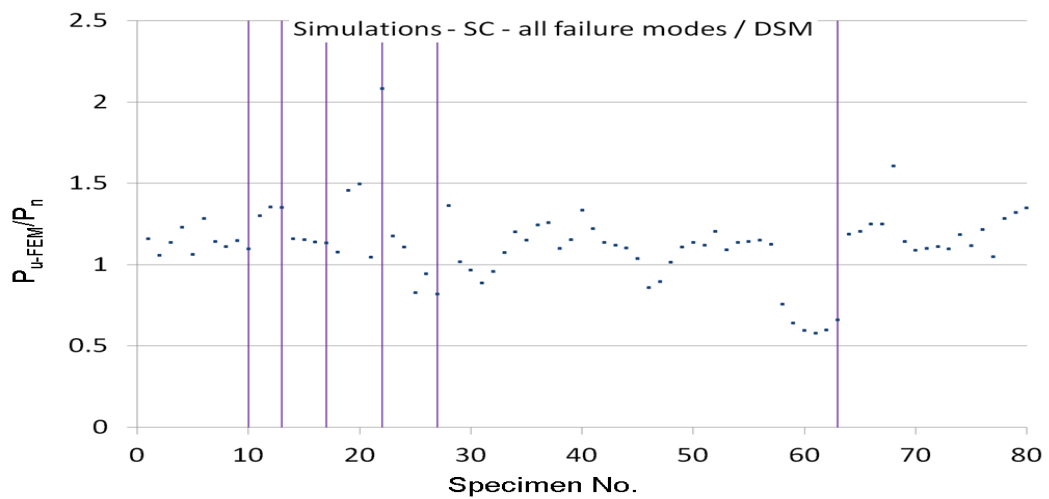
Fig. S.12: Simulation-to-predicted ratios for non-perforated Stiffened C section columns by DSM Method 19 by separate regression parameters with classified failure modes (from left to right: L, LG, G, D, LD, DG, and LDG)

APPENDIX T

Highlights of large discrepancies in the simulation-to-predicted ratios by DSM Method 19

## T.1   non-perforated columns
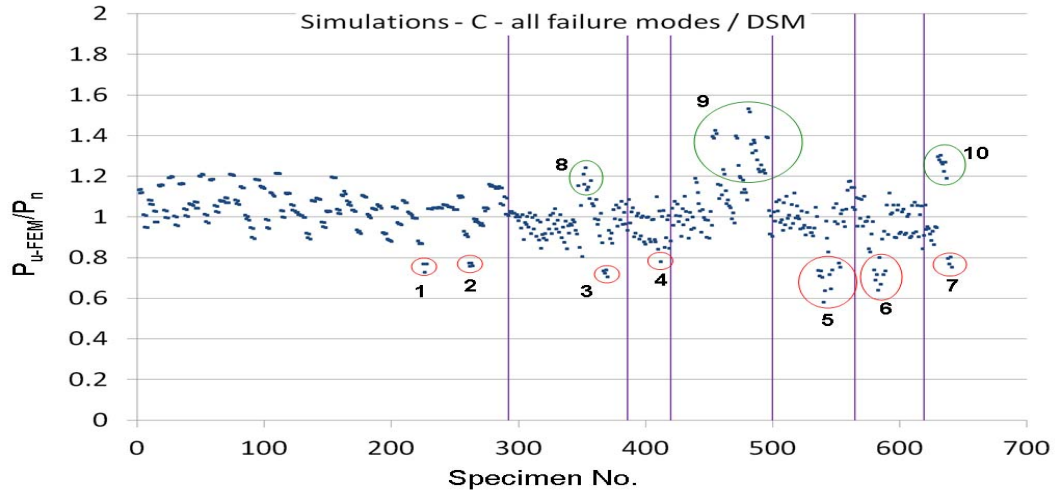
Fig. T.1: Highlight of large discrepancies in the simulation-to-predicted ratios for non-perforated C section columns by DSM Method 19 with classified failure modes (from left to right: L, LG, G, D, LD, DG, and LDG)
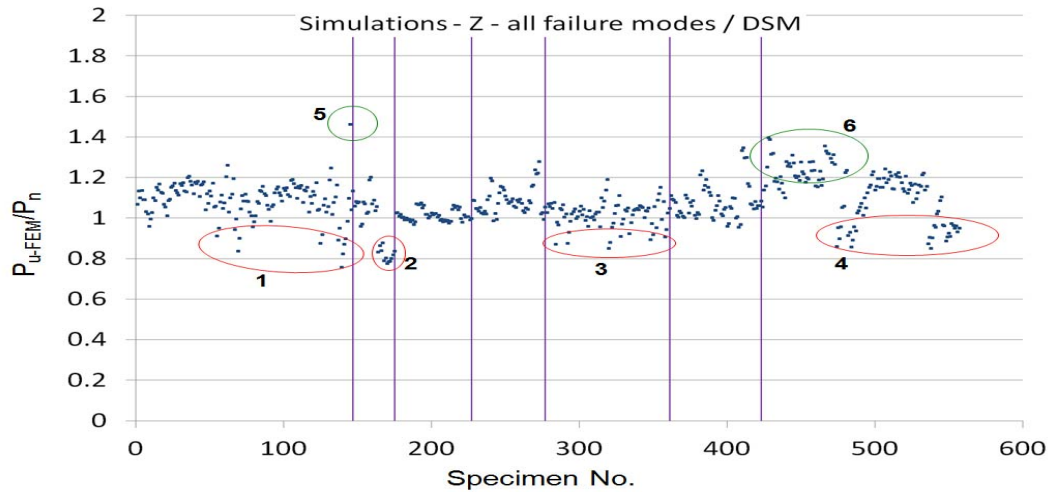

Fig. T.2: Highlight of large discrepancies in the simulation-to-predicted ratios for non-perforated Z section columns by DSM Method 19 with classified failure modes (from left to right: L, LG, G, D, LD, DG, and LDG)
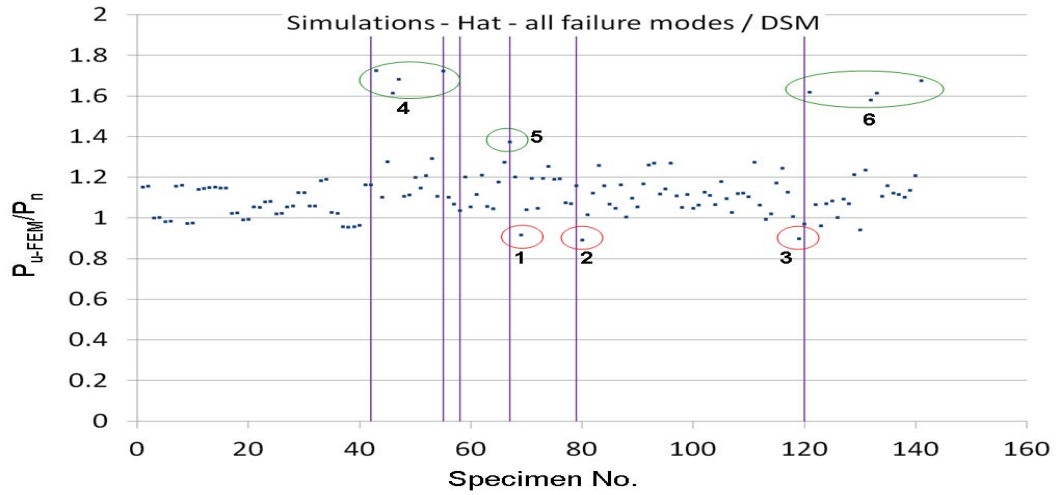
Fig. T.3: Highlight of large discrepancies in the simulation-to-predicted ratios for non-perforated Hat section columns by DSM Method 19 with classified failure modes (from left to right: L, LG, G, D, LD, DG, and LDG)
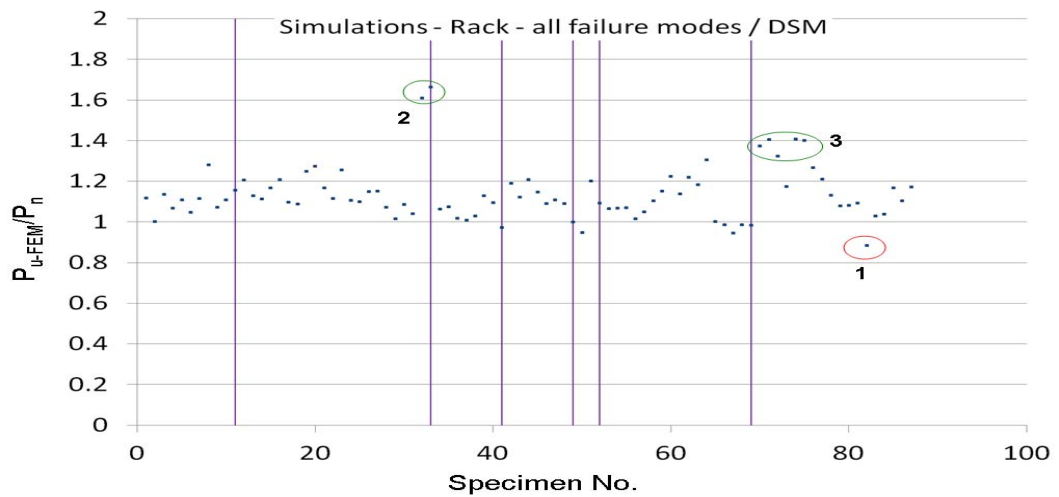
Fig. T.4: Highlight of large discrepancies in the simulation-to-predicted ratios for non-perforated Rack section columns by DSM Method 19 with classified failure modes (from left to right: L, LG, G, D, LD, DG, and LDG)
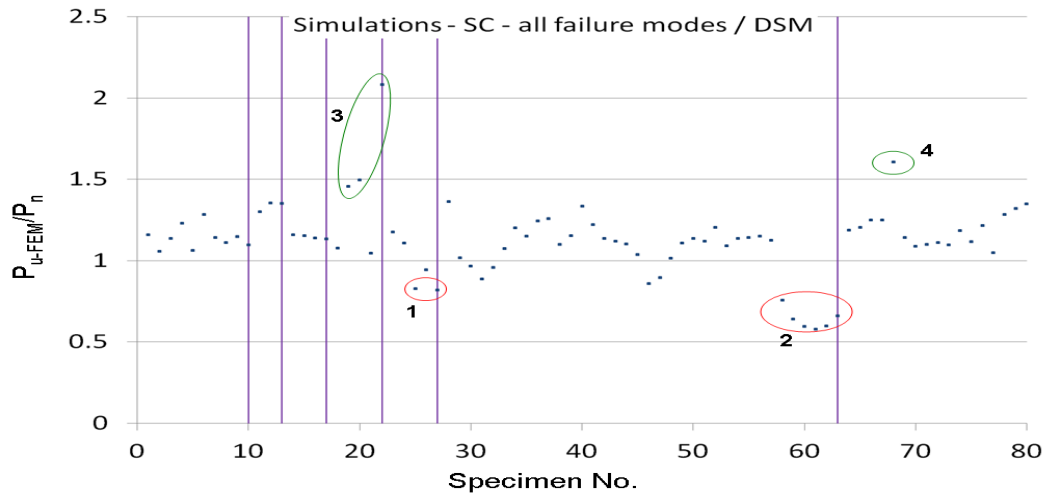
Fig. T.5: Highlight of large discrepancies in the simulation-to-predicted ratios for non-perforated Stiffened C section columns by DSM Method 19 (with separate regression constants) with classified failure modes (from left to right: L, LG, G, D, LD, DG, and LDG)

T.2   non-perforated and perforated columns
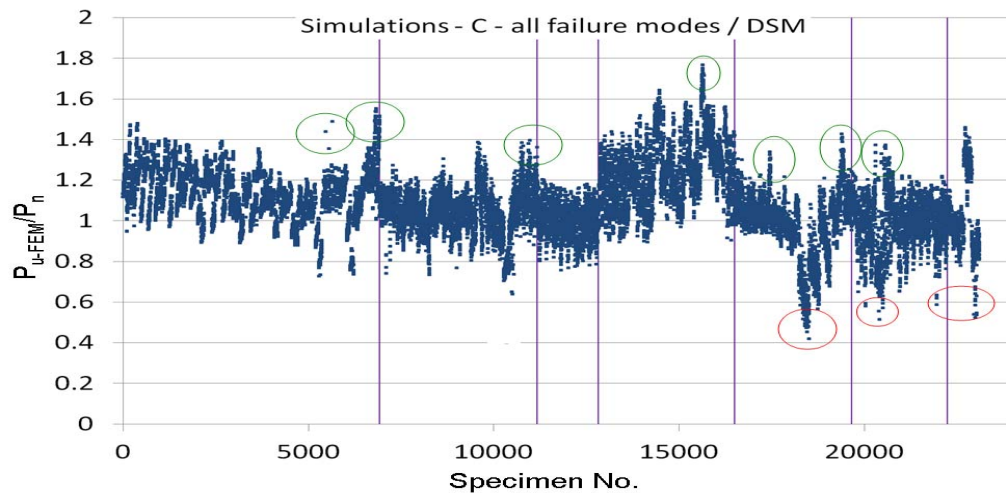
Fig. T.6: Highlight of large discrepancies in the simulation-to-predicted ratios for all C section columns by DSM Method 19 with classified failure modes (from left to right: L, LG, G, D, LD, DG, and LDG)
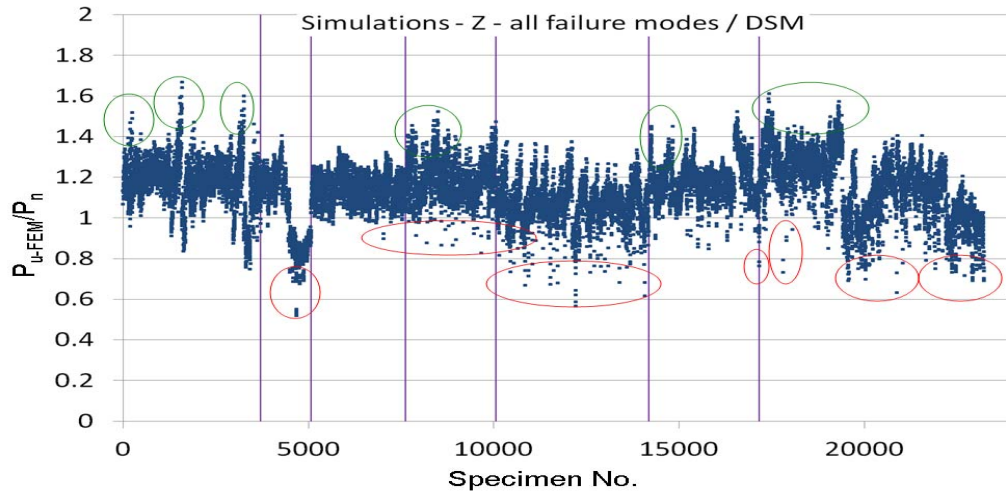
Fig. T.7: Highlight of large discrepancies in the simulation-to-predicted ratios for all Z section columns by DSM Method 19 with classified failure modes (from left to right: L, LG, G, D, LD, DG, and LDG)
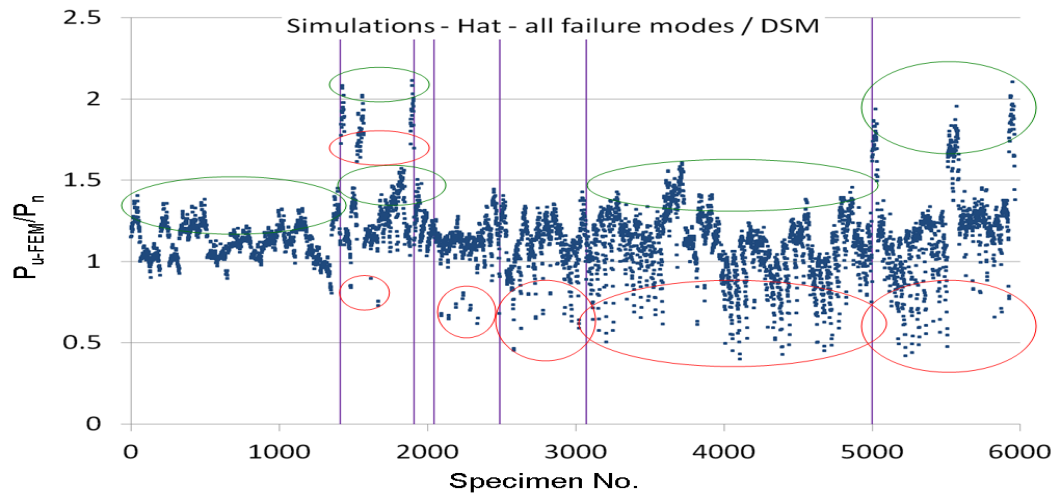
Fig. T.8: Highlight of large discrepancies in the simulation-to-predicted ratios for all Hat section columns by DSM Method 19 with classified failure modes (from left to right: L, LG, G, D, LD, DG, and LDG)
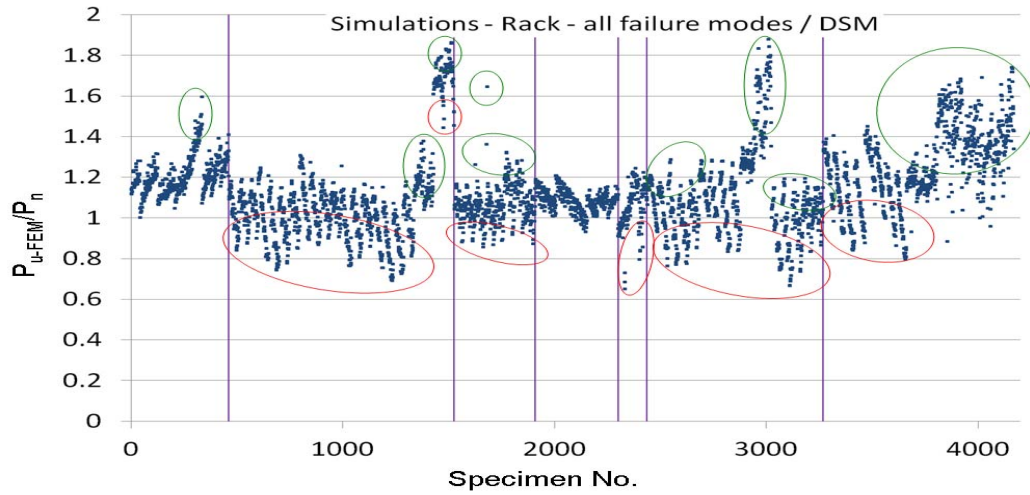
Fig. T.9: Highlight of large discrepancies in the simulation-to-predicted ratios for all Rack section columns by DSM Method 19 with classified failure modes (from left to right: L, LG, G, D, LD, DG, and LDG)
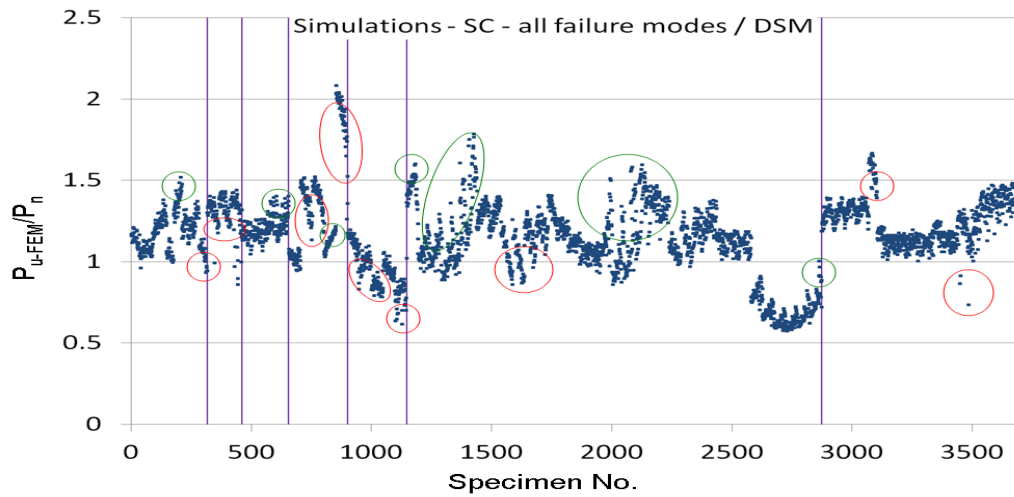
Fig. T.10: Highlight of large discrepancies in the simulation-to-predicted ratios for all Stiffened C section columns by DSM Method 19 (with separate regression constants) with classified failure modes (from left to right: L, LG, G, D, LD, DG, and LDG)

APPENDIX U

SIMULATION-TO-PREDICTED RATIOS BY DSM METHOD 19 –for columns with *Hole Width Factor*=0, 0.2, 0.4, and 0.6

U.1   non-perforated and perforated columns
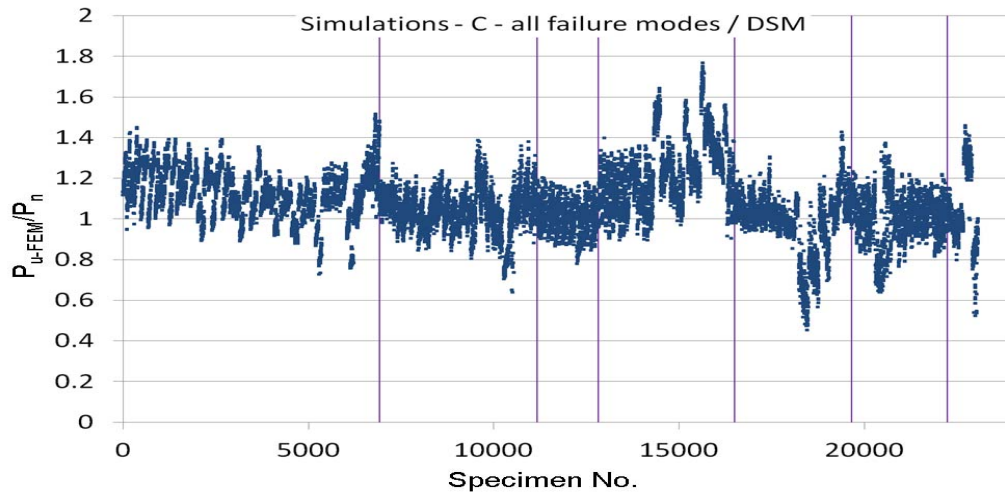
Fig. U.1: Simulation-to-predicted ratios for C section columns with Hole Width Factor=0, 0.2, 0.4, and 0.6

by DSM Method 19 with classified failure modes (from left to right: L, LG, G, D, LD, DG, and LDG)
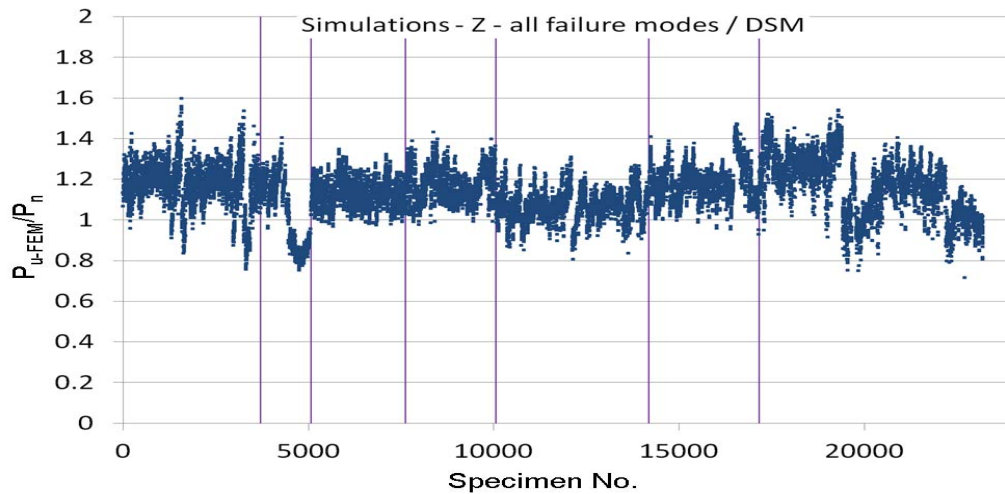

Fig. U.2: Simulation-to-predicted ratios for Z section columns with Hole Width Factor=0, 0.2, 0.4, and 0.6

by DSM Method 19 with classified failure modes (from left to right: L, LG, G, D, LD, DG, and LDG)
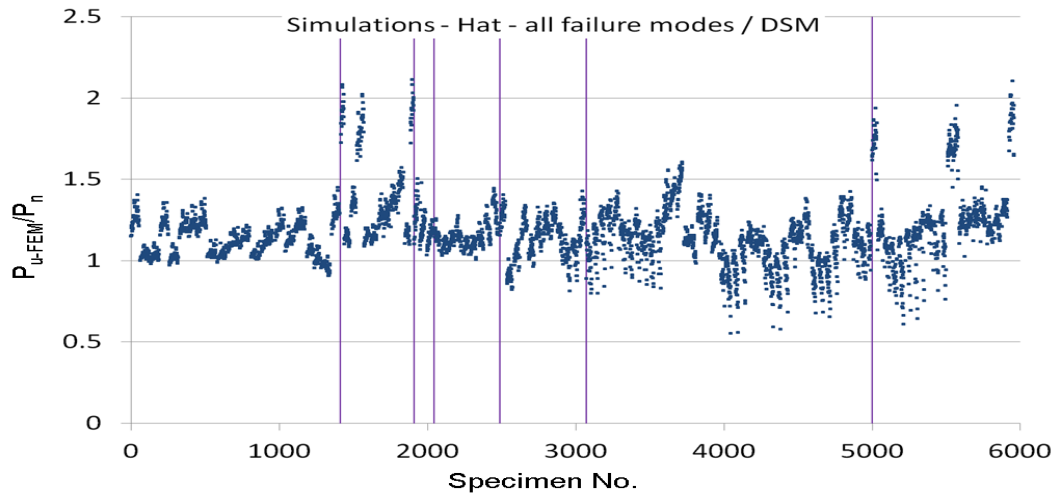
Fig. U.3: Simulation-to-predicted ratios for Hat section columns with Hole Width Factor=0, 0.2, 0.4, and 0.6 by DSM Method 19 with classified failure modes (from left to right: L, LG, G, D, LD, DG, and LDG)
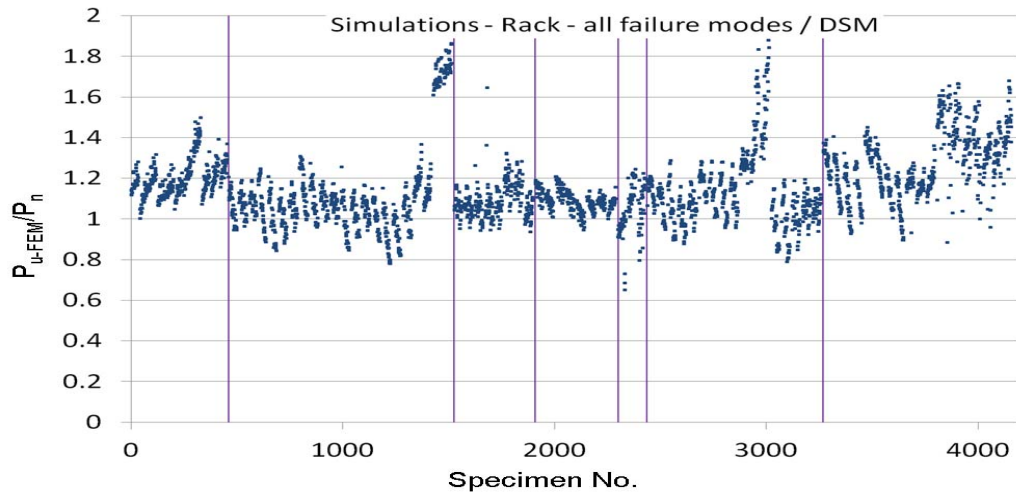
Fig. U.4: Simulation-to-predicted ratios for Rack section columns with Hole Width Factor=0, 0.2, 0.4, and 0.6 by DSM Method 19 with classified failure modes (from left to right: L, LG, G, D, LD, DG, and LDG)
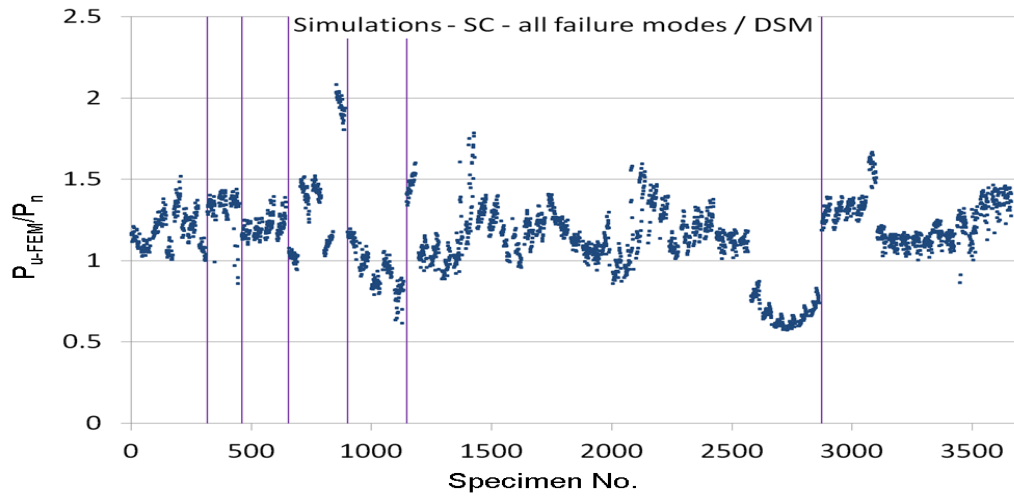
Fig. U.5: Simulation-to-predicted ratios for Stiffened C columns with Hole Width Factor=0, 0.2, 0.4, and 0.6 by DSM Method 19 (with separate regression constants) with classified failure modes (from left to right: L, LG, G, D, LD, DG, and LDG)

APPENDIX V

SIMULATION-TO-PREDICTED RATIOS BY DSM METHOD 19 –for columns with *Hole Width Factor*=0, 0.2, and 0.4

V.1 non-perforated and perforated columns
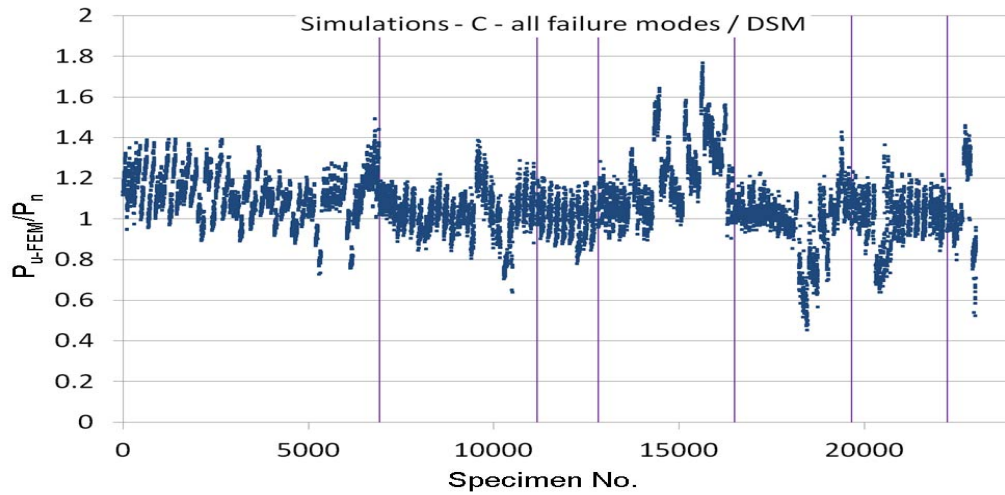
Fig. V.1: Simulation-to-predicted ratios for C section columns with Hole Width Factor=0, 0.2, and 0.4 by DSM Method 19 with classified failure modes (from left to right: L, LG, G, D, LD, DG, and LDG)
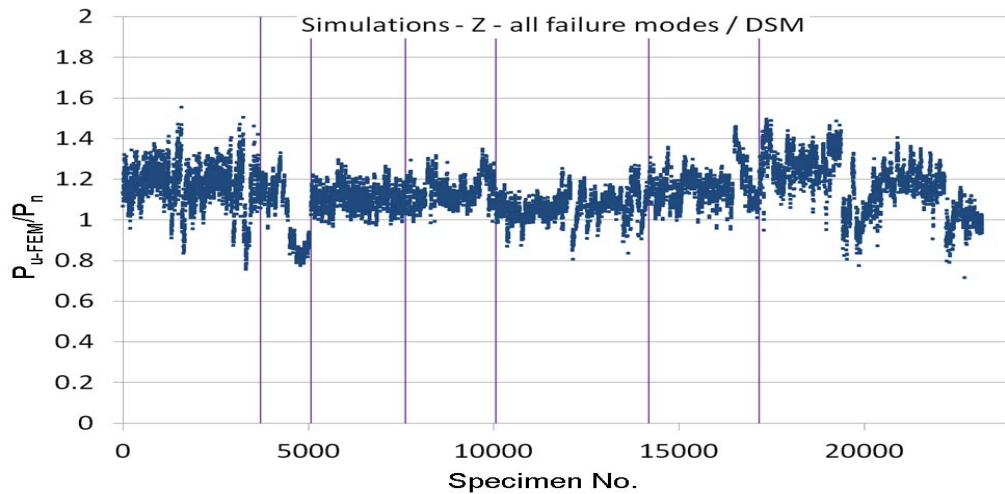

Fig. V.2: Simulation-to-predicted ratios for Z section columns with Hole Width Factor=0, 0.2, and 0.4 by DSM Method 19 with classified failure modes (from left to right: L, LG, G, D, LD, DG, and LDG)
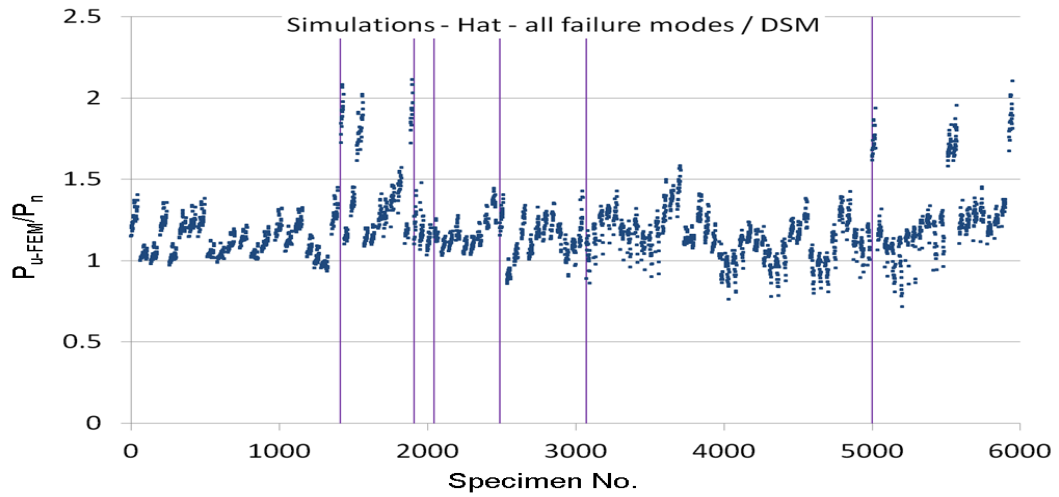
Fig. V.3: Simulation-to-predicted ratios for Hat section columns with Hole Width Factor=0, 0.2, and 0.4 by DSM Method 19 with classified failure modes (from left to right: L, LG, G, D, LD, DG, and LDG)
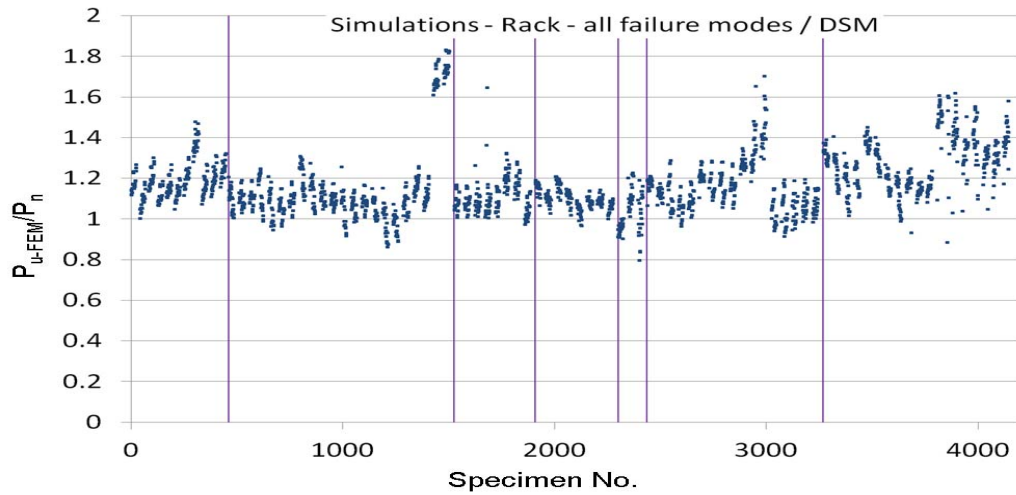
Fig. V.4: Simulation-to-predicted ratios for Rack section columns with Hole Width Factor=0, 0.2, and 0.4 by DSM Method 19 with classified failure modes (from left to right: L, LG, G, D, LD, DG, and LDG)

Fig. V.5: Simulation-to-predicted ratios for Stiffened C columns with Hole Width Factor=0, 0.2, and 0.4 by DSM Method 19 (with separate regression constants) with classified failure modes (from left to right: L, LG, G, D, LD, DG, and LDG)